THE INTRINSIC HOST FACTORS ASSOCIATED WITH INTRASPECIFIC VIRAL SHEDDING VARIATION IN LOW-PATH AVIAN INFLUENZA-INFECTED WILD DUCKS

By

Amanda C. Dolinski

A DISSERTATION

Submitted to
Michigan State University
in partial fulfillment of the requirements
for the degree of

Fisheries and Wildlife – Doctor of Philosophy

2021

ABSTRACT

THE INTRINSIC HOST FACTORS ASSOCIATED WITH INTRASPECIFIC VIRAL SHEDDING VARIATION IN LOW-PATH AVIAN INFLUENZA-INFECTED WILD DUCKS

By

Amanda C. Dolinski

In this dissertation I, with co-authors and co-collaborators, evaluated the association between intraspecific viral shedding variation and intrinsic host factors in low-path avian influenza virus (LPAIV) infected mallards and blue-winged teals. We hypothesized that intraspecific viral shedding variation would be associated with intraspecific variation in virus receptor occurrence frequency and gene expression at the host tissue site of viral replication.

Chapter one is a literature review of super-shedding effects on pathogen transmission dynamics and highlights the importance of studying super-shedding in wildlife from a zoonotic spillover and conservation perspective. Conclusions drawn include the recognition that many different wildlife host-pathogen systems exhibit intraspecific variation in pathogen load, and various techniques/technologies should be utilized for expanding current knowledge of wildlife pathogen transmission dynamics in the purpose of developing innovative wildlife disease management programs.

In chapter two we evaluated the association between intraspecific variation in LPAIV load and alpha-2,3 sialic acid viral receptors ($SA\alpha2,3Gal$) in the intestines and bursa of mallards and blue-winged teals. Our hypotheses were supported in that we detected a significant relationship between LPAIV load and $SA\alpha2,3Gal$ occurrence frequency in the ileum of mallards. $SA\alpha2,3Gal$ in teals did not have a significant relationship with LPAIV load; however, teals had higher virus titers and $SA\alpha2,3Gal$ occurrence frequency than mallards. In conclusion, we

determined that higher $SA\alpha 2,3Gal$ occurrence frequency was associated with higher virus titers and may also be a contributing host factor for intraspecific LPAIV shedding in mallards.

In chapters three and four we evaluated differential gene expression in association with intraspecific individual viral shedding in wild mallards and blue-winged teals, respectively. We found that several genes of the innate immune system and pro-viral cell entry and replication were up-regulated in higher shedding LPAIV-infected birds than lower shedding birds. For both species, most of the differential gene expression was observed in the ileum compared to the bursa. Early in the infection, mallards showed most differential gene expression between viral shed level groups and teals showed most differential gene expression between LPAIV-infected and uninfected birds. Later in the infection, differential gene expression was not observed in mallards, but in teals several genes were down regulated in high shedders. We also found statistically significant positive linear relationships for expression of innate immune genes and viral shedding, but mostly early in the infection. We concluded that intraspecific LPAIV shedding variability was closely related to innate immune gene expression, and that genes which promote viral cell entry and viral replication were likely impacting viral shedding load.

Chapter five is a dissertation summary where I draw conclusions based on the previous chapters, suggest hypotheses for potential mechanisms responsible for intraspecific variation in LPAIV shedding, and recommend how the dissertation data and results could be used for future research. Collectively, the research in this dissertation provides evidence that physiological, genetic, and immunogenic host factors were associated with intraspecific variation in viral shedding.



ACKNOWLEDGEMENTS

Looking back on my time spent at Michigan State University, I am beyond grateful to those who helped me get to this point. I first have to thank my academic adviser, Dr. Jen Owen, for molding me into the scientist I have become. This project was beyond ambitious and definitely had its trials and tribulations. In the end, I think we can be very proud of the product. With Jen's guidance, I learned how to organize and conduct experimental research, improved my communication skills, and become a better writer. I have no doubt that my future success as a scientist will be attributed to having Jen as my academic adviser.

A huge thanks also goes out to the other members of my graduate committee, Dr. Mark Jankowski, Dr. Scott Fitzgerald, and Dr. Paul Coussens. They provided excellent guidance, assistance, and expertise to elevate this massive research project. Furthermore, they provided me with the knowledge I needed to become a successful scientist.

I also need to thank Dr. Jared Homola, Dr. John Robinson, and Dr. Juan Steibel for their assistance with bioinformatics. Juan provided guidance on the initial experimental design and further direction on differential gene expression. John provided the initial groundwork for the mallard bioinformatics creating a smooth pipeline to follow for differential expression analysis. Jared not only assisted this project by providing his expertise in bioinformatics analyses for this dissertation, but he was also my personal mentor in navigating these analyses. Almost everything I learned concerning bioinformatics is thanks to Jared.

It is also imperative for me to thank the many individuals who assisted with the experimental aspect of this project. First, a huge thank you to all the undergraduate research assistants who helped with duck care, sample collection, and lab work: Darren Incorvaia, Evan

Nelson, Marni Gutman, and Jared Emerson were NSF funded undergraduate interns (REU), and Elizabeth Hergert, Craig Sklarczyk, Mercedes Yang, Taylor McCord, Mark Phillips, Olivia Lefere, William Decker, Valeria Colberg, Veronika Olszewski, Karee Lesko, Olivia Rose, Joseph Shemanski, Elyse Goran, Rebecca Cena, Amber Bedore, and Laura Carlson. Thanks to Frank Rowher and Mike Buxtan from Delta Waterfowl for the training and assistance in collecting duck eggs. Thank you to former MSU Genomics Core assistant researcher, Jeff Landgraff, who taught me most of the laboratory techniques needed for this project. Thanks to CSTAT at MSU and consultants Andrew Dennhardt, Daewoo Pak, and Dr. Dhruv Sharma for providing guidance on statistical analyses and statistical writing. Thank you to members of the disease ecology team, Jean Tsao, Kim Fake, Gena Pang, Megan Porter, and Viva Kobbedad, who provided advice and friendship along the way.

I would also like to thank the many individuals and organizations at MSU who helped me grow as a better educator and professional during my time at MSU. Dr. Ryan Kimbirauskas and Dr. Melinda Wilkins were excellent teaching mentors, and with their guidance I can confidently continue to train the next generation of veterinarians and scientists. Dr. William Cunningham and Ann Marie Schneider provided me with campus wide One Health outreach opportunities. I thank the Wildlife Disease Organization for the ability to form a student chapter at MSU which connected me to other wildlife disease students and professionals on MSU's campus.

I thank the National Research Foundation (Career Grant 135077 awarded to Dr. Jen Owen) for funding this research and financially supporting my work. I also would like to thank the Hal and Jean Glassen Memorial Foundation for awarding me a fellowship in wildlife disease research and MSU's College of Agriculture and Natural Resources along with the Graduate School for awarding me a dissertation completion fellowship.

Finally, I would like to thank my family and friends. My mother, Margie Dolinski, was the ultimate cheerleader. She provided much needed financial and emotional support throughout my entire educational journey. My very proud father, Antoni Dolinski, was always bragging to his friends about me. Although he passed away two years prior to my graduation, I can feel his spirit still wondering when I will have my own PBS nature show. A huge thank you to my husband and ultimate life partner, Andrew Dennhardt, who I met on my first day at MSU. Andrew is constantly by my side providing strength, laughter, and much needed statistical expertise. I also thank my in-laws, Eugene, Beri, Christian, and Shelby for providing a home away from home. The financial and emotional support has truly been an overwhelming gift. A special thanks to friends and colleagues Rebecca Cain, Gena Pang, and Remington Moll, for their advice and emotional support.

PREFACE

The second chapter of this dissertation was published in an open-source, online, peer-reviewed journal with co-authors and was modified from its original format for this dissertation.

TABLE OF CONTENTS

LIST OF TABLES	xii
LIST OF FIGURES	xv
KEY TO ABBREVIATIONS	xix
CHAPTER 1: SUPER-SHEDDERS IN WILDLIFE - THE IMPORTANCE OF	
HIGHLY INFECTIOUS INDIVIDUALS FOR WILDLIFE DISEASE	
TRANSMISSION	1
Background	
Modeling Heterogeneity in Pathogen Transmission and Identifying	
Super-Shedders	3
Quantifying Pathogen Load	
Determining the Factors Responsible for Variation in Pathogen Load	
Super-shedding and Implications for Control of Disease Outbreaks	
Intraspecific Variation in Pathogen Load Observed in Wildlife	
Applications of Super-shedding Research and Wildlife Disease	
Management	15
Rationale For This Study	
Avian Influenza Virus, Ducks, and Transmission	
Super-shedding in LPAIV-infected Mallards and Blue-winged Teals	
CHAPTER 2: THE ASSOCIATION BETWEEN SAα2,3GAL OCCURRENCE	
FREQUENCY AND AVIAN INFLUENZA VIRAL LOAD IN MALLARDS	
(ANAS PLATYRHYNCHOS) AND BLUE-WINGED TEALS (SPATULA DISCORS)	21
Abstract	
Introduction	
Methods	
Permits and Protocols	
Study Species and Locations	
Virus	
Experimental Design	
1 0	
Euthanasia	
Necropsy and Tissue Collection	
Lectin Histochemistry	
· · · · · · · · · · · · · · · · · · ·	
Statistical Analysis	
Results	
Viral Infection of Mallards and Teals	
Relationship of Virus Titers in Cloacal Swab, Ileum Tissue, and	30
Bursa of Fabricius Tissue	37
Dui su 0/1 uu i ilius 1 issue	/

Species and Sex-based Differences in Viral Shedding	39
Evaluating SAα2,3Gal in Intestines and Bursa of Fabricius	
Lectin Score Differences Between Infected and Control Birds	
Species and Sex-based Differences in Lectin Score	
Relationship Between Lectin Score and Virus Titer – Mallard	
Relationship Between Lectin Score and Virus Titer – Teal	
Discussion	51
CHAPTER 3: DIFFERENTIAL GENE EXPRESSION REVEALS HOST FACTORS	
FOR VIRAL SHEDDING VARIATION IN MALLARDS (ANAS PLATYRHYNCHOS)	
INFECTED WITH LOW-PATH AVIAN INFLUENZA VIRUS	59
Abstract	59
Introduction	
Methods	63
Permits and Protocols	63
Birds and Virus	64
Experimental Design	64
Viral RNA Extraction and Quantification from Cloacal Swabs	66
Determining Shed Level Groups	66
mRNA Extraction, cDNA Library Preparation, and Sequencing	69
RNA-seq Read Processing	70
Differential Expression Analyses	71
Candidate Gene Analysis	
Results	74
RNA Sequencing	74
Differential Gene Expression Between LPAIV-infected and Uninfected	
Control Groups	
Differential Gene Expression of LPAIV-infected Birds Over Time	75
Differential Gene Expression Between Virus Shed Level Groups During	
Early Stage Infection	76
Differential Gene Expression Between Virus Shed Level Groups During	
Late Stage Infection	94
Candidate Gene Analysis	94
Discussion	95
CHAPTER 4: DIFFERENTIAL GENE EXPRESSION REVEALS HOST FACTORS	
FOR VIRAL SHEDDING VARIATION IN BLUE-WINGED TEALS (SPATULA	
DISCORS) INFECTED WITH LOW-PATH AVIAN INFLUENZA VIRUS	102
Abstract	
Introduction	
Methods	
Permits and Protocols	
Birds and Virus	
Experimental Design	
Viral RNA Extraction and Quantification from Cloacal Swabs	
MIKNA EXITACIION. CIJNA LIDTATV FYEDATAIION. ANA SEAUENCING	1 1 0

RNA-seq Read Processing	110
Differential Expression Analyses	111
Candidate Gene Analysis	
Results	
Viral Infection	
RNA Sequencing	
Differential Gene Expression Between LPAIV-infected and Uninfected	
Control Groups	117
Differential Gene Expression of LPAIV-infected Birds Over Time	
Differential Gene Expression Between Virus Shed Level Groups During	
Early Stage Infection	130
Differential Gene Expression Between Virus Shed Level Groups During	
Late Stage Infection	135
Candidate Gene Analysis	
Discussion	
CHAPTER 5: CONCLUSION	149
Summary	
Conclusions Across Dissertation Chapters	
Interspecific Differences	
Future Contributions	
APPENDIX	163
REFERENCES	169

LIST OF TABLES

Table 2.1: Virus titer descriptive statistics for mallard and blue-winged teal cloacal swabs. $N = total$ sample size, $DL = detection$ limit of $0.04 Log10(EID_{50}/mL)$, $QL = quantification$ limit of $2.60 Log10(EID_{50}/mL)$, min $+ = minimum$ N>DL, mean is the geometric mean, and std.dev = one standard deviation. (*) signifies significantly higher titer variation for each DPI between species.
Table 2.2: Lectin histochemistry score descriptive statistics. Proximal includes duodenum and jejunum. N = total sample size and std.dev = one standard deviation. (*) signifies significantly higher lectin score variation for each tissue/cell type between species
Table 2.3: Sex and ileum lectin scores are associated with LPAIV H5N9 virus titers in mallards. Y = dependent variable, N = number of individual birds in model, X = independent variables in final model, CI = 95% confidence interval, p = p-value. Dependent variable "mallard cloaca virus titer" includes virus titers from cloacal swabs collected on the DPI each bird was sacrificed. Proximal includes the duodenum and jejunum. PC1 represents the principal component variable for the proximal villi enterocytes, brush border, and crypt enterocytes combined. BCS = Body Condition Score. Group and Sex were treated as factors in each model, and if present in final model, group T1 and females are represented in the intercept.
Table 3.1: Sample size used in differential gene expression analyses for uninfected control (C) and LPAIV-infected mallards on one (I1), two (I2), five (I5), 15 (I15), and 29 (I29) days post infection (DPI). Groups I1, I2, and I5 were further divided into low (L), moderate (M), or high (H) viral shedding groups
Table 3.2: Immune genes differentially expressed (DEGs) in the ileum between low (L), moderate (M), and high (H) LPAIV shedders on one (I1) and two (I2) days post infection. Alt.LvH is an alternative shed status grouping scheme that divided birds into two groups rather than three. Comparisons without DEGs are not shown. DEGs are designated by log ₂ fold count differences for each comparison. Up regulated genes are positive and down regulated genes are negative corresponding to the first shed level group in each comparison. Gene symbols in parentheses indicate alternative nomenclature. ns = non-significant.
Table 3.3: Immune genes in the bursa with statistically significant differential expression between low (L) and high (H) LPAIV shedders two (I2) days post infection. Differential expression is designated by log ₂ fold count differences for each comparison. Up-regulated genes are positive and down-regulated genes are negative corresponding to the first shed level group in each comparison. Gene symbols in parentheses indicate alternative nomenclature.

Table 3.4: Host cell factors of viral replication differentially expressed between low (L), moderate (M), and high (H) LPAIV shedders on one (I1) and two (I2) days post infection. Alt.LvAlt.H is an alternative shed level grouping scheme that divided birds into two groups rather than three. Differential expression is designated by log ₂ fold count differences for each comparison. Up regulated genes are positive and down regulated genes are negative corresponding to the first shed level group in each comparison. Gene names in parenthesis indicate alternative nomenclature. ns = non-significant	90
Table 4.1: Summary of KEGG BRITE pathways for differentially expressed transcripts/genes (DET/DEG) of LPAIV-infected blue-winged teals. A) DET/DEGs are either down (↓) or up regulated (↑) in infected birds compared to control birds on 1, 3, 5, or 14 DPI. B) LPAIV shed level group comparisons in early-stage infection (I1, I3). DET/DEGs shown are up regulated in low shedders compared to moderate or high shedders, or up regulated in high shedders compared to low and moderate shedders. C) LPAIV shed level group comparisons in late-stage infection (I5). DET/DEGs shown are all down regulated in high shedders compared to low or moderate shedders. See supplementary file for full list of KEGG BRITE pathways	119
Table 4.2: Immune transcripts/genes with significant differential expression between LPAIV-infected and uninfected (control) birds and between low and high viral shedders on one (I1), three (I3), and five (I5) days post infection. Immune genes up regulated (\uparrow) or down regulated (\downarrow) corresponds to the infected and low shedders. Significant linear relationships (p < 0.05) between candidate gene expression and cloacal virus titers are positive (+) or negative (-) at the transcript and/or gene level across all bird samples with (w/) and without (w/o) uninfected controls and on one (I1), three (I3), and five (I5) days post infection. Blank cells are non-significant.	125
Table 4.3: Significant (p<0.05) linear relationships between viral load and candidate gene expression for LPAIV-infected blue-winged teals and uninfected controls. Genes were significant at either the transcript level, gene level, or both. All results are for the ileum only, unless otherwise stated.	138
Table 5.1: Dissertation conclusions and the results in each chapter that provide evidence to support each conclusion.	150
Table 5.2: Interspecific and inter-tissue comparisons of supported hypotheses in this dissertation. Yes = hypothesis was supported based on dissertation results. No = hypothesis was not supported based on dissertation results. Early = early in the infection. Late = late in the infection.	151
Table A2.1: Pearson's r correlation matrix for mallard lectin histochemistry scores. Crypts = crypt enterocytes, villi = villi enterocytes, and BB = brush border	164
Table A3.1: Mallard RNA integrity number (RIN) and sequencing pool at Michigan State University (MSU) and University of Minnesota (UMN). Ns = not sequenced	165

Table A4.1: Mallard RNA integrity number (RIN) and sequencing pool at Michigan	
State University (MSU) and University of Minnesota (UMN)	167

LIST OF FIGURES

Figure 1.1: Cumulative percent graphs for LPAIV-infected mallards and blue-winged teals. The x-axis represents the percentage of the total number of birds, and the y-axis represents the percentage of total virus detected in cloacal swabs. Each dot represents an individual's additive contribution to the overall virus shed on each day post infection (DPI). n = number of individuals.
Figure 2.1: Timeline of Sample Collection for Mallards and Blue-winged Teals. Experimental groups are designated by species (M = mallard, B = blue-winged teal), infection status (T = LPAIV treatment/inoculation with LPAIV H5N9, C = control/shaminoculated), and day post infection (DPI) the group of birds was sacrificed. Two mm sections of bursa of Fabricius tissue and ileum tissue were collected from each bird on the DPI of sacrifice. Cloacal swabs were collected from all living birds at each DPI designated by an asterisk.
Figure 2.2: LPAIV H5N9 virus titers in the bursa, ileum, and cloacal swabs are positively related. Black trendline is the linear regression for all birds sacrificed on $1-5$ days post infection (DPI) with the 95% confidence interval shaded in gray. Colored trendlines represent each treatment group: T1 represents birds sacrificed on 1 DPI, etc. Trendlines indicated with a (*) indicate a statistically significant relationship (p < 0.05)
Figure 2.3: Cloacal swab virus titer boxplots for mallard and blue-winged teals infected with LPAIV H5N9. Horizontal bar within the box is the median value, solid dots indicate values falling above the upper or below the lower quartile $+ 1.5$ times the interquartile distance. (*) indicates statistically higher variation between species for each day post infection (DPI; $p < 0.05$)
Figure 2.4: Mean virus titer ± 95% confidence interval for (a) species, (b) days post infection (DPI), and (c) the interaction of species and DPI for mallard and blue-winged teal cloacal swab samples one to five DPI.
Figure 2.5: Mean virus titer + 95% confidence intervals for (a,c) sex, and (b,d) the interaction of sex and days post infection (DPI) for male (M) and female (F) mallard and teal blue-winged teal cloacal swab samples one to five DPI.
Figure 2.6: Lectin staining of mallard and blue-winged teal intestines and bursa of Fabricius. Lectin binding is positive where the brown colored stain is visible. The individual bird ID, tissue, and lectin score (villi enterocyte/epithelial cells) are given for each histological photograph. Scores were determined by averaging the scores for each field of view evaluated at 400x. Each field of view was given the following score: 0, no cells stained; 5, 1–10% of cells were stained; 35, 11–60% of cells stained; and 80, 61–100% of cells stained. Segments (a) and (b) show the range of lectin scores between sections of intestinal tissue in one individual (proximal represents duodenum or jejunum). Segments (c) and (d) show the range of lectin between individuals for the

Fabricius. All photos were taken at 200x brightfield microscopy	2
Figure 2.7: Lectin score differences between control and LPAIV-infected birds. Mean lectin scores $+95\%$ confidence intervals of intestinal tissues proximal (duodenum and jejunum), ileum, cecum, and colon for LPAIV H5N9 infected and control mallards and blue-winged teals. Bursa epithelial cells are included for teals only. (*) indicates tissue/cell type with a statistically significant difference between control and infected birds (p < 0.05).	4
Figure 2.8: Lectin score differences between mallard and blue-winged teal intestinal tissues. Mean lectin scores $+95\%$ confidence intervals for intestinal tissues proximal (duodenum and jejunum), ileum, cecum, and colon for LPAIV H5N9 infected mallards and blue-winged teals. Across all panels, points with different letters are considered significantly different (p < 0.05).	5
Figure 2.9: Mean lectin scores \pm 95% confidence intervals for intestinal tissues proximal (duodenum and jejunum), ileum, cecum, and colon for LPAIV H5N9 infected male (M) and female (F) mallards and blue-winged teals.	3
Figure 3.1: Experimental timeline of sample collection days post infection (DPI). Groups are designated by infection status (I = LPAIV-infected, C = uninfected control), DPI sacrificed and (N) quantity of birds in each group. Ileum and bursa of Fabricius were collected upon sacrifice. Cloacal swabs were collected from all living birds designated with the swab icon.	5
Figure 3.2: Cloacal swab virus titer profiles for LPAIV-infected mallards sacrificed on one (I1), two (I2), and five (I5) days post infection (DPI). Shed status of high (H), moderate (M), or low (L) was assigned to individuals by their last virus titer (I1, I2) or the average virus titer across all DPI (I5). Alternative high (Alt.H) and alternative low (Alt.L) shed status groupings were assigned to individuals in I2 based on cumulative virus titers clustered across one and two DPI. Due to low host RNA quality, *individuals were not included in ileum differential gene expression analyses	8
Figure 3.3: Multidimensional scaling (MDS) plot of bursa and ileum samples shows that tissue samples cluster based on tissue type gene expression. Bursa and ileum samples from bird 1 and 72 were removed from differential expression analysis due to opposite tissue grouping.	2
Figure 3.4: Gene expression of FOSB and HSPA8 in the bursa of uninfected control and LPAIV-infected mallards on one (I1), two (I2), five (I5), 15 (I15), and 29 (I29) days post infection (DPI). Differential expression (FDR <0.1, LFC >0.5) was only observed between I2 and I29. HSPA8 at the transcript (trans) and gene levels had identical gene expression.	5

Figure 3.5: Differentially expressed genes (DEG) between shed level groups (low,

moderate, high) of LPAIV-infected mallards in the ileum and bursa on one (I1) and two (I2) days post infection. An additional analysis for I2 divided birds evenly into low and high shedders (Alt.L vs. Alt.H). Each value represents the quantity of DEGs per comparison, and/or shared between comparisons. The arrows reflect the number of DEGs that are up (↑) or down (↓) regulated in the first shed level group listed in each comparison.	77
Figure 3.6: KEGG pathways associated with differentially expressed genes (DEG) in shed level group comparisons (low, moderate, high) on one day post infection (I1). KEGG pathways in darker colors indicate statistically enriched pathways (p < 0.05). Abbreviations: biosynthesis (bs), signaling pathway (sp), glycosaminoglycan (ga), glycosphingolipid (gs), phosphate pathway (pp).	79
Figure 3.7: KEGG pathways associated with differentially expressed genes (DEG) in shed level group comparisons (low, moderate, high) on two days post infection (I2). KEGG pathways in darker colors indicate statistically enriched pathways ($p < 0.05$). Abbreviations: signaling pathway (sp), protein processing (pp)	80
Figure 3.8: KEGG pathways associated with differentially expressed genes (DEG) in alternative shed level group comparisons (Alt.L vs. Alt.H) on two days post infection (I2). KEGG pathways in darker colors indicate statistically enriched pathways (p < 0.05). Abbreviations: biosynthesis (bs), protein processing (pp), signaling pathway (sp), glycosaminoglycan (ga), glycosphingolipid (gs).	81
Figure 3.9: Immune genes differentially expressed in the bursa (A) and ileum (B) on one-and two-days post-infection. Individuals and their shed status group are on the x-axis and gene names are on the y-axis. Expression of genes is designated by color corresponding to the row Z-score (distance from the mean). Colors of gene names corresponds to their immune functional category.	83
Figure 3.10: Conditional R ² values for candidate genes with significant (p <0.05) linear relationships to cloacal swab virus titers on one, two, and five days post infection (DPI). All significant relationships were positive. Candidate genes in the bursa were evaluated at the gene and transcript level. Candidate genes in the ileum were only evaluated at the gene level. Immune gene categories are designated by color.	95
Figure 4.1: Experimental timeline of sample collection days post infection (DPI). Groups are designated by infection status (I = LPAIV-infected, C = uninfected control), DPI sacrificed, (N) quantity of birds in each group. Ileum and bursa of Fabricius were on DPI designated by group identification. Cloacal swabs were collected from all living birds designated with the swab icon.	108
Figure 4.2: Multidimensional scaling (MDS) plot of bursa and ileum samples shows that tissue samples cluster based on tissue type gene expression. The bursa sample for bird 19 was grouping with ileum samples; therefore, bird 19 was removed from differential expression analysis due to likelihood of mislabeled samples	111

Figure 4.3: Cloacal swab virus titer profiles for LPAIV-infected blue-winged teals sacrificed on one (I1), three (I3), and five (I5) days post infection (DPI). Shed level of high (H), moderate (M), or low (L) was assigned to individuals by their last virus titer (I1, I3) or the average virus titer across all DPI (I5).
Figure 4.4: Differentially expressed transcripts/genes between LPAIV-infected and uninfected control blue-winged teals in the ileum. LPAIV-infected birds were sacrificed on one (I1), three (I3), five (I5), and 14 (I14) days post infection (DPI). Each number represents the quantity of DET/DEGs per comparison, and/or shared between comparisons. DEGs/DETs up-regulated (↑) or down-regulated (↓) in each group corresponds to the LPAIV-infected group. Numbers preceding arrows indicate the number of unique transcripts/genes per annotation. (*) indicates LPAIV genes.
Figure 4.5: A. Heat map for differentially expressed genes in the ileum between uninfected (control) and LPAIV-infected mallards on one, three, five, and 14 days post infection (DPI). Illustrated are the relative expression levels of each transcript (rows) in each sample (column). Rows are hierarchically clustered by expression. Log2-transformed expression values are z-transformed. Box plots are provided for each visually observed gene cluster. B. Enriched GO terms corresponding to each cluster
Figure 4.6: Differentially expressed transcripts/genes between shed level groups (Low, Moderate, High) of LPAIV-infected blue-winged teals on one (I1), three (I3), and five (I5) days post infection for (A) bursa and (B) ileum tissues. Each number represents the quantity of DET/DEGs per comparison, and/or shared between comparisons. Transcripts/Genes upregulated (\(\epsilon\)) or down-regulated (\(\epsilon\)) corresponds to the first shed level group listed in the comparison. See supplementary material for additional gene information and log2(fold count).
Figure 4.7: Expression of endogenous retroviral genes differentially expressed in the ileum between shed level groups of LPAIV-infected blue-winged teals on one (I1), three (I3), and five (I5) days post infection (DPI). POL_BAEVM was down regulated in high shedders compared to moderate shedders on one DPI (I1) at the transcript level. No retroviral genes were differentially expressed on three DPI. POL_MLVFF was down regulated in high shedders compared to moderate and low shedders on five DPI (I5) at the transcript level. POL_SFV1 and SYNA_MOUSE were both down regulated in high shedders compared to low shedders on five DPI at the gene level. Expression of uninfected (control) birds is displayed for reference
Figure 4.8: Heat map for differentially expressed genes in the ileum between shed level groups of LPAIV-infected blue-winged teals on five days post infection. Illustrated are the relative expression levels of each transcript (rows) in each sample (column). Rows are hierarchically clustered by expression. Log2-transformed expression values are z-transformed. Box plots are provided for each visually observed gene cluster. B. Enriched GO terms corresponding to each cluster.

KEY TO ABBREVIATIONS

MAP: Mycobacterium avium subspecies paratuberculosis

QMRA: Quantitative microbial risk assessment

TCID_{50:} Fifty-percent tissue culture infective dose

EID₅₀: Fifty-percent egg infection dose

qPCR: reverse-transcription quantitative polymerase chain reaction

cfu/g: colony forming units per gram

BLV: bovine leukemia virus

AIV: Avian influenza virus

LPAIV: Low pathogenic avian influenza virus

HPAIV: Highly pathogenic avian influenza virus

WNV: West Nile virus

CWD: Chronic wasting disease

PrP^{Sc}: Chronic wasting disease prion

PRNP: prion protein

Bd: Batrachochytrium dendrobatidis

IHNV: Infectious hematopoietic necrosis virus

pfu/mL: Plaque forming units per milliliter

DPI: Days post infection

HA: Hemagglutinin

NA: Neuraminidase

SAα2,3Gal: alpha-2,3 sialic acid receptor

MAL I: Maackia Amurensis I

MAL II: Maackia Amurensis II

MSU: Michigan State University

ECE: embryonated chicken eggs

DMEM: Dulbecco's modified eagle medium

FOV: Fields of view

PCA: Principle component analysis

MLR: Multiple linear regression

BCS: Body condition score

AIC: Akaike's information criteria

VIF: Variance inflation factor

PRR: Pattern recognition receptor

ISG: interferon stimulated gene

NWHC: USGS National wildlife health center

MDS: Multidimensional scaling

DEG: Differentially expressed gene

DET: Differential expressed transcript

MHC: Major histocompatibility complex

ERV: Endogenous retrovirus

CHAPTER 1: SUPER-SHEDDERS IN WILDLIFE: THE IMPORTANCE OF HIGHLY INFECTIOUS INDIVIDUALS FOR WILDLIFE DISEASE TRANSMISSION

Background

Heterogeneity in disease transmission is an important factor to consider in infectious disease ecology yet has been understudied as a potential factor in wildlife disease transmission. For many pathogens, whether they involve an arthropod vector, a multi-host life cycle, or are directly transmitted, heterogeneities of individual host attributes can disproportionately affect the progress and outcome of a disease (Dushoff and Levin 1995; Lloyd-Smith et al. 2005; Woolhouse et al. 1996). Disease ecologists and epidemiologists use mathematical models to study how heterogeneity in transmission affects disease outcomes; however, the majority of models are specific to mixing patterns associated with human social structures (Edmunds et al. 2006; Mossong et al. 2008). While measuring contacts and group mixing is certainly an important factor for disease transmission in wild animal populations, it is also important to recognize that infected populations may also vary in their infectiousness, or their capacity to transmit an infection following contact with a susceptible host (Beldomenico and Begon 2010). With infectious disease as a cause of wildlife population decline (MacPhee and Greenwood 2013) and 70% of emerging zoonotic diseases originating from wildlife (Jones et al. 2008), it is critical to understand how heterogeneity in infectiousness impacts wildlife disease transmission.

One of the most notable examples of host heterogeneity influencing disease transmission is the 2003 SARS super-spreading event which was pivotal in the global spread of the disease (Zhuang et al. 2004). During this outbreak, one Hong Kong hotel patron is credited with spreading the virus to 12 other hotel patrons, one of which is responsible for the infections of 69 health care workers and sixteen medical students (Tsang et al. 2003). One epidemiologic investigation of Beijing hospitals found that out of 77 patients, 66 infected individuals did not

transmit the virus to others, seven transmitted the virus to less than three contacts each, and four persons transmitted the virus to eight or more individuals (Zhuang et al. 2004). The authors of this epidemiological analysis suggest that the viral load of the patient played a role in the likelihood of being a super-spreader. From observing this extreme heterogeneity in transmission of SARS and analyzing transmission of other infectious diseases, it has been found that many obligatory host pathogens are transmitted according to the 20/80 rule, where mathematically, it is recognized that 20% of infected individuals are responsible for 80% of transmission events (Lloyd-Smith et al. 2005; Woolhouse et al. 1996). From these analyses, we can conclude that most cases of secondary transmission in super-spreading events are dependent on a minority of individuals.

Super-spreading of infectious diseases is dependent on two key factors: 1) contact rate — the number of individuals a single individual contacts during the infectious period, and 2) infectiousness — the quantity of infectious particles the infected individual can shed during the infectious period (Vanderwaal and Ezenwa 2016). A "super-shedder" has therefore been identified as an individual who, for a period, yields many more infectious organisms of a particular type than most other individuals of the same host species (Chase-Topping et al. 2008). Therefore, "super-spreading" and "super-shedding" have been identified as independent traits: super-spreading as a reflection of the interaction between hosts, and super-shedding as a reflection of the interaction between the host and the pathogen (Chase-Topping et al. 2008). Identifying super-shedders are of particular interest, because if we can target the super-shedders specifically, we can increase efficiency in controlling outbreaks by 1) removing them from the population (Matthews, Low, et al. 2006) or 2) actively restricting their individual contacts (Woolhouse et al. 1996). For already infected individuals during a current outbreak, super-

shedders are identified by simply measuring how much pathogen they are actively shedding; however, for better use as a preventative management strategy to reduce pathogen transmission, it would be advantageous to identify the super-shedders prior to them becoming infected. Identifying super-shedders prior to infection would require the disease ecologist or public health official to identify individuals based on certain host factors that predisposes an individual to becoming a super-shedder; therefore, it is important to understand the host factors that are associated with intraspecific pathogen shedding variation.

In this review, heterogeneity in infectiousness is explored as a potential factor affecting wildlife disease dynamics, as well as the identification and control of super-shedders as a critical tool in wildlife disease management. I will describe how super-shedders are identified, the host factors, both intrinsic and extrinsic, that are contributing to individual variation in pathogen load, and how targeting super-shedders has been used to control disease outbreaks. A majority of this work has been done in domestic and laboratory animals, but a knowledge gap exists in wildlife host-pathogen systems. Examples of observed variation in pathogen load in wildlife host-pathogen systems are given across various taxa to highlight where super-shedding research could be applied to better predict emerging infectious diseases.

Modeling Heterogeneity in Pathogen Transmission and Identifying Super-Shedders

Disease modeling and analytical statistics are used to determine if targeting super-shedders is an effective strategy in controlling or preventing disease outbreaks. Traditional compartmental models are generally used to determine the speed and efficiency of a disease outbreak by grouping individuals based on their pathogen exposure status as infected, susceptible, or recovered. The rate of transmission is measured with the basic reproductive number or R_0 , that is the average number of susceptible individuals that will become infected after exposure to an

infected individual. Disease ecologists and public health officials use these models to determine how to reduce the spread of infection, for when R₀ is less than one, an outbreak comes to an end. R₀, however is a population average and does not account for individual heterogeneity in infectiousness; therefore, Lloyd-Smith et. al (2005) proposed a model that introduces the individual reproductive number "v", which accounts for the heterogeneity in the infectiousness of the infected population. By applying the individual reproductive number to disease transmission models, the most infectious individuals can be identified, and control efforts such as quarantine, vaccination, and culling can be focused on the super-spreaders, which reduces time and cost spent on control measures (Lloyd-Smith et al. 2005; Matthews, Low, et al. 2006).

Lloyd-Smith's individual reproductive number has been used to detect the pathogen threshold for identifying super-shedders in cattle infected with *Escherichia coli* O157 and Johne's disease, (*Mycobacterium avium subspecies paratuberculosis* - MAP). Super-shedders of *E. coli* O157 have been identified as the few individuals with a bacterial carriage at very high levels (10⁴ to 10⁵ cfu/g) (Chase-Topping et al. 2008; Matthews, Low, et al. 2006). This quantity represented the 9% of the cattle shedding greater than 96% of all bacteria in samples tested. This was also determined to be the super-shedding threshold for control. When the animals shedding more than 10⁴ cfu/g of bacteria are removed from the population, the spread of the pathogen is reduced to the point of eliminating the outbreak (Matthews, Low, et al. 2006). Similar to cattle infected with E. coli, cows infected with MAP are called super-shedders when fecal shedding of the pathogen exceeds 10⁴ cfu/g which represents 7.1% of culture-positive cattle (Whitlock et al. 2006) and 10% of qPCR positive cattle (Aly et al. 2012). Recognizing these pathogen shedding thresholds makes it easier to identify the requirements to call an individual a super-shedder. In addition to being the first species in which super-shedders have been quantified, cattle have also

been a good host to study the implications of super-shedding in disease control because they represent a closed population of animals which can easily be identified and handled.

In wildlife, identifying super-shedders based on a pathogen threshold is challenging considering no wildlife-pathogen system is a closed system, meaning that individuals and environmental factors within each host-pathogen system are constantly changing. If a supershedding threshold is identified for one population, it may not be the same for another, since the threshold depends not only on the type of pathogen, but also the route of transmission and quantity of pathogen particles needed to cause infection in the host. It might therefore be more important to understand the pathogen dose required for an individual to become infected and a source of secondary transmission. This is where the field of quantitative microbial risk assessment (QMRA) is useful (Haas, Rose, and Gerba 2014). For example, risk of being infected by a pathogen that is transmitted via the fecal-oral route and a contaminated water source (Tolouei et al. 2019) would be assessed differently than a pathogen transmitted via a mosquito vector (Kilpatrick et al. 2006). All pathogens require a specific dose threshold for infection, but the route of transmission will dictate how pathogen shedding load from an infected individual impacts the occurrence of a secondary transmission; therefore, each host-pathogen system needs to be researched independently to further identify the factors contributing to individual variation in pathogen load.

Quantifying Pathogen Load

Various methods have been developed to quantify infectious pathogens in excretory fluids. The traditional methods used for quantifying bacteria involve bacterial culture using media specific to the type of bacteria and enumeration (Feng et al. 2002). Viruses are quantified by detecting the virus titer using plaque assays (Baer and Kehn-Hall 2014), focus forming assays (Payne et al.

2006), the fifty-percent tissue culture infective dose (TCID₅₀) (Nadgir et al. 2013), or the fifty-percent egg infective dose (EID₅₀) (Spackman and Killian 2014). With the development reverse-transcription, quantitative polymerase chain reaction (qPCR), the DNA or RNA from pathogens can be isolated from host excreta and quantified by amplifying the pathogen's unique nucleic acid sequence in repetitive cycles (Heid et al. 1996; Rio 2014). These latter methods have revolutionized quantifying infectious pathogen load because of the ability to analyze multiple samples in a short amount of time. With the use of this technology, studying the effects of supershedders is practical and efficient.

Methods used to measure pathogen load and identify super-shedders was first accomplished in cattle. Immunomagnetic separation and evaluating the density of bacterial colony forming units per gram of feces (cfu/g) were the quantitative methods used to determine the threshold for super-shedding cattle infected with *E. coli* O157 (Pearce et al. 2004).

Quantifying pathogen load has been particularly challenging for cattle infected with MAP. Most of the research done with MAP and super-shedders has been to develop better diagnostic tools to accurately quantify the pathogen (Aly et al. 2009, 2012) since traditional culture methods using Herold's egg yolk medium could not quantify the pathogen above 50 cfu/g (Whitlock et al. 2000). The serial dilution method first used to quantify MAP in culture above 50 cfu/g determined quantities to range from 7,000 to 1,470,000 cfu/g (Whitlock et al. 2006). Methods using qPCR have obtained similar results with quantities ranging from 12,600 to 1,260,000 cfu/g (Aly et al. 2012).

For each host-pathogen system, quantifying pathogen load is helpful for identifying the super-shedders; however, in wildlife species, this is not an easy task. Very rarely is the source and time of exposure known. However, if the laboratory methods used to quantify pathogen are

standardized across populations, the potential for determining a pathogen threshold for each host-pathogen system may be possible.

Determining the Factors Responsible for Variation in Pathogen Load

The route of pathogen transmission, how the pathogen replicates in the host, and which species are susceptible to infection are used to evaluate the host factors impacting super-shedding for each host-pathogen system. Super-shedding research depends on studying the host-pathogen interaction; therefore, in vivo studies are required in order to fully evaluate differences between higher and lower pathogen shedding individuals. Below are some examples of host factors that have been determined for a few host-pathogen systems. They include intrinsic host factors, such as physiological, genetic, and immunogenic traits, and extrinsic factors, such as diet, co-infection stress, and exposure to environmental contaminants.

The search into genetic variation has already shown promising results for finding causes of super-shedding. Cattle have been used to show how specific genes can affect host shedding and susceptibility to disease. Asymptomatic cattle infected with bovine leukemia virus (BLV) are either recognized as having a high proviral load or a low proviral load, and the cattle with the low proviral load have been shown to not contribute to the spread of the disease (Juliarena et al. 2016). Further, the low proviral cattle carry the BoLA-DRB3*0902 allele, and when cattle were selected for this gene, the chain of viral transmission was stopped (Juliarena et al. 2008).

Looking at variation in microbiota can also shed some light into variation in pathogen load. Studies in mice infected with salmonella have shown that the intestinal microbiota plays a critical role in controlling Salmonella serovar Typhimurium infection, disease, and transmissibility (Lawley et al. 2008). The mucosal carriage at the recto-anal junction in cattle

infected with *E. coli* O157 has been determined to be a key physiological feature contributing to the super-shedding threshold of cattle (Cobbold et al. 2007; Low et al. 2005).

Other factors such as age, have been shown to affect viral load. For instance, the age that mallards are infected with influenza virus might have an effect on the extent of viral shedding, thereby impacting transmission of low-path avian influenza viruses (LPAIV) within the wild bird reservoir system (Costa et al. 2010). These intrinsic factors mentioned, such as specific alleles, microbiota, and age provide promising results to indicate that putting resources into studying other host-pathogen systems would greatly impact current knowledge concerning the host factors which contribute to variation in viral load.

Extrinsic factors which can influence the host pathogen load are mostly environmental factors or external stressors. Diet and food availability can impact an individual's health regardless of pathogen presence. In the case of mallards experimentally infected with LPAIV, birds that experienced reduced food availability and body condition shed lower quantities of LPAIV than birds provided with abundant access to food (Arsnoe, Ip, and Owen 2011). Another study assessing parasite loads and transmission dynamics in fish found that low food availability increased the strength of the associations between parasite peak burden and aggregation (Tadiri, Dargent, and Scott 2013). It is important to point out that access to food can also affect intrinsic host factors such as metabolic activity (Stahlschmidt and Glass 2020); therefore, extrinsic and intrinsic factors can be, and should be, studied simultaneously when possible.

Co-infection with two or more pathogens has also been observed to impact pathogen load. In an experimental study using mice infected with the gastrointestinal helminth Heligmosomoides polygyrus and the respiratory bacterial pathogen Bordetella bronchiseptica, it was found that individuals infected with both pathogens had higher bacterial and helminth egg loads than individuals infected with only one of the pathogens (Lass et al. 2013). By studying coinfection, we may observe interactions between pathogens that could affect transmission outcomes.

Stress and exposure to toxicants has also been shown to affect pathogen load. Nine-week old chickens experimentally infected with West Nile Virus (WNV) were exposed to synergized resmetherin (SR), an ingredient in mosquito insecticide, and subacute levels of corticosterone (CORT) to assess the immunological effects of the toxicant on an avian species (Jankowski et al. 2010). SR treatment alone extended viremia by one day while SR and CORT treatment together increased the number of chickens that shed WNV orally. Diet, co-infection, stress, and exposure to toxicants are all examples of extrinsic factors involved in super-shedding; however, many other extrinsic factors, such as temperature, humidity, precipitation, and other host-pathogen systems need to be studied to analyze super-shedding impacts.

Super-shedding and Implications for Control of Disease Outbreaks

Before discussing how super-shedding can be applied to control and management of disease in wild animal populations, it is best to see if it is an attainable strategy at all. In addition to being the first species in which super-shedders have been identified, cattle have also been a good host to study the implications of super-shedding in disease control because they represent a closed population of animals which can easily be identified and handled.

Variation in individual pathogen load has been used in models to describe the transmission dynamics in cattle infected with *E.coli* (Matthews, McKendrick, et al. 2006) and campylobacter (Marshall and French 2011). Results from these models indicate that only when heterogeneity in individual infectiousness is incorporated into the model, does the model effectively represent the transmission and infection trends seen in dairy herds. This indicates that

high-shedding animals may have a large impact on prevalence and environmental loading of these pathogens.

Even though controlling disease in free-ranging wild animals poses its unique challenges, these methods used in cattle to identify super-shedders and study the impacts of transmission have the potential to be applied to wildlife disease ecology. Super-shedding is a new area of study in disease ecology, but it seems the more it is being looked for, the more often it is found; therefore, super-shedding should be included in future modeling of infectious diseases, especially in wildlife.

Intraspecific Variation in Pathogen Load Observed in Wildlife

Historically, and more commonly in recent years, wild animals have been a source of emerging infectious diseases (Jones et al. 2008). Zoonotic pathogens that involve a wild animal reservoir, such as leptospirosis and avian influenza, and pathogens of conservation concern, such as chytridiomycosis in amphibians depend on innovative and cost-effective methods of control to better predict and treat disease outbreaks. It is important to recognize that super-shedding could have major impacts on how these diseases are sustained in their natural systems. Variation in pathogen load has been observed in a variety of wild animal host-pathogen systems. With a bit of tweaking, the tools and techniques used in cattle to identify and model super-shedders can be applied to wild animals. By reviewing where variation in pathogen load has been observed in various wildlife host-pathogen systems, we can better understand how super-shedding could be incorporated into disease control and management.

Starting with mammals, heterogeneity of leptospiral load in Norway rats (*Rattus norvegicus*) has been associated with varying demographics of the species (Costa et al. 2015). Between June and August of 2010, urine and kidney samples were obtained and then analyzed

for leptospiral load from 82 Norway rats. Urine samples' leptospiral loads varied between 5.9 and 6.1×10^6 GEq (Genomic equivalents of Leptospira per ml) (Costa et al. 2015). Multivariate analysis revealed that leptospiral load increased with increasing weight to length ratio of the rat, increasing number of wounds/scars, and varied with location of capture. Although no direct association was made between high pathogen load and leptospirosis in people, variation in leptospiral load could contribute to the disease transmission dynamics of this system (Costa et al. 2015).

Chronic wasting disease (CWD) is an infectious disease of free-ranging and captive cervids, such as deer, elk, and moose, which is caused by a misfolded protein called a prion (PrPSc) (Saunders, Bartlet-Hunt, and Bartz 2012). This disease is slowly emerging to new areas of the United States every year and has posed great challenges for wildlife management. Because prions do not contain nucleoproteins like other infectious organisms, they cannot be studied using traditional laboratory methods. A new method called "Real-time quaking-induced conversion (RT-QuIC)" has been developed which can be used to quantify prion seeding activity (Atarashi et al. 2011). Variation in prion quantity has been observed over the course of an infection, between infected tissues, and more infectious prions are found in feces compared to saliva and urine (Henderson et al. 2015; Plummer et al. 2017). The host genotype has also been suggested to influence prion shedding where cervids with genotypes for the prion protein (PRNP) were considered to be more susceptible to CWD and excrete CWD prions (94 %) than cervids with genotypes considered to be less susceptible (64 %) (Plummer et al. 2017). We also know that individuals can start shedding prions in their saliva and urine as early as three months of age (Henderson et al. 2015) or even one month of age (Cheng et al. 2016) and will continue to shed these infectious particles until death by the disease. Although PrPSc variation is seen in

different types of samples and over the course of an infection, no work has been conducted to analyze the impacts of individual variation in prion shedding. This will be an important area to study in the future because it may provide insights into more cost-efficient management.

Amphibians infected with the chytrid fungus *Batrachochytrium dendrobatidis* (Bd), a devastating fungal pathogen which has been responsible for endangering a large variety of the world's amphibians, have experienced devastating impacts surrounding individuals with high pathogen loads. In a study involving experimental infections of the Boreal toad (*Bufo boreas*) with Bd, it has been found that mortality is positively correlated with individuals who are infected with a higher dose and have a high fungal load (Carey et al. 2006). Due to the method in which Bd is transmitted, the direct contact dosage of zoospores with the skin is an important factor for super-shedding. This important revelation of this disease leads us to believe that when the density of the population is high and infected individuals have high fungal loads, a massive and quick mortality event will occur. Super-shedding in this case, is vitally important, because it could mean extinction of a population.

Wild birds have also been implicated in super-shedding patterns. Mallards (*Anas platyrhynchos*) infected with LPAIV have been observed to have large variation in viral shedding. In field studies, juveniles account for the largest percentage of positive samples collected (Papp et al. 2017). An experimental study found that younger birds (1 to 2 months old) shed more virus than older birds (3 to 4 months old) (Costa et al. 2010). In a study looking at how nutritional condition affects a mallard's ability to replicate and shed LPAIV, variation was not only seen between the treatment groups, but also within treatment groups, suggesting intrinsic factors may be responsible for the observed variation in viral load (Arsnoe, Ip, and Owen 2011).

In addition to mallards infected with LPAIV, super-shedding has been observed in other avian-pathogen systems. Using data from 17 bird-RNA virus/host-pathogen systems, it was found that birds shed RNA virus according to the pareto principle; that is, 20% of the individuals are responsible for 80% of the virus being shed (Jankowski et al. 2013). A conclusion one may draw from this finding is that epidemiological models used to develop control programs designed to reduce prevalence of these RNA viruses should be incorporating individual pathogen load heterogeneity.

Reptile pathogens are also included in this super-shedding phenomenon. Mojave desert tortoises (Gopherus agassizii) infected with Mycoplasma agassizii show variation in pathogen load, which is related to prevalence in populations and to clinical signs and disease progression (Weitzman, Sandmeier, and Tracy 2017). Quantitative PCR was used to quantify bacterial DNA from nasal lavage samples collected from 402 wild Mojave Desert tortoises from 2010 to 2012. The results of this method were evaluated based upon the Cq value, a calculation of the number of cycles necessary for amplification of the desired region above a given threshold. (Weitzman, Sandmeier, and Tracy 2017). 198 positive samples were detected with Cq values less than 40, which ranged from 28.98 to 39.3. The Cq value negatively correlated with prevalence at each collection site, meaning that prevalence of the pathogen was higher in populations with a higher pathogen load (Weitzman, Sandmeier, and Tracy 2017). This result suggests that higher pathogen load may result in more infections within a population, or that more infections in a location may increase the overall pathogen burden due to increased contacts. In addition, presence of clinical signs similarly correlated with prevalence. This may suggest that the use of syndromic surveillance in these tortoise populations and removal of ones with clinical signs and higher pathogen loads could help control disease prevalence.

One of the most intensive studies looking at variation in viral load in a non-domestic animal species is in fish which are an important economic commodity and ecological staple in freshwater and marine systems and are commonly plagued with infectious disease. Infectious hematopoietic necrosis virus (IHNV), a negative-sense, single-stranded RNA virus in the family Rhabdoviridae, is endemic in salmonid fish in the Pacific Coast from Alaska to California. Variation in viral load has been observed on several different occasions. One of the first reports of IHNV individual load variation found that viral titers varied from just 5 plaque forming units (pfu)/mL to 10⁹ pfu/mL between individual fish (Mulcahy et al. 1982). Initially this variation was suspected to be due to asynchronous timing of sampling and diversity of fish demographics. However, individual variation in viral titers as high as five orders of magnitude have also been observed in tightly controlled experiments (Peñaranda, Wargo, and Kurath 2011; Purcell et al. 2010; Wargo et al. 2012). Viral variation was significantly correlated with interferon gene expression and to be a predictor of cumulative percent mortality between families of rainbow trout (Oncorhynchus mykiss) (Purcell et al. 2010). It is unclear whether viral load influenced interferon expression or the opposite in this study; however, the correlation between viral load and gene expression provides new knowledge of the association between the innate immune system and viral load in this system. Interestingly, a different study in rainbow trout found that genetic diversity did not play a significant role in viral load variation (Wargo et al. 2012), indicating there may be some unknown physiological factor involved. These conflicting findings indicate that more research is warranted into the host factors associated with viral load.

Controlling pathogen load has even been a target of disease treatment in arthropods.

Crithidia bombi, an endoparasite of bumble bees (Bombus impatiens), can cause reduced pollinating efficiency. Bees with higher infection intensities, measured at >1000 C. bombi cells,

compared to bees infected with low intensities, measured at 10-1000 *C. bombi* cells, have been found to have lower learning rates, less access time at flowers, and decreased pollinating efficiency at visited flowers (Gegear 2005). When provided with the nectar alkaloid of the beepollinated plant *Gelsemium sempervi*, pathogen load, clinical disease, and transmission decreases (Manson, Otterstatter, and Thomson 2010). This treatment not only benefits bees in captive hives, but also could be used for conservation of free-ranging bee populations since the treatment is applied by self-medication with the plant nectar.

The examples of individual variation in pathogen load provided above are a short list of host-pathogen systems in which pathogen load heterogeneity has been observed and studied. Individual variation in pathogen load is not specific to a certain taxon of animals nor a type of pathogen. It could be assumed that in any host-pathogen system, if variation is looked for, it will be found. Testing the observed variation is the next step in determining if heterogeneity in pathogen load a target for control. It is important to recognize, however, that just because heterogeneity in pathogen load is observed, it does not mean that it is the driving factor for transmission of pathogens in every circumstance. The relationship between pathogen load, route of transmission, host factors, and environmental factors all need to be evaluated together to determine the impact super-shedding may have.

Applications of Super-shedding Research and Wildlife Disease Management

Super-shedding is a phenomenon seen in many host-pathogen systems. It is best described in cattle infected with *E. coli* O157 where management strategies targeting the super-shedders has been used successfully. Research has been conducted in a variety of systems to identify the intrinsic and extrinsic factors responsible for variation in pathogen load ranging from specific genes to co-infection. Disease modeling has been used to look at the effects of heterogeneity of

infectiousness in cattle, which has been shown to be a key component in transmission dynamics and control. With the background work that has already been done in this and other host-pathogen systems, these tools and techniques can, and should, be applied to wildlife disease systems.

Variation in pathogen load has been identified in many wildlife-pathogen systems, and some factors have been determined; however, due to the complexities and unknowns in identifying super-shedders and evaluating the transmission dynamics in wild animal populations, management and disease control strategies are yet to be implemented. Currently disease management programs target geographical areas at highest risk for disease, whether that be on migratory flyways for birds carrying WNV or AIV (Dusek et al. 2009; Gubler 2007; Ip et al. 2008), in a newly identified infected zone of CWD (DelGiudice 2002), or at the interface between wild animals and livestock/production animal facilities (O'Brien et al. 2011). Culling operations have been used as a management tool, but the animals are usually selected at random within a geographical area at risk (Wasserberg et al. 2009). Culling animals is also a controversial management tool due to ethical and economic concerns, especially for threatened species, and it has not been successful in eliminating the disease in most situations (Wobeser 2007). If more research is done to identify the factors involved in super-shedding, then individuals may be identifiable in the future, and more targeted, cost-effective approaches could be used to control the spread of disease between wildlife, domestic animals, and people.

Rationale For This Study

The experimental research conducted for this dissertation takes the ideas outlined in this literature review and applies them to an essential wildlife reservoir host for a potential zoonotic pathogen: wild ducks infected with avian influenza viruses. Based on previous work, where it

was found that mallards shed LPAIV according to the 20/80 rule (Jankowski et al. 2013) independent of the extrinsic factor of variation of food availability (Arsnoe, Ip, and Owen 2011), we were interested in understanding the genetic, immunogenic, and physiological factors associated with individual variation in LPAIV load in mallards and blue-winged teals. The approach of this experimental study was to 1) collect mallard and blue-winged teal eggs from the nests of free-ranging birds, 2) hatch and raise birds in captivity, 3) infect a proportion of the birds with a low-pathogenic strain of avian influenza virus, 4) collect cloacal swab samples for detection of influenza virus, 5) sacrifice birds at various intervals post infection to collect tissue samples for host physiological and genetic evaluation, and 6) statistically evaluate the relationship between viral load and target host factors.

Avian Influenza Virus, Ducks, and Transmission

Avian influenza viruses (AIV) are influenza A viruses belonging to the family of orthomyxoviruses (Suarez 2009). They are negative-sense RNA viruses with eight different gene segments that code for at least ten viral proteins. These viruses are classified by their surface proteins hemagglutinin (HA) and neuraminidase (NA) of which there are 16 antigenically different HA and nine NA serotypes (excluding bat influenza A-like viruses; (Krammer et al. 2018). Avian influenza viruses are also classified by their pathogenicity in poultry. Low-path avian influenza viruses (LPAIV) have low morbidity and mortality rates in domestic poultry, while high-path avian influenza viruses (HPAIV) have high rates of morbidity and mortality in poultry (Hooper and Selleck 2003). HPAIV serotypes of H5 and H7 have caused significant mortality in humans (Kalthoff, Globig, and Beer 2010). There is evidence to support that HPAIV serotypes evolved from LPAIVs circulating in wild waterfowl (Van der Goot et al. 2003; Lee et al. 2017). LPAIVs in wild waterfowl are transmitted via the fecal-oral route and replicate in the

intestines and bursa of Fabricius (Franca, Stallknecht, et al. 2012; Webster et al. 1978) of wild waterfowl. Based on previous knowledge concerning the transmission and replication of LPAIV, we hypothesized that physiological, immunogenic, and genetic host factors would be associated with intraspecific variation in LPAIV-infected mallards and blue-winged teals.

Super-shedding in LPAIV-infected Mallards and Blue-winged Teals

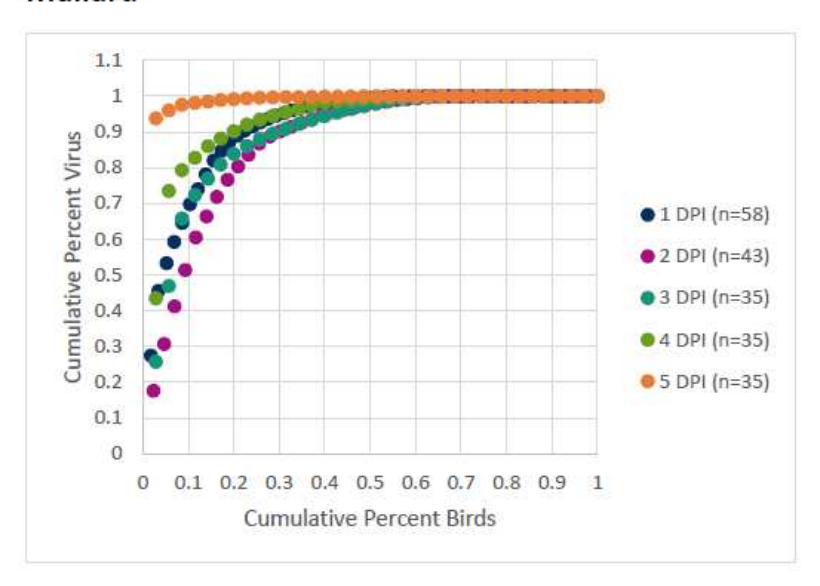
Currently, no study has been conducted to identify a super-shedder threshold for LPAIV-infected ducks or to determine if super-shedding could be used as a potential method of controlling the spread of LPAIV between wild ducks or to domestic poultry. Since LPAIV is transmitted via the fecal-oral route, similar to *E. coli* transmission in cattle, reason would suggest that super-shedders are also important in LPAIV transmission dynamics, similar to what has been demonstrated in *E. coli*-infected cattle (Matthews, McKendrick, et al. 2006). Although a viral shedding threshold for LPAIV-infected ducks is not yet determined, because mallards shed LPAIV according to the Pareto Principle (Jankowski et al. 2013), we hypothesized that the mallards and blue-winged teals in our study will also shed LPAIV according to the Pareto Principle where 20% of the birds are responsible for 80% of the overall virus shed. Thus, we predicted that the top 20% of viral shedders are super-shedders and are physiologically and genetically different from the rest of non-super-shedders.

We collected virus titer data from LPAIV-infected mallards and blue-winged teals according to methods detailed in Dolinski et. al (2020). In support of our hypothesis, both mallards and blue-winged teals shed LPAIV with variation according to the pareto principle (Figure 1.1). Mallards on one to four days post infection had proportional distributions where 10-25% of the birds were shedding 80% of overall virus shed. One individual in our study shed over 90% of virus shed on five days post infection (DPI); however, this observation was only

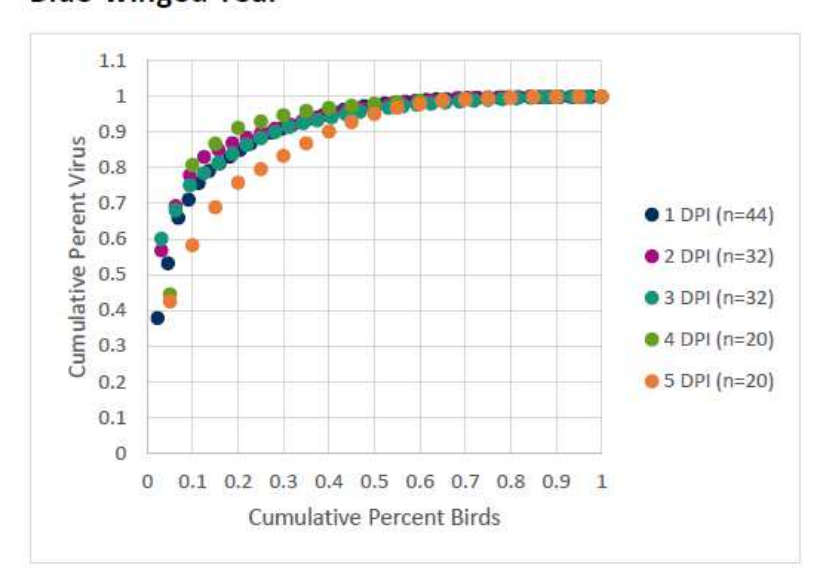
observed on five DPI. Blue-winged teals shed LPAIV with similar variation, with 10-25% of birds shedding 80% of overall virus shed. These results are consistent with previous findings (Jankowski et al. 2013).

Figure 1.1: Cumulative percent graphs for LPAIV-infected mallards and blue-winged teals. The x-axis represents the percentage of the total number of birds, and the y-axis represents the percentage of total virus detected in cloacal swabs. Each dot represents an individual's additive contribution to the overall virus shed on each day post infection (DPI). n = number of individuals.

Mallard



Blue-winged Teal



In this dissertation, we explored the relationship between intrinsic factors and viral load to identify which factors are associated with LPAIV super-shedding. Chapter two evaluates $\alpha 2,3$ sialic acid receptors (SA $\alpha 2,3$ Gal), the viral receptor required for LPAIV cell entry (Ito et al. 2000), in both mallards and blue-winged teals to determine if viral receptors are associated with viral shedding. Chapters three and four evaluates gene expression of LPAIV-infected mallards and blue-winged teals, respectively, to determine the genetic factors and immune response are associated with super-shedders. Chapter five synthesizes the work from chapters one, two, and three to highlight the major findings and provide suggestions for future research. The results of this dissertation provide new knowledge to the field of avian disease ecology as we can better understand the factors responsible for variation in LPAIV-shedding in wild ducks. Virologists, wildlife disease managers, and public health officials can use this information to better inform disease prevention strategies as well as perform future genetic studies to better understand the genetic factors involved in LPAIV replication.

CHAPTER 2: THE ASSOCIATION BETWEEN SAα2,3GAL OCCURRENCE FREQUENCY AND AVIAN INFLUENZA VIRAL LOAD IN MALLARDS (ANAS PLATYRHYNCHOS) AND BLUE-WINGED TEALS (SPATULA DISCORS)

Dolinski, Amanda, Mark Jankowski, Jeanne Fair, and Jennifer Owen. 2020. "The Association Between SAα2,3Gal Occurrence Frequency and Avian Influenza Viral Load in Mallards (Anas Platyrhynchos) and Blue-Winged Teals (Spatula Discors)." *BMC Veterinary Research* 16(430): 1–17.

Abstract

Individual heterogeneity in pathogen load can affect disease transmission dynamics; therefore, identifying intrinsic factors responsible for variation in pathogen load is necessary for determining which individuals are prone to be most infectious. Because low pathogenic avian influenza viruses (LPAIV) preferentially bind to alpha-2,3 sialic acid receptors (SAα2,3Gal) in the intestines and bursa of Fabricius in wild ducks (Anas and Spatula spp.), we investigated juvenile mallards (Anas platyrhyncos) and blue-winged teals (Anas discors) orally inoculated with A/northern pintail/California/44221-761/2006 (H5N9) and the virus titer relationship to occurrence frequency of SAα2,3Gal in the intestines and bursa. To test the natural variation of free-ranging duck populations, birds were hatched and raised in captivity from eggs collected from nests of free-ranging birds in North Dakota, USA. Data generated from qPCR were used to quantify virus titers in cloacal swabs, ileum tissue, and bursa of Fabricius tissue, and lectin histochemistry was used to quantify the occurrence frequency of SAα2,3Gal. Linear mixed models were used to analyze infection status, species, and sex-based differences. Multiple linear regression was used to analyze the relationship between virus titer and SAα2,3Gal occurrence frequency. In mallards, we found high individual variation in virus titers significantly related to high variation of $SA\alpha 2$, 3Gal in the ileum. In contrast to mallards, individual variation in teals was minimal and significant relationships between virus titers and SAα2,3Gal were not determined. Collectively, teals had both higher virus titers and a higher occurrence frequency of

 $SA\alpha2,3Gal$ compared to mallards, which may indicate a positive association between viral load and $SA\alpha2,3Gal$. Statistically significant differences were observed between infected and control birds indicating that LPAIV infection may influence the occurrence frequency of $SA\alpha2,3Gal$, or vice versa, but only in specific tissues. The results of this study provide quantitative evidence that $SA\alpha2,3Gal$ abundance is related to LPAIV titers; thus, $SA\alpha2,3Gal$ should be considered a potential intrinsic factor influencing variation in LPAIV load.

Introduction

Wild waterfowl are the natural reservoir for avian influenza viruses (AIV) and a source of infection for domestic poultry (Halvorson et al. 1983; Halvorson 2008; Stallknecht and Shane 1988). Highly pathogenic avian influenza virus (HPAIV), which causes devastating impacts to poultry worldwide with some strains fatal to humans, originates from strains of low pathogenic avian influenza virus (LPAIV) circulating in wild ducks (Röhm et al. 1995). LPAIV is transmitted most efficiently via the fecal-oral route (Mamlouk et al. 2011) and transmitted to poultry via direct contact, contaminated fomites, or contaminated water sources (Koch and Elbers 2006); hence, understanding the wild waterfowl host factors responsible for the dissemination of AIV is crucial for improving disease management.

Individual heterogeneity in infectiousness is considered to be a driving force in the development of infectious disease epidemics (Woolhouse et al. 1996), with high shedding individuals thought to be key in enhancing outbreak intensity (Lloyd-Smith et al. 2005; Matthews, McKendrick, et al. 2006). Birds infected with RNA viruses, including LPAIV-infected mallards (*Anas platyrhynchos*), are observed to shed virus with high heterogeneity, where 20% of the birds shed 80% of the total virus shed by all birds (Jankowski et al. 2013).

While this pattern in infectiousness has been observed and hypothesized to contribute to the dynamics of disease transmission, we know little about what drives this variation.

The intestines and bursa of Fabricius are important sites for LPAIV replication in wild waterfowl (Daoust et al. 2011; Franca, Stallknecht, et al. 2012; Webster et al. 1978). Most LPAIVs circulating in waterfowl preferentially bind to glycans tipped with sialic acid bound to galactose (Gal) in an α-2,3 position (SAα2,3Gal) (Gambaryan et al. 2005; Ito et al. 2000). These receptors found on epithelial cells are throughout the bird's respiratory tract, intestinal tract (Costa et al. 2012; Franca, Stallknecht, and Howerth 2013; Kimble, Nieto, and Perez 2010), and bursa of Fabricius (Franca, Stallknecht, et al. 2012). In birds, the nucleoprotein antigen for LPAIV has most frequently been detected in the intestines and bursa (Daoust et al. 2011; Franca, Stallknecht, et al. 2012; Wille et al. 2014). Additionally, LPAIV-infected birds have more virus isolated from cloacal swab samples than oropharyngeal swabs (Ellstrom et al. 2008). Therefore, the distribution and abundance of these receptors in avian intestines and bursa are likely to determine the host's susceptibility to infection and the virus's ability to replicate.

Similar to the observation of individual heterogeneity in mallard viral load, variation in sialic acid receptor expression has also been observed. In 76 avian species assessed, 20% of them expressed 80% of the sialic acid receptors observed on erythrocytes in all species (Jankowski et al. 2019). Similarly, 20% of 340 birds expressed 80% of the sialic acid receptors expressed on erythrocytes in all birds assessed (Jankowski et al. 2019). Individual variation of $SA\alpha 2,3Gal$ expression in mallard intestines has been observed with some individuals having lower expression of $SA\alpha 2,3Gal$ in the ileum, cecum, colon, and bursa compared to other individuals (Franca, Stallknecht, et al. 2012). Differences in the distribution and intensity of $SA\alpha 2,3Gal$ between wild bird species have also been observed, such as red head ducks (*Aythya Americana*),

black swans (*Cygnus atratus*), and northern pintails (*Anas acuta*) having limited $SA\alpha2,3Gal$ expression in the duodenum and jejunum compared to other Anseriformes (Franca, Stallknecht, and Howerth 2013). Variation was also found within species, such as mallards, based on the lectin used, *Maackia amurensis* I (MAL I) vs. *Maackia amurensis* II (MAL II) (Franca, Stallknecht, and Howerth 2013). While previous literature suggests there is variation in $SA\alpha2,3Gal$ abundance and distribution within and across species, the occurrence frequency of $SA\alpha2,3Gal$ in the intestines and bursa has yet to be statistically quantified and related to LPAIV load, a first step in understanding this potential source of AIV variability across individuals and species.

In this study, we address this knowledge gap by investigating the relationship between SAα2,3Gal and LPAIV load in mallards and blue-winged teals (*Spatula discors*, hereafter referred to as "teal"). Both species are important hosts for LPAIV. The mallard is important because of their worldwide distribution, their periodomesticity, and the large diversity of AIV strains isolated from them, including highly pathogenic strains causing high mortality in poultry and people (Munster et al. 2005; Stallknecht and Shane 1988; Takekawa et al. 2010). Teals have high infection prevalence (Papp et al. 2017) and an important role in over-wintering the virus in the southern United States (Ferro et al. 2010; Stallknecht et al. 1990).

We hypothesized that a higher occurrence frequency of $SA\alpha 2,3Gal$ in mallards and teals corresponds with higher LPAIV titers. Additionally, we hypothesized that the relationship between virus titers in cloacal swab, ileum tissue, and bursa tissue would all be positively related to each other. Sex-based differences, species-based differences, and comparisons in the occurrence frequency of $SA\alpha 2,3Gal$ between control and infected birds was also analyzed, where

we did not expect to see differences. This research provides a first look into this putative intrinsic factor responsible for LPAIV individual variation in mallards and blue-winged teals.

Methods

Permits and Protocols

Protocols for animal care and experimental sampling procedures were approved by Michigan State University (MSU) Institutional Animal Care and Use Committee (AUF 12/16-211-00). All euthanasia procedures were in accordance with the Animal Welfare Act and Guidelines to the Use of Wild Birds in Research (Fair, Paul, and Jones 2010). Duck eggs were collected with permission from the U.S. Fish and Wildlife Permit (M Bl 94270-2) and North Dakota Game and Fish Department License #GNF03639403.

Study Species and Locations

Mallards and teals used for this study were collected as eggs from the nests of wild birds in the southwest corner of Towner County, North Dakota, USA (48.4431853, -99.3156225). In May - June 2015 we collected 90 mallard eggs (1 – 2 per nest) from a total of 50 nests, with each nest containing an average of eight eggs per clutch. The following summer, May – June 2016 we collected 80 blue-winged teal eggs (1 – 2 per nest) from a total of 40 nests. Nests were found and eggs collected by dragging a heavy metal-link chain behind two ATVs driving in parallel which initiated hens to fly off their nest (Higgins, Kirsch, and Ball Jr. 1969). Eggs were candled in field to determine age, and any eggs that either had not started incubation or were between 15 and 22 days of incubation were shipped overnight to MSU in East Lansing, Michigan. Each year we made 2 – 4 shipments of 15 to 40 eggs each over a period of 6 weeks. Unless specified otherwise, all procedures were the same for each species/year.

Upon arrival at MSU, eggs were immediately placed into a climate-controlled egg incubator (Sportsman 1502 Egg Incubator, GQF Manufacturing Co., Savannah, GA) housed within a biosafety level two room within the MSU Research Confinement Facility. Eggs were incubated at 37.5°C with 45-50% humidity and rotated electronically ten times per day. Eggs were candled for viability and age once every three days. As soon as eggs pipped, they were moved into a hatching incubator (Sportsman 1502 Egg Incubator, GQF Manufacturing Co., Savannah, GA) at 37.2°C with 70-80% humidity. Chicks remained in the hatcher until they were dry, approximately 12-24 hours post hatching. Each bird was then weighed to the nearest 0.1g, banded with a uniquely numbered plastic leg band, and placed in a brooder (30 - 35 °C). Birds were kept in brooders for two weeks, then moved to open-room housing where a maximum of 35 birds were housed per room (400sq feet). Each room maintained a temperature of 23°C and 45-55% humidity, had two swimming pools (45" diameter, 10" depth), and two dry pools with aspen chip bedding. In both years, birds were maintained on a 13:11hr light:dark photoperiod.

Birds were fed ad libitum Purina® Flock Raiser® Crumbles (Purina, St. Louis, MO, USA) and supplemented with chopped dandelion greens twice per day. Rooms were fully cleaned twice per day. Birds were routinely checked for normal health and weighed every five days. One week prior to inoculation, mallards were separated into individual cages of 20 cages per room. Blue-winged teals were kept in the open room housing separated by experimental group.

Virus

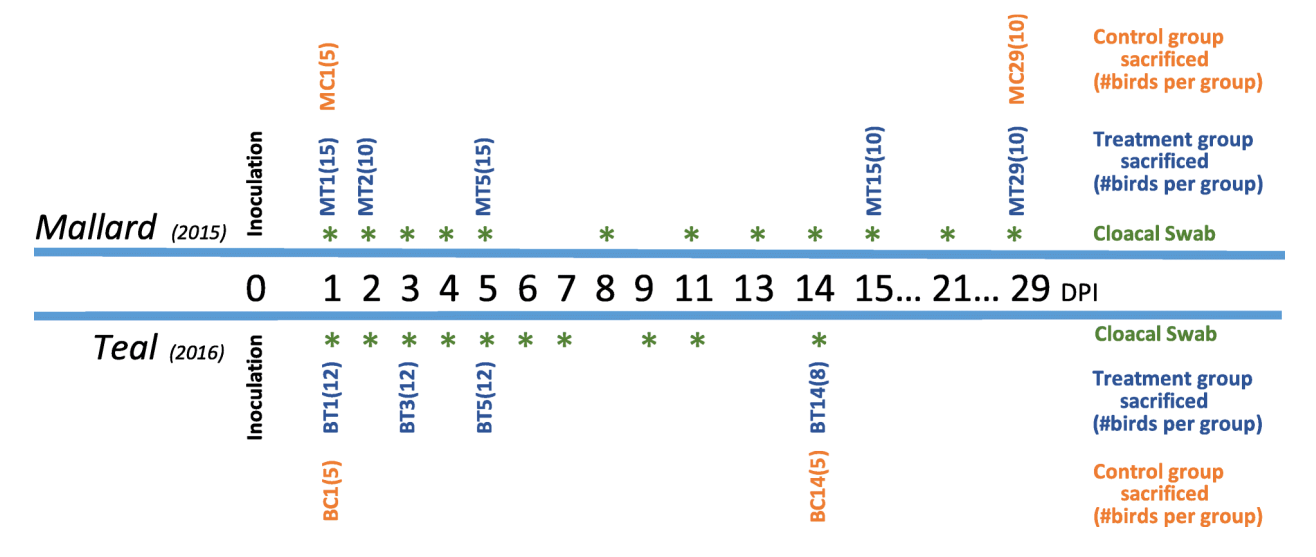
LPAIV A/northern pintail/California/44221-761/2006 (H5N9), originally collected from a northern pintail cloacal swab and isolated in specific pathogen free embryonated chicken eggs (ECE), was acquired from the USGS National Wildlife Health Center in Madison, WI (USDA)

Veterinary Permit 44372). We prepared stock virus propagating the virus in 9 to 11-day old ECE (Charles River, Norwich, CT, USA) (Woolcock 2008). The infectious titer of the stock virus of 7.63 log EID₅₀/ml was determined using the 50% egg infectious dose (EID₅₀) and calculated using the Reed & Muench method (Reed and Muench 1938). The viral inoculum was prepared by diluting the stock virus in Dulbecco's Modified Eagle Medium (DMEM) (Gibco® by Life Technologies, Grand Island, NY, USA) to yield a final titer of 5.63 log EID₅₀/ml.

Experimental Design

Individual birds were assigned to one of two control groups for each species, one of five mallard LPAIV treatment groups, or one of four teal LPAIV treatment groups (Figure 2.1). Experimental group assignment was done using pseudo-stratified randomization with birds being stratified by body mass, age, and sex. Additionally, individuals from the same nests were assigned to separate groups. Group names refer to their species (mallard = M, teal = B), whether they received LPAIV treatment (inoculated with virus= T, control = C), and the DPI they were sacrificed (# to follow T/C). The minimum sample size per group was based on individual viral load variation observed in populations as small as ten individuals (Jankowski et al. 2013). Additional birds were placed in groups on DPI of most importance such as high viral shedding (DPI 1-3) and early detection of antibody titer (DPI 5) (Jourdain et al. 2010).

Figure 2.1: Timeline of Sample Collection for Mallards and Blue-winged Teals. Experimental groups are designated by species (M = mallard, B = blue-winged teal), infection status (T = LPAIV treatment/inoculation with LPAIV H5N9, C = control/sham-inoculated), and day post infection (DPI) the group of birds was sacrificed. Two mm sections of bursa of Fabricius tissue and ileum tissue were collected from each bird on the DPI of sacrifice. Cloacal swabs were collected from all living birds at each DPI designated by an asterisk.



All LPAIV treatment group birds (also referred to as "LPAIV-infected") were inoculated with 1.0 mL of 5.63 log EID₅₀/ml viral inoculum on zero DPI, diluted in DMEM by placing one drop on each eye and each nare, then dispensing the rest in the esophagus (Cardona et al. 2014; Franca, Poulson, et al. 2012). All control birds were sham-inoculated with 1.0 mL of sterile DMEM in a similar fashion. During the inoculation and after inoculation, birds were kept in biosafety level two conditions and personal protective equipment consisted of non-vented, full coverage eye goggles, hair cap, N95 respirator, double gloves, tyvek suit, and plastic booties.

We collected cloacal swabs on all live individuals. Cotton tipped swabs were collected from mallards on 1-5, 8, 11, 13, 15, 17, 19, 22, 24, 26, and 29 DPI, and from teals on 1-7, 9, 11, and 14 DPI (Figure 2.1). Swabs were stored in 3.0mL of brain-heart infusion broth (BHI), transported on ice, and stored in -80°C until sample processing.

Euthanasia

Mallards, as described by their assigned groups, were sacrificed on 1, 2, 5, 15, and 29 DPI, and teals were sacrificed on 1, 3, 5, and 14 DPI (Figure 2.1). Mallards sacrificed on one DPI were euthanized by intravenous lethal injection of pentobarbital sodium and phenytoin sodium solution (Beuthanasia-D Special, Merck Animal Health, Madison, NJ, USA). All other birds were euthanized by carbon dioxide inhalation. Bird carcasses were preserved on ice until necropsy was performed.

Necropsy and Tissue Collection

Mallard necropsy was performed in the same room where birds were kept under biosafety level two conditions mentioned above. Teal necropsies were performed under a biosafety cabinet. Necropsies were performed on mallards within one to six hours of being euthanized, with an average time of approximately four hours post euthanasia. Due to autolysis of tissue samples observed with mallards, we performed necropsies on teals within one hour of being euthanized, with the average time of 22 minutes post euthanasia. We examined birds for any abnormalities and the coelomic cavity for any gross pathology. We also assessed the birds' body condition using a scale of one to five: one being emaciated and five being over-conditioned with presence of fat in intestinal mesentery. Sex was determined by examining the syrinx (Mohamed 2017).

We collected 0.5 to 2 cm sections of intestine (duodenum, jejunum, ileum, cecum, colon) and bursa of Fabricius in 10% buffered formalin. The tissues were incubated at room temperature for 24-48 hours to allow time for fixation, then transferred to a histological sectioning cassette in 70% ethanol and embedded in paraffin within 24 hours. We also collected 2 mm sections of ileum and bursa in RNA stabilizing solution (RNAlater®, Sigma-Aldrich, St. Louis, MO, USA) for viral RNA analysis in these tissues.

Viral RNA Isolation and qPCR

Virus in cloacal swabs, ileum tissue, and bursa tissue was quantified by isolating viral RNA using qPCR targeting the matrix protein gene (Spackman and Suarez 2008). Unlike immunohistochemistry which stains for nucleoprotein antigen, qPCR is quantitative and can detect lower quantities of virus (Ward et al. 2004). Viral RNA was isolated from cloacal swab material using the MagMAXTM-96 AI/ND Viral RNA Isolation Kit (Applied Biosystems® by Thermo Fisher Scientific, Vilnius, Lithuania) with modifications to the manufacturer protocol previously described (Das et al. 2009b). Viral RNA was extracted with host mRNA from 15-30mg of ileum and bursa tissue from each bird using the Qiagen RNeasy Mini Kit (QIAGEN®, Hilden, Germany) according to the manufacturer's protocol. For the RT-PCR working solution we used the TaqMan® RNA-to-CtTM 1-Step Kit (Applied Biosystems® by Thermo Fisher Scientific, Foster City, CA, USA), primer 5'-AGATGAGTCTTCTAACCGTCTCTG (Sigma-Aldrich, St. Louis, MO, USA), probe 5'-[6FAM]TCAGGCCCCTCAAAGCCGA[BHQ1] (Sigma-Aldrich, St. Louis, MO, USA), and 2µL of sample RNA for a final well volume of 10µL. Each sample was processed at least three times on a 384 well plate with a minimum of three negative control wells and three positive control wells. We used LPAIV H5N9 stock virus in a 10-fold dilution on each plate in three replicates to create a reference standard curve. Ct values less than 40 were considered positive for virus. Using QuantStudio™ 6 and 7 Flex Real-Time PCR Software System v1.3, we calculated the standard curve, which was used to estimate virus quantity of each sample by correlating Ct values to 50% egg infectious dose per milliliter (EID₅₀/mL). The reported limit of detection is 0.1 EID₅₀ (Spackman et al. 2002); therefore, any samples with undetectable viral RNA were considered negative and assumed to be 0.00

EID₅₀/mL. Virus quantity for each sample was averaged across sample replicates. Failed wells and suspected contaminated wells were removed from final calculations.

The quantification limit of the stock virus 10-fold dilution was approximately 400 EID₅₀; however, 21% of our samples were detected to have positive virus between this threshold and 0.1 EID₅₀. To validate the stability of our statistical analysis, multiple value random imputation (Pleil 2016) was used for any sample with positive virus between 0.1 and 400 EID₅₀, and statistical analysis was repeated. Methods and results of this validation technique are outlined in Dolinski et. al (2020).

Lectin Histochemistry

We used lectin histochemistry to detect SAα2,3Gal in formalin fixed and paraffin embedded tissues of the intestines and bursa of Fabricius of each bird. *Maackia amurensis* I (MAL I) agglutinin is a plant lectin which binds specifically to Siaα2-3Galβ1-4Glc(NAc) (Geisler and Jarvis 2011; Knibbs et al. 1991) and has been used in multiple receptor distribution studies in ducks and other influenza hosts (Pillai and Lee 2010; Yu et al. 2011) to detect SAα2,3Gal. MAL II, which specifically binds Siaα2-3Galβ1-3 (Neu5Acα2-6)GalNAc (Geisler and Jarvis 2011), is another lectin commonly used in place of, or in conjunction with MAL I (Costa et al. 2012; Franca, Stallknecht, et al. 2012; Franca, Stallknecht, and Howerth 2013; Kuchipudi et al. 2009). Trial protocols were tested to determine the proper concentration of each lectin needed for proper binding and visual staining of SAα2,3Gal. The trial protocol resulted in a determined concentration for MAL I, but not MAL II; hence MAL I was the only lectin used given that H5 LPAIVs have similar affinity for the receptors targeted by each lectin (Gambaryan et al. 2006; Geisler and Jarvis 2011); furthermore, any lack of specificity for sialic acid receptors is shared by both lectins (Geisler and Jarvis 2011).

Paraffin embedded tissue (duodenum, jejunum, ileum, cecum, colon, and bursa of Fabricius) from each bird was sectioned and stained with biotinylated lectin MAL I (Vector Laboratories, Burlingame, CA, USA), using previous described methods (Costa et al. 2012; Pillai and Lee 2010) with minor modifications. Paraffin embedded tissue sections were deparaffinized and processed with the EnVision FLEX Target Retrieval Solution, Low pH kit wash buffers, blocking agents, and DAB plus chromogen working solution (Agilent, Dako Omnis, Santa Clara, CA, USA). Tissue sections were first treated with 100μL of 3% Peroxide Block, then Avidin/Biotin blocking agent (Agilent, Dako Omnis, Santa Clara, CA, USA), and protein blocking. The tissue sections were incubated in 100μL of MAL I for 32 minutes, and then treated for 20 minutes in 100μL of streptavidin peroxidase (Agilent, Dako Omnis, Santa Clara, CA, USA). The working solution (200μL) was applied and tissue sections were finally counter stained with 100μL of hematoxylin (Gill's III, 1:10 dilution) (Astral Diagnostics Incorporated, West Deptford, New Jersey, USA). All tissue sections stained in the same batch were also stained with a known positive control of duck (*Anas platyrhynchos domesticus*) tissue.

We assessed the abundance of SAα2,3Gal in the proximal intestine (combined duodenum and jejunum), ileum, cecum, colon, and bursa of Fabricius by estimating occurrence frequency of lectin stained cells. We estimated the percentage of lectin stained cells per 5mm sections of tissue and cell type via an ordinal visual scoring method commonly used in histochemistry (Meyerholz and Beck 2018), which we called "lectin score." Using brightfield microscopy (400x), we looked specifically at the bursa epithelial cells, and three cell types in each intestinal tissue: the brush border, villi enterocytes, and crypt enterocytes. We scored as many fields of view (FOV) as possible with a maximum of 10 FOVs per cell type in each tissue. Each FOV received a score based on the estimated percentage of cells stained in that FOV. A score of zero

indicated that no cells were stained in that field of view. A score of 5 indicated that 1-10% of cells were stained. A score of 35 indicated that 11-60% of cells were stained. A score of 80 indicated that 61-100% of cells were stained. The scores for the FOVs were averaged to obtain a single score for each tissue and cell type, providing 13 separate lectin scores per bird. All samples were scored by the same individual (AD) to eliminate inter-observer error. In some cases, the tissue had become autolyzed and could not be scored, which was more common for the ileum and bursa tissues in mallards possibly due to longer processing times compared to teals.

Since the scoring method used to quantify the frequency of SA α 2,3Gal was based off four categories of scores compared to a quantitative continuous scale, we validated our scoring method with the absolute counts of stained cells for 20 randomly selected birds from mallard groups MT1, MT2, and MT5. For each tissue, a single observer (AD) counted the number of stained cells out of 500 cells for each cell type of the ileum and colon, then calculated the percentage. With a total of 108 counts for 20 birds, we found high agreement between our scoring method and the absolute counts ($R^2 = 0.79$, p <0.001).

Statistical Analysis

Statistical software R version 3.4.4 (Team 2013) was used for all statistical analyses. P-values of less than 0.05 were considered statistically significant and assumptions of normality were met by Log₁₀(value + 1) transforming all virus titer and lectin histochemistry data. These methods were performed for both mallards and teals unless otherwise indicated. All analyses only included virus titer data collected on one to five DPI, when the majority of virus was shed.

For birds sacrificed during the first five DPI, we used simple linear regression to analyze the relationship between virus titers in the cloacal swab, ileum tissue, and bursa tissue, since all three of these variables were collected at the time the bird was sacrificed. Only the cloacal swab

collected on the day the bird was sacrificed was used in this analysis. Six total comparisons were evaluated, three for each species (swab vs. ileum, swab vs. bursa, ileum vs. bursa). In each comparison, the effect of DPI was also evaluated.

A repeated measures, linear mixed effects model (Searle and McCulloch 2001) was used to test for differences in virus titer or lectin score between species, between sexes, and between control and infected birds (lectin score only). To account for repeated measures of individuals birds, each model was adjusted with a random intercept for each bird. Additionally, when variances of virus titer were different between the factors of the main effects, the model was adjusted to allow for unequal variances. Differences in variance were detected using the Fligner-Killeen test (Conover, Johnson, and Johnson 1981). ANOVA tables were visualized, and the post-hoc Tukey's test was used to assess pairwise differences.

To analyze the effect of species on virus titer, species, DPI, and the species*DPI interaction were included in the model. To analyze the effect of sex on virus titer, we assembled two separate models: one for mallards and one for teals. Sex and DPI, plus their interaction, were included in each model.

To analyze the effect of lectin score on infection status (infected vs. control), mallards and teals were assessed in two separate models. For each species, infection status and tissue/cell-type, plus their interaction, were included in their respective model.

Using data from infected birds only, we also assessed species and sex-based differences in lectin score. To analyze the effect of species on lectin score, species, tissue/cell type, and their interaction, were included in the model. To analyze the effect of sex on lectin score, mallards and teals were analyzed in separate models. Sex and tissue/cell type, plus their interaction, were included in each model.

We also looked at lectin score correlations between cell types within intestinal tissue type using Pearson's r coefficient. We considered cell types within a tissue type (proximal, ileum, cecum, colon) with a coefficient of 0.8 or higher to indicate a strong correlation. If all three cell types within a tissue were highly correlated, we used PCA to reduce the data into one component variable we called "[tissue type] PC." Each PC variable accounted for greater than 80% of the variation between the cell types of that particular tissue. PC variables generated from the PCA were used in the MLR models to determine the relationship between virus titer and lectin score.

Virus titer and lectin score relationship was determined by assessing three different MLR models for each species using virus titer as the dependent variable. The virus titer variable in the first model consisted of virus titers from cloacal swabs collected on the DPI each bird was sacrificed. The second model used virus titers in ileum tissue, and the third model used virus titers in bursa tissue. Independent variables for the cloacal swab virus titer model consisted of the lectin score variables, the principal components described above (when appropriate), and five control variables: sex, BCS, LPAIV treatment group, body mass in grams at 55 days after hatch, and inoculation age in days. Independent variables for the ileum virus titer model included only the ileum lectin score variables and the five control variables. Only the bursa epithelium lectin score variable and the five control variables were included in the bursa virus titer model.

To determine the best fitting MLR model for each dependent variable, we followed a consistent procedure. Global linear models were tested for each dependent variable separately. To select parsimonious model fits to the data, we used stepwise variable selection based on the generalized Akaike's Information Criterion (AIC). We then used variance inflation factor (VIF) scores to identify problematic co-linear predictors from the stepwise-chosen models. Independent variables with VIFs > 3.0 were determined problematic and were removed from the

model one at a time until all VIFs < 3.0 (Zuur, Ieno, and Elphick 2010). When two VIFs were > 3.0 and < 1.0 in difference, we tested alternative models. Stepwise variable selection was used for each model to ensure the best fitting model. Residual plots were reviewed. For each of the three dependent variables, the model with both the lowest AIC, highest adjusted R², and satisfactory residual patterns (e.g., no linear or nonlinear trend in residuals, little to no heterogeneous variance in residuals, and no suspected outlier observations) was chosen as the best fitting model to the data.

Results

Distribution of Birds in Experimental Groups

Mallards (n=70) and teals (n=54) were assigned to LPAIV treatment (inoculated with LPAIV H5N9) and control groups (sham-inoculated) prior to LPAIV inoculation and sample collection (cloacal swab, ileum tissue, and bursa of Fabricius tissue; Figure 2.1). Birds in both treatment groups and control groups were assigned to smaller groups based on the day post infection (DPI) they were sacrificed. Body mass (mallard: range = 640 to 1020g, mean = 849g; teal: range = 285 to 473g, mean = 362g), age (mallard: range = 60 to 120 days, mean = 87 days; teal: range = 64 to 86 days, mean = 76), and sex (mallard: male = 34, female = 36; teal: male = 26, female = 28) were equally distributed across experimental groups.

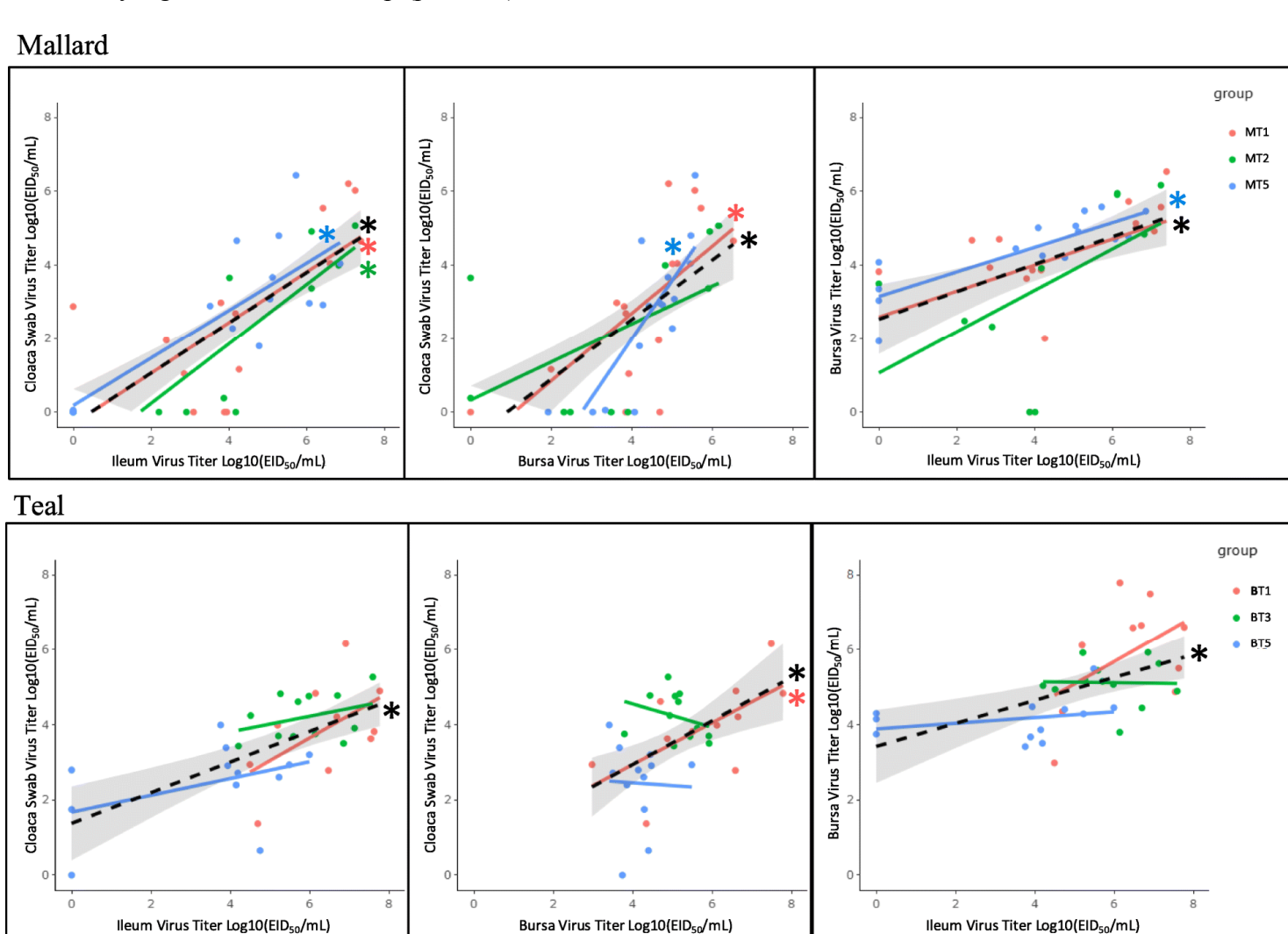
Viral Infection of Mallards and Teals

All birds inoculated with LPAIV H5N9 (mallard=60, teal=44) were infected as demonstrated by detection of LPAIV RNA (qPCR Ct values <40) in cloacal swabs, ileum tissue, and/or bursa tissue collected during the first five DPI. No birds shed virus past 15 DPI, and of the birds that survived to 15 DPI, 99.9 (mallard) and 98.5 (teal) percent of the total virus shed by those birds

occurred in the first five DPI. As expected with LPAIV, we observed no clinical signs of disease such as ruffled feathers, lethargy, respiratory distress, or any pathology.

Statistically significant (p < 0.05) positive linear relationships were observed between virus titers in cloacal swabs collected at DPI of sacrifice, ileum tissue, and bursa tissue for mallard LPAIV treatment groups MT1, MT2, MT5 and teal LPAIV treatment groups BT1, BT3, BT5 (Figure 2.2). In mallards, statistically significant positive relationships were observed between ileum virus titers and cloacal swab virus titers for all LPAIV treatment groups (MT1, slope parameter estimate (Est.) = 0.69, $R^2 = 0.43$, p = 0.005; MT2, Est. = 0.81, $R^2 = 0.64$, p = 0.003; and MT5, Est. = 0.65, $R^2 = 0.66$, p < 0.001). Statistically significant positive relationships were observed between bursa virus titers and cloacal swab virus titers for LPAIV treatment groups MT1 (Est. = 0.92, $R^2 = 0.41$, p = 0.006) and MT5 (Est. = 1.60, $R^2 = 0.63$, p < 0.001). Only MT5 (Est. = 0.33, $R^2 = 0.68$, p < 0.001) had a statistically significant positive relationship between ileum virus titers and bursa virus titers. In teals, the only statistically significant positive relationship for LPAIV treatment groups was observed for BT1 (Est. = 0.56, $R^2 = 0.34$, p = 0.036) between cloacal swab virus titers and bursa virus titers and bursa virus titers.

Figure 2.2: LPAIV H5N9 virus titers in the bursa, ileum, and cloacal swabs are positively related. Black trendline is the linear regression for all birds sacrificed on 1-5 days post infection (DPI) with the 95% confidence interval shaded in gray. Colored trendlines represent each treatment group: T1 represents birds sacrificed on 1 DPI, etc. Trendlines indicated with a (*) indicate a statistically significant relationship (p < 0.05).



Species and Sex-based Differences in Viral Shedding

Looking at all virus titers from cloacal swab samples collected from LPAIV treatment groups in the first five DPI, statistically significant differences were found between mallards and teals, but not between males and females within species. Mallards had statistically higher variation than teals in cloacal swab viral titers on one, two, three, and five DPI (Fligner-Killeen p < 0.05; Table 2.1, Figure 2.3). For both species, mean cloacal swab virus titers on one, two, and three DPI were statistically higher than virus titers on four and five DPI ($F_{4,242} = 17.61$, p < 0.001). Teals shed statistically more virus than mallards ($F_{1,102} = 14.60$, p < 0.001) with no interaction between species and DPI ($F_{4,242} = 0.91$, p = 0.456; Figure 2.4). No sex-based differences were observed in cloacal swab virus titers for either species (mallard: $F_{1,58} = 0.05$, p = 0.818; teal: $F_{1,42} = 2.49$, p = 0.122) with no statistically significant interaction between sex and DPI (mallard: $F_{4,138} = 0.39$, p = 0.818; teal: $F_{4,96} = 2.43$, p = 0.053; Figure 2.5).

Table 2.1: Virus titer descriptive statistics for mallard and blue-winged teal cloacal swabs. N = total sample size, DL = detection limit of 0.04 Log10(EID₅₀/mL), QL = quantification limit of 2.60 Log10(EID₅₀/mL), min + = minimum N>DL, mean is the geometric mean, and std.dev = one standard deviation. (*) signifies significantly higher titer variation for each DPI between species.

DPI	Species	N	N>DL	N>QL	min + Log10(EID ₅₀ /mL)	max Log10(EID ₅₀ /mL)	mean Log10(EID50/mL)	std.dev Log10(EID50/mL)
DPI 1	mallard	58	52	38	0.13	6.21	3.26	*1.94
	teal	44	44	41	1.37	6.16	4.06	0.99
DPI 2	mallard	43	38	28	0.38	5.2	3.11	*1.64
	teal	32	32	29	1.78	6.12	3.96	0.97
DPI 3	mallard	35	29	26	0.06	5.72	3.33	*1.90
	teal	32	32	29	0.5	6.15	4.05	0.98
DPI 4	mallard	35	29	19	0.19	5.03	2.38	1.54
	teal	20	19	15	0.98	5.04	3.08	1.16
DPI 5	mallard	35	28	18	0.05	6.43	2.29	*1.75
	teal	20	19	10	0.65	3.99	2.37	1.01

Figure 2.3: Cloacal swab virus titer boxplots for mallard and blue-winged teals infected with LPAIV H5N9. Horizontal bar within the box is the median value, solid dots indicate values falling above the upper or below the lower quartile + 1.5 times the interquartile distance. (*) indicates statistically higher variation between species for each day post infection (DPI; p < 0.05).

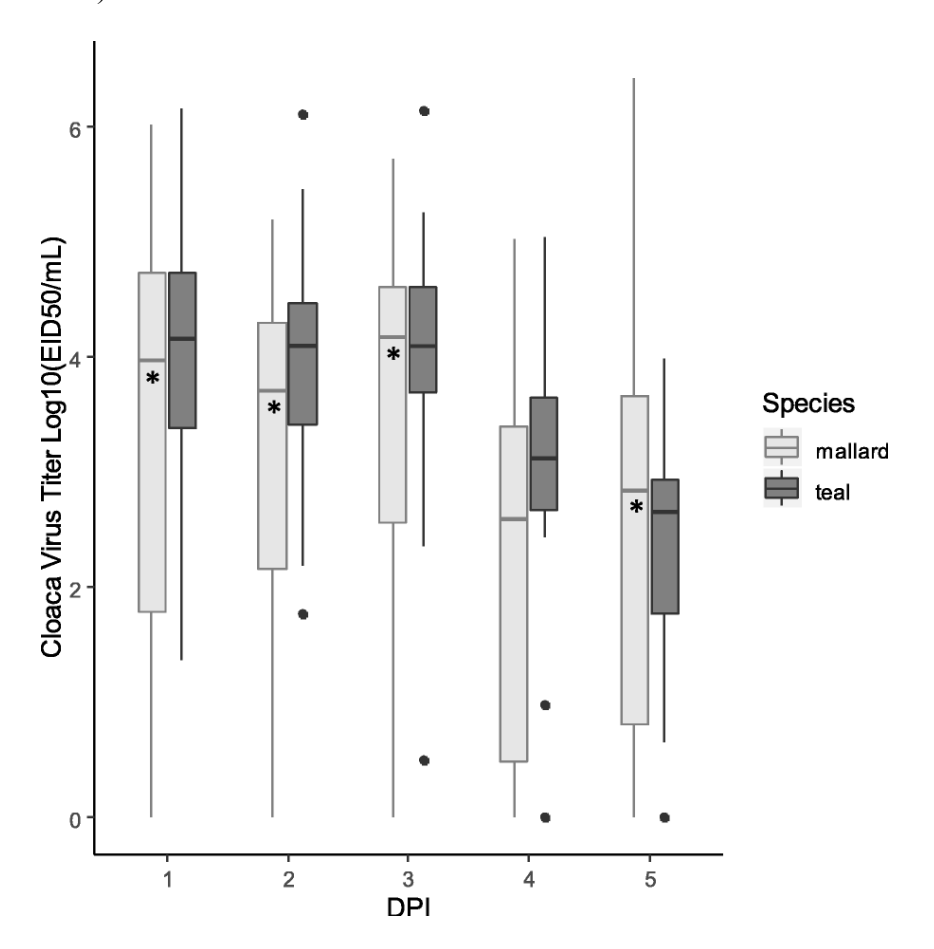


Figure 2.4: Mean virus titer \pm 95% confidence interval for (a) species, (b) days post infection (DPI), and (c) the interaction of species and DPI for mallard and blue-winged teal cloacal swab samples one to five DPI.

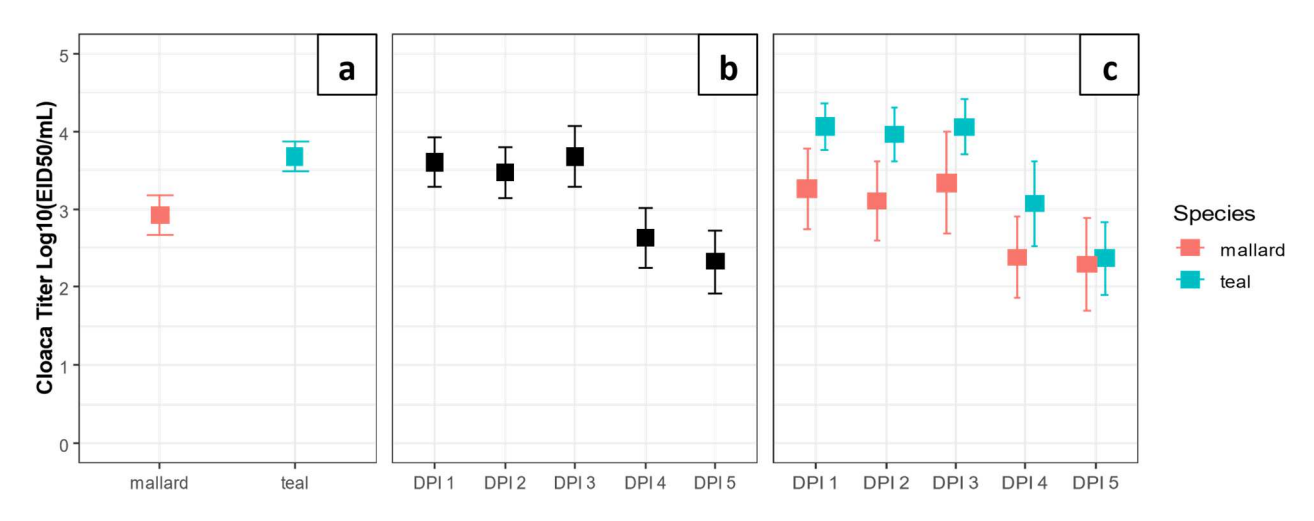
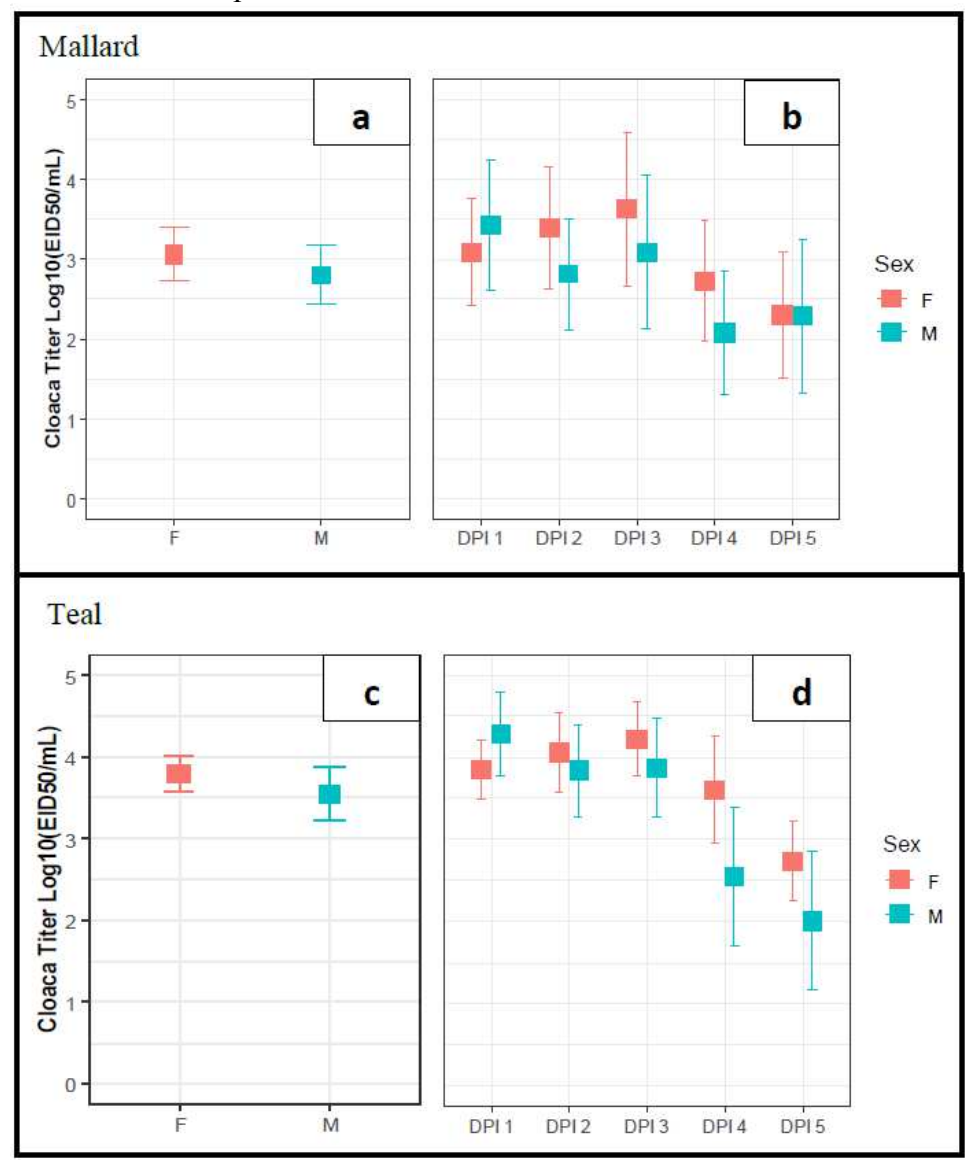


Figure 2.5: Mean virus titer +95% confidence intervals for (a,c) sex, and (b,d) the interaction of sex and days post infection (DPI) for male (M) and female (F) mallard and teal blue-winged teal cloacal swab samples one to five DPI.

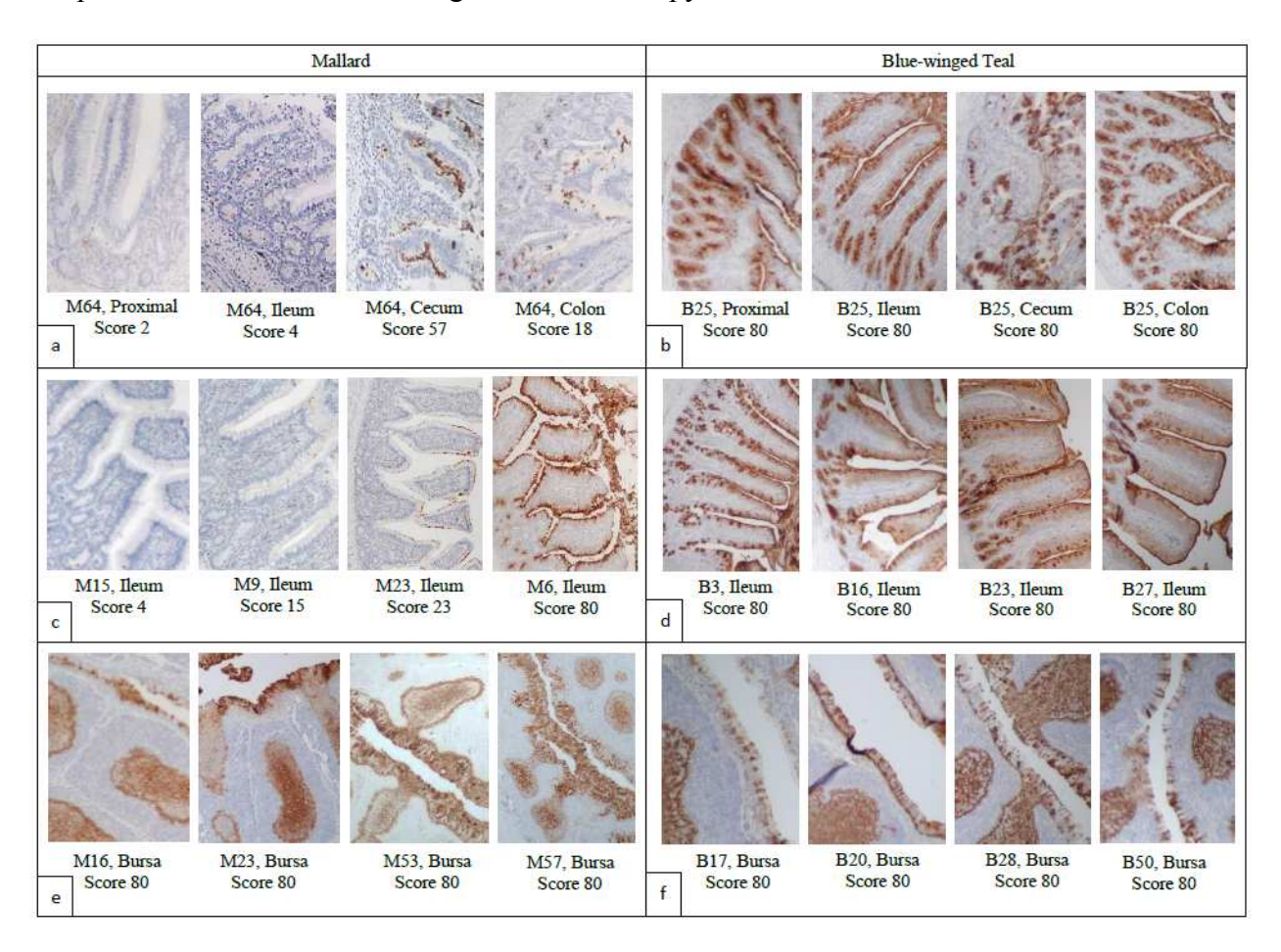


Evaluating SAa2,3Gal in Intestines and Bursa of Fabricius

Frequency of $SA\alpha 2,3Gal$ occurrence in the intestines and bursa of Fabricius was determined by visually assessing MAL I lectin stained cells and assigning a "lectin score" based on the estimated percentage of cells stained in each microscopic field of view (400x) per tissue sample. Initial observation of lectin staining in mallard intestinal tissues revealed incongruent staining of the intestinal brush border, villi enterocytes, and crypt enterocytes; therefore, these three "cell

types" of the duodenum, jejunum, ileum, cecum, and colon of each bird were assessed separately and received their own lectin score (Figure 2.6). The majority of mallard bursa epithelial cells were autolyzed, thus the lectin score for mallard bursa was not evaluated. Autolysis also affected 5.7% of intestinal tissue/cell types assessed. Any individual tissue/cell type that could not be scored was removed from analysis.

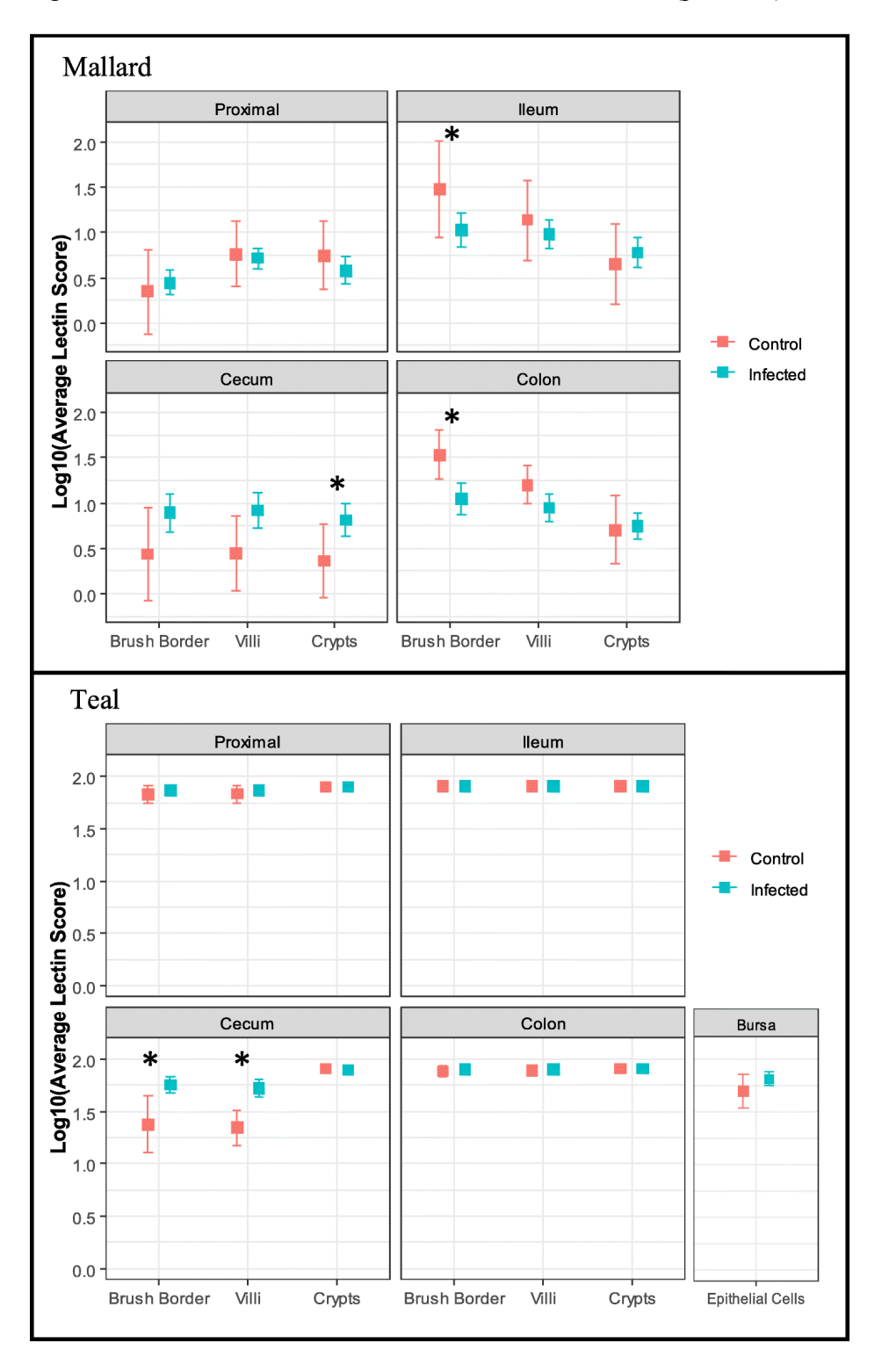
Figure 2.6: Lectin staining of mallard and blue-winged teal intestines and bursa of Fabricius. Lectin binding is positive where the brown colored stain is visible. The individual bird ID, tissue, and lectin score (villi enterocyte/epithelial cells) are given for each histological photograph. Scores were determined by averaging the scores for each field of view evaluated at 400x. Each field of view was given the following score: 0, no cells stained; 5, 1–10% of cells were stained; 35, 11–60% of cells stained; and 80, 61–100% of cells stained. Segments (a) and (b) show the range of lectin scores between sections of intestinal tissue in one individual (proximal represents duodenum or jejunum). Segments (c) and (d) show the range of lectin between individuals for the ileum tissue specifically. Segments (e) and (f) show lectin scores in the bursa of Fabricius. All photos were taken at 200x brightfield microscopy.



Lectin Score Differences Between Infected and Control Birds

Analyzing mallards and teals in two separate statistical models, lectin scores were not statistically different between LPAIV treatment and control mallards ($F_{1.68} = 0.11$, p = 0.746); however, there was a statistically significant interaction between infection status and tissue/cell type ($F_{11,693} = 4.08$, p < 0.001). We found the cecum crypt lectin score in LPAIV treatment mallards to be statistically higher than control mallards (p = 0.046; Figure 2.7). Conversely, lectin scores of control mallards' ileum brush border (p = 0.017) and colon brush border (p = 0.015) were statistically significantly higher than LPAIV treatment mallards (Figure 2.7). Unlike mallards, LPAIV treatment teals had statistically higher lectin scores than control teals ($F_{1,52} = 15.20$, p < 0.001), with a statistically significant interaction between infection status and tissue/cell type ($F_{12,611} = 8.66$, p < 0.001). Post-hoc analysis shows the lectin score in the cecum brush border (p < 0.001) and cecum villi (p < 0.001) was higher in LPAIV treatment birds than control birds (Figure 2.7).

Figure 2.7: Lectin score differences between control and LPAIV-infected birds. Mean lectin scores +95% confidence intervals of intestinal tissues proximal (duodenum and jejunum), ileum, cecum, and colon for LPAIV H5N9 infected and control mallards and blue-winged teals. Bursa epithelial cells are included for teals only. (*) indicates tissue/cell type with a statistically significant difference between control and infected birds (p < 0.05).



Species and Sex-based Differences in Lectin Score

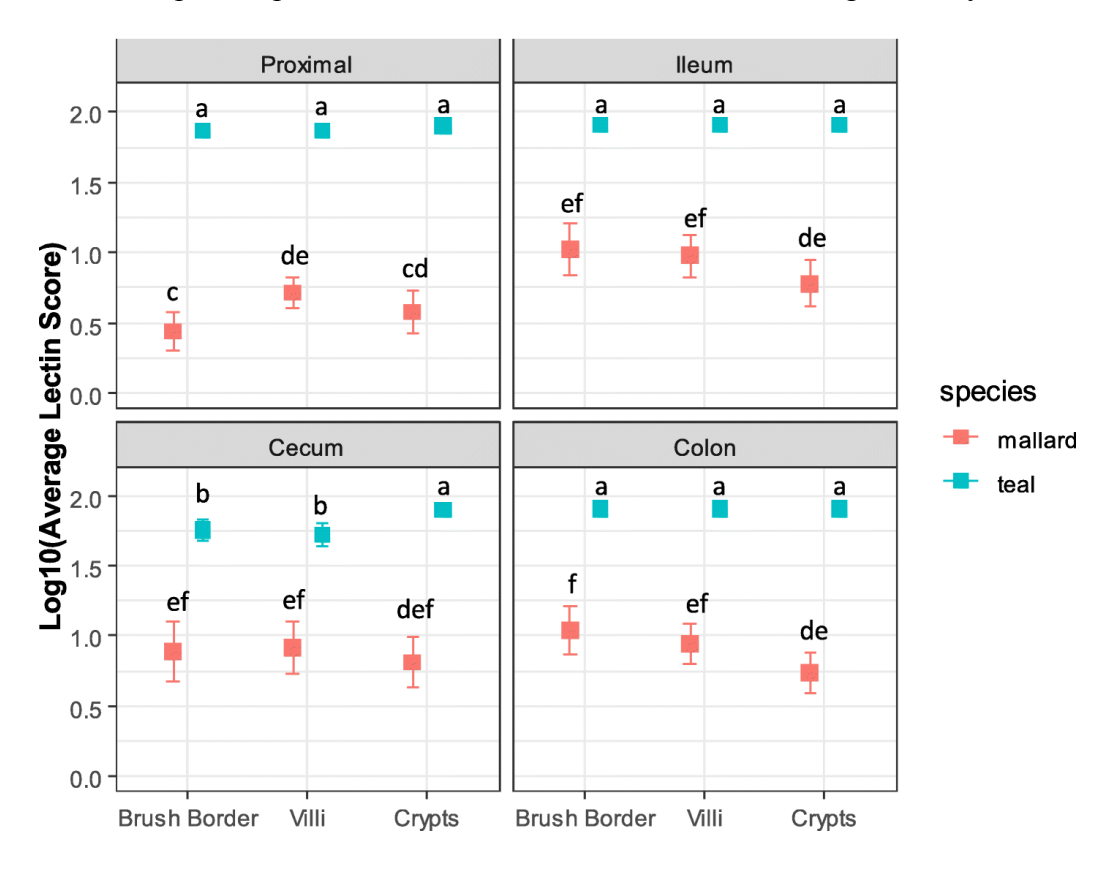
Looking at birds only in LPAIV treatment groups, higher inter-tissue and inter-individual variation was observed in mallards compared to teals for all tissue/cell types (Fligner-Killeen p < 0.001; Table 2.2).

Table 2.2: Lectin histochemistry score descriptive statistics. Proximal includes duodenum and jejunum. N = total sample size and std.dev = one standard deviation. (*) signifies significantly higher lectin score variation for each tissue/cell type between species.

Tissue	Cell Type	Species	N	min (%)	max (%)	mean (%)	std.dev (%)
		teal	44	44.25	80.00	79.19	5.39
	crypts	mallard	60	0.00	80.00	10.22	*19.92
D1	brush	teal	44	40.25	80.00	74.24	12.12
Proximal	border	mallard	60	0.00	80.00	6.91	*16.99
	villi	teal	44	40.55	80.00	74.46	12.12
		mallard	60	0.00	80.00	8.82	*16.12
	crypts	teal	44	80.00	80.00	80.00	0.00
		mallard	54	0.00	80.00	14.51	*22.26
Hayres	brush	teal	43	80.00	80.00	80.00	0.00
Ileum	border	mallard	47	0.00	80.00	23.36	*27.30
	villi	teal	43	80.00	80.00	80.00	0.00
		mallard	47	0.00	80.00	16.87	*20.47
	crypts	teal	44	38.00	80.00	78.82	6.47
		mallard	58	0.00	80.00	18.97	*27.25
Caayee	brush	teal	43	7.00	80.00	62.96	23.49
Cecum	border	mallard	54	0.00	80.00	26.24	*33.35
	villi	teal	43	8.00	80.00	59.21	24.95
		mallard	54	0.00	80.00	23.12	*30.47
	or rota	teal	44	80.00	80.00	80.00	0.00
	crypts	mallard	59	0.00	80.00	11.66	*19.36
Calan	brush	teal	44	76.00	80.00	79.91	0.60
Colon	border	mallard	58	0.00	80.00	23.55	*24.91
	:11:	teal	44	76.00	80.00	79.91	0.60
	villi	mallard	58	0.00	80.00	16.35	*18.98
Bursa	Epithelial	teal	42	10.00	80.00	68.57	20.61
Duisa	Cells	mallard	NA	NA	NA	NA	NA

LPAIV treatment teals had statistically higher lectin staining than LPAIV treatment mallards $(F_{1,102}=309.92,\,p<0.001)$ with a statistically significant interaction between species and tissue/cell type $(F_{11,1067}=9.95,\,p<0.001)$. In mallards, the ileum, cecum, and colon had statistically similar lectin scores for most cell types; however, lectin scores for most cell types in the proximal intestine were significantly lower (p<0.05) than the lectin scores in ileum, cecum, and colon (Figure 2.8). In teals, most tissues/cell types had similar lectin scores, except for the cecum brush border and cecum villi, which were statistically significantly lower than all other tissue/cell types (Figure 2.8).

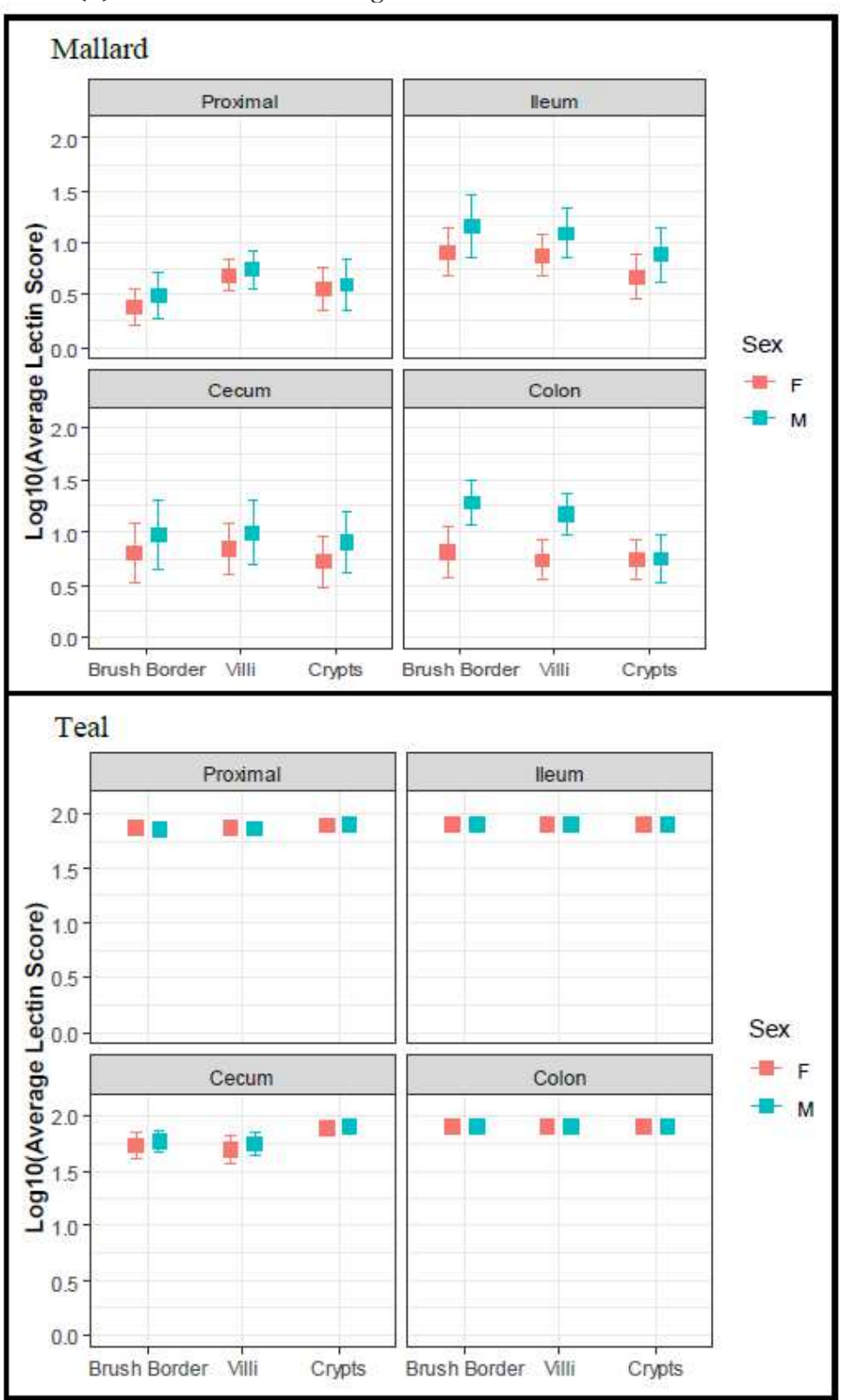
Figure 2.8: Lectin score differences between mallard and blue-winged teal intestinal tissues. Mean lectin scores +95% confidence intervals for intestinal tissues proximal (duodenum and jejunum), ileum, cecum, and colon for LPAIV H5N9 infected mallards and blue-winged teals. Across all panels, points with different letters are considered significantly different (p < 0.05).



Analyzing LPAIV treatment mallards and teals in separate models, we found that lectin staining was not significantly different between males and females (mallard: $F_{1,58} = 2.243 p =$

0.141; teal: $F_{1,42} = 0.24$, p = 0.626) for either species, and there was no significant interaction between sex and tissue/cell type (mallard, $F_{11,587} = 1.48$, p = 0.136; teal, $F_{11,458} = 0.42$, p = 0.947; Figure 2.9).

Figure 2.9: Mean lectin scores \pm 95% confidence intervals for intestinal tissues proximal (duodenum and jejunum), ileum, cecum, and colon for LPAIV H5N9 infected male (M) and female (F) mallards and blue-winged teals.



Relationship Between Lectin Score and Virus Titer – Mallard

With 99% of positive virus titers on 1-5 DPI, mallards in LPAIV treatment groups MT1, MT2, and MT5 were used in each model to evaluate the association between virus titers and lectin scores. Because lectin scores could not be obtained for mallard bursa tissue due to autolysis, only cloacal swab virus titers and ileum tissue virus titers were analyzed. Missing intestinal lectin scores due to autolysis reduced the sample size for each model from 40 to 25 birds (MT1 = 6; MT2 = 8; MT5 = 11). High correlations (Pearson's r > 0.8) between lectin scores for proximal brush border, villi enterocytes, and crypt enterocytes, as well as between lectin scores for cecum brush border, villi enterocytes, and crypt enterocytes were observed (Appendix Table A2.1); therefore, singular variables (proximal PC, cecum PC) for each respective tissue were created using principal component analysis (PCA).

For cloacal swab virus titers on the DPI of sacrifice, initial stepwise variable selection rendered a multiple linear regression (MLR) model which included sex, proximal PC, ileum villi, and ileum brush border (AIC = 11.44, Δ AIC = 1.77). This reduced model was tested for colinearity issues and residual plots were evaluated with no serious statistical problems detected, so the reduced model was selected as the best fitting model (R² = 0.66, p < 0.001; Table 2.3). Our results show that lectin staining in the ileum villi and being male were positively associated with a higher virus titer, while lectin staining in the ileum brush border was negatively associated with a higher virus titer. Lectin staining in the proximal intestine was not a significant term in the model.

For mallard ileum virus titer, initial stepwise variable selection rendered a model which included sex, ileum villi, and ileum brush border (AIC = 33.57, Δ AIC = 1.32). This reduced model was tested for co-linearity issues and residual plots were evaluated with no serious

statistical problems detected, thus this model ($R^2 = 0.33$, p < 0.010, Table 2.3) was selected as the best fitting model. Our results show that the lectin score of the ileum villi was positively associated with a higher virus titer. The lectin score in the ileum brush border was negatively associated with a higher virus titer. Sex was not a significant factor in this model.

Table 2.3: Sex and ileum lectin scores are associated with LPAIV H5N9 virus titers in mallards. Y = dependent variable, N = number of individual birds in model, X = independent variables in final model, CI = 95% confidence interval, p = p-value. Dependent variable "mallard cloaca virus titer" includes virus titers from cloacal swabs collected on the DPI each bird was sacrificed. Proximal includes the duodenum and jejunum. PC1 represents the principal component variable for the proximal villi enterocytes, brush border, and crypt enterocytes combined. BCS = Body Condition Score. Group and Sex were treated as factors in each model, and if present in final model, group T1 and females are represented in the intercept.

y	y n R		X	Est. (95% CI) Log10(EID50/mL)	P
	25	0.66	Intercept	1.37 (0.14 to 2.60)	0.031
M-111 C1			Sex (Male)	1.66 (0.60 to 2.73)	0.004
Mallard Cloaca Virus Titer			Proximal PC1	0.50 (-0.22 to 1.22)	0.166
VII US TITE			Ileum Villi	2.93 (1.42 to 4.44)	< 0.001
			Ileum Brush Border	-1.96 (-3.12 to -0.80)	0.002
	25	0.33	Intercept	2.86 (1.21 to 4.52)	0.002
Mallard Ileum Virus			Sex (Male)	1.36 (-0.19 to 2.92))	0.083
Titer			Ileum Villi	3.27 (1.18 to 5.36)	0.004
			Ileum Brush Border	-1.93 (-3.73 to -0.14)	0.036

Relationship Between Lectin Score and Virus Titer – Teal

With 98% of positive virus titers on 1-5 DPI, teals in LPAIV treatment groups BT1, BT3, and BT5 were used in each model to evaluate the association between virus titers and lectin scores. Missing lectin scores due to autolysis reduced the sample size for each model from 36 to 32 birds (T1=9, T3=11, T=12).

For cloacal swab virus titers on the DPI of sacrifice, initial stepwise variable selection rendered a model which included sex, mass, body condition score (BCS), LPAIV treatment group, proximal crypts, and bursa (AIC = -8.31, Δ AIC = 0.10). This reduced model was tested

for co-linearity issues and residual plots were evaluated with no serious problems detected, thus this model ($R^2 = 0.61$, p < 0.010) was selected as the best fitting model; however, inconsistent results were observed when validating results with respect to quantification limit assumptions. Due to these inconsistencies, we conclude the model to be unstable and results unreliable.

For teal ileum virus titer, initial stepwise variable selection rendered a model which included BCS and LPAIV treatment group (AIC = 32.41, Δ AIC = 1.99). This reduced model was tested for co-linearity issues and residual plots were evaluated with no serious problems detected, thus this model (R² = 0.44, p < 0.001) was selected as the best fitting model. Our results show that virus titers were lower on five DPI compared to one and three DPI. BCS was not a significant term in the model.

For teal bursa virus titer, initial stepwise variable selection rendered a model which included mass, BCS, and treatment group (AIC = -1.6, Δ AIC = 1.75). The reduced model was tested for co-linearity issues with no problems detected. Residual plots were evaluated, and the model did not fit normality assumptions. Mass was removed from the model since it was an insignificant factor, and the residual plots improved; therefore, the model which included BCS and LPAIV treatment group was accepted as the best fitting model (R² = 0.37, p = 0.001). Our results show that virus titer was highest on one DPI, and significantly lower on three and five DPI. BCS was not a significant term in the final model.

Discussion

Mallards and blue-winged teals are important reservoir hosts for avian influenza viruses (Papp et al. 2017; Stallknecht et al. 1990; Stallknecht and Shane 1988); they are both widely distributed waterfowl species and commonly infected with both LPAIV and HPAIV. Our study documents both within and between-species variation in viral shedding and occurrence frequency of

 $SA\alpha2,3Gal$, the viral receptor for many LPAIVs. In mallards, but not teals, we found viral shedding was related to lectin scores, which represent the occurrence frequency of $SA\alpha2,3Gal$. While we expected to see positive linear relationships between virus titers and $SA\alpha2,3Gal$ in all tissues and cell types, the mallard ileum was the most predictive of virus titers, with a positive relationship between virus titers and $SA\alpha2,3Gal$ in ileum villi enterocytes, and a negative relationship between virus titers and $SA\alpha2,3Gal$ in the ileum brush border. Despite the lack of relationship between viral shedding and $SA\alpha2,3Gal$ in teals, we observed significantly higher viral shedding by teals, and a higher occurrence frequency of $SA\alpha2,3Gal$ compared to mallards.

As the direction (positive or negative) of the correlation between $SA\alpha2,3Gal$ occurrence frequency and virus titer varied across mallard tissue locations, our data highlight the importance of understanding tissue-specific tropism as it relates to cell surface $SA\alpha2,3Gal$ distribution. Within mallards, the positive relationship between virus titer and $SA\alpha2,3Gal$ in the ileum villi enterocytes was expected given that LPAIV replicates in intestinal enterocytes by binding $SA\alpha2,3Gal$ on the surface of the cell for cell entry (Cheung and Poon 2007). A reason ileum villi enterocytes were most correlated with viral titer compared to ileum crypt enterocytes may be that the villi have closer direct contact with digesta and as a result, closer direct contact with virus passing through the gut. For example, previous studies have found LPAIV antigen via immunohistochemistry more consistently in mallard villi enterocytes compared to the crypts (Daoust et al. 2011; Franca, Stallknecht, et al. 2012).

Two hypotheses could explain the negative relationship between $SA\alpha 2,3Gal$ in the ileum brush border and virus titer. Initially, we expected to see a positive relationship between $SA\alpha 2,3Gal$ in the brush border of all intestinal tissues and virus titers since the receptors are on the surface of the cell and more likely to be exposed to virus (Kelm and Schauer 1997).

However, as a virion attaches to a receptor, the virion along with the receptor becomes engulfed by the cell for replication, therefore removing the receptor from the surface of the cell (Samji 2009). This idea is also consistent with the differences observed in occurrence frequency of $SA\alpha2,3Gal$ between LPAIV treatment and control mallards, where control mallards had higher $SA\alpha2,3Gal$ in the ileum and colon brush border compared to LPAIV treatment birds. Second, mucus is also found along the brush border and LPAIV has been found to bind $SA\alpha2,3Gal$ in mucus, which would prohibit the virus from reaching the enterocyte for virus replication (Ito et al. 2000; Linden et al. 2008; McAuley et al. 2017); thereby reducing the quantity of virus shed. Up-regulation of mucins have also been observed in response to other viruses which bind sialic acid receptors (Kim and Ho 2010), such as human rotavirus infections (Matrosovich, Herrler, and Klenk 2013). To understand the true source for the negative relationship between occurrence frequency of $SA\alpha2,3Gal$ in the ileum brush border and virus titers, further experimental research is warranted.

Our results do not show a relationship between virus titer and $SA\alpha2,3Gal$ occurrence frequency in the other three intestinal tissue types: proximal, cecum, and colon. The lack of a statistically significant relationship between $SA\alpha2,3Gal$ and virus titer in the mallard colon was unexpected, given many studies have showed the colon as a site for high LPAIV replication (Daoust et al. 2011; Franca, Stallknecht, et al. 2012; Kida, Yanagawa, and Matsuoka 1980; Webster et al. 1978). Since $SA\alpha2,3Gal$ in the ileum and colon were 63% correlated with each other (Appendix Table A2.1), the colon could also have a contributing effect to viral load, but not as strongly as the ileum. Because the cecal tonsils, a major lymphoid tissue in the cecum, enlarge during gut infections due to infiltration of immune cells (Davison, Kaspers, and Schat 2008), perhaps a relationship between virus titer and $SA\alpha2,3Gal$ in the cecum could not be

detected because of the interference of immune cells which may have been identified as enterocytes when stained. $SA\alpha2,3Gal$ in the mallard proximal intestine did not show a relationship with virus titers likely because we observed a lower frequency of $SA\alpha2,3Gal$ in the proximal intestine compared to the ileum, cecum, and colon. Previous findings show that positive viral antigen is more commonly found in the ileum, cecum, and colon when cloacal swab virus titers are high (Daoust et al. 2011; Franca, Stallknecht, et al. 2012), which would suggest that the proximal intestine is not a prime site of LPAIV replication. While we did not detect statistically significant relationships between virus titers and $SA\alpha2,3Gal$ in the proximal intestine, cecum, or colon, we cannot say for certain these tissues do not contribute to viral shedding. Our results indicate, however, that ileum $SA\alpha2,3Gal$ occurrence frequency has the strongest relationship to viral load in mallards.

The bursa epithelial cells are also considered an important site of replication for LPAIV in waterfowl, including mallards (Daoust et al. 2011; Franca, Stallknecht, et al. 2012). However, given autolysis of tissue samples, we could not analyze the relationship between $SA\alpha2,3Gal$ in the bursa and viral shedding in mallards. In teals, lectin staining was very high in the bursa; however, it was not significantly related to viral shedding. Lack of a significant relationship to viral titer in teals could be attributed to the lack of individual variation in $SA\alpha2,3Gal$ expression in the bursa or to a sporadic correlation between bursa and cloacal swab virus quantity. Further analysis of bursa sialic acid receptors is therefore warranted to determine relationships with LPAIV viral load.

Although we did not determine a linear relationship between $SA\alpha 2,3Gal$ and virus titers in blue-winged teals, significantly higher virus titers and a higher occurrence frequency of $SA\alpha 2,3Gal$ with less variation were observed in teals compared to mallards. We hypothesize that

the higher teal virus titers resulted from higher SAα2,3Gal occurrence frequency. Teals have already been shown to have a higher binding affinity to MAL I lectin than mallards (Franca, Stallknecht, and Howerth 2013). Different LPAIV strains also vary in binding affinity to SAα2,3Gal with different molecular structures (Gambaryan et al. 2006). Although, LPAIV H5N9 (Ratite/New York/12716/94) has a similar affinity for the receptors targeted by MAL I (Gambaryan et al. 2006; Geisler and Jarvis 2011), we did not test the specific receptor affinity of the LPAIV H5N9 (A/northern pintail/California/44221-761/2006) used in this study. If LPAIV H5N9 (A/northern pintail/California/44221-761/2006) has a higher affinity for SAα2,3Gal with a β1-4Glc(NAc) linkage, the preferred binding affinity of MAL I, then our results provide further evidence to explain the higher LPAIV H5N9 virus titers in teals. However, the converse is at least theoretically possible; that is, higher receptor abundance was a result rather than a cause of higher viral titers in teal. Receptor abundance would have to be assayed prior to and during viral infection to disentangle these issues, which is a significant experimental hurdle.

Species-based variation in SA α 2,3Gal has been observed in other experimental infection studies (Franca, Stallknecht, and Howerth 2013; Jankowski et al. 2019). Jankowski et al. (2019) analyzed the variation of sialic acid receptors expressed by erythrocytes in various avian species and found that approximately 20% of the species expressed 80% of the overall sialic acid receptor quantity in all species studied. Although teals were not included in the Jankowski et. al. (2019) study, mallards and three other *Anas* species (*A. acuta, A. Americana, and A. crecca*) were among the species assessed. Interestingly, mallards had the lowest quantity of sialic acid receptors on erythrocytes compared to the other three *Anas* species. Our results which show mallards with lower frequencies of SA α 2,3Gal compared to teals provide further evidence of species-based differences in sialic acid receptors.

The premise of our study was to determine if the occurrence frequency of SAα2,3Gal in the intestines and bursa may be associated with cloacal shedding; hence, we predicted the variation of SAα2,3Gal in control and infected birds would not differ. Our data suggest this is not the case. In the cecum, the occurrence frequency of $SA\alpha 2.3Gal$ was higher in the crypts of infected mallards compared to their conspecific controls. Similarly, in teals the frequency of SAα2,3Gal was higher in the cecum villi and brush border of infected birds. The ceca have a unique role in the functioning of the vertebrate immune system. As stated previously, the cecal tonsils, a major lymphoid tissue in the cecum, enlarge during gut infections due to infiltration of immune cells, which also includes macrophages (Davison, Kaspers, and Schat 2008). Macrophages express Gal-specific receptors (Munday, Floyd, and Crocker 1999), which could explain the higher abundance of $SA\alpha 2,3Gal$ in the cecum of infected birds relative to controls. Evidence of macrophages expressing Gal-specific receptors are seen in white leghorn chickens, which in one study had a greater abundance of sialic acid receptors than silky fowl because of a higher number of immune cells in the leghorns' cecum (Han et al. 2016). The cecum has a unique response to LPAIV infection compared to other intestinal tissues, which warrants further analysis of $SA\alpha 2,3Gal$ in this tissue.

Contrary to differences in SAα2,3Gal expression between LPAIV-infected and control birds in the cecum, control mallards expressed more SAα2,3Gal in the ileum and colon brush border than infected mallards. Franca et. al (2012) found that SAα2,3Gal was lower in the cecum, colon, and bursa of infected birds compared to control birds. Their hypothesis indicated that the SAα2,3Gal expression level may decrease after infection because the neuraminidase function of the virus allows cleaving of the receptor releasing virions from the cell (Byrd-Leotis, Cummings, and Steinhauer 2017). When the receptor is cleaved, it is no longer present on the

cell surface which would reduce lectin binding. While Franca et. al (2012) did not specify whether the decrease in lectin staining was on the surface of the enterocyte, we found mallards to have a higher occurrence frequency of $SA\alpha2,3Gal$ only in the brush border. Our results indicate the importance of assessing the specific location of $SA\alpha2,3Gal$ in determining their function in influenza studies.

No difference was detected between males and females in virus titers or frequency of $SA\alpha2,3Gal$ when examined separately in either species; yet, when $SA\alpha2,3Gal$ in the ileum villi enterocytes and brush border are held constant, a statistically significant difference in cloacal swab virus titer was detected between male and female mallards. Biologically, our results show that due to the natural variation of $SA\alpha2,3Gal$ frequency in the ileum of mallards, sex is not important to the viral shedding variation observed in the population; however, it may be a contributing factor in the relationship between viral load and $SA\alpha2,3Gal$ frequency in the ileum. The unique relationship between sex, $SA\alpha2,3Gal$ in the ileum, and cloacal swab virus titers in mallards warrants further research for understanding why sex would be important for the relationship between viral load and $SA\alpha2,3Gal$ in the mallard ileum.

The identified positive relationships between viral RNA in cloacal swabs, ileum tissue, and bursa tissue further supports the importance of the ileum and bursa for cloacal shedding of LPAIV. Prior to this study, it was well known that LPAIV replicates in duck intestines and the bursa of Fabricius (Daoust et al. 2011; Franca, Stallknecht, et al. 2012; Webster et al. 1978). While testing for virus in cloacal swabs is the standard method for determining AIV fecal shedding (Ellstrom et al. 2008; Killian 2014), the direct relationship between tissue replication and virus shed by the cloaca was unknown. Through quantifying viral RNA via qPCR in ileum and bursa tissue, significant positive relationships were found between virus titers in cloacal

swabs, ileum tissue, and bursa tissue, showing the contribution of these tissues to the cloacal virus shed. The positive relationship between virus titers in the ileum and cloacal swabs provides additional evidence to support our conclusion that ileum $SA\alpha2,3Gal$ was associated with virus titer. These positive relationships add validity to collecting cloacal swabs as an indicator of virus titer in the ileum and bursa and perhaps the infection status of individual birds.

Understanding the mechanism underlying variation in infection severity and viral shedding can provide insight into why a few individuals in a population are more infected than others, and perhaps, why some species are more infectious than others. LPAIV is a gutassociated pathogen in wild waterfowl; hence, the physiology of the host's gut is an important determinant of within-host-pathogen interaction. Our results provide evidence that sialic acid receptors in the gut are associated with viral load. Since sialic acid expression varies both between species (Franca, Stallknecht, and Howerth 2013; Jankowski et al. 2019) and within species (Franca, Stallknecht, et al. 2012), this variation has implications for a species' and/or individual bird's contribution to the transmission of avian influenza virus. Furthermore, sialic acid is the cellular receptor for other viruses such as parainfluenza, mumps, corona, noro, rota, and DNA tumor viruses, some of which infect humans (Matrosovich, Herrler, and Klenk 2013), leading to similar questions regarding the effect of sialic acid receptor variation across individuals and species on host-virus interactions. Pathogen receptors are not the only contributing factor to a host's infectiousness. Other intrinsic factors and their relationship to pathogen shedding warrant further investigation. Because the quantity of virus shed can directly affect transmission dynamics and is an important parameter for predicting disease risk in a population (Henaux and Samuel 2011), identifying individuals or certain species as more infectious could improve our ability to predict and mitigate disease.

CHAPTER 3: DIFFERENTIAL GENE EXPRESSION REVEALS HOST FACTORS FOR VIRAL SHEDDING VARIATION IN MALLARDS (ANAS PLATYRHYNCHOS) INFECTED WITH LOW-PATH AVIAN INFLUENZA VIRUS

By: Amanda C. Dolinski^{1*}, Jared J. Homola^{1*}, Mark D. Jankowski^{1,2}, John D. Robinson¹, Jennifer C. Owen^{1,3}

*These authors contributed equally

- 1. Department of Fisheries and Wildlife, Michigan State University, East Lansing, MI
- 2. U.S. Environmental Protection Agency, Region 10, Seattle, WA 98101
- 3. Department of Large Animal Clinical Sciences, Michigan State University, East Lansing, MI, USA

Abstract

Intraspecific variation in pathogen load is a key factor in disease transmission dynamics; therefore, understanding the host factors associated with individual variation in pathogen shedding is key to controlling and preventing outbreaks. In this study, bursa and ileum tissues of low-path avian influenza (LPAIV) infected mallards (Anas platyrhynchos) were evaluated at various time points post infection to determine genetic host factors associated with intraspecific variation in viral shedding. By analyzing transcriptomic sequencing, we found that LPAIVinfected mallards do not exhibit differential gene expression compared to uninfected birds, but that gene expression was associated with viral shedding load early in the infection. In both tissues, immune genes were mostly up regulated in higher shedding birds and had significant positive relationships with viral load. In the ileum, host genes involved in viral cell entry were down regulated in low shedders on one DPI, and host genes promoting viral replication were up regulated in high shedders on two DPI. Our findings indicate that viral shedding is a key factor for gene expression differences in LPAIV-infected mallards, and the genes identified in this study could be important for understanding the molecular mechanisms driving intraspecific variation in pathogen load.

Introduction

Individual heterogeneity in pathogen transmission can impact the magnitude and duration of a disease outbreak (Lloyd-Smith et al. 2005; Vanderwaal and Ezenwa 2016). Some individuals in a population are super-spreaders, that is they are disproportionately responsible for secondary transmission cases of a contagious pathogen through increased contact rate and/or higher infectiousness (Stein 2011). Recently, super-spreaders were linked to human outbreaks of novel coronaviruses (Al-Tawfiq and Rodriguez-Morales 2020), yet the super-spreader phenomenon can be traced back to Typhoid Mary in the early 1900s (Paull et al. 2012), humans infected with human immunodeficiency virus (HIV) in the 1980s (Galvani and May 2005; Gupta, Anderson, and May 1989), and wildlife spillover events in recent decades (Hudson, Perkins, and Cattadori 2010; Paull et al. 2012). Super-spreading events are more often attributed to higher contact rates by some infected individuals in a population (Godfrey 2013; Mossong et al. 2008; Vanderwaal and Ezenwa 2016) rather than to variation in infectiousness; however, the individuals with the highest pathogen loads, i.e. the "super-shedders" (Chase-Topping et al. 2008), have been shown to be drivers of super-spreading events as demonstrated in cattle infected with Escherichia coli O157 (Matthews, McKendrick, et al. 2006) and *Brucella abortus* (Capparelli et al. 2009). Despite the apparent importance of individual variation in pathogen load to transmission dynamics, we know little about the mechanisms underlying differential pathogen shedding.

Identifying the extrinsic and intrinsic factors that affect an individual host's pathogen load can help to understand mechanisms perpetuating super-spreading events. Extrinsic host factors linked to heterogeneity in pathogen load include food availability (Arsnoe, Ip, and Owen 2011; Tadiri, Dargent, and Scott 2013), geographical location (Costa et al. 2015), toxicant exposure (Jolly et al. 2013), and myriad environmental factors that can affect host immune

competence through chronically elevated stress hormones (Jankowski et al. 2010). Intrinsic factors linked to pathogen load are inherent conditions of the host such as age (Costa et al. 2010), sex (Zuk and McKean 1996), and genetically based traits affecting host growth (Boddicker and Garrick 2011), physiology (Cobbold et al. 2007; Dolinski, Jankowski, et al. 2020), the immune response (Juliarena et al. 2008; Purcell et al. 2010; O. Wang et al. 2017), and metabolism (Wang et al. 2017). In particular, intraspecific variation linking immune responses and biological processes to observed variation in pathogen load can improve our understanding of host factors involved in disease transmission.

With the advancement of transcriptomics in the past decade, gene expression studies identified host immune responses and other biological processes related to variation in pathogen load. For instance, evaluating the bovine intestinal tract transcriptome revealed that T-cell responses and cholesterol metabolism were associated with super-shedding of *E. coli* O157 (Wang et al. 2017). Another study found that viral load in rainbow trout (*Oncorhynchus mykiss*) infected with infectious hematopoietic necrosis virus was correlated with type I and type II interferon transcript levels early in the infection (Purcell et al. 2010). Analyzing gene expression simultaneously with viral load improves our understanding of infectious disease progression and the mechanisms driving transmission dynamics, but due to limited studies in only a few host-pathogen systems, further investigation is warranted.

Gene expression studies have also highlighted the value of examining multiple tissues at various time points post infection since immune responses are tissue-specific and change over time (Cornelissen et al. 2012; Deist et al. 2017; Hu and Pasare 2013). Successful viral infections, for example, are dependent upon cellular entry and the ability to evade the host immune response. The host provides initial protection by activating the innate immune response through

pattern recognition receptors (PRR) that activate the transcription of interferons, which leads to the production of anti-viral interferon-stimulated genes (ISGs) (Koyama et al. 2008; Santhakumar et al. 2017). This process provides protection to the host since many ISGs are known to inhibit virus cell entry and replication, degrade viral RNA, regulate cell apoptosis, and have regulatory effects on the interferon pathway (Santhakumar et al. 2017; Schoggins and Rice 2011). The host also stimulates immune cell dependent mechanisms (cellular immunity) to eliminate infected cells and activate adaptive immunity consisting of antigen recognition by major histocompatibility complex (MHC) molecules, T-cell activation, and B-cell activation for the production of antibodies later in the infection (Bonilla and Oettgen 2010; Rong, Wang, et al. 2018; Suarez and Schultz-Cherry 2000). Depending on the type of tissue infected, the innate and adaptive immune systems respond differently (Hu and Pasare 2013), thus it's important to evaluate tissue-specific host gene expression at various time-points post infection.

In this study, we analyzed the association between gene expression and viral load variation in avian influenza virus (AIV) infected mallards (*Anas platyrhynchos*). AIVs are type A influenza viruses that can spillover into domestic swine and poultry posing a significant health risk to domestic animal and human populations (Webster et al. 1992). Previous studies have shown that AIV-infected mallards exhibit extreme heterogeneity in pathogen shedding (Jankowski et al 2013), which has been linked to both extrinsic (food availability) (Arsnoe, Ip, and Owen 2011) and intrinsic (gut physiology) (Dolinski, Jankowski, et al. 2020) host factors. Yet, these factors alone do not explain all the observed variation in viral load. Previous gene expression studies of AIV-infected poultry consistently show that gene expression is upregulated in AIV-infected birds, many of which are associated with the immune response (Cornelissen et al. 2012; Huang et al. 2013; Ranaware et al. 2016; Smith et al. 2015; Vanderven et al. 2012);

however, a longitudinal transcriptome-wide study is yet to be conducted to analyze the association between gene expression and viral shedding.

Given what is currently known regarding cell infectivity (Costa et al. 2012; Daoust et al. 2011; Gambaryan et al. 2005; Webster et al. 1978) and the avian immune response to AIV (Campbell and Magor 2020; Chen et al. 2018; Evseev and Magor 2019; Santhakumar et al. 2017), we hypothesized that gene expression in the ileum and bursa of Fabricius (hereafter referred to as "bursa") is associated with viral shedding in low pathogenic AIV (LPAIV)infected mallards. Specifically, we predicted that gene expression would differ (1) between infected and uninfected birds, (2) between days post-infection, with innate immunity genes expressed early in the infection and adaptive immunity genes expressed later in the infection, and (3) between birds with various viral shedding levels. Further, we predicted that viral shedding would be correlated with expression of genes involved in cell entry and the immune response. We accomplished our objectives by evaluating gene expression at various time points post infection to detect differential expression with respect to infection stage, infection site, and viral shedding load in an important reservoir host for AIV, the mallard (Halvorson et al. 1983; Jimenez-Bluhm et al. 2018; Li et al. 2010; Stallknecht and Brown 2008). This research provides virologists and disease ecologists with a larger body of information about LPAIV infections in mallards, as well as new knowledge of genes associated with individual heterogeneity in pathogen load.

Methods

Permits and Protocols

Eggs were collected under the U.S. Fish and Wildlife Permit (M Bl 94270-2) and North Dakota Game and Fish Department License #GNF03639403. All capture, handling, infections, and

sampling of mallards was approved by the Michigan State University (MSU) Institutional Animal Care and Use Committee (AUF 12/16-211-00).

Birds and Virus

Wild mallards collected in ovo were used for this study. Analyzing the gene expression of wild birds is important due to the inherent genetic variation within the population (Svobodová et al. 2020) and how that could influence variation in viral load (Arsnoe, Ip, and Owen 2011). Eggs were collected from hen nests located in uncultivated fields of Towner County, North Dakota, USA (48.44, -99.31) in May - June 2015, and shipped to MSU where they were incubated (Sportsman 1502 Egg Incubator, GQF Manufacturing Co., Savannah, GA) at 37.5°C with 45-50% humidity until hatched. Full details of egg collection and raising ducks can be found in Dolinski et al. (2020).

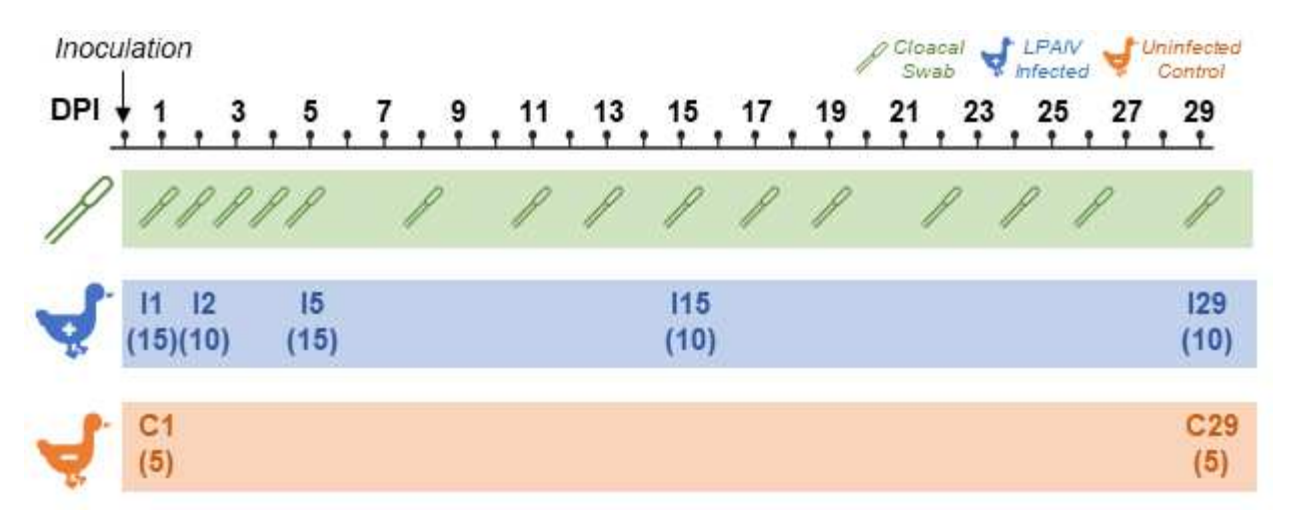
LPAIV A/northern pintail/California/44221-761/2006 (H5N9) was acquired from the USGS National Wildlife Health Center (NWHC) in Madison, WI (USDA Veterinary Permit 44372). The virus was propagated in embryonated pathogen free eggs (Charles River, Norwich, CT, USA) under biosafety level two laboratory conditions at MSU (Woolcock 2008). The propagated virus (stock) was sent to USGS NWHC and determined to have a viral titer of 7.63 log EID₅₀/ml using the Reed-Munch 50% egg infectious dose method (Reed and Muench 1938).

Experimental Design

Once all the birds were eight weeks or older, they were moved to individual cages (76x61x41cm) and randomly assigned to one of seven experimental groups using a random-pseudostratified method controlling for age, weight, and nest. Group identification and size are shown in Figure 1, with the group name referring to infection status and the day post infection (DPI) when the group was sacrificed for tissue sample collection (Figure 3.1).

At inoculation, mallards (n = 60) were inoculated with 5.63 log EID₅₀/ml of LPAIV H5N9 in Dulbecco's Modified Eagle Medium (DMEM; Gibco® by Life Technologies, Grand Island, NY, USA) and the remainder mallards (n = 10) were sham inoculated with sterile DMEM. Inoculum (1.0 mL) was administered to birds with one drop in each eye and nare, then the rest dispensed in the bird's esophagus.

Figure 3.1: Experimental timeline of sample collection days post infection (DPI). Groups are designated by infection status (I = LPAIV-infected, C = uninfected control), DPI sacrificed and (N) quantity of birds in each group. Ileum and bursa of Fabricius were collected upon sacrifice. Cloacal swabs were collected from all living birds designated with the swab icon.



Cloacal swabs for quantification of virus shedding (virus titers) were collected on days shown in Figure 3.1 using cotton-tipped swabs (Puritan, Guilford, ME), placed in 3.0 mL of brain-heart infusion broth (Sigma-Aldrich, St. Louis, MO, USA), and immediately placed on wet ice and stored at -80°C within three hours after collection.

Birds in each group were euthanized and necropsied as shown in Figure 3.1. Birds sacrificed on one DPI (I1, C1) were euthanized via lethal injection with pentobarbital sodium and phenytoin sodium solution (Beuthanasia-D Special, Merck Animal Health, Madison, NJ, USA), but due to complications with intravenous injections, all other birds were sacrificed by CO₂ inhalation. Birds were stored on beds of ice until necropsies were conducted one to six

hours after being euthanized. During necropsies, tissue sections (2 mm³) of ileum and bursa were collected, and the coelomic cavity was assessed for gross pathology. Each tissue section was placed in 1.0 mL of room temperature RNA stabilizing solution (RNAlater®, Sigma-Aldrich, St. Louis, MO, USA), then removed from the solution after 24 hours and stored at -80°C.

Viral RNA Extraction and Quantification from Cloacal Swabs

Cloacal swab samples were thawed at room temperature and viral RNA was extracted from 200 μL of each sample using the MagMAXTM-96 AI/ND Viral RNA Isolation Kit (Applied Biosystems® by Thermo Fisher Scientific, Vilnius, Lithuania) with modifications (Das et al. 2009b). Extracted viral RNA was stored in 500 μL of elution buffer. The virus titer for each cloacal swab sample was quantified by real time reverse transcription-quantitative polymerase chain reaction (RT-qPCR) targeting the matrix protein gene. We used the TaqMan® RNA-to-CtTM 1- Step Kit (Applied Biosystems® by Thermo Fisher Scientific, Foster City, CA, USA), primers/probe specified by Spackman et. al (Spackman and Suarez 2008), and 2 μL of sample RNA in three replicates. CT values were used to estimate virus quantity as EID₅₀/mL via standard curve (QuantStudioTM 7 Flex Real-Time PCR Software System v1.3) of stock viral RNA (7.63 log EID₅₀/ml) in a series of 10-fold dilutions. The three replicates per sample were averaged to derive a single estimated virus titer for each sample.

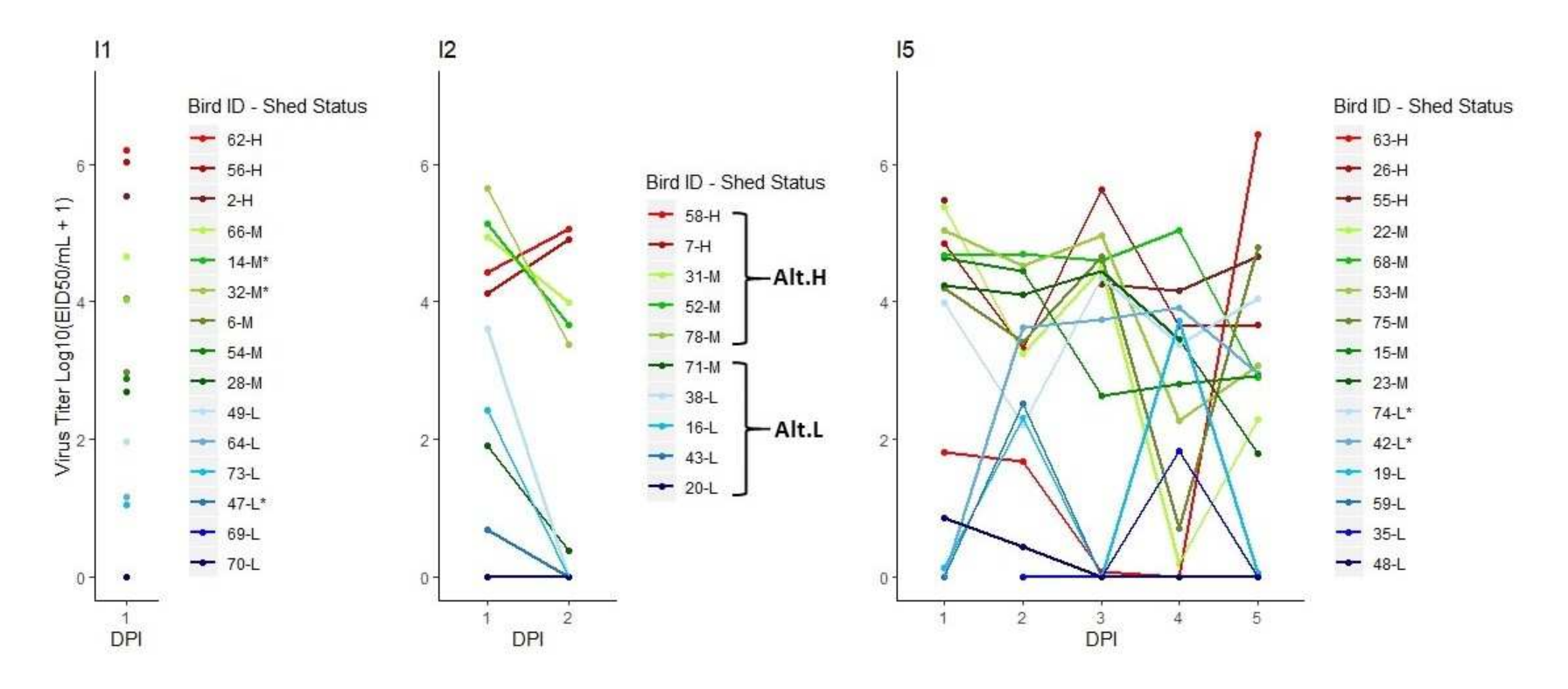
Determining Shed Level Groups

Previous analysis of virus titer data in mallards determined that 99% of cumulative LPAIV was detected during the first five DPI (Dolinski, Jankowski, et al. 2020), and birds were observed to disproportionately shed LPAIV according to the 20/80 rule (Jankowski et al. 2013); therefore, birds in LPAIV-infected groups (I1, I2, I5) were subdivided into three shed level groups (Figure 3.2). High shedders (H) were the top 20% of birds with the highest cloacal virus titer, moderate

shedders (M) were the top half of the lowest 80% of virus titers, and low shedders (L) were the bottom half of the lowest 80% of virus titers in each group. To detect differential gene expression as it directly relates to active viral shedding during the innate immune response (Campbell and Magor 2020; Evseev and Magor 2019), only the virus titer collected on the day the bird was sacrificed was used to categorize shed level groups in early-stage infection (I1, I2). To detect differential gene expression as it relates to the adaptive immune response (Jourdain et al. 2010; Suarez and Schultz-Cherry 2000), cloacal virus titers on one to five DPI were averaged to create a cumulative virus titer for late-stage infection (I5).

After evaluating virus titer data, we observed that I2 cumulative virus titer data clustered into two distinct shed level groups (Figure 3.2); therefore, we also provided an alternative two-group shed level classification of high shedders (Alt.H) and low shedders (Alt.L) for I2.

Figure 3.2: Cloacal swab virus titer profiles for LPAIV-infected mallards sacrificed on one (I1), two (I2), and five (I5) days post infection (DPI). Shed status of high (H), moderate (M), or low (L) was assigned to individuals by their last virus titer (I1, I2) or the average virus titer across all DPI (I5). Alternative high (Alt.H) and alternative low (Alt.L) shed status groupings were assigned to individuals in I2 based on cumulative virus titers clustered across one and two DPI. Due to low host RNA quality, *individuals were not included in ileum differential gene expression analyses.



mRNA Extraction, cDNA Library Preparation, and Sequencing

Total mRNA was extracted from ileum and bursa tissue (15-30 mg) using the Qiagen RNeasy mini kit (QIAGEN®, Hilden, Germany) following the manufacturer's protocol. Total mRNA was stored in 500 μL of RNase free water at -80°C.

RNA quality was determined prior to library preparation using a Qubit® Fluorometer 1.0 (Molecular Probes, Life Technologies, Eugene, OR, USA). Sixty-six of 70 bursa samples had RNA integrity number (RIN) scores >8.0 and one bursa sample had a RIN score of <7.0 (Appendix Table A3.1). All 70 bursa samples were sequenced at the MSU Research Technology Support Facility. Thirty of the 70 ileum samples had RIN scores >8.0 and 35 had RIN scores <7.0. Library preparation and RNA sequencing was performed at MSU for 22 ileum samples with RIN scores >8.0 in groups I2, I5, and C1. Due to lack of availability at MSU, library preparation and RNA sequencing for an additional 20 ileum samples with RIN scores between 4.9 and 9.4 was conducted at the University of Minnesota (UMN) Genomics Center in St. Paul, MN.

Sequencing libraries were prepared using the NuGEN Ovation® Universal RNA preparation kit (Tecan Genomics, Chesapeake Drive, CA, USA) according to the manufacturer's specifications. Custom probes complementary to mallard rRNA sequences were designed and used for the Insert Dependent Adaptor Cleavage (InDA-C) portion of the protocol. Completed library quality was assessed using Qubit® dsDNA HS (Molecular Probes, Life Technologies, Eugene, OR, USA) and Caliper LabChip® GX DNA HS (Caliper, A PerkinElmer Company, Hopkinton, MA, USA) assays. Libraries sequenced at MSU were combined into six pools for multiplexed sequencing, including five pools of 16 libraries each, and a sixth pool of 13 libraries. Library pools were quantified using Kapa Biosystems Illumina Library Quantification qPCR

assay prior to sequencing. Each pool was loaded on one lane of an Illumina HiSeq 2500 High Output flow cell (v4) and sequencing was performed in a 2x150bp paired end format using HiSeq SBS reagents. Libraries at UMN were combined into a single pool and sequenced in one lane of an Illumina NovaSeq S1 2x150-bp run. Base calling was done by Illumina Real Time Analysis (RTA) v1.18.64 and output of RTA was demultiplexed and converted to FastQ format with Illumina Bcl2fastq v1.8.4.

RNA-seq Read Processing

Quality of raw cDNA reads was assessed using FastQC (Andrews 2011) prior to trimming and filtering. Sequence regions with a quality score below 15 and sequences shorter than 40bp were removed using Trimmomatic (Bolger, Lohse, and Usadel 2014). FastQC was used again to verify quality and trimming.

Sequences were aligned to the most recent mallard reference genome, Ensembl ASM874695v1 (Mallard assembly and gene annotation 2019), using STAR (Dobin et al. 2013; Dobin and Gingeras 2015). Gene-specific read counts for bursa samples were acquired with HT-seq using the STAR output, then RSEM (Li and Dewey 2011) was used to estimate read abundance. Due to low RIN scores of 14 ileum samples (RIN = 4.9 – 7.3), we used DegNorm (Xiong et al. 2019) to normalize read counts and model read abundance for ileum samples. Low RIN scores (RIN <8.0) can negatively impact analyses by misaligning sequences resulting in inaccurate transcript counts (Copois et al. 2007; Romero et al. 2014). DegNorm adjusts read counts for heterogeneity in mRNA sequence degradation on an individual gene basis while also accounting for sequencing depth (Xiong et al. 2019).

Differential Expression Analyses

We performed differential gene expression analyses using the R packages "EdgeR" (McCarthy, Chen, and Smyth 2012; Robinson, McCarthy, and Smyth 2010) and "limma" (Ritchie et al. 2015) in R version 4.0.0, using the approach outlined by Law et al. (Law et al. 2018). Differential expression analysis was performed separately for each tissue and included gene- and transcript-level analyses for the bursa and only gene-level for the ileum because isoform counts are not estimated by DegNorm.

Lowly expressed genes and transcripts were filtered by requiring expression of >0.5 counts per million in at least 25% of the birds. A false discovery rate (FDR) corrected alpha value of 0.1 and a required log fold count difference (LFC) of 0.5 was required to establish differential expression. To account for sex-based differences and variation in sequencing pool, sex and pool were included as covariates in each analysis. Gene names (HGNC symbols) were assigned based on ENSEMBL annotation information that accompanied the reference genome. KEGG pathway analyses were performed using the "kegga" function of "limma". Pathways with p-values <0.05 were determined as over-represented (enriched) pathways of differentially expressed genes or transcripts (DEG, DET) per analysis.

Preliminary differential expression analysis showed that ileum and bursa samples clustered based on tissue-specific gene expression (Figure 3.3). Two individuals (1 and 72), both in group C1, had tissue samples clustering opposite of the rest of the tissue samples suggesting improper sample labels; therefore, these two individuals were removed from differential expression analyses, leaving a total of 68 bursa samples and 40 ileum samples. Additionally, due to an absence of differential gene expression between C1 and C29 (Supplemental File S1), we

combined the two control groups into one group "C" for subsequent analyses. Sample size for each group in each differential expression analysis is provided in Table 3.1.

Figure 3.3: Multidimensional scaling (MDS) plot of bursa and ileum samples shows that tissue samples cluster based on tissue type gene expression. Bursa and ileum samples from bird 1 and 72 were removed from differential expression analysis due to opposite tissue grouping.

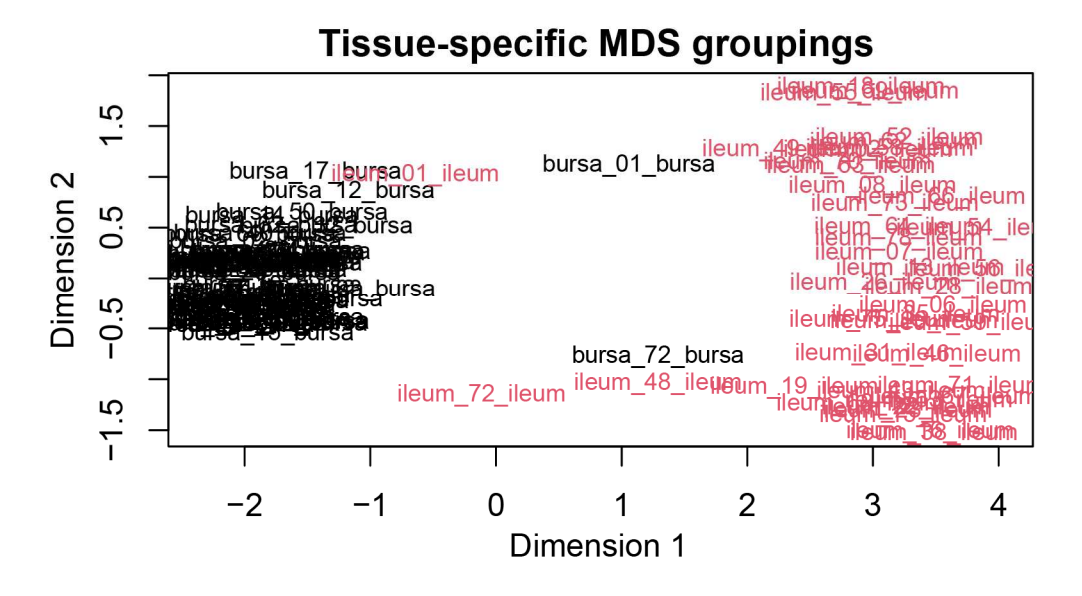


Table 3.1: Sample size used in differential gene expression analyses for uninfected control (C) and LPAIV-infected mallards on one (I1), two (I2), five (I5), 15 (I15), and 29 (I29) days post infection (DPI). Groups I1, I2, and I5 were further divided into low (L), moderate (M), or high (H) viral shedding groups.

Comparison	Tissue	C	I1	I2	I5	I15	I29
Infected vs control	Bursa	8	15	10	15	15	10
	Ileum	5	12	10	13		
Infection by DPI	Bursa		15	10	15	15	10
	Ileum		12	10	13		
		Sample size per shedding group					
		L, M, H					
Shed Level	Bursa		3,6,6	2,4,4	3,6,6		
	Ileum		3,4,5	2,4,4	3,4,6		

To address our hypothesis and predictions, differential gene expression comparisons were conducted separately for ileum and bursa tissues. For our prediction that infection status induces

differential gene expression, we compared LPAIV-infected groups on each DPI to the uninfected control group. For our prediction that LPAIV infection induces differential gene expression over time, we also compared each LPAIV-infected group to each other. For our prediction that virus shed level induces differential gene expression, we conducted analyses for early (I1, I2) and late-stage infection (I5) by comparing high, moderate, and low shed level groups for each DPI.

Additionally, an alternative analysis was conducted for I2 using the Alt.L and Alt.H comparison.

Once analyses were complete, a literature search was conducted for DET/DEGs using search terms "immune response," "influenza virus," and "viral infection" on google scholar.

Genes that were involved with the immune response (Schoggins 2019; Shim et al. 2017; Zhang et al. 2018) were classified as immune genes. Genes previously identified as host cell factors of influenza A virus replication (Dubois, Terrier, and Rosa-Calatrava 2014; König et al. 2010; Peacock et al. 2019; Shaw and Stertz 2017), are similar to influenza host factors, or were involved in the replication of other viruses were classified as potential host cell factors associated with LPAIV replication.

Candidate Gene Analysis

We selected candidate genes based on what is broadly known about the host's immune response to viral infections and more specifically about the avian response to AIV infection (Barber et al. 2013; Evseev and Magor 2019; Huang et al. 2013; Kuchipudi et al. 2014; Ranaware et al. 2016; Santhakumar et al. 2017; Smith et al. 2015; Vanderven et al. 2012). We also selected genes associated with production of sialic acid receptors (i.e. sialyltransferase genes) (Harduin-lepers 2010). Seventy-six search terms were identified based on gene function or name (e.g., interferon, IFIT; Supplemental File S2) for an automated search of the ENSEMBL *Anas platyrhynchos* genome using 'hgnc_symbol' and 'description' fields. This search identified a list of candidate

genes and transcripts which were manually filtered to only include relevant genes. Using only transcripts and genes that showed variability in expression, we used linear mixed models to assess the relationship between gene expression and a bird's virus titer on the day they were sacrificed. Virus titers were adjusted to Log₁₀(virus titer +1) transformed values and gene expression was analyzed as log₂ transformed. Each targeted gene and transcript were assessed separately using automated sub-setting and looping through the dataset. Statistical significance was assessed based on a 0.05 false discovery rate. Sex and DPI were included as fixed effects to account for sex and time-point related differences in gene expression and sequencing pool was a random effect. P-values and conditional R² were reported for each significant model, as well as each LPAIV-infected bird group. The "nlme" R package was used for all linear mixed model analyses (Pinheiro et al. 2007).

Results

All LPAIV-infected birds tested positive for LPAIV as demonstrated by at least one cloacal swab, ileum tissue, or bursa tissue sample with a Ct value <40 on qRT-PCR (Costa et al. 2011), whereas all uninfected control birds tested negative. No individuals died prior to scheduled euthanasia or exhibited signs of disease, such as ruffled feathers, lethargy, or gross pathology.

RNA Sequencing

Library preparations generated \geq 750 M pass filter reads for each lane. Mean quality scores for all libraries were \geq Q30. Bursa tissue samples yielded an average of 9,261,147 raw reads (range: 4,141,232 – 14,172,345) and ileum samples yielded an average of 10,881,788 raw reads (range 6,737,825 – 17,963,033). After filtering, we retained an average of 8,984,110 bursa reads (range: 4,062,211 – 13,742,163) and an average of 10,526,592 ileum reads (range: 6,567,571 – 17,444,644) per individual for analyses.

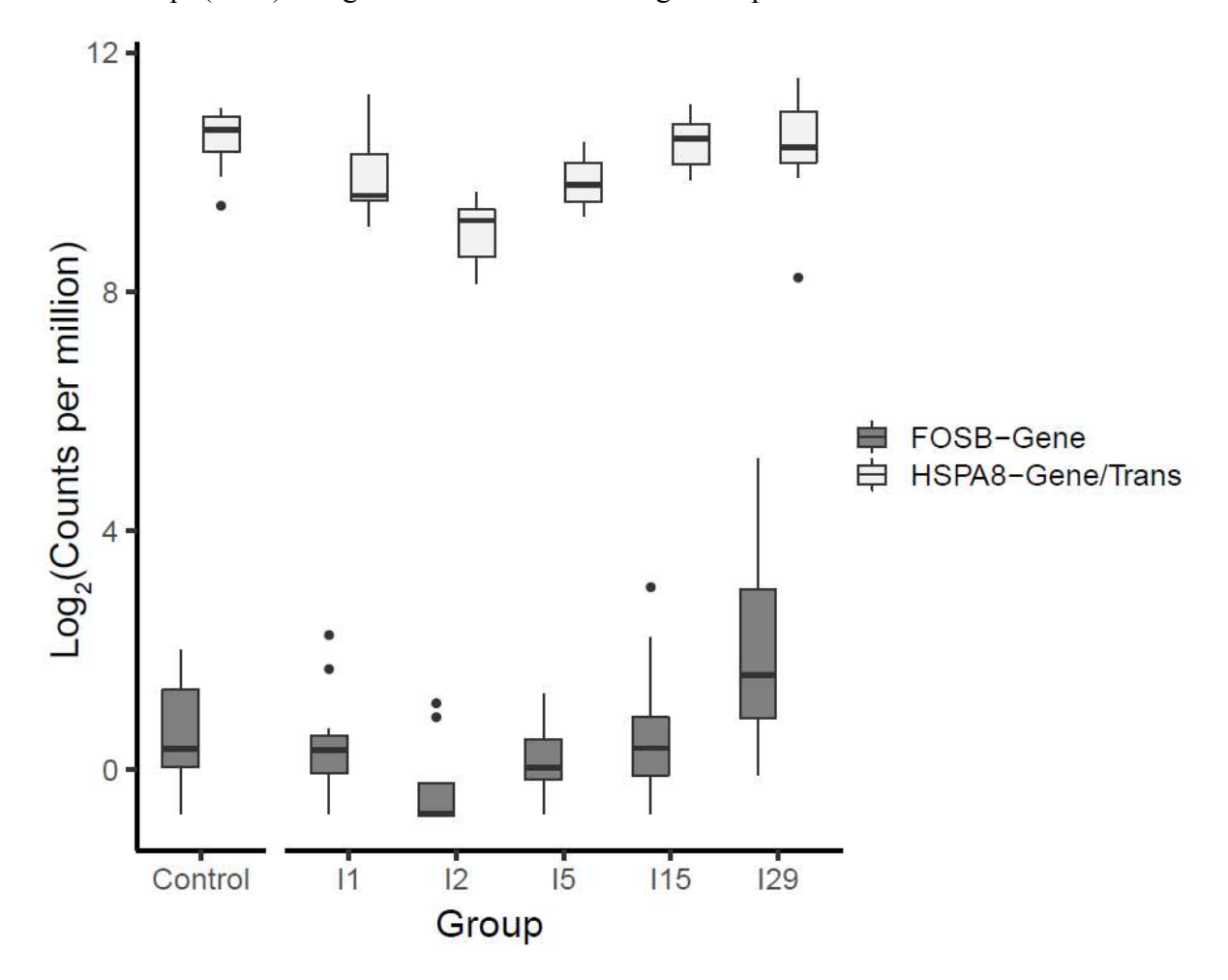
Differential Gene Expression Between LPAIV-infected and Uninfected Control Groups

Differential gene expression was not observed between LPAIV-infected and uninfected control birds at each DPI in the bursa or ileum (Supplemental File S1).

Differential Gene Expression of LPAIV-infected Birds Over Time

Differential expression was only observed between I2 and I29 for LPAIV-infected group comparisons across DPI. One transcript (HSPA8) and two genes (FOSB, HSPA8) were down regulated in I2 compared to I29, and also had similar expression patterns over the course of the infection (Figure 3.4). Both HSPA8 and FOSB were expressed lowest on two DPI, with a gradual increase in expression after two DPI. KEGG pathway analysis revealed four enriched pathways associated only with HSPA8 which included spliceosome, MAPK signaling, protein processing in the endoplasmic reticulum, and endocytosis (detailed results can be viewed in Supplemental File S1).

Figure 3.4: Gene expression of FOSB and HSPA8 in the bursa of uninfected control and LPAIV-infected mallards on one (I1), two (I2), five (I5), 15 (I15), and 29 (I29) days post infection (DPI). Differential expression (FDR <0.1, LFC >0.5) was only observed between I2 and I29. HSPA8 at the transcript (trans) and gene levels had identical gene expression.

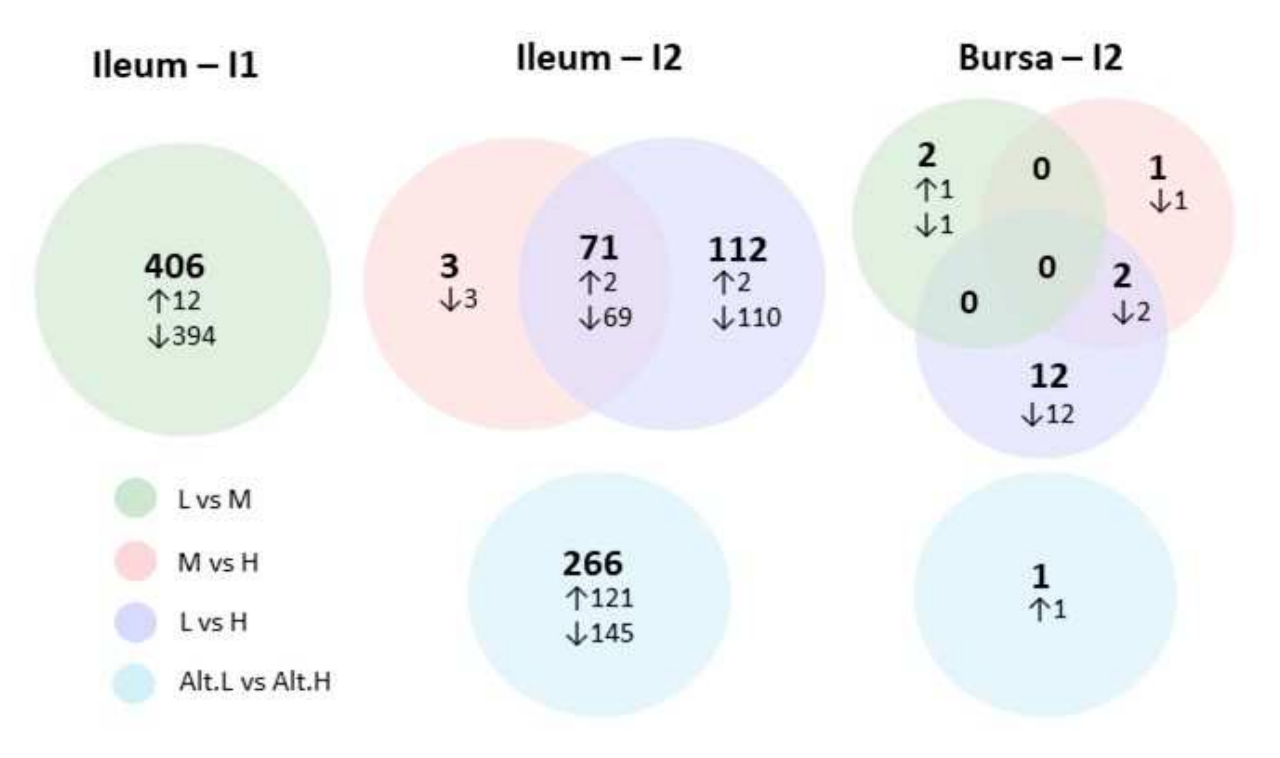


In the ileum, one gene was differentially expressed between LPAIV-infected groups I1 and I2. S100A12, a gene that codes for a calcium binding protein was down regulated in I1 compared to I2. No KEGG pathways were enriched in the ileum.

*Differential Gene Expression Between Virus Shed Level Groups During Early Stage Infection*We observed differential gene expression between shed level groups early in the infection,
mostly in the ileum compared to the bursa (Figure 3.5). In the ileum, we observed 406 DEGs on
one DPI (I1) and 186 DEGs on 2 DPI (I2) between shed level groups. DEGs in I1 were only

observed between low and moderate shedders with 97% of the DEGs up regulated in moderate shedders. DEGs in I2 were observed between high shedders and low/moderate shedders with 98% of the DEGs up regulated in high shedders. We observed 266 DEGs in the I2 alternative shed level comparison (Alt.L vs Alt.H) with 54% of the DEGs up regulated in high shedders. In the bursa, we did not observe any DETs in I1 or I2, but we observed 17 DEGs in I2, 88% of which were up regulated in high shedders. In I2 Alt.L vs. Alt.H, we observed only one up regulated gene in low shedders compared to high shedders. Fold count differences for all DEGs can be viewed in Supplemental File S1.

Figure 3.5: Differentially expressed genes (DEG) between shed level groups (low, moderate, high) of LPAIV-infected mallards in the ileum and bursa on one (I1) and two (I2) days post infection. An additional analysis for I2 divided birds evenly into low and high shedders (Alt.L vs. Alt.H). Each value represents the quantity of DEGs per comparison, and/or shared between comparisons. The arrows reflect the number of DEGs that are up (↑) or down (↓) regulated in the first shed level group listed in each comparison.



In the ileum, KEGG pathways were recognized for DEGs between shed level groups on one and two DPI. On one DPI, KEGG pathways were recognized for 51 out of the 406 DEGs observed which represented a variety of metabolic pathways, cellular processes, signal transduction/cell signaling, the endocrine system, and the immune system (Figure 3.6). Out of all the I1 KEGG pathways recognized, 11 metabolic and two cellular process pathways were enriched (p < 0.05), signifying likely biological significance. On two DPI, KEGG pathways were recognized for 28 out of the 186 DEGs between the three shed level groups (Figure 3.7), and 31 out of the 266 DEGs between Alt.L and Alt.H (Figure 3.8). Enriched pathways on I2 were mostly involved in genetic information processing. Across all shed level analyses, the bursa had only one DEG associated with one KEGG pathway in genetic information processing. Detailed KEGG pathway results can be viewed in Supplemental File S1.

Figure 3.6: KEGG pathways associated with differentially expressed genes (DEG) in shed level group comparisons (low, moderate, high) on one day post infection (I1). KEGG pathways in darker colors indicate statistically enriched pathways (p < 0.05). Abbreviations: biosynthesis (bs), signaling pathway (sp), glycosaminoglycan (ga), glycosphingolipid (gs), phosphate pathway (pp).

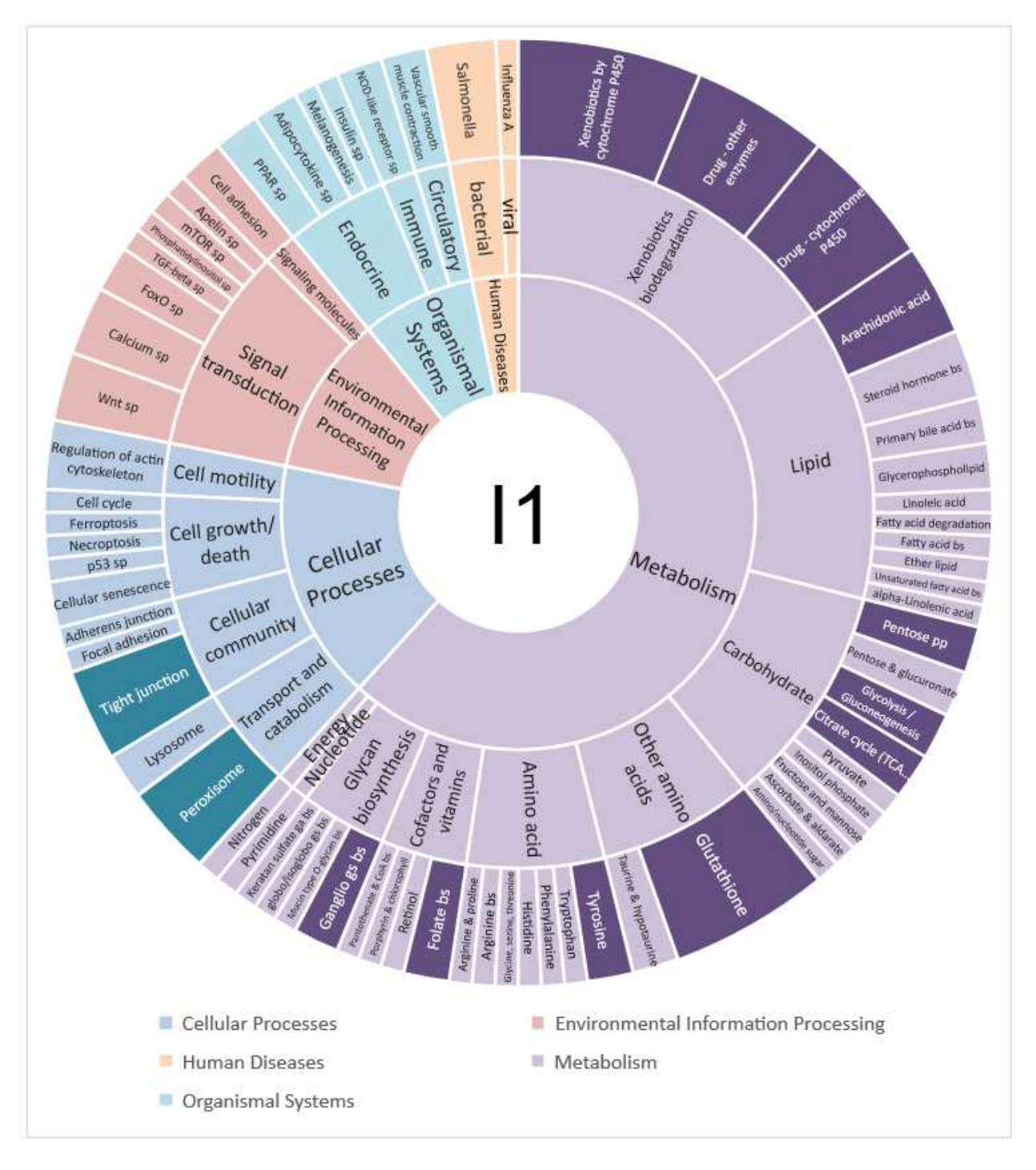


Figure 3.7: KEGG pathways associated with differentially expressed genes (DEG) in shed level group comparisons (low, moderate, high) on two days post infection (I2). KEGG pathways in darker colors indicate statistically enriched pathways (p < 0.05). Abbreviations: signaling pathway (sp), protein processing (pp).

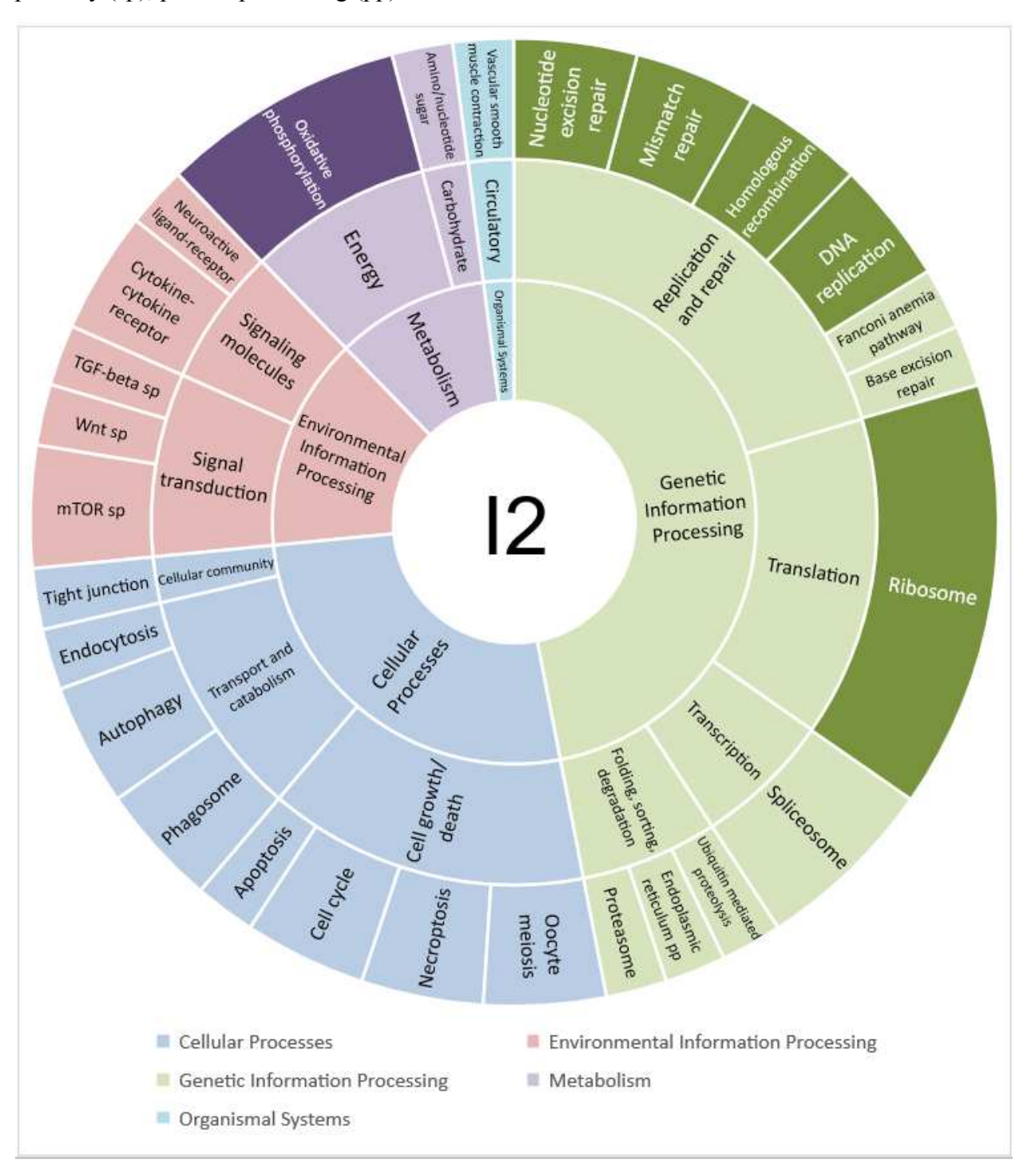
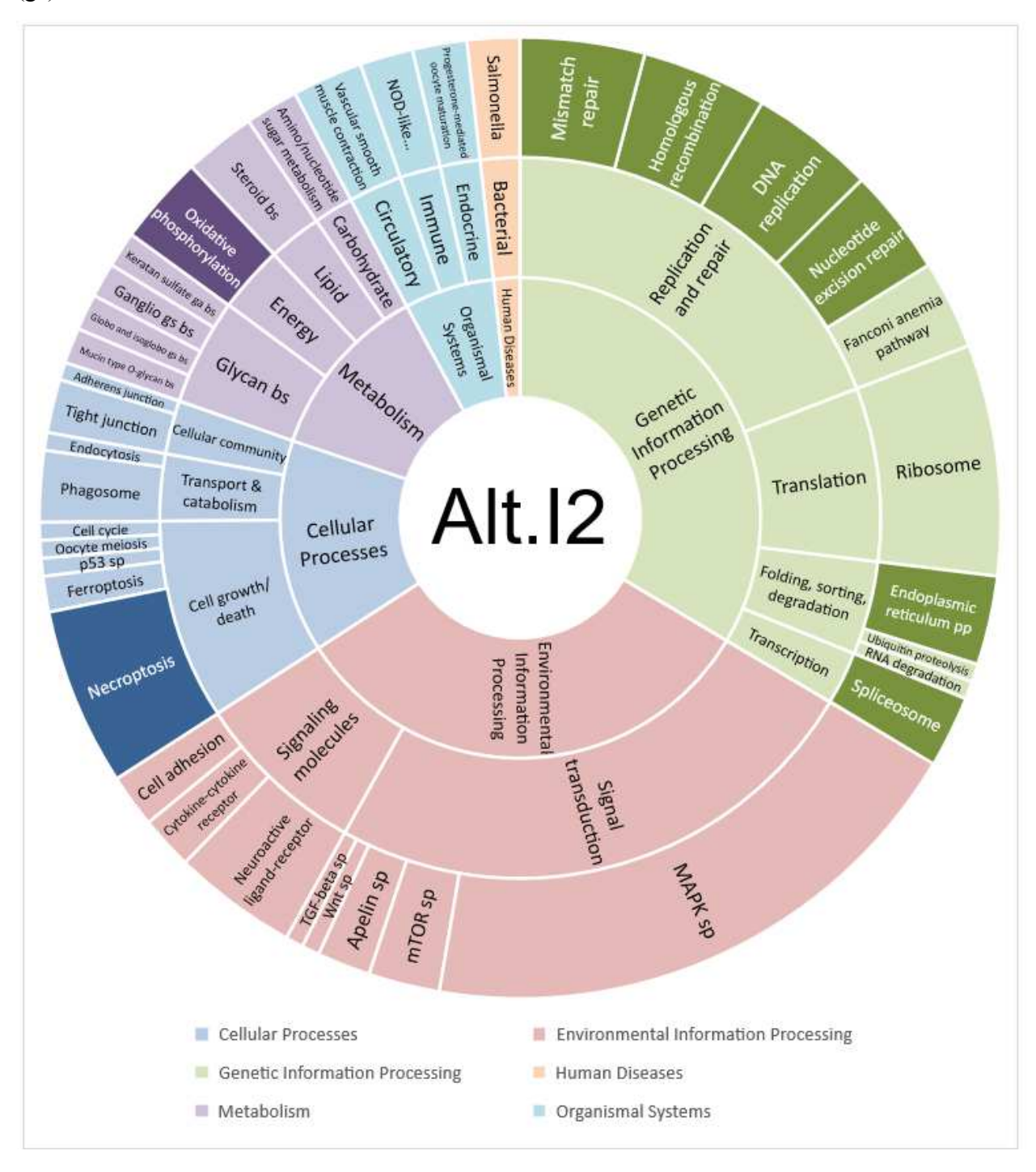
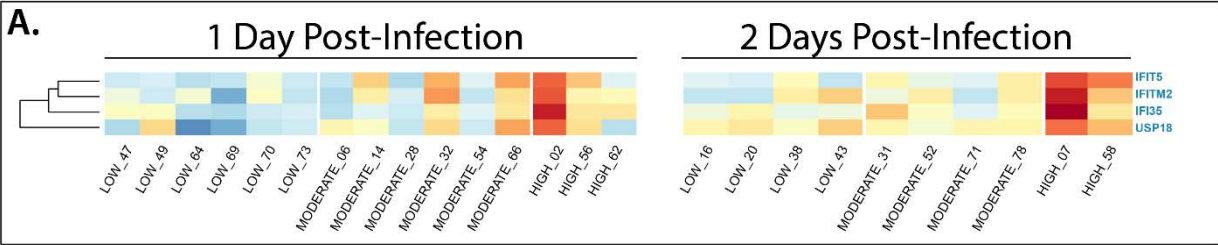


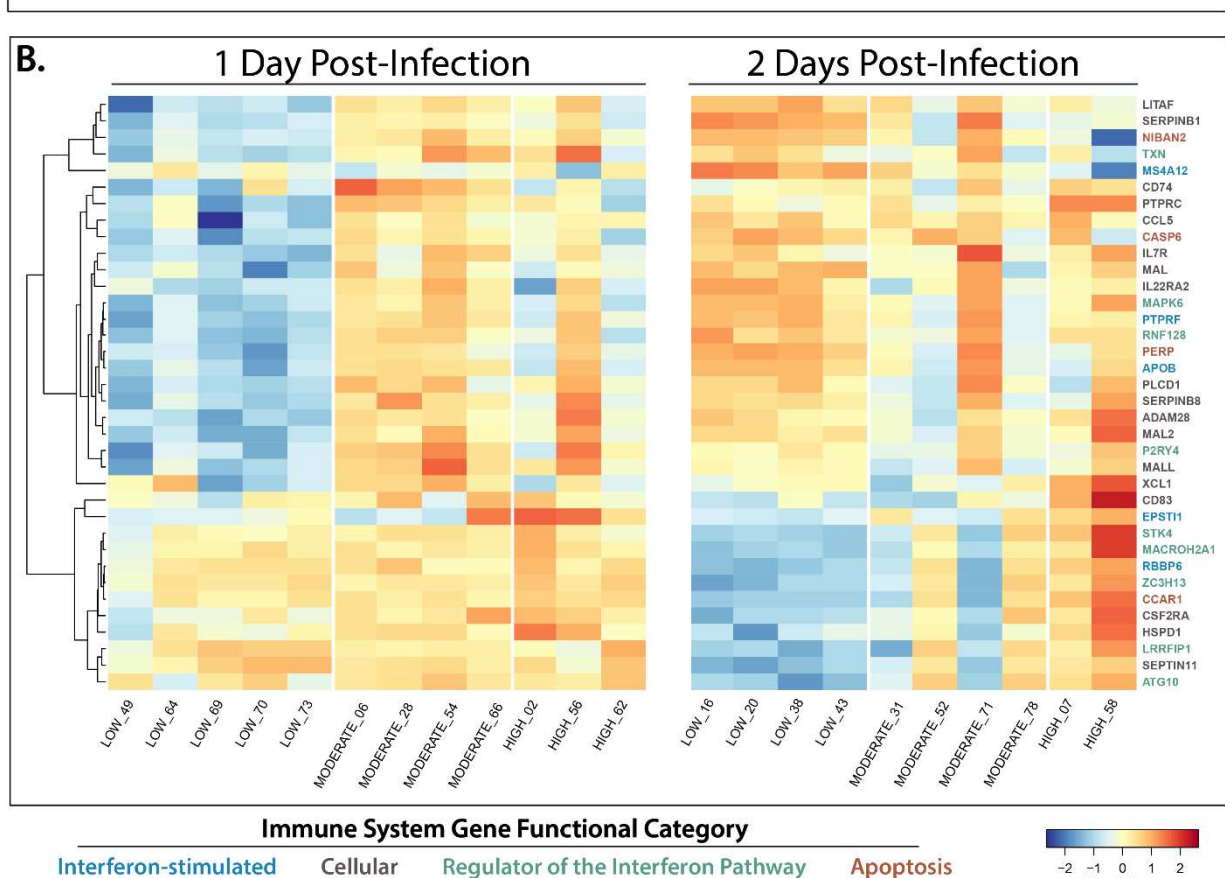
Figure 3.8: KEGG pathways associated with differentially expressed genes (DEG) in alternative shed level group comparisons (Alt.L vs. Alt.H) on two days post infection (I2). KEGG pathways in darker colors indicate statistically enriched pathways (p < 0.05). Abbreviations: biosynthesis (bs), protein processing (pp), signaling pathway (sp), glycosaminoglycan (ga), glycosphingolipid (gs).



Genes of the innate immune system were differentially expressed between shed level groups early in the infection in both the ileum and the bursa. In the ileum, genes of the interferon pathway, cellular immunity, and regulators of apoptosis were differentially expressed between shed level groups on both one and two DPI (Figure 3.9, Table 3.2). In the bursa, interferon-stimulated genes (ISG) were differentially expressed between low and high shedders on two DPI (Table 3.3).

Figure 3.9: Immune genes differentially expressed in the bursa (A) and ileum (B) on one- and two-days post-infection. Individuals and their shed status group are on the x-axis and gene names are on the y-axis. Expression of genes is designated by color corresponding to the row Z-score (distance from the mean). Colors of gene names corresponds to their immune functional category.





83

Table 3.2: Immune genes differentially expressed (DEGs) in the ileum between low (L), moderate (M), and high (H) LPAIV shedders on one (I1) and two (I2) days post infection. Alt.LvH is an alternative shed status grouping scheme that divided birds into two groups rather than three. Comparisons without DEGs are not shown. DEGs are designated by log₂ fold count differences for each comparison. Up regulated genes are positive and down regulated genes are negative corresponding to the first shed level group in each comparison. Gene symbols in parentheses indicate alternative nomenclature. ns = non-significant.

		I1	12			
	Gene	LvM	MvH	LvH	Alt.L v Alt.H	Immune Function
	P2RY4 (P2Y4)	-2.24	ns	ns	ns	ligands of P2RY4 are inhibitors of IFN-α (Shin et al. 2008)
way	MAPK6 (ERK3, PRKM6, MK06)	-1.73	ns	ns	ns	regulator of AP-1 activity, NFκβ activity (Tripathi et al. 2015)
con Path	RNF128 (GRAIL, GREUL1, RN128)	-1.67	ns	ns	ns	pos. reg. TBK1/IFNbeta (Song et al. 2016)
Interfer	TXN (ADF, TRX)	-1.64	ns	ns	ns	AP-1/NFκβ Transcriptional Activity (Hirota et al. 1997)
Regulator of Interferon Pathway	ATG10 (APG10)	ns	ns	-2.31	-1.97	Autophagy, can activate expression of IFN regulating genes (Zhao et al. 2017)
Reg	MACROH2A1 (MH2AFY)	ns	ns	-2.02	-1.54	interferes with binding of NFκβ (Angelov et al. 2003)
	ZC3H13 (KIAA0853, Xio)	ns	ns	-1.78	-1.49	LMP1-mediated NFκβ activation (Gewurz et al. 2012)

Table 3.2 (cont'd)

ıf	HSPD1 (HSP60, CPN60)	ns	ns	-2.06	-1.75	Interacts with IRF3 to enhance IFN-β induction (Lin et al. 2014)
Regulator of Interferon Pathway	STK4 (MST1, KRS2)	ns	ns	-1.76	ns	neg. reg. TBK1-IRF3 signaling (Jorgensen et al. 2020)
Re Interf	LRRFIP1 (TRIP)	ns	ns	-1.68	ns	activation of Type I IFN, increases NFκβ activity (Bagashev et al. 2010; Dai et al. 2009; Shim et al. 2017)
e	APOB (APOBEC)	-3.57	ns	ns	2.79	inhibition of HIV/HepB replication – unknown for AIV (Bonvin et al. 2006; Wang et al. 2008)
ted Gen	PTPRF (LAR)	-1.71	ns	ns	ns	STAT regulation – PTPRK (Chen et al. 2015; Lin et al. 2006)
Interferon Stimulated Gene	EPSTI1 (ESIP1)	ns	ns	-5.61	-5.2	expressed in macrophages exposed to IFNγ (Evseev and Magor 2019; Kim, Lee, and Hahn 2018)
ıterferor	IFIT5 (AvIFIT)*	ns	ns	ns	-4.16	broad anti-viral activity (Rong, Hu, et al. 2018; Schoggins 2019)
I	MS4A12 (FLJ20217)	ns	ns	ns	3.5	enhances IFN-β activation (Zhang et al. 2018)

^{*}Also differentially expressed in the bursa.

Table 3.2 (cont'd)

	MAL (MAL, VIP17)	-2.91	ns	ns	ns	Membrane signaling in T-cells (Alonso and Weissman 1987)
	MAL2	-2.52	ns	ns	ns	Paralog of MAL (Alonso and Weissman 1987)
	MALL (MAL, BENE)	-1.71	ns	ns	ns	Paralog of MAL (Alonso and Weissman 1987)
unity	SERPINB8 (PI8, CAP2, PSS5)	-2.54	ns	ns	ns	restricts pro-inflammatory cytokine production (Bao et al. 2018; Gatto et al. 2013)
Cellular Immunity	SERPINB1 (PI2, MNEI, ELANH2, LEI)	-1.92	ns	ns	2.4	restricts pro-inflammatory cytokine production (Bao et al. 2018; Gatto et al. 2013)
Cellu	LITAF (SIMPLE, PIG7)	-2.45	ns	ns	ns	stimulator of monocytes and macrophages and regulator of TNF-α (Hong et al. 2006)
	CCL5 (TCP228, RANTES, SCYA5)	-2.05	ns	ns	ns	Chemokine: Promotes leukocyte proliferation (Kaiser and Staheli 2013)
	IL7R (CD127)	-1.5	ns	ns	ns	Chemokine receptor (Kaiser and Staheli 2013)
	IL22RA2 (IL22BP, CRF2X, ZCYTOR16)	-2.52	ns	ns	ns	IL-22 receptor subunit: defense/repair to epithelial cells post infections (Perusina Lanfranca et al. 2016)

Table 3.2 (cont'd)

	PLCD1 (PLCδ1, NDNC3)	-1.57	ns	ns	ns	neg. reg. IL-1β/Fcγ mediated phagocytosis in macrophages
	CD74 (HLADG, P33)	-1.56	ns	ns	ns	neg. reg. dendritic cell motility (Kudo et al. 2016; Shaw and Stertz 2017; Zhu, Ly, and Liang 2014)
	ADAM28 (ADA28, ADAM23, MDCL)	-1.3	ns	ns	ns	transendothelial migration of lymphocytes (McGinn et al. 2011)
Cellular Immunity	PTPRC (CD45, T200, GP180, LCA)	-1.05	ns	ns	ns	required for T-cell activation (Chen et al. 2015; Koretzky et al. 1991; Lin et al. 2006)
ellular I	CSF2RA (GMCSFR, CD116)	ns	ns	-3.31	-2.78	macrophage and T-cell regulation (Hercus et al. 2009)
	XCL1 (SCM1, LPTN, LTN)	ns	-3.45	-2.29	ns	dendritic-cell-mediated cytotoxic immune response (Lei and Takahama 2012)
	CD83 (HCD83, BL11, HB15)	ns	ns	-1.88	ns	antigen presentation, MHC class II (Hansell et al. 2007; Kuwano et al. 2007)
	SEPTIN11 (SEPT11)	ns	ns	-1.61	-1.43	required for FcγR-mediated phagocytosis (Huang et al. 2008)

Table 3.2 (cont'd.)

	PERP (KCP1, THW, PIGPC1, KRTCAP1)	-2.59	ns	ns	2.07	p53-dependent apoptosis (Attardi et al. 2000)
Apoptosis	CASP6	-1.45	ns	ns	ns	ZBP1-mediated apoptosis (Zheng et al. 2020)
Арор	NIBAN2 (MINERVA, FAM129B)	-1.19	ns	ns	ns	suppression of apoptosis (Chen, Evan, and Evans 2011)
	CCAR1 (CARP1, DIS)	ns	ns	-1.53	ns	CD437-dependent apoptosis (Rishi et al. 2003)

Table 3.3: Immune genes in the bursa with statistically significant differential expression between low (L) and high (H) LPAIV shedders two (I2) days post infection. Differential expression is designated by log₂fold count differences for each comparison. Up-regulated genes are positive and down-regulated genes are negative corresponding to the first shed level group in each comparison. Gene symbols in parentheses indicate alternative nomenclature.

	Gene	I2 - LvH	Immune Function
Gene	IFIT5 (AvIFIT)*	-6.57	Broad anti-viral activity (Rong, Hu, et al. 2018)
Stimulated Gene	IFITM2 (DSPA2c)	-5.55	Inhibition of viral replication by multiple mechanisms (Brass et al. 2009; Schoggins 2019)
	USP18 (UBP18, ISG43)	-3.56	Neg. reg. type I IFN (Basters, Knobeloch, and Fritz 2018)
Interferon	IFI35 (IFP35)	-3.36	Neg. reg. RIG-I (Das et al. 2014)

^{*}Also differentially expressed in ileum.

DEGs that are host cell factors promoting or inhibiting viral replication, or genes that are related to host factors (paralogs, orthologs), were also found between shed level groups early in the infection (Table 3.4). Inhibitors of viral replication were mostly up regulated in high shedders on two DPI. Host cell factors which support viral replication were differentially expressed on both one and two DPI. Genes involved in viral cell entry were mostly down regulated in low shedders on one DPI, and genes involved in viral transcription, translation, and intracellular transport were up regulated in high shedders on two DPI.

Table 3.4: Host cell factors of viral replication differentially expressed between low (L), moderate (M), and high (H) LPAIV shedders on one (I1) and two (I2) days post infection. Alt.LvAlt.H is an alternative shed level grouping scheme that divided birds into two groups rather than three. Differential expression is designated by log_2 fold count differences for each comparison. Up regulated genes are positive and down regulated genes are negative corresponding to the first shed level group in each comparison. Gene names in parenthesis indicate alternative nomenclature. ns = non-significant.

		II I2					
	Function	Gene	LvM	MvH	LvH	Alt.Lv Alt.H	References
	Cell Entry	H4	ns	ns	ns	3.79	(Hoeksema et al. 2015)
ation	Transcription	RBBP6 (PACT, SNAMA, P2PR, RBQ1, MY038)	ns	-1.9	-2.03	-1.72	(Batra et al. 2018)
eplic	/ Translation	LSM14B (RAP55B)	ns	ns	ns	-1.49	(Mok et al. 2012) ^a
ral R		HNRNPH3 (2H9)	ns	-2.62	-2.53	-1.89	(Wang, Zhou, and Du 2014) ^a
Inhibits Viral Replication	Nuclear Export of Viral mRNA/RNP	HNRNPA2B1 (IBMPFD2, SNRPB1, RNPA2)	ns	-2.25	-2.25	-1.73	(Wang, Zhou, and Du 2014)
Inhi		HNRNPAB (ABBP1)	ns	-1.81	-1.67	ns	(Wang, Zhou, and Du 2014) ^a
		EEF1B2 (EF1B)	ns	ns	-1.64	ns	(Gao et al. 2020) ^a
al		TMPRSS15 (PRSS7, ENTK)	-3.7	ns	ns	ns	(Hayashi et al. 2018)
Promotes Viral Replication	Cell Entry	TSPAN1 (NET1, TM4C, TM4SF)	-2.66	ns	ns	1.39	(Florin and Lang 2018) ^a
	Cen Linuy	TSPAN8 (TM4SF3)	-2.56	ns	ns	ns	(Florin and Lang 2018) ^a
Pr 1		ANXA13 (ISA)	-2.31	ns	ns	ns	(Ampomah et al. 2018) ^a

^aReferences an isoform, paralog, or family of genes related to the corresponding DEG

Table 3.4 (cont'd)

		ANXA2 (ANX2, LPC2D, LIP2, P36)	-1.4	ns	ns	ns	(Ampomah et al. 2018; LeBouder et al. 2008) ^a
		ST3GAL5 (SIAT9, SPDRS, SATI)	-2.25	ns	ns	ns	(Harduin-lepers 2010)
		ST3GAL1 (ST3O, SIATFL, SIAT4A)	-1.62	ns	ns	1.74	(Harduin-lepers 2010)
		EPS8 (DFNB102)	-1.5	ns	ns	ns	(Larson et al. 2019)
uo		EPS8L2 (DFNB106)	-2.07	ns	ns	ns	(Larson et al. 2019) ^a
olicati	Cell Entry	EPS8L3 (HYPT5)	-1.89	ns	ns	ns	(Larson et al. 2019) ^a
ıl Reț		MAL, (MAL, VIP17)	-2.91	ns	ns	ns	(Puertollano et al. 1999)
s Vira		CLTA (LCA)	-1.59	ns	ns	ns	(Wang and Jiang 2009) ^a
Promotes Viral Replication		PLCD1 (PLCδ1, NDNC3)	-1.57	ns	ns	ns	(Kudo et al. 2016; Zhu, Ly, and Liang 2014) ^a
Pro		ATP6V1D (VATD, VMA8)	ns	ns	-2.23	-1.74	(Guinea and Carrasco 1995) ^a
		ATP6V1G1 (ATP6G, VMA10)	ns	ns	-1.72	-1.4	(Guinea and Carrasco 1995) ^a
	Nuclear	DNAJC2 (MPHOSPH11, MPP11, ZRF1, ZUO1)	ns	-2.21	-2.49	-2.02	(Qiu et al. 2006) ^a
	Import of Viral	DNAJC8 (SPF31, HSPC331)	ns	-2.02	-1.9	ns	(Qiu et al. 2006) ^a
3D. C	mRNA/RNP	DNAJC21 (DNAJA5, GS3, JJJ1, BMFS3)	ns	ns	-1.84	ns	(Qiu et al. 2006) ^a

^aReferences an isoform, paralog, or family of genes related to the corresponding DEG

Table 3.4 (cont'd)

	Nuclear Import of Viral mRNA/RNP	ST13 (HIP, AAG2, SNC6)	ns	ns	-1.71	ns	(Shi, Zhang, and Zheng 2007)
		ROS1 (MCF3)	-2.38	ns	ns	ns	(Klempner and Ou 2017; Kumar et al. 2011)
		ATP1A1 (CMT2DD)	-1.83	ns	ns	ns	(Mi et al. 2010) ^a
ion		CTSH (ACC4, ACC5, CPSB)	-1.03	ns	ns	ns	(Coleman et al. 2018; Edinger et al. 2015) ^a
plicati		SNRPD1 (SMD1, SNRPD)	ns	ns	-2.62	ns	(Dubois, Terrier, and Rosa- Calatrava 2014)
al Re	Transcription / Translation	SEC61G (SSS1)	ns	ns	-2.19	ns	(Heaton et al. 2016)
Promotes Viral Replication		CDK6 (PLSTIRE, CDKN6, MCPH12)	ns	ns	-2.17	-1.79	(Zhang, Li, and Ye 2010) ^a
mote		CCNK (CPR4, IDDHDF)	ns	-2.16	-2.15	-1.78	(Zhang, Li, and Ye 2010) ^a
Pro		CDK11A (CDC2L3, P58GTA, PITSLRE)	ns	-1.96	-1.87	ns	(Zhang, Li, and Ye 2010) ^a
		CCNI (CYI, CYC1)	ns	ns	2.73	1.96	(Zhang, Li, and Ye 2010) ^a
		RRP15 (KIAA0507, CGI115)	ns	ns	-1.82	ns	(Su et al. 2015) ^a
		PRPF38B (NET1)	ns	ns	-1.77	ns	(Minakuchi et al. 2017) ^a
	·	SNRPD3 (SMD3)	ns	ns	-1.67	ns	(Dubois, Terrier, and Rosa- Calatrava 2014) ^a

^aReferences an isoform, paralog, or family of genes related to the corresponding DEG

Table 3.4 (cont'd)

		YTHDC1 (KIAA1966, YT521)	ns	ns	-1.59	ns	(Bayoumi, Rohaim, and Munir 2020)
ā	Transcription / Translation	DNAJA1 (HSPF4, HSJ2, NEDD&, DNAJ2)	ns	ns	ns	-1.51	(Cao et al. 2014)
Viral Replication	/ Translation	HSP90AA1 (HSP90, HSPCA, HSP86, HSP89, LAP2, HSPN, EL52)	ns	ns	ns	-1.36	(Naito et al. 2007)
iral R	Nuclear Export of	HSPA8 (HSC70, HSP73, LAP1, NIP71)	ns	ns	ns	-1.25	(Stricher et al. 2013)
	Viral mRNA/RNP	RANBP1 (HTF9A)	ns	ns	ns	-1.19	(Predicala and Zhou 2013) ^a
Promotes		RAB11B (YPT3, NDAGSCW)	-1.92	ns	ns	ns	(Amorim et al. 2011; Bruce, Digard, and Stuart 2010)
d	Cell Exit	HSPA5 (BIP, GRP78)	ns	ns	ns	-1.23	(Hogue and Nayak 1992; Singh et al. 1990)
		SEPTIN11 (SEPT11)	ns	ns	-1.61	-1.43	(Tokhtaeva et al. 2015) ^a

^aReferences an isoform, paralog, or family of genes related to the corresponding DEG

Differential Gene Expression Between Virus Shed Level Groups During Late Stage Infection

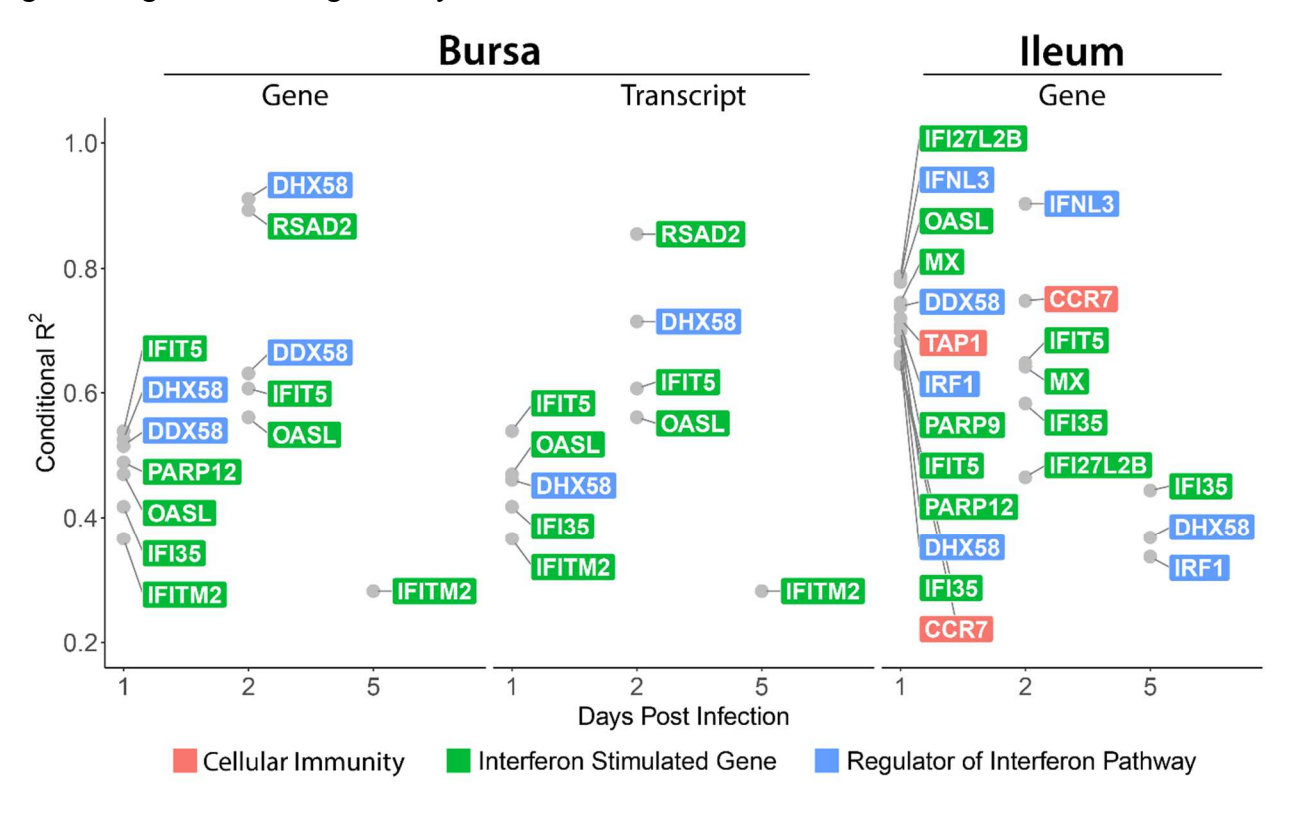
Differential expression was not observed between shed level groups during late-stage infection

(I5) at the gene or transcript level in the bursa or ileum (Supplementary File S1).

Candidate Gene Analysis

Manual identification of candidate gene names in the mallard reference genome resulted in 268 candidate genes and 433 candidate transcripts that we assessed for associations with viral shedding rates (Supplemental File S2). Eleven genes and seven transcripts in the bursa had significant positive linear relationships with cloacal virus titers. Thirteen genes in the ileum had significant positive linear relationships with cloacal virus titers. No genes or transcripts had negative linear relationships. All significant candidate genes have functions relating to the host immune system (Figure 3.10), and no sialyltransferase candidate genes had statistically significant linear relationships with cloacal virus titers. Expression levels of most genes were significantly associated with virus titers early in the infection (I1, I2), but not late in the infection (I5).

Figure 3.10: Conditional R^2 values for candidate genes with significant (p <0.05) linear relationships to cloacal swab virus titers on one, two, and five days post infection (DPI). All significant relationships were positive. Candidate genes in the bursa were evaluated at the gene and transcript level. Candidate genes in the ileum were only evaluated at the gene level. Immune gene categories are designated by color.



PRRs DDX58 (RIG-I) and DHX58 (LGP2), along with several ISGs were among the candidate genes with significant linear relationships to virus titers. In the bursa, higher conditional R² values were observed on two DPI compared to one DPI (Figure 3.10). Higher R² values were observed in the ileum on one DPI compared to the bursa on one DPI. Both tissues had few significant relationships on five DPI with significantly lower R² values. Detailed candidate gene analysis results can be viewed in Supplemental File S3.

Discussion

Individual heterogeneity in pathogen load can alter the magnitude and duration of infectious disease outbreaks; hence, understanding the host intrinsic factors associated with variation in pathogen shedding is key. Here, we evaluated the variation in tissue-specific gene expression as

it relates to infection status, DPI, and pathogen load in LPAIV-infected mallards to obtain a better understanding of the molecular mechanisms underlying intraspecific variation in pathogen shedding. Our findings not only provide evidence that gene expression of the host innate immune system is closely associated with viral shedding, but also provide insight into the host cell machinery utilized by the virus to successfully replicate. These data improve the current understanding of avian host genes involved in LPAIV-infections and the molecular mechanisms associated with viral shedding magnitude.

The ileum and bursa are main sites of LPAIV binding and replication in ducks (Costa et al. 2012; Daoust et al. 2011; Webster et al. 1978); therefore, we assessed both tissues to determine the association between cloacal viral shedding and gene expression. Cloacal shedding was measured because it can be repeated over time, and because it represents the transmissible fraction of virus, thus providing a direct link to questions of transmission dynamics. Innate immune gene expression was positively related to cloacal virus titers in both tissues; however, higher R² values were observed in the ileum on one DPI (Figure 3.10), indicating a stronger relationship (Kasuya 2019). Also, early in the infection, significantly more DEGs were observed in the ileum compared to the bursa between shed level groups (Figure 3.9). Differences in gene expression between the ileum and bursa were previously observed in LPAIV H7N1-infected ducks when Cornelissen et. al (2012) found that PRR gene expression was higher in the ileum than the bursa on one DPI. Collectively, these results may suggest that the ileum is more involved than the bursa in the initiation of the immune response and variation in viral shedding.

Contrary to other studies (Cornelissen et al. 2012; Fleming-Canepa et al. 2019; Maughan et al. 2013; Smith et al. 2015; Vanderven et al. 2012) and despite our lenient DEG screening criteria, we did not observe differential gene expression between LPAIV-infected and uninfected

mallards, nor did we observe many DEGs between the collective group of LPAIV-infected birds at different time points post infection. We hypothesize this difference between our findings and previous studies is due to the extreme individual viral load variation observed in LPAIV-infected wild mallards (Arsnoe, Ip, and Owen 2011; Dolinski, Jankowski, et al. 2020; Jankowski et al. 2013), which was closely associated with gene expression in our results. We demonstrated positive relationships between viral shedding and gene expression for select immune genes and also showed that low viral shedders had similar gene expression to uninfected control birds (Supplemental File S3). In previous studies comparing gene expression between LPAIV and highly pathogenic AIV (HPAIV) infected ducks, LPAIVs elicit lower magnitudes of gene expression than HPAIV (Fleming-Canepa et al. 2019; Smith et al. 2015; Vanderven et al. 2012). We hypothesize that the limited host response to LPAIV combined with high genetic variability of wild birds (Svobodová et al. 2020) is preventing detection of statistically significant differences between uninfected and LPAIV-infected birds. These results may suggest that in wild mallards, genes of the innate immune system are more influenced by viral load than just by infection status alone; therefore, gene expression studies of LPAIV-infected wild mallards should not only evaluate infection status, but also incorporate individual variation of virus shed.

Immune genes differentially expressed between shed level groups on one and two DPI supports our prediction that viral shedding is closely associated with innate immunity early in the infection. Several of the up-regulated immune DEGs in higher shedding birds are involved in the interferon pathway (Table 3.3), which is characterized by PRRs recognizing intracellular viruses, initiating the transcription of type I and II interferons, and leading to the production of antiviral ISGs (Santhakumar et al. 2017). Several of the DEGs involved in interferon pathway regulation have not been identified in previous AIV infection studies, such as P2RY4, MAPK6, RNF128,

ATG10, MACROH2A1, ZC3H13, STK4, and LRRFIP1; however, thioredoxin (TXN2) was down regulated in LPAIV-infected chickens (Ranaware et al. 2016). Antiviral ISGs up regulated in high shedders such as IFIT5, EPST11, IFITM2, USP18, and IFI35 were also up regulated in previously AIV-infected poultry (Evseev and Magor 2019; Rohaim et al. 2018; Smith et al. 2015). Among the regulators of the interferon pathway, we observed mediators of transcription factors NFκβ (Hayden, West, and Ghosh 2006) and AP-1 (Foletta, Segal, and Cohen 1998) up regulated in high and moderate shedders compared to low shedders, but differential expression was not observed for the transcription factors themselves. While our results show that regulation of the interferon pathway and viral load are closely related, we cannot conclude mechanistically how these genes contribute to the overall immune response. We also cannot conclude whether gene expression is influencing viral load or if viral load is influencing gene expression. Future research is warranted to determine the molecular pathways influencing or that are influenced by viral replication.

Furthermore, we detected statistically significant positive relationships between viral shedding and expression of immune genes in both the ileum and bursa (Figure 3.10). PRRs such as DDX58 (RIG-1) and DHX58 (LGP2), and ISGs such as IFIT5, IFITM2, OASL, RSAD2, MX, PARP12 were also previously up-regulated LPAIV-infected ducks (Barber et al. 2013; Cao et al. 2017; Ranaware et al. 2016; Vanderven et al. 2012; Zhang et al. 2020). Our results are consistent with previous studies that also found positive associations between viral load and immune genes (Cornelissen et al. 2012; Smith et al. 2015). These results provide further evidence of the close relationship between viral shedding and the host immune response.

Differential gene expression between shed level groups differed between one and two DPI (Figure 3.9, Table 3.3). We hypothesize these DPI-dependent immune gene expression

differences were influenced by the expression of the non-immune DEGs also observed, some of which are known to promote influenza A virus replication (Dubois, Terrier, and Rosa-Calatrava 2014; König et al. 2010; Peacock et al. 2019; Shaw and Stertz 2017). In the ileum on one DPI, two sialyltransferases of SAα2,3Gal plus other pro-viral genes involved in cell entry were up regulated in moderate shedders compared to low shedders (Table 3.4). Up regulation of sialyltransferases in the ileum was expected since previous work detected a statistically significant positive relationship between LPAIV shedding and SAα2,3Gal in ileum enterocytes of mallards (Dolinski, Jankowski, et al. 2020). Most viral cell-entry DEGs on one DPI were not differentially expressed on two DPI, which is expected given the variation in the virus's latent period, which in poultry ranges from one to two days (Van der Goot et al. 2003). Likely, the variation in viral shedding on one DPI is dependent upon the latent period and viral cell-entry, which is a factor driving the differences in immune gene expression between one and two DPI.

Another key difference between DEGs for shed level groups on one and two DPI are the biological processes associated with the DEGs on each DPI. In the ileum on one DPI, many of the DEGs had biological processes associated with metabolism (Figure 3.6). In chickens infected with HPAIV H5N1, lipid metabolism was also enriched on one DPI (Smith et al. 2015). Metabolic functions are commonly linked to viral infections (Sanchez and Lagunoff 2015) with lipid metabolism (Zhou, Pu, and Wu 2021) and cellular kinases (Meineke, Rimmelzwaan, and Elbahesh 2019) most associated with influenza infections. Smith et. al (2015) suggested that membrane trafficking due to viral cell entry early in the infections was likely the reason for increased lipid metabolism since the cell membrane is made of primarily phospholipids. Interestingly, cholesterol metabolism was recently associated with super-shedding cattle infected with *E.coli* O157 (Wang et al. 2017), which is also an intestinal pathogen. On two DPI in the

ileum, fewer metabolic genes were differentially expressed, and a higher proportion of DEGs were associated with genetic information processing pathways (Figure 3.7 and Figure 3.8). Many of the DEGs up regulated in high shedders on two DPI promote transcription, translation, and nuclear transport of influenza A viruses (Table 3.4). Genes involved in viral entry up regulated in high shedders on one DPI and genes involved in promoting viral transcription/translation up regulated in high shedders one two DPI follows the timeline of the influenza A virus life cycle (Watanabe, Watanabe, and Kawaoka 2010) early in the infection. Even though we cannot confirm mechanistically that these genes are involved in LPAIV replication in mallards, our results highly suggest this may be the case; therefore, future research should focus on the DEGs reported here to understand the molecular mechanisms involved.

The variety of DEGs between virus shed level groups showcases the complexity of host cell activity during active LPAIV replication in mallards. At five DPI, when viral shedding is decreasing and production of LPAIV-antibodies are detected (Suarez and Schultz-Cherry 2000), we did not observe any DEGs between shed level groups. Hence, our prediction that genes of the adaptive immune system would be differentially expressed later in the infection is not supported. Early in the infection we did observe cellular immunity DEGs between shed level groups in the ileum on one and two DPI that are involved in T-cell regulation and MHC class II expression (Table 3.2). CD4+ T-helper cells recognize antigen presentation on MHC class II molecules of dendritic cells which leads to B cell activation for the production of antibodies (Bonilla and Oettgen 2010; Chen et al. 2018; Davison, Magor, and Kaspers 2008). Our results suggest that immune cell mechanisms that lead to adaptive immunity, as it may relate to viral load, occurs earlier in the infection than we had expected.

Most differential expression observed was between shed level groups on one and two DPI; however, two genes: FOSB and HSPA8, were down regulated in the bursa between LPAIV-infected groups 12 and 129. Interestingly, both these genes had similar expression profiles over the course of the infection (Figure 3.4). FOSB is a transcription factor subunit for AP-1 which is a transcription factor for induction of IFN-beta (Foletta, Segal, and Cohen 1998), and HSPA8 (aka hsc70) mediates viral production by binding to viral protein M1 and NP transporting these viral proteins from the nucleus to the cytoplasm after replication (Stricher et al. 2013; Watanabe et al. 2006). The expression profile of these two genes suggests that LPAIV infection may down-regulate these genes early in the infection in the bursa; however, in the ileum, HSPA8 was upregulated in the top half of higher shedding birds on two DPI (Table 3.4, Alt.LvH). These results could suggest that a lack of HSPA8 down regulation in the ileum could be a major contributing factor for higher shedding individuals. More gene-specific research analyzing the biological mechanisms of LPAIV infections is needed to confirm the molecular mechanisms involved.

Even though we found gene expression was associated with viral shedding, our results suggest that assigning the top 20% of birds as the highest shedders may not be the best determination for detecting the genetic factors associated with super-shedding individuals. Our differential expression analysis between the three shed-level groups on two DPI revealed that the moderate group had two individuals with similar gene expression as the high shedding group and two individuals had similar gene expression with the low shedding group. Results from the alternative differential expression analysis on two DPI, where birds were divided into two equal high and low shedding groups, revealed an additional 166 genes to be differently expressed between low and high shedders. These results could indicate that gene expression differences

related to viral load are not necessarily unique to the top 20% of birds, but perhaps a particular virus titer threshold that is yet to be determined.

Collectively, we have identified specific genes and biological processes in the ileum and bursa of LPAIV-infected mallards that are associated with viral shedding heterogeneity; however, this study alone does not confirm an inherent genetic difference between supershedders and non-super-shedders. The differential gene expression and linear mixed model analyses conducted determined associations between viral shedding and gene expression, but they do not imply a cause and effect; therefore, it is unknown whether gene expression is related to an inherent difference between individuals or as a response to the viral infection itself. We expect the genes identified in this study to undergo further examination, utilizing SNP technology and gene-knockout studies to fully understand the molecular mechanisms contributing to viral load variation.

We know that identifying and removing super-shedders is a method of controlling outbreaks as evidenced by modeling the super-shedders of *E.coli* O157-infected cattle (Matthews, Low, et al. 2006). If the individuals with the propensity to be the super-shedders can be determined prior to pathogen exposure, new strategies for outbreak prevention could be realized. This future research depends on applying the knowledge gained from exploratory studies like this one, as well as performing similar studies in multiple host-pathogen systems, to gain a better understanding of how individual host variation contributes to the complexity of disease transmission dynamics. With more knowledge gained, the more tools wildlife managers and public health officials will have to better predict and control future outbreaks.

CHAPTER 4: DIFFERENTIAL GENE EXPRESSION REVEALS HOST FACTORS FOR VIRAL SHEDDING VARIATION IN BLUE-WINGED TEALS (SPATULA DISCORS) INFECTED WITH LOW-PATH AVIAN INFLUENZA VIRUS

By: Amanda C. Dolinski^{1*}, Jared J. Homola^{1*}, Mark D. Jankowski^{1,2}, John D. Robinson¹, Jennifer C. Owen^{1,3}

*These authors contributed equally

- 1. Department of Fisheries and Wildlife, Michigan State University, East Lansing, MI
- 2. U.S. Environmental Protection Agency, Region 10, Seattle, WA 98101
- 3. Department of Large Animal Clinical Sciences, Michigan State University, East Lansing, MI, USA

Abstract

Intraspecific variation in host infectiousness affects disease transmission dynamics in many wildlife host-pathogen systems including avian influenza virus (AIV); therefore, understanding host factors that contribute to this variation is important for understanding, controlling, and preventing future outbreaks. In this study, we evaluate viral shedding and gene expression in LPAIV-infected blue-winged teals (*Spatula discors*) at various time points post infection to understand the host genetic factors associated with intraspecific variation in pathogen load. Using transcriptomic data, we found that host genes were associated with LPAIV infection. Most differential gene expression was observed in the ileum between infected and uninfected birds early in the infection and between viral shed level groups later in the infection. Genes of the innate immune system had positive linear relationship with cloacal viral shedding. These findings will assist future researchers in determining the molecular mechanisms driving replication and variation in viral load in LPAIV wildlife reservoirs.

Introduction

Determining host factors driving wildlife reservoir competence for zoonotic and other pathogens is crucial to understanding how wildlife hosts contribute to the persistence and distribution of pathogens. Heterogeneity in transmission rates, for example, have an impact on pathogen

transmission dynamics, where only a few infectious individuals, known as "super-spreaders," disproportionately influence the intensity of a disease outbreak (Lloyd-Smith et al. 2005; Woolhouse et al. 1996). One factor of heterogeneity in transmission rate is infectiousness, where "super-shedders," defined as individuals that yield many more infectious units of a particular type than most other individuals in the same host species (Chase-Topping et al. 2008), are responsible for the majority of secondary transmissions. Lloyd-Smith et. al (Lloyd-Smith et al. 2005) predict that if the highly infectious individuals can be identified, the efficacy of outbreak control can be greatly increased. Targeting super-shedders as a control method was demonstrated with cattle heterogeneously infected with Escherichia coli O157, whereby removing individuals with high fecal bacterial carriage >10⁴ colony-forming units per gram (cfu/g) reduced the reproductive number, R₀ (i.e., the average number of secondary transmissions per infected individual), below one, thus reducing prevalence and halting the outbreak. By understanding the host factors that contribute to individual pathogen load heterogeneity in wild animal populations, better management strategies could be developed to control and prevent the spread of zoonotic diseases.

Wild waterfowl are important hosts in the ecology of avian influenza virus (AIV) as a natural wildlife reservoir for low pathogenic avian influenza viruses (LPAIV) (Webster et al. 1992). Wild birds infected with RNA viruses, including mallards (*Anas platyrhynchos*) infected with LPAIV, have been shown to shed (replicate and excrete from the body) virus according to the pareto principle, where 20% of the individuals are responsible for 80% of the overall virus shed (Jankowski et al. 2013). Highly pathogenic avian influenza viruses (HPAIV), some of which are zoonotic, are the cause of human fatalities and devastating impacts to the poultry industry worldwide (Swayne 2009). HPAIVs are known to emerge from domestic poultry

infected with LPAIV potentially originating from wild birds (Duan et al. 2007; Monne et al. 2014). The blue-winged teal (*Spatula discors*; hereafter referred to as teals), a common dabbling duck species of North America (Rohwer, Johnson, and Loos 2002), is one species frequently infected with LPAIV (Carter et al. 2019; Papp et al. 2017; Stallknecht et al. 1990) and has been implicated in introducing AIV to poultry flocks in the United States (US) (Lee et al. 2017). For example, a strain of HPAIV H7N9 that caused high morbidity and mortality in US poultry in 2017 shared a high level of nucleotide identity to an LPAIV H7N9 strain isolated from a bluewinged teal in Wyoming, US the previous year (Lee et al. 2017). Teals are also implicated in maintaining LPAIV over winter along the Atlantic gulf coast of the US (Ferro et al. 2010; Hanson et al. 2005), which could be a factor for introducing the virus to naïve migrating waterfowl in the spring. Given their importance as a wildlife reservoir for LPAIV, blue-winged teals are an ideal candidate for studying host factors responsible for heterogeneity in LPAIV infectiousness.

Several prevalence studies show blue-winged teals frequently infected with LPAIV in the wild (Carter et al. 2019; Papp et al. 2017; Stallknecht et al. 1990); however, experimental studies assessing heterogeneity in infectiousness among blue-winged teals is lacking. Previously published data showed that blue-winged teals shed LPAIV H5N9 in a similar pattern to mallards with viral shedding beginning at one day post inoculation (DPI) and 98.7% of the total viral load being shed during the first five DPI (Dolinski, Jankowski, et al. 2020). During peak viral shedding (1-3 DPI), teals had virus titers which ranged from 2.46 Log₁₀(EID₅₀/mL) to 6.16 Log₁₀(EID₅₀/mL), indicating significant variation in viral load. Identifying the intrinsic factors associated with this high variation in viral load is crucial for understanding LPAIV transmission dynamics.

The objective of this study was to determine if LPAIV in blue-winged teals generates tissue-specific gene expression responses associated with individual heterogeneity in viral load. Previous studies in AIV-infected domestic poultry have shown genes of the innate immune system, consisting of the interferon pathways and cellular immunity, up-regulated in infected birds (Cornelissen et al. 2012; Huang et al. 2013; Ranaware et al. 2016; Smith et al. 2015; Vanderven et al. 2012); however, full transcriptomic analyses of LPAIV-infected wild ducks are lacking. We hypothesized that LPAIV infections are associated with gene expression in bluewinged teals, similar to our previous study in mallards (Chapter 3). Specifically, we predicted that gene expression would differ (1) between infected and uninfected birds, (2) between days post-infection, with innate immunity genes expressed early in the infection and adaptive immunity genes expressed later in the infection, and (3) between birds with various viral shedding levels. Our approach included transcriptome wide mRNA sequencing of LPAIV replication sites, the ileum and bursa of Fabricius (hereafter referred to as "bursa") (Daoust et al. 2011), to discover associated genes and to evaluate a select set of candidate genes involved in immunity and viral binding. These data and analyses provide new knowledge for virologists and disease ecologists concerning the genetic factors associated with LPAIV infections in bluewinged teals and individual variation in viral load.

Methods

Permits and Protocols

Protocols for animal care and experimental sampling procedures were approved by Michigan State University (MSU) Institutional Animal Care and Use Committee (AUF 12/16-211-00). All euthanasia procedures were performed in accordance with the Animal Welfare Act and Guidelines to the Use of Wild Birds in Research (Fair, Paul, and Jones 2010). Duck eggs were

collected with permission from the U.S. Fish and Wildlife Permit (M Bl 94270-2) and North Dakota Game and Fish Department License #GNF03639403.

Birds and Virus

Teals were collected in ovo (n=80, 1-2 eggs per nest) from wild teal nests in uncultivated fields of Towner County, North Dakota, USA (48.443, -99.316) and shipped to Michigan State University (MSU). Egg incubation, hatching, and bird rearing was conducted in a climate controlled animal containment facility at MSU according to protocols previously described (Dolinski, Jankowski, et al. 2020).

LPAIV A/northern pintail/California/44221-761/2006 (H5N9) was acquired from the USGS National Wildlife Health Center in Madison, WI (USDA Veterinary Permit 44372). The virus was propagated in embryonated pathogen free chicken eggs (Charles River, Norwich, CT, USA) at MSU under biosafety level two laboratory conditions (Woolcock 2008). The propagated virus (stock) had a viral titer of 7.63 log EID₅₀/ml calculated using the Reed-Munch 50% egg infectious dose method (Reed and Muench 1938). Inoculum for experimental infection was generated by diluting the stock virus in Dulbecco's Modified Eagle Medium (DMEM; Gibco® by Life Technologies, Grand Island, NY, USA) to a concentration of 5.63 log EID₅₀/ml.

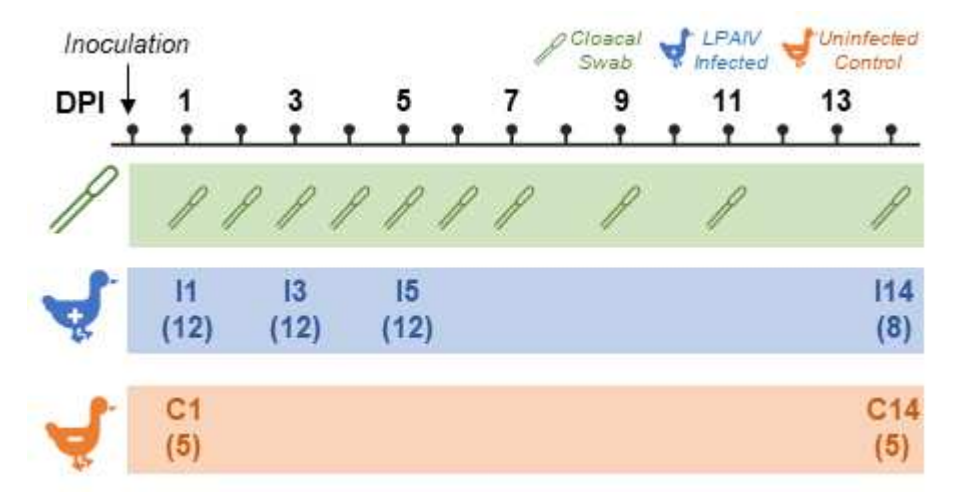
Experimental Design

Birds that survived to the experimental phase (n = 54; 9-12 weeks of age) were divided into LPAIV-infected (n = 44) and uninfected control groups (n = 10). Viral inoculum (1.0mL) was administered to LPAIV-infected birds with one drop in each eye and nare, and the rest in the bird's esophagus. Birds in control groups were sham-inoculated with sterile DMEM in a similar fashion. Birds were kept under biosafety level two conditions during and post inoculation where

personal protective equipment of Tyvek suits, plastic booties, double gloves, full coverage non-vented safety eye goggles, hair cap, and N95 respirators were worn by all personnel.

Bird groups were further subdivided into four LPAIV-infected and two uninfected control groups based on DPI of sacrifice (Figure 4.1). Groups were determined by pseudo-stratified randomization based on body mass, age on day of inoculation, sex, and nest (Dolinski, Jankowski, et al. 2020). Sex was determined by the color of the feathers on the speculum of the wing (Carney 1992), and no two birds from the same nest were placed in the same group. Body mass for group assignments was standardized based on weight at 55 days old, when birds were considered full grown.

Figure 4.1: Experimental timeline of sample collection days post infection (DPI). Groups are designated by infection status (I = LPAIV-infected, C = uninfected control), DPI sacrificed, (N) quantity of birds in each group. Ileum and bursa of Fabricius were on DPI designated by group identification. Cloacal swabs were collected from all living birds designated with the swab icon.



Cotton swabs (Puritan, Guilford, ME) were used to collect cloacal samples according to Figure 4.1, which were used to quantify virus shedding. Swabs were inserted into the cloaca, twisted back and forth 3-4 times, and then placed in 3.0 mL of brain-heart infusion broth and stored at -80°C until sample processing (Killian 2014). Birds were sacrificed according to Figure 4.1 via carbon dioxide inhalation and necropsied within one hour (mean time to necropsy: 15

minutes ± 10 SD). The coelomic cavity was examined for any abnormal gross pathology. Sex was confirmed by examining the syrinx (Mohamed 2017). Two cubic millimeter sections of ileum and bursa were collected and placed in one milliliter of RNA stabilizing solution (RNAlater®, Sigma-Aldrich, St. Louis, MO, USA). After 24 hours, tissues were removed from RNAlater and stored at -80°C.

Viral RNA Extraction and Quantification from Cloacal Swabs

Virus was isolated from cloacal swab material using the MagMAXTM-96 AI/ND Viral RNA Isolation Kit (Applied Biosystems® by Thermo Fisher Scientific, Vilnius, Lithuania) with modifications to the manufacturer protocol previously described (Das et al. 2009a). Viral RNA was quantified using real time reverse transcription-quantitative polymerase chain reaction (RTqPCR) targeting the matrix protein gene (Spackman and Suarez 2008). For the RT-qPCR working solution we used the TaqMan® RNA-to-CtTM 1-Step Kit (Applied Biosystems® by Thermo Fisher Scientific, Foster City, CA, USA), probe and primer sequences (Sigma-Aldrich, St. Louis, MO) specified by Spackman and Suarez (2008) and 2µL of sample RNA for a final well volume of 10µL. Each sample was processed at least three times on a 384 well plate with a minimum of three negative control wells and three positive control wells. We used LPAIV H5N9 stock virus in a 10-fold dilution on each plate in three replicates to create a reference standard curve. Ct values less than 40 were considered positive for virus (Costa et al. 2011). Using QuantStudio[™] Flex Real-Time PCR Software System v1.3, we calculated the standard curve, which was used to estimate virus quantity of each sample by correlating Ct values to 50% egg infectious dose per milliliter (EID₅₀/mL).

mRNA Extraction, cDNA Library Preparation, and Sequencing

Total mRNA was extracted from 15-30 mg of ileum and bursa tissue samples using the Qiagen RNeasy Mini Kit (QIAGEN®, Hilden, Germany) according to the manufacturer's protocol and stored in 500μ L of RNAse-free water at -80°C. RNA integrity number (RIN) were evaluated and all but two samples had RIN scores >8.0 (Appendix Table A4.1). The two scores lower than 8.0 were >7.0.

Library preparation was performed using TruSeq stranded mRNA library prep kits (Illumina, San Diego, CA) to generate 108 dual indexed libraries that were combined into 3 uniquely barcoded pools containing 36 samples each. The libraries were gel size selected using a Sage Science PippinHT (Beverly, MA) to have inserts of ≈ 200 bp. Each pool was sequenced in a single lane of a NovaSeq S1 using a 2x150-bp run. Library preparation did not select for only host mRNA. Library preparation and sequencing was performed at the University of Minnesota Genomics Center, St. Paul, MN.

RNA-seq Read Processing

Raw cDNA reads were quality screened using FastQC (Andrews 2011) to establish baseline measures of read quality prior to trimming and filtering. We used Trimmomatic (Bolger, Lohse, and Usadel 2014) to remove Illumina adapters, sequence regions with a quality score below 15 based across a four-base sliding window, and sequences shorter than 40bp. FastQC was again used to verify adapter and quality trimming. Next, we estimated expression levels using RSEM (B. Li and Dewey 2011), with alignment to the annotated blue-winged teal transcriptome (Dolinski, Homola, et al. 2020) performed using Bowtie (Langmead et al. 2009) with the aid of the Trinity (Grabherr et al. 2013) *align_and_estimate_abundance* Python script. Resulting gene-

and transcript-level expression estimates were combined into separate expression level matrices using the Trinity *abundance estimates to matrix* Python script.

Differential Expression Analyses

Two birds were removed prior to performing differential expression analyses. One bird in LPAIV treatment group I14 was removed due to missing weight data, reducing the sample size of that group from n = 8 to n = 7. A second bird from control group C1 was removed because of improper tissue grouping in the multidimensional scaling (MDS) ordination suggesting potential incorrect sample labeling (Figure 4.2), reducing the sample size of C1 from n = 5 to n = 4.

Figure 4.2: Multidimensional scaling (MDS) plot of bursa and ileum samples shows that tissue samples cluster based on tissue type gene expression. The bursa sample for bird 19 was grouping with ileum samples; therefore, bird 19 was removed from differential expression analysis due to likelihood of mislabeled samples.

Tissue-specific MDS groupings 48 Ileum 49 Bursa 2013a 48 Bursa 2 20 Heum 19 Ileum 54_Bursa 56 Bursa 19 Bursalleum 9-lleum lleum 0.5 5eBHIMB Bursa Dimension 2 57 Ileum 51 Bursa -0.5 4 Bursa 3 -2 -1 0 1 2 Dimension 1

We performed differential gene expression analyses using the R packages "EdgeR" (McCarthy, Chen, and Smyth 2012; Robinson, McCarthy, and Smyth 2010) and "limma" (Ritchie et al. 2015) in R version 4.0.0, following the approach outlined by Law et al. (Law et al.

2018). In cases where a gene has multiple isoforms, differential gene expression only detects changes across the sum of expression for all gene isoforms and may miss changes at the isoform level; therefore, differential expression analysis was conducted at both the transcript and gene level. We filtered lowly expressed genes and transcripts by requiring expression of >0.5 counts per million in at least 25% of the birds. Differential expression was established based on a false discovery rate (FDR) corrected alpha value of 0.1 and required log fold count difference (LFC) of 1.0. Sex, age at inoculation, weight at 55 days old, and sample sequencing pool were included as covariates in each analysis. Putative gene names were assigned to genes and transcripts based on existing SwissProt annotations of the blue-winged teal reference transcriptome (Dolinski, Homola, et al. 2020). KEGG BRITE hierarchical pathways were determined for annotated transcripts/genes with available KO identification numbers using "KEGG Mapper – Reconstruct Pathway" v4.2 (Kanehisa and Sato 2020).

We conducted two preliminary analyses to establish appropriate sample groupings for differential expression analysis. First, we performed a differential expression analysis that included both tissue types and group (C1, C14, I1, I3, I5, I14) including all birds (n = 54). This process identified 9261 transcripts and 8879 genes that were differentially expressed between the ileum and bursa (FDR adjusted p < 0.1 and LFC > 1.0), highlighting the need to analyze these tissues separately. Second, we assessed differential expression between control groups C1 and C14 to determine whether combining them into a single control sample set was appropriate. This analysis identified no differentially expressed genes between C1 and C14 for either tissue and only two differentially expressed transcripts each for bursa and ileum (Supplementary File S4). Given these extremely minor differences, we combined C1 and C14 into a single control group (C) for subsequent analyses.

To determine how gene expression differs between LPAIV-infected birds and control birds at various time intervals following viral inoculation, birds in each LPAIV-infected group (I1, I3, I5, I14) were compared to control birds (C). We also compared LPAIV treatment groups to each other to determine how gene expression changes in LPAIV infected birds over time by conducting differential expression analyses between I1 and I3, I3 and I5, and I5 and I14 groups.

To determine how gene expression differed between birds with different LPAIV shedding load, birds within each LPAIV-infected group I1, I3, and I5 were ranked from highest to lowest virus titer and divided into three "shed level" groups. Using the 20/80 rule for determining super-shedding individuals as a reference (Jankowski et al. 2013), the top 20% of individuals with the highest virus titers (n = 2) were classified as high shedders (H). The bottom 80% were then divided in half, classifying the top half (n = 5) as moderate shedders (M) and the bottom half (n = 5) as low shedders (L). To analyze gene expression early in the infection as it relates to active viral shedding, groups I1 and I3 were analyzed using only the cloacal swab virus titer data collected on the DPI the bird was sacrificed. Later in the infection, as viral load decreases and antibodies start to develop (Suarez and Schultz-Cherry 2000), we were interested in differential gene expression based on shedding status over the course of the infection; therefore group I5 shed level groups were determined using each individual's average cloacal swab virus titer over the first five DPI. Each LPAIV-infected group was analyzed with the following group comparisons: LvM, MvH, and LvH,

We performed enrichment analyses to identify over-represented gene ontology (GO) terms. GO enrichment was performed with the R package "topGO" (Alexa and Rahnenfuhrer 2020) using the elimination algorithm and Fisher statistic to determine significance using a maximum p-value of 0.01. Differentially expressed genes and transcripts in the ileum and bursa

were visualized in heat maps to identify gene clusters in each differential expression analysis. Clusters of similarly expressed genes/transcripts were delineated visually based on heatmap shading as determined by expression-level derived Z-scores.

Candidate Gene Analysis

A literature review was conducted to identify genes associated with the avian immune response, sialyltransferase, and AIV infections in birds (Barber et al. 2013; Cao et al. 2017; Cornelissen et al. 2012; Harduin-lepers 2010; Huang et al. 2013; Kuchipudi et al. 2014; Petit et al. 2018; Santhakumar et al. 2017; Stambas et al. 2017; Vanderven et al. 2012). We identified 76 search terms that were based on gene functions or names (e.g., sialyltransferase or NODAL) to help identify individual genes and transcripts of interest. An automated search of the teal de novo transcriptome 'SProt Gene Name', 'SProt Gene Function', 'KEGG Pathway', or 'EGGNOG ortholog' fields was performed for concordance with the list of search terms using a custom R script. The resulting list was manually filtered to remove transcripts that were erroneously included. Transcripts/genes with zero expression variability for each tissue type were also removed prior to analyses.

We used a linear mixed model to evaluate associations between candidate gene expression and viral load of all birds included in the differential expression analyses. Analyses were conducted with and without the inclusion of uninfected control birds. Expression levels were assessed as log₂ transformed counts per million, and viral load was assessed as log₁₀ transformed viral titers of the cloacal swab collected on the DPI the bird was sacrificed. Linear mixed models were assessed separately for every targeted transcript and gene using automated sub-setting and looping through the dataset. Significant relationships were identified by adjusting our false discovery rate (Benjamini and Hochberg 1995) to an alpha level of 0.05 for each tissue

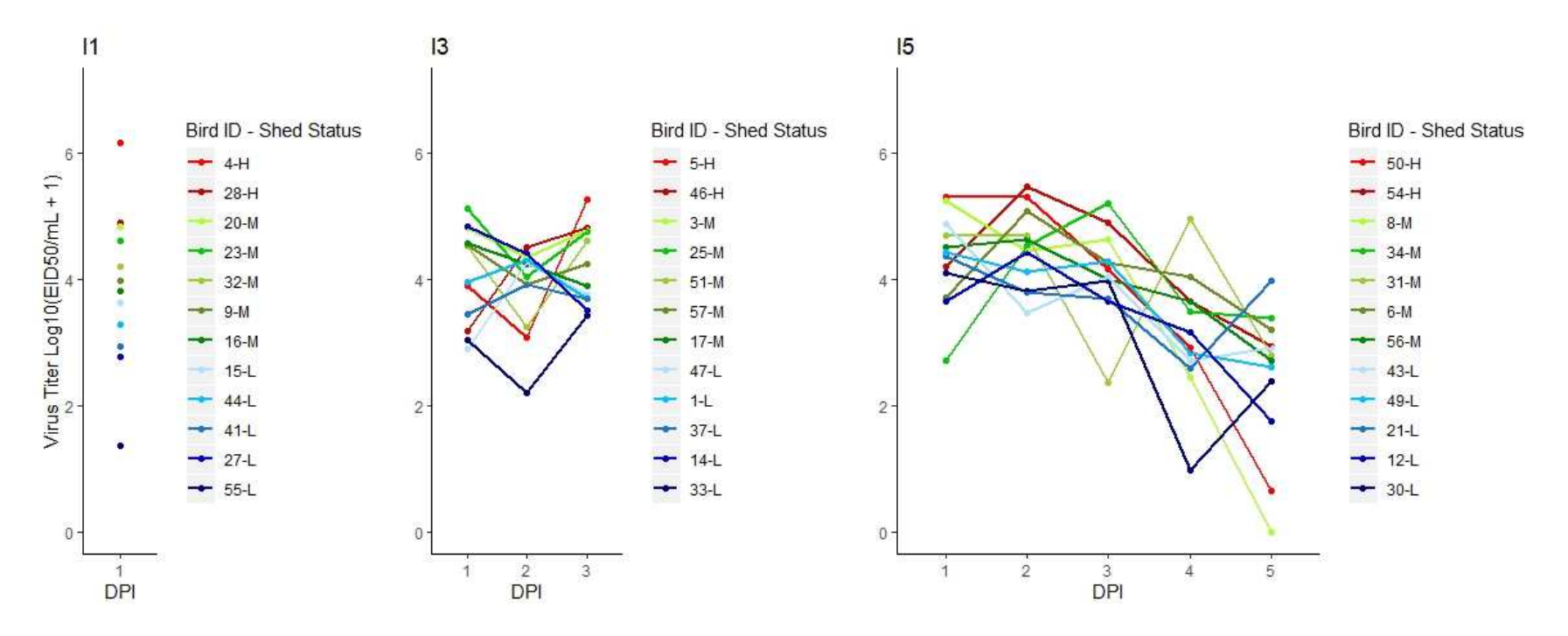
type and transcript/gene analysis combination. Sex, weight at age 55 days, and age at inoculation were included as fixed effects and sequencing pool was included as a random effect. P-values for the full model were recorded in addition to the p-values for each LPAIV-infected group. Models were constructed using the R package "nlme" (Pinheiro et al. 2007).

Results

Viral Infection

All LPAIV-infected birds had at least one positive virus titer following inoculation (Ct values < 40) (Costa et al. 2011; Dolinski, Jankowski, et al. 2020). All uninfected control birds had negative virus titers (Ct values undetermined) throughout the course of the study. We observed virus titer variation in LPAIV-infected groups I1, I3, and I5 and individuals were assigned to their respective shed level groups (Figure 4.3). No birds, infected or control, exhibited external signs of disease such as ruffled feathers, lethargy, or gross pathology.

Figure 4.3: Cloacal swab virus titer profiles for LPAIV-infected blue-winged teals sacrificed on one (I1), three (I3), and five (I5) days post infection (DPI). Shed level of high (H), moderate (M), or low (L) was assigned to individuals by their last virus titer (I1, I3) or the average virus titer across all DPI (I5).



RNA Sequencing

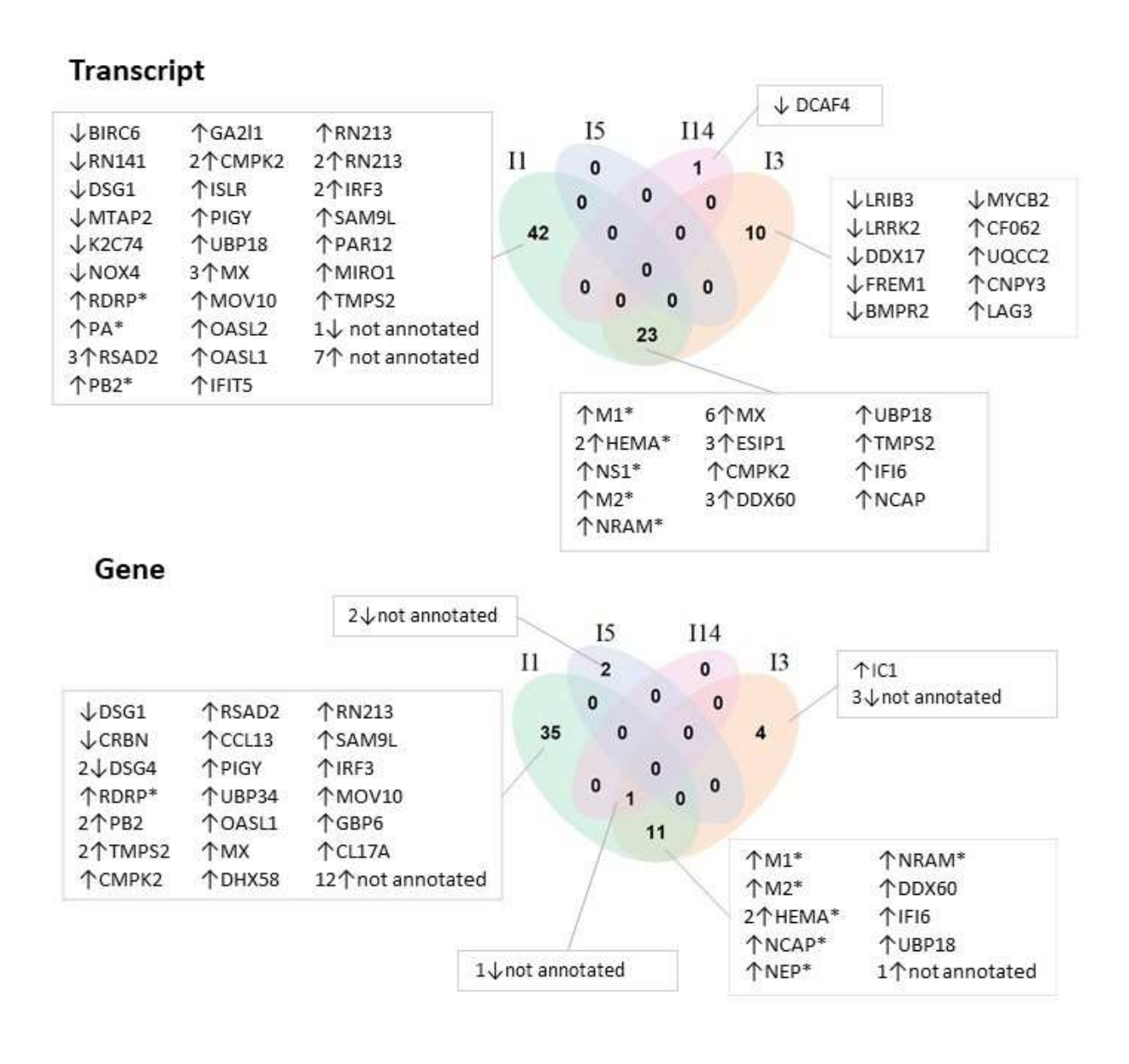
Across the three Hi-Seq lanes ≥750 M reads were generated. Mean quality scores for all libraries were greater than Q30. Bursa tissue samples yielded an average of 30,013,700 raw reads (range: 9,991,624 − 53,617,872) and ileum samples yielded an average of 31,833,779 raw reads (range: 22,623,885 − 52,693,669). After filtering, we retained an average of 29,517,172 bursa reads (range: 9,810,509 − 53,158,765) and an average of 31,483,391 ileum reads (range: 21,956,196 − 52,154,936) per individual for analyses.

Differential Gene Expression Between LPAIV-infected and Uninfected Control Groups

In the ileum, 76 transcripts and 53 genes were differentially expressed between LPAIV-infected and uninfected control teals across DPI. Fifty-eight unique annotations were recognized for 68 of the transcripts and 36 of the genes (Figure 4.4). Twenty-five of the annotated genes were also differentially expressed at the transcript level. Out of the 58 unique annotations identified, nine were LPAIV genes. In the bursa, only one unannotated gene was differentially expressed, and it was up regulated in I1 compared to uninfected controls. Fold count differences were calculated for each DET/DEG per comparison and can be viewed in supplemental material.

Across all LPAIV-infected groups, more differentially expressed transcripts (DETs) and genes (DEGs) were up regulated in LPAIV infected birds compared to down regulated genes, and more differential expression was observed early in the infection compared to later in the infection. Up regulated DETs and DEGs accounted for 82% and 81% of all observed differential expression, respectively. Ninety-nine percent of DETs and 96% of DEGs were observed early in the infection (I1, I3), while only 1% of DETs and 6% of DEGs were observed later in the infection (I5, I14).

Figure 4.4: Differentially expressed transcripts/genes between LPAIV-infected and uninfected control blue-winged teals in the ileum. LPAIV-infected birds were sacrificed on one (I1), three (I3), five (I5), and 14 (I14) days post infection (DPI). Each number represents the quantity of DET/DEGs per comparison, and/or shared between comparisons. DEGs/DETs up-regulated (↑) or down-regulated (↓) in each group corresponds to the LPAIV-infected group. Numbers preceding arrows indicate the number of unique transcripts/genes per annotation. (*) indicates LPAIV genes.



KEGG BRITE pathways in metabolism, genetic information processing, and cell signaling were associated with DET/DEGs between LPAIV-infected and uninfected control birds (Table 4.1). Protein kinases were down regulated in infected birds, while more peptidases were up regulated. More DET/DEGs involved in cell signaling were up regulated in infected birds than were down regulated. DET/DEGs associated with spliceosomes and membrane trafficking were down regulated in LPAIV-infected birds, and DET/DEGs associated with transcription, mRNA biogenesis, and folding catalysts were down regulated in LPAIV infected birds. Three DET/DEGs of the ubiquitin system were up regulated and three were down regulated in LPAIV-infected birds.

Table 4.1: Summary of KEGG BRITE pathways for differentially expressed transcripts/genes (DET/DEG) of LPAIV-infected bluewinged teals. A) DET/DEGs are either down (↓) or up regulated (↑) in infected birds compared to control birds on 1, 3, 5, or 14 DPI. B) LPAIV shed level group comparisons in early-stage infection (I1, I3). DET/DEGs shown are up regulated in low shedders compared to moderate or high shedders, or up regulated in high shedders compared to low and moderate shedders. C) LPAIV shed level group comparisons in late-stage infection (I5). DET/DEGs shown are all down regulated in high shedders compared to low or moderate shedders. See supplementary file for full list of KEGG BRITE pathways.

		A) LPAIV-Infected vs. Control		B) Shed le	evel Early	C) Shed level Late
	Type	↓Infected	↑Infected	↑Low	↑High	↓High
Metabolism	Enzyme	LRRK2, BIRC6, BMPR2, MYCB2, NOX4, DDX17	MIRO1, TMPS2, UBP18, UBP34, DHX58, CMPK2, OASL1, OASL2, PAR12, MOV10,	ACS2L, TALDO, TRAF6, PUR4, DEGS1, WWP2, FASTK, RNF34	GLSK, SYIM, KMT5B, DDX3X, ANPRB,	GSHR, GLT12, KHK, PFKAL, PARN, AT8B2, KYNU, PMGE, IRAK4, PGAP1, PTPRK, CARM1, PTPRK, CHAC1, ALG13, PCSK6, TERT, DKC1, SIR5, SETMR, UBP24, CNOT6, LPIN1

Table 4.1 (cont'd)

	Enzyme		DDX60, RN213			
	Protein Kinases	LRRK2, BMPR2		FASTK	ANPRB	IRAK4
ism	Protein Phosphatases and Associated Proteins			AXIN		PFKAL, PTPRK, LPIN1, CAMP1
Metabolism	Peptidases and Inhibitors	BIRC6	IC1, TMPS2, UBP18, UBP34			CFLAR, AGRG5, PCSK6, UBP24, PEDF
	Lipid Biosynthesis Proteins			ACS2L, DEGS1		
	Amino Acid Related Enzymes				SYIM	
	Glycosyltransferases					GLT12, ALG13
1 8	Transcription Factors		IRF3	NR2C2	ZN384	SCRT2, CXXC1, MEIS1, TRPS1
cessin	Transcription Machinery					ARI1B, MD12L
Pr	Translation Factors					
ntion	Messenger RNA Biogenesis		MOV10, DDX60	FASTK, ROA3	DDX3X	PFKAL, PARN, RCC1, CNOT6
ä.	Spliceosome	DDX17		ROA3	DDX3X	BUD31
Genetic Information Processing	Ribosome Biogenesis					DKC1, DIEXF
enetic	Transfer RNA Biogenesis				SYIM	IRAK4
Ğ	Chaperones and Folding Catalysts		CNPY3			PCSK6, TCPD, DJC14

Table 4.1 (cont'd)

ssing	Membrane Trafficking	LRRK2		TRAF6	SH3G1	PGAP1, MRC1, CCN2, SC22A, IQEC1, SEPT7, VLDLR, FBP1L, RHG29, MCF2L, SGSM2
on Proce	Ubiquitin System	BIRC6, MYCB2, DCAF4	UBP18, UBP34, RN213	TRAF6, RNF34, WWP2	FXL15	UBP24, UBA5
atic	Proteosome					HOP2
form	DNA Replication Proteins					DPOG2, CCNE2, TERT, DKC1
Genetic Information Processing	Chromosome and Associated Proteins				KMT5B, DDX3X, SIN3A	CARM1, CCNE2, RAD21, TCPD, SIR5, SETMR, RCC1, CBX1, MBD2, ARI1B, CXXC1, IFT74
	Mitochondrial Biogenesis		MIRO1, UQCC2			DPOG2, ATAD3
ses	Transporters				MRP5	S2611, MCAT, S2536, ELMO2
rocess	Cytoskeleton Proteins		K2C74			K2C75, SEPT7, CAMP1
Signaling and Cellular Processes	Exosome	LRRK2	IC1, K2C74,			KHK, BT2A2, BT3A3, DMB, K2C75, TCPD, SEPT7 BTNL2, MOG
nd Co	G protein-coupled receptors				TMCO4	PACR, AGRG5
ling a	Pattern Recognition Receptors		DHX58		TLR1	MRC1
zna	Nuclear Receptors			NR2C2		
Sig	GTP-binding proteins		MIRO1			KBRS2

Table 4.1 (cont'd)

and 1r es	CD molecules	LA	G3	TLR1	CD69, MRC1, BT2A2, BT3A3
ali ell	Glycosaminoglycan binding proteins	CCI	.13		
Sign C Pr	Lectins	CL1	7A		CD69, MRC1

We found 135 enriched GO terms between LPAIV-infected and uninfected birds across all DPI (Supplementary File S4). Within the ileum, four clusters of DEGs were observed with corresponding GO terms (Figure 4.5). Cluster I is comprised of host genes with higher expression in the uninfected controls compared to all LPAIV-infected groups and no enriched GO terms. Cluster II is comprised of host genes with higher expression in uninfected controls/late infection groups (C, I5, I14) compared to early infection groups (I1, I3), and enriched GO terms were associated with cellular adhesion. Cluster III contains host genes with lower overall expression in control/late infection groups (C, I5, I14) compared to early infection groups, and enriched GO terms were associated with transcription, virus replication, and the immune system. Cluster IV is comprised of LPAIV genes and follows a similar pattern to Cluster III.

Figure 4.5: A. Heat map for differentially expressed genes in the ileum between uninfected (control) and LPAIV-infected mallards on one, three, five, and 14 days post infection (DPI). Illustrated are the relative expression levels of each transcript (rows) in each sample (column). Rows are hierarchically clustered by expression. Log2-transformed expression values are z-transformed. Box plots are provided for each visually observed gene cluster. B. Enriched GO terms corresponding to each cluster.

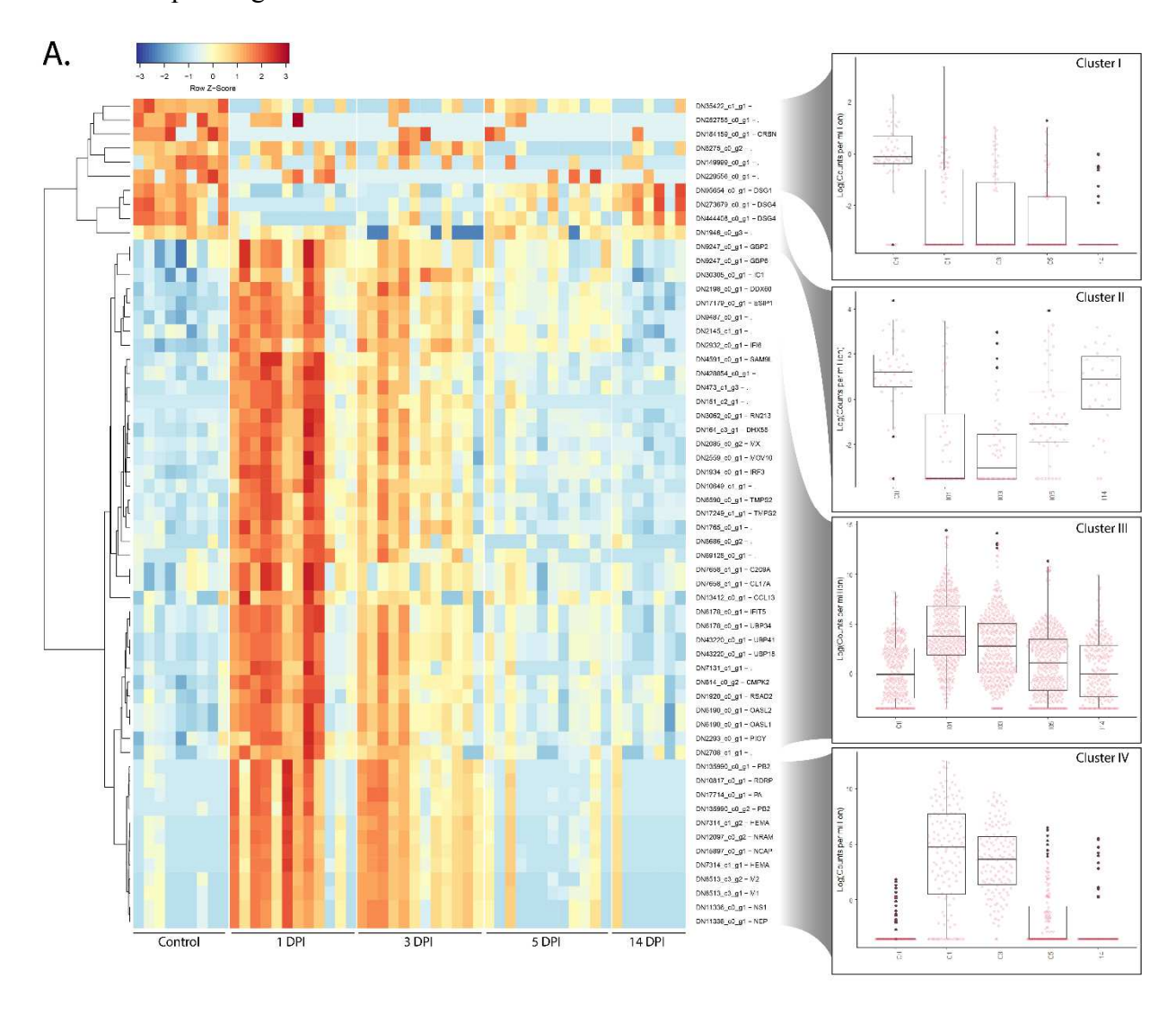


Figure 4.5 (cont'd)

Cluster II No enriched GO terms Hair follicle development В. • Homophilic cell adhesion via plasma membrane desmosome Cluster III • Positive regulation of T cell cytokine production Fibrinolysis • Positive regulation of type 2 immune response • Negative regulation of viral genome replication · RNA helicase activity • Innate immune response • Double-stranded RNA binding • Negative regulation of innate immune responses Single-stranded RNA binding · Positive regulation of viral entry into host cell Scavenger receptor activity • Defense response to virus • Blood coagulation, intrinsic pathway · Regulation of type I interferon-mediated • Negative regulation of endopeptidase activity responses · Protein autoprocessing Positive regulation of MDA-5 signaling pathway • Positive regulation of type I interferon production • Positive regulation of RIG-I signaling pathway Cluster IV • RNA-directed 5'3' RNA polymerase activity • Host cell plasma membrane host cell cytoplasm • 7-methylguanosine mRNA capping • Suppression by virus of host RNA polymerase • Virion Viral RNA genome replication Viral envelope · Host cell nucleus Virion attachment to host cell Exo-alpha-(2,3)-sialidase activity • Fusion of virus membrane with host plasma · Exo-alpha-(2,6)-sialidase activity Viral transcription Virion membrane

DET/DEGs with functions associated with the immune system were all up regulated in infected birds compared to uninfected birds on one and three DPI (Table 4.2). Regulators of the interferon pathway are involved in RIG I/MDA5 signaling, toll-like signaling, and transcription of interferons. Interferon-stimulated genes (ISGs) have various anti-viral activity. Regulators of cellular immunity are involved in inflammation (proliferation of leukocytes at the site of infection) and complement activation.

Table 4.2: Immune transcripts/genes with significant differential expression between LPAIV-infected and uninfected (control) birds and between low and high viral shedders on one (I1), three (I3), and five (I5) days post infection. Immune genes up regulated (\uparrow) or down regulated (\downarrow) corresponds to the infected and low shedders. Significant linear relationships (p < 0.05) between candidate gene expression and cloacal virus titers are positive (+) or negative (-) at the transcript and/or gene level across all bird samples with (w/) and without (w/o) uninfected controls and on one (I1), three (I3), and five (I5) days post infection. Blank cells are non-significant.

			Infected vs. Control		Low vs. High Shedders		Candidate Gene Linear Mixed Models							
	Gene ID (other known IDs)	I1	I3	15	I1	13	15	w/controls*	w/o controls*	I 1	13	15	Gene Function	
	CNPY3		1										Toll-like receptor chaperone (Liu et al. 2012)	
way	DDX3X (DBX, DDX3)					1							Required for IFN-β production (Soulat et al. 2008)	
on Path	DDX58 (RIG-I)							+	+	+			Pattern Recognition Receptor (Santhakumar et al. 2017; Schoggins and Rice 2011)	
iterfer	DDX60	1	1										Regulates RIG-1/MDA5 signaling (Oshiumi et al. 2015)	
Regulator of Interferon Pathway	DHX58 (D11LGP2E, LGP2)	1						+	+	+		+	Regulates RIG-1/MDA5 signaling (Rothenfusser et al. 2005; Santhakumar et al. 2017)	
Regula	FGFR3 (Mfr3, Sam3)							-					Activation of STAT1/3 (Hart et al. 2000)	
	IFIH1 (MDA5, RH116)							+					Pattern Recognition Receptor (Santhakumar et al. 2017; Schoggins and Rice 2011)	

Table 4.2 (cont'd)

	IFNA2						+				Type I interferon (Santhakumar et al. 2017)
	IFNL3 (IFNL, IL28, IL28B)						+				Type III interferon (Santhakumar et al. 2017)
	IFRD1						-				Suppression of NFkB activation (Tummers et al. 2015)
	IKBE (Nfkbie)						+				Inhibits NFkB-directed transactivation (Whiteside et al. 1997)
Ma	IRF1						+				Regulator of IFN-β (Liu et al. 2018)
ı Path	IRF3 (IRF7)	1					+	+	+		Interferon transcription activator (Santhakumar et al. 2017)
Regulator of Interferon Pathway	KBRS2 (NKIRAS2, KappaB-Ras2)					1					Regulator of NFkB (Sarais et al. 2020)
f Inte	NFKB1							+	+	+	Interferon transcription activator (Santhakumar et al. 2017)
itor o	PARP9 (BAL, BAL1, ARTD9)						+	+			Enhances STAT1 activity (Zhang et al. 2015)
Regula	PTPRK (R-PTP-kappa, PTPK)					1					Negatively regulates STAT3 activity (Chen et al. 2015)
	SIN3A (Kiaa4126)			1							Regulator of STAT activity (Icardi et al. 2012)
	STAT1						+	+	+		Initiates transcription of ISGs (Santhakumar et al. 2017)
	TRAF6				↑b						Activates NFkB/IRF7 (Konno et al. 2009)
	UBP18 (USP18, hUBP43, ISG43)	1	1								Type I interferon negative regulator (Basters, Knobeloch, and Fritz 2018)

^bAlso significant in the bursa.

Table 4.2 (cont'd)

E2AK2 (PKR, PRKR, EIF2AK2)						+	+	+		+	Inhibition of translation (Ko et al. 2004; Santhakumar et al. 2017; Schoggins and Rice 2011)	
GVIN1 (GTPase-1, VLIG-1)					1						Antiviral function unknown (Klamp et al. 2003)	
IFI6	1	1				+	+	+		+	Regulation of apoptosis (Schoggins and Rice 2011)	
IFIT5 (ISG58, RI58, P58, AvIFIT)	1					+	+	+			Inhibits viral replication (Rong, Hu, et al. 2018)	
IFM5 (IFITM5)						+	+				No antiviral activity in ducks (Evseev and Magor 2019)	
IN35 (IFI35, IFP35)						+	+	+			Negative regulation RIG-1 (Das et al. 2014)	
MX	1	1				+ b	+	+ b		+	No antiviral activity in ducks (Bazzigher, Schwartz, and Staeheli 1993)	
OASL1	1					+	+	+	+		Dual antiviral functions (Choi et al. 2015)	
OASL2						+					Dual antiviral functions (Choi et al. 2015)	
PAR12 (PARP12, ZC3HDC1)	1					+	+	+			Increased NFkB signaling (Welsby et al. 2014)	
RSAD2 (viperin)	↑					+b	+	+b			Prevents virion release/unknown in ducks (Evseev and Magor 2019)	
BT2A2 (Btn2a2)					1						Inhibits CD4+ and CD8+ T cell activation (Smith et al. 2010)	
BTNL2 (BTL-II)					1						Inhibits T cell proliferation (Nguyen et al. 2006)	
	EIF2AK2) GVIN1 (GTPase-1, VLIG-1) IFI6 IFI6 IFIT5 (ISG58, RI58, P58, AvIFIT) IFM5 (IFITM5) IN35 (IFI35, IFP35) MX OASL1 OASL1 OASL2 PAR12 (PARP12, ZC3HDC1) RSAD2 (viperin) BT2A2 (Btn2a2)	EIF2AK2) GVIN1 (GTPase-1, VLIG-1) IFI6 ↑ IFIT5 (ISG58, RI58, P58, AvIFIT) ↑ IFM5 (IFITM5) IN35 (IFI35, IFP35) MX ↑ OASL1 ↑ OASL2 PAR12 (PARP12, ZC3HDC1) ↑ RSAD2 (viperin) ↑ BT2A2 (Btn2a2) BTNL2 (BTL-II)	EIF2AK2) GVIN1 (GTPase-1, VLIG-1) IFI6 ↑ ↑ IFIT5 (ISG58, RI58, P58, AvIFIT) ↑ IFM5 (IFITM5) IN35 (IFI35, IFP35) MX ↑ ↑ OASL1 ↑ OASL2 PAR12 (PARP12, ZC3HDC1) PAR3 (Viperin) ↑ BT2A2 (Btn2a2) BTNL2 (BTL-II)	EIF2AK2) GVIN1 (GTPase-1, VLIG-1) IFI6 ↑ ↑ IFIT5 (ISG58, RI58, P58, AvIFIT) ↑ IFM5 (IFITM5) IN35 (IFI35, IFP35) MX ↑ ↑ OASL1 ↑ OASL2 PAR12 (PARP12, ZC3HDC1) PASAD2 (viperin) ↑ BT2A2 (Btn2a2) BTNL2 (BTL-II)	EIF2AK2) GVIN1 (GTPase-1, VLIG-1) IFI6 ↑ ↑ IFIT5 (ISG58, RI58, P58, AvIFIT) ↑ IFM5 (IFITM5) IN35 (IFI35, IFP35) MX ↑ ↑ OASL1 ↑ OASL2 PAR12 (PARP12, ZC3HDC1) RSAD2 (viperin) ↑ BT2A2 (Btn2a2) BTNL2 (BTL-II)	GVIN1 (GTPase-1, VLIG-1) ↑ IFI6 ↑ ↑ IFIT5 (ISG58, RI58, P58, AvIFIT) ↑ IFM5 (IFITM5) IN35 (IFI35, IFP35) MX ↑ ↑ OASL1 ↑ OASL2 PAR12 (PARP12, ZC3HDC1) RSAD2 (viperin) ↑ BT2A2 (Btn2a2) ↑ BTNL2 (BTL-II) ↑	EIF2AK2) ↑ GVIN1 (GTPase-1, VLIG-1) ↑ IFI6 ↑ ↑ IFIT5 (ISG58, RI58, P58, AvIFIT) ↑ + IFM5 (IFITM5) + + IN35 (IFI35, IFP35) + + MX ↑ ↑ + OASL1 ↑ + + OASL2 + + PAR12 (PARP12, ZC3HDC1) ↑ + + RSAD2 (viperin) ↑ + + BT2A2 (Btn2a2) ↑ + + BTNL2 (BTL-II) ↑ + +	EIF2AK2) ↑ ↑ ↑ GVIN1 (GTPase-1, VLIG-1) ↑ ↑ + + IFI6 ↑ ↑ + + + IFIT5 (ISG58, RI58, P58, AvIFIT) ↑ +	EIF2AK2)	EIF2AK2) ↑ ↑ ↑ ↑ ↑ ↑ ↑ ↑ ↑ □	EIF2AK2) ↑	

^bAlso significant in the bursa.

Table 4.2 (cont'd)

	CC4L (CCL4L, SCYA4L2)					+	+			Chemokine function similar to CCL4 (Howard et al. 2004)
	CCL13 (MCP4, NCC1, SCYA13	1				+				Chemokine: attracts leukocytes (Kim, Lee, and Hahn 2018)
	CCL26 (Eotaxin-3)					+				Chemokine: attracts leukocytes, STAT6/IL4 signaling (Chen and Jiang 2013)
	CCL4 (SCYA4, MIP-1β, LAG1)					+	+	+		Chemokine: attracts leukocytes, associated with H5N1 pathogenesis (Betakova et al. 2017)
it.	CCR5 (CMKBR5)					+	+		+	Binding receptor for CCL4 and CCL4 (Howard et al. 2004)
ımun)	CD4					+				CD4 T-cell surface glycoprotein (Veillette et al. 1988)
Cellular Immunity	CD59 (P-18, MACIF, MIRL, HRF-20, 1F5 antigen, MEM-43 antigen, H19, protectin)						-			Inhibitor of the membrane attack complex (MAC) (Davies and Lachmann 1993)
	DMB (HLA-DMB, RING7)				1					MHC class II component (Denzin and Cresswell 1995)
	ELMO2 (CED12A, KIAA1834)				1					Phagocytosis of apoptotic cells (Hamann et al. 2016)
	ESIP1 (EPSTI1)	1	1							Modulator of macrophage activation (Kim, Lee, and Hahn 2018)
	IC1 (SERPING1, C1IN, C1NH)		1							Regulates complement activation (Davis, Mejia, and Lu 2008)
	IL10					+				Down regulates effects of IFNγ (Kapczynski, Jiang, and Kogut 2014)
	IL18					+				Promotes IFNγ production by CD8+ T cells (Iwasaki and Pillai 2014)

Table 4.2 (cont'd)

S	IL8 (CXCL8, CEF4, EMF1)			+				Chemokine: attracts leukocytes (Kaiser and Staheli 2013)
munity	LAG3 (Aida, CD223)	1						Regulator of T cell proliferation (Huang et al. 2004)
Im	LY6E (SCA2)			+		+		Regulator of T cell proliferation (Yu and Liu 2019)
Cellular	MXRA5 (Adlican)			+/				Anti-inflammatory properties (Poveda et al. 2017)
	TAP1 (APT1)			+	+	+	+	Component of MHC class I (MacDonald et al. 2007)

Differential Gene Expression of LPAIV-infected Birds Over Time

Between LPAIV-infected groups (I1vI3, I3vI5, I5vI14), only three transcripts were differentially expressed in the ileum. Transcript DDX17 was up regulated in I1 compared to I3, an unannotated transcript was down regulated in I3 compared to I5, and transcript DCAF4 was up regulated in I5 compared to I14. Fold count differences for each DET can be viewed in supplemental material (Supplementary File S4). Transcripts in the bursa were not differentially expressed, and differential expression at the gene level was not observed in either tissue.

Nine enriched GO terms were significant (p < 0.05) in the ileum between LPAIV-infected group comparisons (Supplementary File S4). Regulation of mRNA splicing, RNA helicase activity, miRNA metabolic processes, miRNA transcription, and cellular structure processes were enriched in I1 compared to I3. Ubiquitin processes were enriched in I5 compared to I14.

Differential Gene Expression Between Virus Shed Level Groups During Early Stage Infection

Differential gene expression was observed between shed level groups (LvM, MvH, LvH) in

early-stage infection (I1, I3) at both the transcript and gene level of the bursa and ileum (Figure
4.6). Among all DEG/DETs, 49 unique annotations were recognized for 46 transcripts and five
genes (Figure 4.6). Only one annotation was differentially expressed at both the transcript and
gene level (EFGM in I1), and only one annotated transcript was differentially expressed in both
the ileum and the bursa (TRAF6 in I3). We observed more DETs in the ileum than the bursa; but
in group I1, more DEGs were observed in the bursa than the ileum. In the ileum, the comparison
with the most differentially expressed genes was LvH in group I3 at the transcript level. In the
bursa, the comparison with the most differentially expressed genes was MvH in group I1 at the

gene level. Most instances of differential expression were present in only one shed level comparison. No DETs/DEGs were differentially expressed in all three shed level comparisons.

Figure 4.6: Differentially expressed transcripts/genes between shed level groups (Low, Moderate, High) of LPAIV-infected blue-winged teals on one (I1), three (I3), and five (I5) days post infection for (A) bursa and (B) ileum tissues. Each number represents the quantity of DET/DEGs per comparison, and/or shared between comparisons. Transcripts/Genes up-regulated (\(\epsilon\)) or down-regulated (\(\epsilon\)) corresponds to the first shed level group listed in the comparison. See supplementary material for additional gene information and log2(fold count).

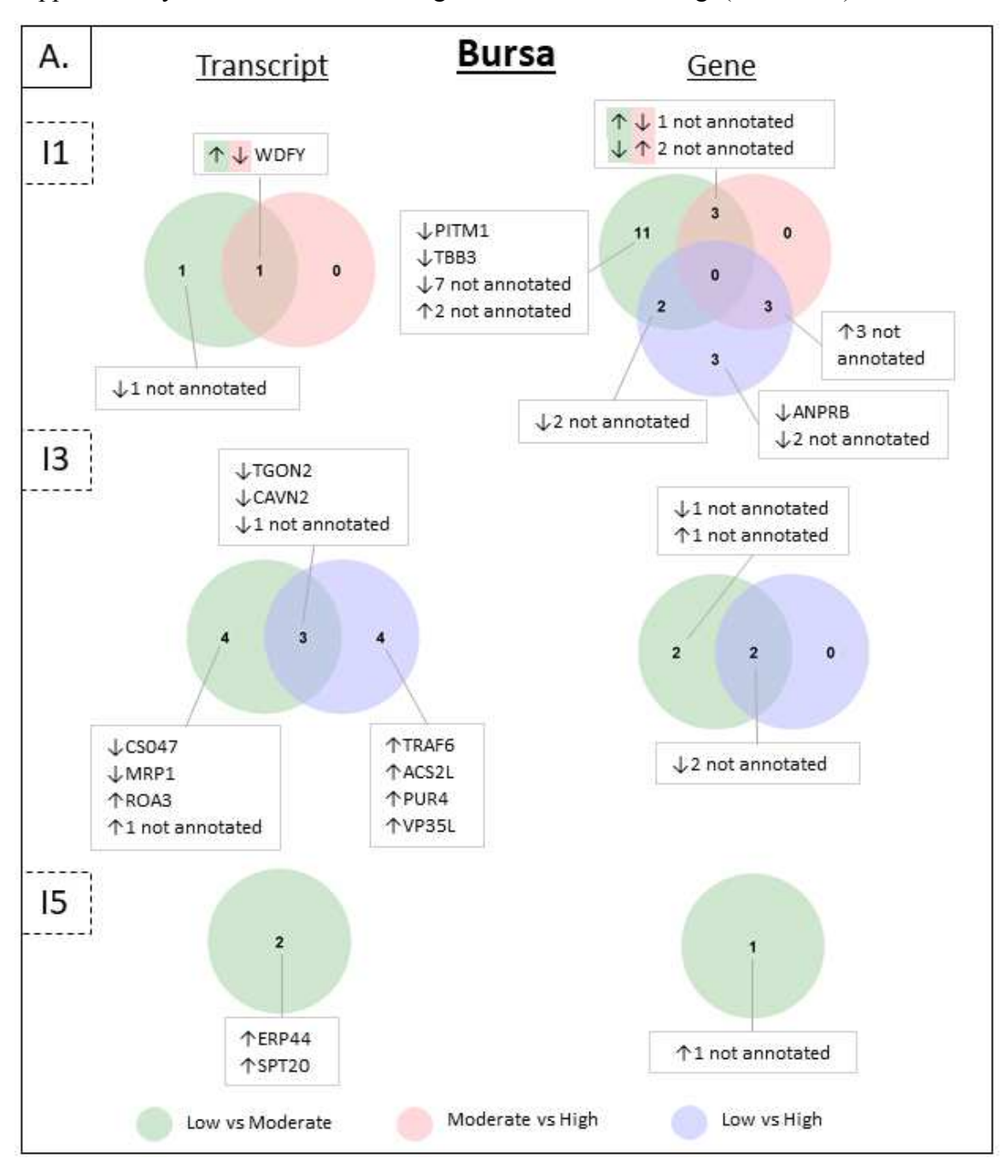
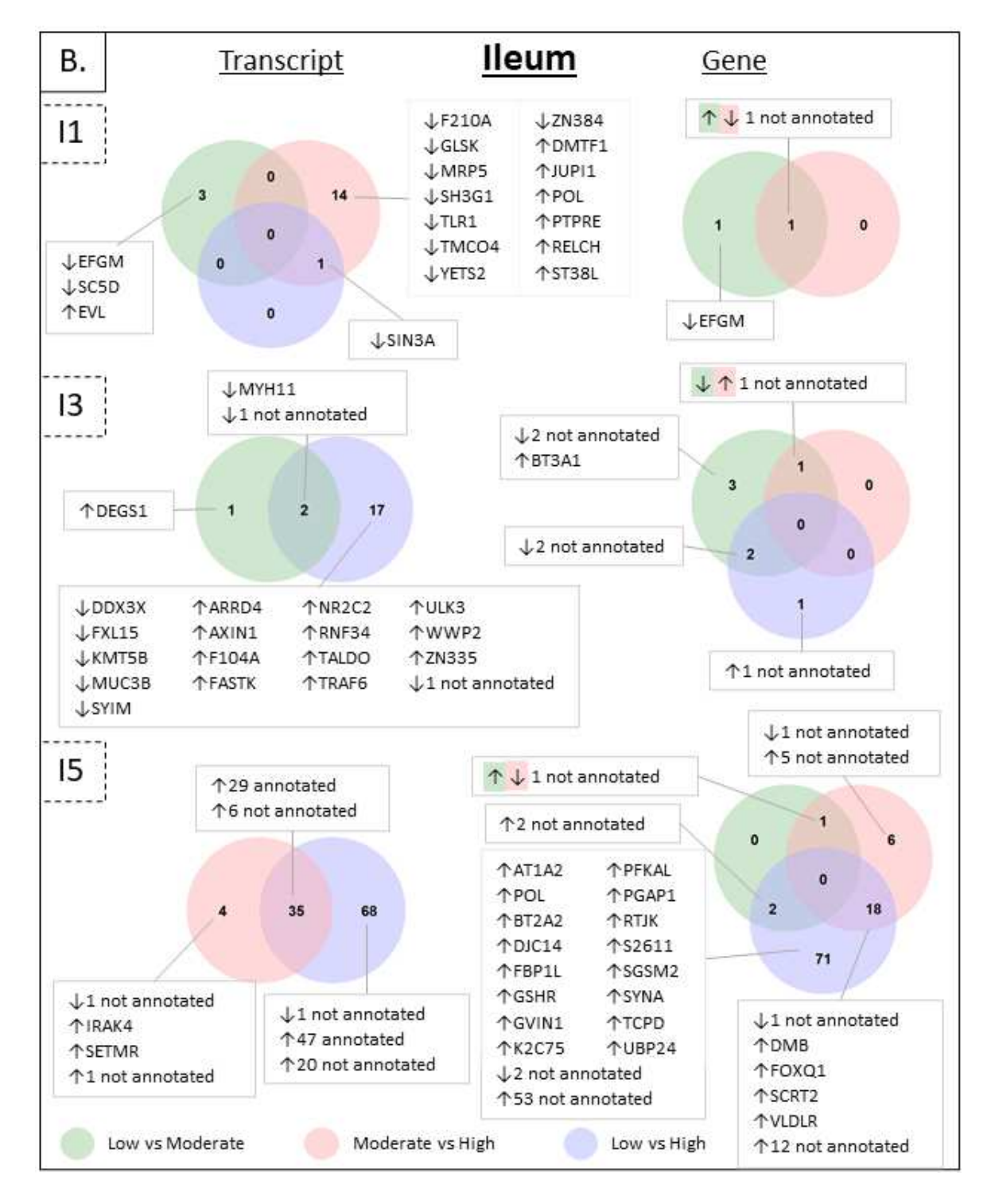


Figure 4.6 (cont'd)



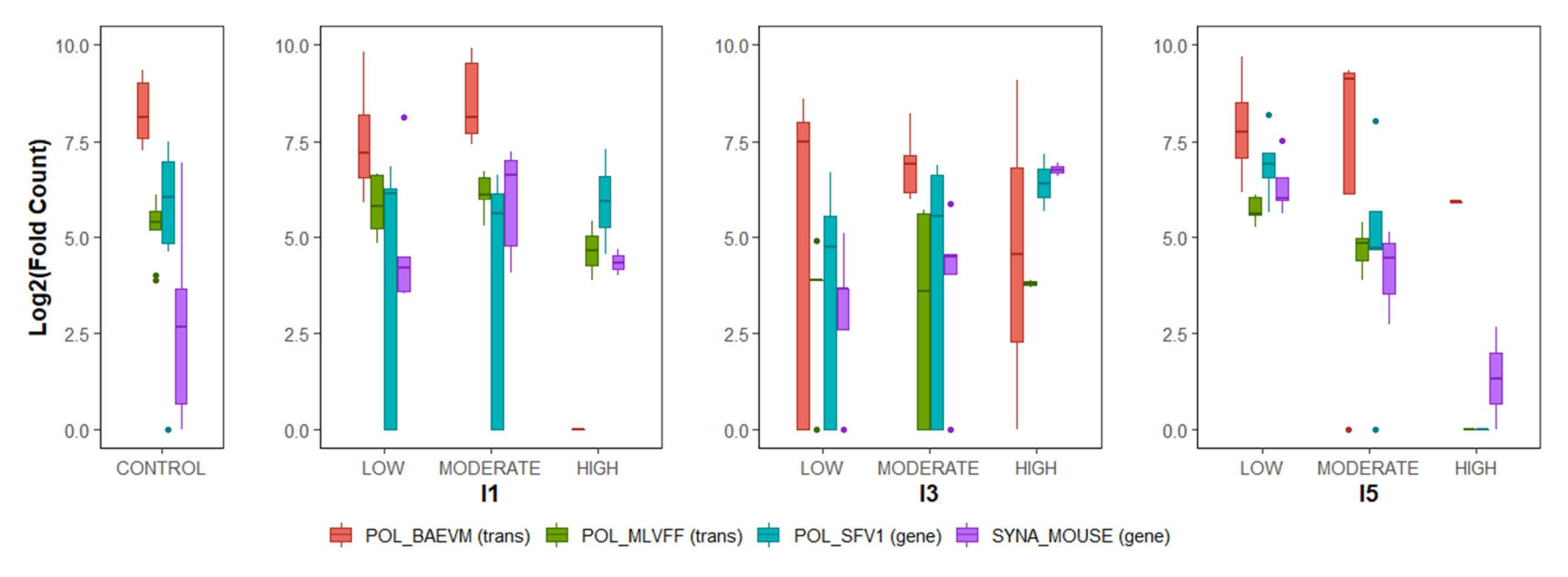
KEGG BRITE pathways in metabolism, genetic information processing, and cell signaling were associated with DET/DEGs between shed level groups early in the infection

(Table 4.1). Metabolic enzymes, such as phosphatases and lipid biosynthesis proteins were up regulated in low shedding birds, while an amino acid related enzyme was up regulated in high shedders. Protein kinases were up regulated in both low and high shedding birds. DET/DEGs of the genetic information processing pathways involved in transcription, RNA biogenesis, membrane trafficking, and the ubiquitin system were up regulated in both low and high shedders. But only chromosome proteins were up regulated in high shedders. We also observed fewer cell signaling DET/DEGs up regulated in low shedders compared to high shedders.

We found 139 enriched GO terms between shed level groups early in the infection; however, no obvious visual gene clusters were observed (Supplementary File S4). DETs/DEGs were enriched in biological processes associated with the host immune/defense processes, ubiquitination, kinase activity, cellular proliferation, and nucleic acid synthesis. While we found GO terms enriched in immune processes between shed level groups early in the infection, few DET/DEGs of the immune system were observed between low and high shedders (Table 4.2).

LPAIV genes were not differentially expressed between shed level groups early in the infection, as was observed between LPAIV-infected and uninfected birds; however, one endogenous retroviral (ERV) transcript (POL_BAEVM) was down regulated in high shedders compared to moderate shedders on one DPI (Figure 4.7).

Figure 4.7: Expression of endogenous retroviral genes differentially expressed in the ileum between shed level groups of LPAIV-infected blue-winged teals on one (I1), three (I3), and five (I5) days post infection (DPI). POL_BAEVM was down regulated in high shedders compared to moderate shedders on one DPI (I1) at the transcript level. No retroviral genes were differentially expressed on three DPI. POL_MLVFF was down regulated in high shedders compared to moderate and low shedders on five DPI (I5) at the transcript level. POL_SFV1 and SYNA_MOUSE were both down regulated in high shedders compared to low shedders on five DPI at the gene level. Expression of uninfected (control) birds is displayed for reference.



Differential Gene Expression Between Virus Shed Level Groups During Late Stage Infection

During late-stage infection (I5) more DETs/DEGs were expressed in the ileum (107 DETs and 98 DEGs) compared to the bursa (2 DETs and 1 DEG; Figure 4.6). Among all DET/DEGs, 101 annotations were recognized for 79 transcripts and 22 genes. In the ileum, most DETs/DEGs were observed between low and high LPAIV shedders. All DETs and 94% of DEGs were down regulated in high shedders compared to low and moderate shedders, and all annotated DET/DEGs were down regulated in high shedders compared to low and moderate shedders.

Eighty-five percent of DETs and 92% of DEGs expressed in low and moderate shedders were not expressed at all in high shedders.

KEGG BRITE pathways in metabolism, genetic information processing, and cell signaling were associated with down regulated DET/DEGs in high shedders late in the infection (Table 4.1). Metabolic pathways included enzymes, one protein kinase, phosphatases, peptidases, and glycosyltransferases. Genetic information processing DET/DEGs were mainly involved in transcription, RNA biogenesis, membrane trafficking, the ubiquitin system, and chromosome proteins. DET/DEGs associated with cell signaling were observed, with most DET/DEGs involved in exosome signaling.

We found 62 GO terms enriched in the ileum and two GO terms enriched in the bursa for DET/DEGs between shed level groups late in the infection (Supplementary File S4). Two distinct DEG clusters were observed in the ileum (Figure 4.8). Cluster I, which consists of the majority of DEGs in late-stage infection, is defined by significant down-regulation of DEGs in high shedders compared to low and moderate shedders. Cluster I is associated with 16 enriched GO terms, many of which are related to an immune system process. Cluster II consists of DEGs

up regulated in high shedders compared to low and moderate shedders, with only one enriched

GO term related to membrane trafficking.

Figure 4.8: Heat map for differentially expressed genes in the ileum between shed level groups of LPAIV-infected blue-winged teals on five days post infection. Illustrated are the relative expression levels of each transcript (rows) in each sample (column). Rows are hierarchically clustered by expression. Log2-transformed expression values are z-transformed. Box plots are provided for each visually observed gene cluster. B. Enriched GO terms corresponding to each cluster.

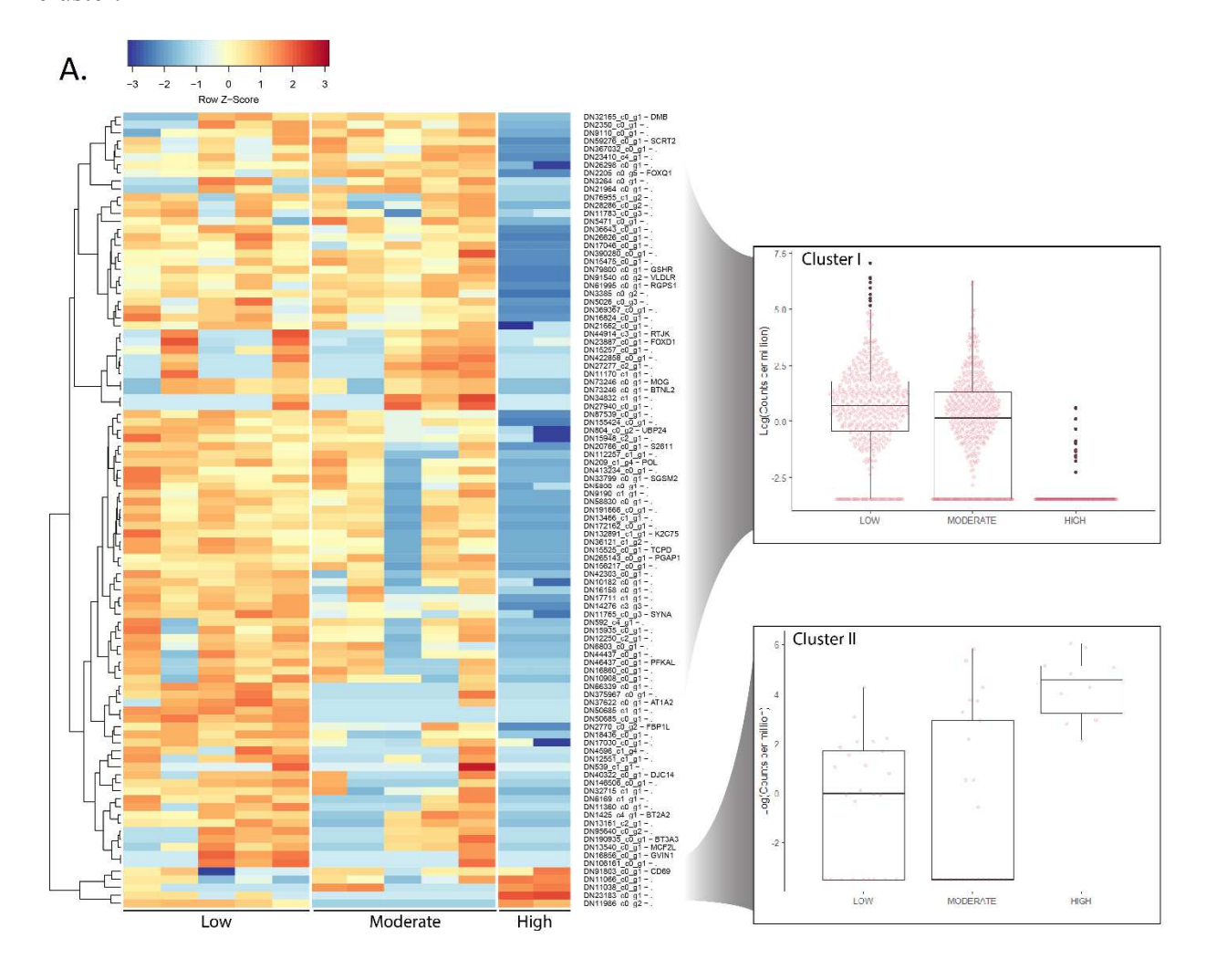


Figure 4.8 (cont'd)

В.

Cluster I

- Peptide antigen assembly with MHC class II protein complex
- Glutathione-disulfide reductase activity
- 6-phosphofructokinase complex
- Ral guanyl-nucleotide exchange factor activity
- External side of plasma membrane
- Myo-inositol transport
- MHC class II protein complex binding
- Very-low-density lipoprotein particle receptor activity
- Regulation of Ral protein signal transduction

- Late endosome to Golgi transport
- Positive regulation of T cell proliferation
- MHC class II protein complex
- T cell receptor signaling pathway
- Negative regulation of T cell receptor signaling pathway
- Positive regulation of interleukin-2 secretion
- Positive regulation of T cell activation via T cell receptor contact with antigen bound to MHC molecule on antigen presenting cell

Cluster II

• External side of plasma membrane

We observed DET/DEGs associated with the immune system down regulated in high shedders compared to low shedders late in the infection (Table 4.2). Immune functions of DET/DEGs include regulators of NFκβ and STAT activity, an ISG with unknown antiviral activity, T cell activation/proliferation, an MHC component, and phagocytosis/apoptosis.

LPAIV genes were not differentially expressed between shed level groups in late-stage infection, as was observed between LPAIV-infected and uninfected birds; however, one ERV transcript (POL_MLVFF) and two ERV genes (POL, SFV1, SYNA_MOUSE) were down-regulated in high shedders compared to low and moderate shedders on five DPI (Figure 4.7).

Candidate Gene Analysis

Identification of candidate genes in the blue-winged teal de novo transcriptome resulted in a final set of 2,125 candidate transcripts and 869 candidate genes associated with 76 search terms (Supplemental File S2). Analysis including LPAIV-infected and uninfected control birds identified 38 unique candidate genes with significant positive linear relationships and 11 unique candidate transcript/genes with negative linear relationships between expression level and viral

load (Table 4.3, Supplemental File S5). Analysis including only LPAIV-infected birds identified 22 unique candidate genes with significant positive linear relationships and three unique candidate transcript/genes with negative linear relationships between expression level and viral load (Table 4.3). All transcripts and genes were significant in the ileum, but only four genes were significant in the bursa.

Table 4.3: Significant (p<0.05) linear relationships between viral load and candidate gene expression for LPAIV-infected blue-winged teals and uninfected controls. Genes were significant at either the transcript level, gene level, or both. All results are for the ileum only, unless otherwise stated.

	Cellular Immunity	Regulator of Interferon Pathway	Interferon Stimulated Genes	Ubiquitination or Kinase Activity	Sialyltransferases	Other
Positive	CC4Lbe5 CCL13° CCL26° CCL4bc CCR5be5 CD4° IL10° IL18° IL8° IL8H° LY6Ec5 MXAR5° TAP1bc15	DDX58bc1 DHX58bc5 IFIH1c IFNA2c IFNL3c IKBEc IRF1c IRF3lbc NFKB1bl5 PARP9bc STAT1bc1	E2AK2 ^{bc15} IFI6 ^{bc15} IFIT5 ^{bc1} IFM5 ^{bc} IN35 ^{bc1} MX ^{abc15} OASL1 ^{bc13} OASL2 ^{bc} PAR12 ^{bc1} RSAD2 ^{abc1}	PARP9 ^{bc} UBP34 ^{bc}		DSA2B ^{c1} FOXC2 ^c GBA2 ^{abc} MIRO1 ^{c1}
Negative	CD59 ^b MXRA5 ^c	FGFR2° FGFR3° IFRD1°		CDC37 ^{b5} FGFR2 ^c FGFR3 ^c	SIAT6° SIA4A° SIA7C°	BMP6 ^c FGF14 ^c FGF4 ^c IRF6 ^c PDE4D ^{c5} RPGF2 ^b

^aalso significant in bursa

^bsignificant in all LPAIV-infected birds without uninfected controls

^csignificant in all LPAIV-infected birds with uninfected controls

¹I1 significant

³I3 significant

⁵I5 significant

Gene expression of many cytokines, chemokines, and interleukins involved in inflammation and signaling of leukocytes had positive linear relationships with virus titers. Pattern recognition receptors, specific transcription factors, and interferons responsible for regulating the interferon pathway also had positive linear relationships between gene expression and viral load. Only three regulators of the interferon pathway had negative linear relationships. All ISGs had positive linear relationships between gene expression and viral load. Three sialyltransferases had significant negative linear relationships between gene expression and viral load, but only when uninfected control birds were included in the analysis. Additionally, gene functions in ubiquitination and kinase activity were among significant candidate genes. Several immune genes with significant linear relationships were also differentially expressed between LPAIV-infected and uninfected control birds (Table 4.2).

Discussion

In this study, we analyzed gene expression in LPAIV-infected blue-winged teals to determine the genetic factors associated with potential viral transmissibility as indicated by cloacal shedding magnitude. We found that genes associated with the host immune response were positively associated with viral shedding. We also observed differential gene expression between high viral shedders and low/moderate viral shedders to be associated with biological processes known to influence influenza replication. Later in the infection, we observed that many genes were down regulated in high shedders compared to low/moderate shedders, which could suggest that a high viral load is associated with the suppression of gene expression. Additionally, our results show distinct differential gene expression between the ileum and bursa, suggesting tissue-specific host responses to LPAIV infections in blue-winged teals. Given what is known about AIV infections and avian host responses, we propose mechanisms for how viral load may influence gene

expression over time and highlight how these data can guide future research into understanding the intrinsic factors associated with intraspecific variation in blue-winged teal LPAIV shedding.

Our results indicate that the interferon pathway plays an active role in the ileum of LPAIV-infected blue-winged teals early in the infection (1-3 DPI). On one and three DPI, we observed up-regulation of interferon pathway regulators and antiviral ISGs between infected and uninfected birds (Table 4.2). The interferon pathway is considered an important innate immune response to viral infections since it initiates the activation of several antiviral ISGs (Schoggins and Rice 2011). When host cells are exposed to viral RNA, pattern recognition receptors RIG-1 (also known as DDX58), MDA5, and LGP2 activate transcription factors IRF3/IRF7, NF-kB, and AP-1 to initiate the production of interferons, which signal the JAK-STAT pathway to produce ISGs(Loo et al. 2008; Santhakumar et al. 2017). This process provides protection to the host since many ISGs are known to inhibit virus cell entry, inhibit virus replication, degrade viral RNA, regulate cell apoptosis, and have negative regulatory effects on IFN pathways (Santhakumar et al. 2017; Schoggins and Rice 2011). Our results are consistent with other AIV studies where lung/intestinal tissue from ducks infected with LPAIV H5N2 (Vanderven et al. 2012) and lung tissue from chickens infected with LPAIV H9N2 (Ranaware et al. 2016) also showed upregulation of interferon pathway genes. Our results suggest that the innate immune response to LPAIV in blue-winged is similar to what has been observed in other avian species; however, these results differ from what we observed in mallards (Chapter 3).

In LPAIV-infected teals, we also found that up-regulated innate immune response genes are positively associated with viral shedding. We found that several interferon regulating genes, ISGs, cytokines, interleukins, and chemokines had significant positive linear relationships to cloacal swab virus titers (Tables 4.2 and 4.3). These results are not surprising given that

interferon pathway activation is a response to virus exposure via the IFN pathways (Schoggins and Rice 2011; Sen and Peters 2007). Similar to our results, positive correlations have been observed previously between virus titers and MX transcripts in the ileum of ducks infected with LPAIV H7N1 (Volmer et al. 2011). Additionally, viral RNA expression was found to be correlated with interleukin and interferon expression in H9N2 infected chickens (Reemers et al. 2010). We also observed that viral genes in the ileum had similar gene expression patterns to interferon pathway genes over time (Figure 4.5). Cornelissen et. al (2012) suggested that immune gene expression is related to LPAIV H7N1 virus titers since expression levels of RIG-I and MDA5 matched virus titer quantities in the ileum, bursa, and lung. These results are also similar to the positive relationships we observed in mallards (Chapter 3) for similar immune genes. Overall, our results provide further evidence that the innate host innate immune response is positively related to viral load.

Early in the infection, no ISGs were found to be differentially expressed between high shedders and low/moderate shedders; however, two genes which regulate the interferon pathway were differentially expressed. Transcripts of TRAF6 and DDX3X, which are involved in the activation of transcription factors IRF7 and NF-kβ, were differentially expressed between low and high shedders on three DPI (Table 4.2). Both genes are stimulated by RIG-1 (aka DDX58) (Konno et al. 2009; Niu et al. 2019); however, TRAF6 is down regulated in high shedders and DDX3X is up regulated in high shedders. This oppositional expression of two transcripts with similar functions could explain why interferon pathway genes downstream of IRF7 and NF-kβ are not differentially expressed between high shedders and low/moderate shedders. The mechanisms underlying the gene expression differences for TRAF6 and DDX58 are unknown; however, a previous study found that miRNA-144 suppressed TRAF6 levels and resulted in

increased viral replication in the lung tissue of mice infected with influenza virus H1N1, encephalomyocarditis virus, and vesicular stomatitis virus (Rosenberger et al. 2017). Mi-RNAs are classified as small non-coding RNAs and are able to control gene expression (Catalanotto, Cogoni, and Zardo 2016). Studies have found that genetic variants of mi-RNA loci are related to the inter-species and inter-individual variation observed in gene expression (Ason et al. 2006; Lu and Clark 2012). We did not evaluate miRNAs in our study; however, future research using a combined sequencing approach of miRNA and mRNA simultaneously could greatly improve our understanding of the mechanisms linking viral load and gene expression.

Expression of innate immune system genes were mostly observed in the ileum compared to the bursa (Table 4.2). Only a few studies have assessed gene expression in the bursa of AIV infected birds, but similar to our results, very little gene expression has been observed in the bursa. In LPAIV H7N1 infected ducks, higher expression of interferon regulator genes were observed in the ileum compared to the bursa early in the infection and exhibited even lower expression later in the infection (Cornelissen et al. 2012). Another study showed only nine miRNAs differentially expressed in the bursa of HPAIV H5N1 ducks (Li et al. 2015). Even though both the ileum and bursa are sites of high LPAIV replication in ducks (*Anas platyrhynchos*) (Daoust et al. 2011), our results suggest that the host immune response is activated mostly in the ileum and not the bursa of blue-winged teals. These findings were also consistent with mallards (Chapter 3). Currently, the mechanism for the immune response differences to influenza virus between the bursa and ileum in this species is still unknown and should be a focus for future research.

Viruses rely on host cellular functions to complete their life cycle and have developed mechanisms for hijacking or suppressing host genes to successfully complete their life cycle

(Watanabe et al. 2012). Previous studies using small interfering RNA (siRNA) have identified host factors involved in the influenza A life cycle (Hao et al. 2008; Karlas et al. 2010; König et al. 2010; Shapira et al. 2009; Shaw and Stertz 2017). Among the host factors associated with influenza virus replication identified in one study (König et al. 2010), kinase-regulated signaling, phosphatase activity, and ubiquitination were the most enriched biological processes. In our study, we found genes involved in ubiquitination, kinase activity, and phosphatase activity differentially expressed between LPAIV-infected birds and uninfected controls early in the infection and between shed level groups early and late in the infection (Table 4.1). Ubiquitination upregulates influenza virus polymerase function (Kirui, Mondal, and Mehle 2016), is involved in virus cell entry (Rudnicka and Yamauchi 2016), and regulates the innate immune response to influenza infection (Rudnicka and Yamauchi 2016). Since the virus does not encode its own kinases, host cellular kinases are used directly or indirectly to regulate phosphorylation-dependent processes during influenza virus replication (Meineke, Rimmelzwaan, and Elbahesh 2019). Some protein kinases are also known to be inhibitors of influenza A virus replication, which is of particular interest for clinical applications in humans (Kumar et al. 2011; Meineke, Rimmelzwaan, and Elbahesh 2019). Our results do not confirm that any of the genes identified in our study enhance or inhibit influenza virus replication in bluewinged teals, but these results do provide new knowledge of differentially expressed genes between low and high shedding individuals. This knowledge will lead future research into identifying the mechanisms used by these genes and their influence on viral load.

Later in the infection, as the host's adaptive immune system begins to respond (Chen et al. 2018), differential expression of genes involved in the regulation of T cells and the major histocompatibility complex (MHC) were observed between high shedders and low shedders

(Table 4.2). Inhibitors of T cell regulation, MHC molecules, regulators of NFκβ activation/degradation, and genes involved in autophagy were among the many genes suppressed in high shedding individuals. The adaptive immune response is characterized by T cells recognizing dendritic cells with viral protein fragments bound to MHC molecules (Guermonprez et al. 2002). CD8+ T cells differentiate into cytotoxic T lymphocytes (CTLs) and are responsible for the production of cytokines and other molecules important for reducing viral replication and killing virus infected cells, while CD4+ T cells contribute to B cell activation and the production of antibodies (Chen et al. 2018). As mentioned previously, NFκβ is a transcription factor of interferons that initiate the expression of ISGs during the innate immune response, but it is also important in the development of T cells, B cells, and lymphoid tissue development (Hayden, West, and Ghosh 2006). Autophagy is the process by which the host recognizes and eliminates virus infected cells; however, influenza viruses can hijack host autophagy processes to enhance viral replication (Zhang et al. 2014). Our results show that specific genes of the adaptive immune system are regulated differently in high shedding individuals compared to low shedding individuals later in the infection. These results are different from what we observed in mallards (Chapter 3), where DEG/DETs were not observed later in the infection. Our findings could indicate that high shedding individuals of different wild duck species respond differently to AIV infections.

Host gene shut-off by viral proteins is a potential explanation for why so many transcripts and genes were not expressed by high shedding blue-winged teals late in the LPAIV infection (I5). Several mechanisms have been proposed that can lead to the reduction of host cell mRNA (Rivas, Schmaling, and Gaglia 2016), one of which involves the viral protein PA-X coded by the viral gene PA, which selectively degrades host transcripts formed by host RNA polymerase II

(Khaperskyy et al. 2016). Our results showed PA to be differentially expressed between infected birds and uninfected controls as well as significantly positively related to cloacal virus titers on one DPI. PA-X might be responsible for host gene shut-off later in the infection due to the low efficiency of ribosomal frameshifting, which is required for the transcription of PA-X (Khaperskyy et al. 2016; Rivas, Schmaling, and Gaglia 2016). Our results suggest that high shedders early in the infection have a higher accumulation of viral gene PA early in the infection, which could lead to host gene shut-off later in the infection. While different mechanisms for host gene shut-off have been proposed, further research of these mechanisms will be required to identify if the large number of downregulated genes in high shedders on five DPI could be related to this proposed phenomena.

Inherent differences between high shedders and low/moderate shedders could potentially be influenced by the down regulation or absence of retroviral genes. ERV genes (POL, SYNA) were down regulated in high shedders on one and five DPI, some of which had no expression at all in high shedders. The effects of ERV gene expression on exogenous viral infections and innate immunity are a current research topic with much discussion (Chuong, Elde, and Feschotte 2016; Grandi and Tramontano 2018; Hu et al. 2017). It is well known that ERV gene expression is increased when exposed to exogenous retroviruses, as is the case with human ERV genes in HIV infections (Gonzalez-Hernandez et al. 2012). Increased ERV gene expression was also observed in non-retroviral infections such as ERV avian leukosis virus (AVLE) in chicken cells infected with Merek's disease virus, an alphaherpesvirus (Hu et al. 2017). ERV genes are also known to affect the immune response, such as T lymphocyte selection and the sensitivity with which T lymphocytes react to retroviral infection strongly influenced by ERV gene expression (Garrison et al. 2007; Takahashi et al. 2008; Young et al. 2012). Specific to influenza virus,

ERVs have been shown to augment antiviral immunity (Schmidt et al. 2019). These findings suggest that endogenous retroviruses could influence exogenous viral replication or the immune response, and therefore warrant further investigation to determine their biological role in viral shedding variation.

Sialyltransferases negatively associated with viral load in the ileum could indicate decreased sialic acid receptor abundance after LPAIV exposure. Sialyltransferases are responsible for the biosynthesis of sialic acid receptors, and receptors with galactose bound in the α 2,3 position (SA α 2,3Gal) are preferred for LPAIV attachment and cell entry (Ito et al. 1997; Skehel and Wiley 2000). It has previously been hypothesized that a decrease in SAα2,3Gal could occur due to the function of neuraminidase cleaving SAα2,3Gal to release virions from the cell membrane (Byrd-Leotis, Cummings, and Steinhauer 2017; Franca, Stallknecht, et al. 2012). While we did not observe any sialyltransferase genes differentially expressed between shed level groups, SIAT4A (ST3Gal I), involved in the synthesis of the sequence NeuAc-alpha-2,3-Galbeta-1,3-GalNAc, SIA7C (ST6GalNAc III), involved in the transfer of an alpha-2,6-linkage to the GalNAc residue on NeuAc-alpha-2,3-Gal-beta-1,3-GalNAc, and SIAT6 (ST3Gal III), involved in the synthesis of the sequence NeuAc-alpha-2,3-Gal-beta-1,4-GlcNAc, all had negative linear relationships with virus titers when uninfected control birds were included in the analysis (Table 4.3). In a previously published manuscript, we found that SAα2,3Gal (NeuAcalpha-2,3-Gal-beta-1,4-GlcNAc) in mallard ileum enterocytes was positively associated with viral shedding, but not associated with viral shedding in blue-winged teals (Dolinski, Jankowski, et al. 2020). Additionally, we observed up regulation in mallard high shedders for two SAα2,3Gal genes early in the infection (Chapter 3). These contradictory results suggest that further research is warranted in determining the relationship between sialyltransferase gene

expression, $SA\alpha 2,3Gal$ abundance, and viral shedding to further explore the differences between these two species.

Overall, this study provides insights into how variation in viral shedding is associated with gene expression over time in LPAIV-infected blue-winged teals. With this comprehensive gene expression analysis between individuals with varying viral shedding loads, we discovered many genes and biological processes that could explain differences between high shedders and low/moderate shedders. Even though our threshold for differential gene expression significance was liberal with parameters of p< 0.1 and an LFC >1.0, our results can still provide novel and biologically meaningful knowledge regarding shed level and viral infections. As previous gene expression studies of LPAIV-infected birds have indicated, gene expression is observed far less in LPAIV infections compared to HPAIV infection (Huang et al. 2013; Ranaware et al. 2016; Vanderven et al. 2012). Differential gene expression observed using these liberal parameters, however, can guide future genetic research determining the relationship between gene expression and viral load in wild ducks.

Our transcriptome-wide investigation provides new knowledge that could guide future research of genes unique to LPAIV-infected blue-winged teals and high shedding individuals. In addition to the known genes and biological processes we identified in this study, 18% of the transcripts and 66% of the genes differentially expressed had no annotation information available. Given the substantial efforts underway to provide better gene annotation resources, our results will only become more comprehensive and informative with time. Such future work includes identifying specific single nucleotide polymorphisms (SNP) that could improve understanding of intrinsic susceptibility to infection and gene silencing studies to confirm involvement of specific genes in viral replication studies. For example, genetic biomarkers are

used in the field of ecogenotoxicology as a method of detecting organisms exposed to environmental contamination and the impact of xenobiotics on ecosystems (Angeletti and Carere 2014). These data could contribute to the development of biomarkers used in field studies to detect highly individuals that are more susceptible to developing high viral loads and thus more likely to by highly infectious. Future studies could also focus on non-lethal approaches to studying gene expression over time, given we could not test gene expression at multiple intervals post infection.

Though the results of this study were specific to LPAIV-infected blue-winged teals, many of the genes identified are involved in biological processes of other host-pathogen systems across species. We showed that genes associated with the interferon pathway are likely driving the innate immune response early in the infection, which is similar to the innate immune response for other viral infections (Purcell et al. 2010); therefore, the positive linear relationships observed between interferon pathway genes and viral load could potentially be observed for other host-pathogen systems. We identified annotated genes as well as novel genes differentially expressed between high-shedders and low/moderate shedders that could provide insight into the genetic factors related to viral shedding load. With human diseases like Covid-19, which is caused by a virus thought to have originated in a wildlife host (Zhang and Holmes 2020), and where secondary transmission is affected by super-spreading events (Al-Tawfiq and Rodriguez-Morales 2020), understanding the host factors responsible for variation in viral load should be a high priority in future host-pathogen studies.

CHAPTER 5: CONCLUSION

Summary

Heterogeneity in pathogen transmission can greatly impact a disease outbreak (Galvani and May 2005; Lloyd-Smith et al. 2005); therefore, the objective of this dissertation research was to determine the intrinsic host factors associated with intraspecific viral shedding variation in LPAIV-infected wild ducks. In chapter one, I discussed how super-shedders, that is the few individuals that shed the highest quantity of pathogen (Chase-Topping et al. 2008), contribute to disease transmission dynamics. I provided examples of wildlife species across taxa with observed intraspecific variation in pathogen load and the methods that could be used for targeting super-shedders in the control of disease outbreaks. Since wild mallards were previously observed to shed LPAIV according to the Pareto Principle, where 20% of the birds are responsible for 80% of the overall virus shed (Jankowski et al. 2013), co-authors and I hypothesized that physiological, immunogenic, and genetic traits of LPAIV-infected mallards and blue-winged teals would be associated with intraspecific variation in viral shedding load. In chapter two we tested our hypothesis by evaluating the physiological trait of viral receptors (SAα2,3Gal) required for LPAIV cell binding and entry that are located in the intestines and bursa of Fabricius. In chapters three (mallards) and four (teals) we evaluated the immunogenic and genetic traits by sequencing the total mRNA in the ileum and bursa of Fabricius to analyze gene expression over the course of the infection. Our hypotheses were supported in that statistically significant associations were found between viral shedding and the intrinsic host factors tested. We also observed differences between tissues and species suggesting that intertissue and interspecific variation are contributors to viral load variation as well. Table 5.1 highlights the results from each chapter that provide supportive evidence for our overall

conclusions. Table 5.2 highlights species and tissue comparisons for our supported hypotheses.

In this dissertation conclusion, I collectively address our research findings and discuss how these data and results could contribute to future research.

Table 5.1: Dissertation conclusions and the results in each chapter that provide evidence to support each conclusion.

		Evidence	
Conclusion	Chapter 2	Chapter 3	Chapter 4
LPAIV receptors are associated with viral shedding	 Teals had higher virus titers and higher SAα2,3Gal than mallards Mallards had higher intraspecific variation in virus titers and SAα2,3Gal than teals SAα2,3Gal in the mallard ileum was associated with viral shedding 	• 13 genes that promote viral cell entry were down regulated in low shedders on one DPI including two sialyltransferase genes ST3GAL5 and ST3GAL1	
Gene expression of the innate immune system is positively influenced by intraspecific viral load variation.		• Genes of the interferon pathway such as DDX58, DHX58, OASL, PARP12, IFIT5, MX, IFI35, RSAD2, and IFNL3 were positively associated with viral shedding (Figure 3.10)	• Genes of the interferon pathway such as DDX58, DHX58, OASL1, PAR12, IFIT5, MX, IN35, RSAD2, and IFNL3 were positively associated with viral shedding (Table 4.3)
The ileum is important for intraspecific LPAIV shedding variation	 SAα2,3Gal in the mallard ileum is associated with viral shedding (Table 2.3) Significant positive relationship between virus titers in the ileum and cloacal swab virus titers (Figure 2.2) 	• 592 genes were differentially expressed between shed level groups early in the infection compared to 17 genes in the bursa	• 97 genes were differentially expressed between shed level groups later in the infection in the ileum compared to one gene in the bursa

Table 5.2: Interspecific and inter-tissue comparisons of supported hypotheses in this dissertation. Yes = hypothesis was supported based on dissertation results. No = hypothesis was not supported based on dissertation results. Early = early in the infection. Late = late in the infection.

	Mal	lard	Te	al
Hypotheses Supported	ileum	bursa	ileum	bursa
LPAIV receptor (SAα2,3Gal) occurrence frequency was associated with viral shedding	yes	NA	no	no
Differential Gene expression was observed between LPAIV- infected and uninfected birds by DPI	no	no	yes - early	no
Differential Gene expression was observed between shed level groups	yes - early	yes - early	yes - early & late	yes - early
Innate immune genes were differentially expressed by shed level groups	yes - early	yes - early	yes - early & late	yes - early
Adaptive immune genes were differentially expressed by shed level groups	yes - early	no	yes - late	no
Gene expression of innate immune genes were positively related to viral shedding	yes	yes	yes	yes

Before we could test our hypotheses, intraspecific variation in LPAIV shedding needed to be confirmed. In chapter one, we showed that both mallards and blue-winged teals in our study shed LPAIV with variation according to the Pareto Principle (Figure 1.1), similar to what has previously been observed (Jankowski et al. 2013). We also confirmed that for both species >98% of viral shedding occurred between one and five DPI with peak viral shedding between one and three DPI (Chapter 2, Dolinski, Jankowski, et al. 2020), which is similar to results observed in previous studies (Jourdain et al. 2010). Interestingly, our virus titer results also indicated that teals had significantly higher virus titers than mallards (Figure 2.4), but mallards shed LPAIV with significantly greater intraspecific variation than teals (Figure 2.3). These results provided

the first indication that while mallards and teals shed LPAIV with a similar viral shedding profile over time, there may be something unique about mallards to indicate why intraspecific variation is greater in mallards, and teals shed more virus than mallards.

Conclusions Across Dissertation Chapters

Evidence from chapters two and three supported our hypothesis in that the physiological host factor of viral receptors, which promote LPAIV cell entry and binding, were associated with viral shedding (Table 5.1). In chapter two, we determined that viral receptor occurrence frequency in the ileum of mallards was significantly related to viral shedding load. Even though we did not find a similar significant relationship in teals, we found that both virus titers and viral receptor occurrence frequency was higher in teals compared to mallards, further suggesting that higher virus receptor occurrence frequency is related to higher viral shedding. The gene expression results of mallards in chapter three provided evidence for a potential mechanism to explain how intraspecific viral receptor occurrence frequency is associated with viral shedding. Sialyltransferase genes, responsible for the production of SAα2,3Gal (Harduin-lepers 2010), and other genes that promote viral cell entry, were down regulated in the ileum of low shedding mallards early in the infection (Table 3.4). It is possible that lower expression of sialyltransferases in the mallard ileum leads to a lower production of viral receptors in the ileum enterocytes, thus causing limited viral cell entry and lower viral replication early in the infection; therefore, causing lower viral shedding.

Some questions still yet to be answered are if sialic acid receptor occurrence frequency in the ileum changes over time, is influenced by LPAIV infection, or if viral receptor occurrence frequency is determined by some other unknown factor. A study where viral receptors are measured over time in association with sialyltransferase gene expression is warranted to

determine this mechanism. Perhaps a gene knockout study or a population evaluation of sialyltransferase SNPs in the genome of wild mallards could provide further insight into identifying the mechanism responsible for these observations. Regardless of what the underlying mechanism is, our results provide collective evidence supporting our hypothesis that intraspecific variation in viral receptors is associated with viral shedding variation.

Another main finding was that gene expression of innate immune genes, particularly of the interferon pathway, are positively related to viral shedding in both species (Table 5.1). For both mallards and teals, we searched the literature and identified immune genes that are associated with AIV infections (Supplemental File S2) to test the linear relationship between gene expression and viral shedding load. Both mallards and teals showed positive linear relationships with genes of the interferon pathway, such as pattern recognition receptors RIG-1 (DDX58) and LGP2 (DHX58), type three interferon IFNL3, and interferon stimulated genes OASL, PARP12 (PAR12), IFIT5, MX, IFI35 (IN35), RSAD2. These genes are consistently up regulated in AIV infections but are also known to have antiviral effects (Santhakumar et al. 2017); therefore, we might expect to see a negative relationship between expression of these genes and viral load. In order to assess gene expression in the ileum and bursa we sacrificed birds to obtain tissue samples; therefore, the relationship we observed between viral shedding and gene expression is likely an effect of viral load on gene expression. Due to our experimental design, we were unable to determine the effects of gene expression on viral load; therefore, in future studies, we suggest designing an experiment where non-lethal samples for gene expression could be collected from each individual at several time points throughout the infection, as this may determine whether high expression of interferon pathway genes are associated with lower viral loads later in the infection. Additionally, determining intraspecific SNP differences for

immune genes, similar to the allele differences detected in super-shedders of BLV-infected cattle (Juliarena et al. 2008), will also determine whether specific immune gene SNPs are associated with variation in viral load.

In chapters two, three, and four we also determined that viral shedding is more closely associated with host factors in the ileum compared to other tissues. Between shed level groups early in the infection of mallards (Figure 3.5) and later in the infection of teals (Figure 4.6), we observed several more genes differently expressed in the ileum compared to the bursa (Table 5.1). Mechanistically, we do not know why gene expression of the ileum is more closely related to intraspecific viral shedding variation than the bursa; however, I propose a few hypotheses. Results from chapter two show that virus titers in the bursa are positively related to cloacal swab virus titers (Figure 2.2), indicating that viral variation in the bursa tissue is similar to viral shedding variation. We also found positive relationships between virus titers in ileum and bursa tissues (Figure 2.2); therefore, perhaps viral load in the bursa is impacted by the quantity of virus replicated in the ileum given that virus replicated in the intestines encounters the bursa prior to excretion. Another possible explanation is that our methods for gene expression captures the total mRNA of the tissue segment collected and not specifically the mRNA in the cells where the virus replicates. In ducks, LPAIV specifically replicates in the epithelial cells of the bursa and the intestines (Daoust et al. 2011; Webster et al. 1978); however, based on tissue processing procedures used, we know that mRNA from other cell types were present in our samples. Given that the epithelium of the ileum is more extensive than the epithelium of the bursa, due to the folding and fingerlike projections of the intestinal villi, perhaps gene expression analysis of total mRNA in the ileum was sufficient to capture gene expression differences for LPAIV infection, but total mRNA in the bursa was not.

It is also possible that we simply did not test for the bursal factors associated with viral shedding variation. The bursa is a transient organ that completely atrophies in mallards between 4 and 6 months of age (Wille et al. 2018), and studies have shown that aging reduces bursal lymphoid follicle associated epithelium (Ciriaco et al. 2003); therefore, perhaps age and size of the bursa could be a contributing factor to viral load variation. Bursal mass or size was not measured in this study; however, age could be analyzed with our data by conducting analyses on different age groups. Given various hypotheses to explain why more genes were differentially expressed in the ileum compared to the bursa and considering the results from all three chapters, we determined that physiological, genetic, and immunogenic host factors of the ileum are important for future work in determining the mechanisms underlying intraspecific LPAIV shedding.

Interspecific Differences

The differences observed between mallards and teals in host factors associated with intraspecific LPAIV shedding variation was a main finding of this research. In chapter two, we observed a significant relationship between SAα2,3Gal occurrence frequency and viral shedding in mallards but not teals, which is likely partly due teals having almost no intraspecific variation in SAα2,3Gal occurrence frequency. In chapter three, differential gene expression was not observed between LPAIV-infected and uninfected mallards at any DPI, as it was for teals and previously studied mallards (Cornelissen et al. 2012; Fleming-Canepa et al. 2019; Maughan et al. 2013; Smith et al. 2015; Vanderven et al. 2012). Additionally, several genes in teals were down regulated in high shedders later in the infection, and no differential gene expression was observed in mallards later in the infection. The ileum of mallards, however, showed extreme

differential gene expression between shed level groups early in the infection, which included immune genes and genes that promote viral cell entry and viral replication.

I hypothesize that the gene expression differences observed between mallards and teals is associated with the intraspecific variation observed in mallard $SA\alpha 2.3Gal$ occurrence frequency. Given that several genes that promote viral cell entry, including sialyltransferases, were down regulated in low viral shedding mallards early in the infection (Table 3.4), it is probable that low SAα2,3Gal occurrence frequency in ileum enterocytes is preventing viral cell entry at an intracellular viral load high enough to trigger the innate immune response. Without an initiation of viral replication or the innate immune response in birds with low SAα2,3Gal occurrence frequency, significant gene expression differences between low shedders and uninfected birds would therefore be undetectable early in infection, which is supported by our analyses of select immune genes (Supplemental File S3). The lower SAα2,3Gal occurrence frequency could be a mechanism affecting the latent period of LPAIV infections by preventing viral loads from getting high enough to trigger an immune response in individuals with low SAα2,3Gal occurrence frequency until later in the infection. This hypothesis could be another explanation for why intraspecific viral shedding variation is much greater in mallards than teals, and differential gene expression could not be detected between mallard shed level groups later in the infection.

Our results also show that the intraspecific LPAIV shedding variation in mallards from one to five DPI (Figure 3.2) is more sporadic than it is in teals (Figure 4.3). If viral receptor occurrence frequency is affecting the latent period of infection, individual mallards would therefore be at different stages of the infection post inoculation based on viral loads getting high enough to trigger a host immune response. If intraspecific variation in SAα2,3Gal occurrence

frequency is the mechanism creating gene expression differences between mallards and teals, I predict that if the low shedders were removed from the mallard analysis, differential gene expression between LPAIV-infected and uninfected mallards would be similar to differential gene expression observed in teals. This prediction has not yet been analyzed, but the data are available for future analysis.

It is possible that there are gene expression differences between mallards and teals that are not caused by differences in $SA\alpha2,3Gal$ occurrence frequency. In 2009, a phylogenetic analysis of mitochondrial genes for several waterfowl species indicated that the teals and shovelers, formerly in the genus Anas, belong in their own genus Spatula, and thus were renamed in 2017 (Chesser et al. 2017; Gonzalez, Düttmann, and Wink 2009). While this certainly could not be the reason for gene expression differences observed between mallards and teals, an assessment of the host intrinsic factors associated with intraspecific LPAIV shedding variation in more waterfowl species is warranted. It would be interesting to see if species belonging to the same genus are more similar than birds in a separate genus.

Future Contributions

One of the unique aspects of this dissertation research is that in addition to the hypothesis testing conducted, our a priori approach used to analyze gene expression by sequencing total mRNA in the ileum and bursa allowed us to discover unknown genes that are associated with LPAIV infections and viral load. We detected several annotated and unannotated genes that were differentially expressed in each analysis that have not previously been association with AIV infections in poultry. These data provide a starting point for determining how these genes function within this system and what role they play in their association with intraspecific variation in pathogen load.

In the past decade, several studies have been conducted to determine the human host genes that are associated with influenza viral infections (Karlas et al. 2010; König et al. 2010; Peacock et al. 2019; Stertz and Shaw 2011). These studies used RNA interference (RNAi) screenings or quantitative proteomic applications of influenza infected cells to detect interactions of RNA molecules (König et al. 2010; Shaw and Stertz 2017). In addition to gene knockout studies and detecting SNP differences in transcript sequences, perhaps an RNAi study could be conducted in duck cells to determine the avian host cell machinery that promotes or inhibits AIV replication.

In addition to the future work that could be conducted to test the hypotheses and molecular mechanisms already suggested, I also recommend improvements for replication studies or adapting these methods to other host-pathogen systems. A major limitation of our experimental design was that birds needed to be sacrificed in order to acquire the tissue samples for evaluating the host factors of interest. This prevented us from being able to observe virus titers on DPI later than tissue samples were collected, thus conclusions drawn which relate SA α 2,3Gal occurrence frequency and gene expression to viral titers is dependent upon virus titers measured prior to tissue collection.

Non-lethal samples collected which could be used for detecting host factors over the course of the infection include fecal and blood samples. Transcriptional analysis of peripheral blood mononuclear cells (PBMCs) in AIV H9N2 infected geese was previously successful in detecting up regulation of interferon stimulated gene MX (Zeng et al. 2016). Evaluating PBMCs would not be able to provide much information about host factors at the site of viral replication, but they could provide insight concerning the host immune response. Fecal samples, however, are rich in recently sloughed enterocytes, and techniques have been developed to isolate these

cells for laboratory analysis in humans (Nair et al. 2003). Perhaps using flow cytometry (Mackenzie and Pinder 1987) and transcriptional analysis on isolated enterocytes in feces could provide a non-lethal method of analyzing host factors contributing to intraspecific LPAIV shedding variation in a longitudinal study over the course of the infection.

Although the nature of the research conducted for this dissertation is not applied research, the data and results generated provide new knowledge that will aide future research in experimental design. For example, prior to this research it was well known that LPAIV replicates in the intestines and bursa of Fabricius, but new knowledge generated from this project suggests that when targeting variation in viral load, the tissue of high priority is the ileum over the bursa. We also showed that significant differences are observed between two species of wild ducks, indicating that evaluating intrinsic factors of species separately is crucial to understanding intraspecific host factors. We also are the first to generate comprehensive transcriptomic data from wild LPAIV-infected ducks. All previous transcriptomic work of LPAIV-infected ducks had only been conducted on farm bred ducks. The data generated from this research can be used to inform future research of potential gene targets for molecular mechanism studies. We suggest looking at the host cell factors, like HSPA8, and genes involved in ubiquitin and kinase activity in controlled experiments to determine the molecular mechanisms involved in intraspecific viral load variation. If confirmed mechanisms are found for specific transcripts, genes, or SNPs, biomarkers could be used for the identification of super-shedders in field studies and the application of disease management.

Targeting super-shedders in wildlife disease management is only useful if the conditions in which super-shedders impact pathogen transmission dynamics are established. Even though we detected significant associations between intrinsic host factors and intraspecific LPAIV

shedding variation in wild ducks, it still is yet to be determined if LPAIV super-shedders affect disease transmission dynamics. In chapter one, I suggested that LPAIV super-shedders are important in LPAIV transmission since LPAIV is transmitted via the fecal-oral route similar to *E. coli*-infected cattle, a known host-pathogen system where super-shedding affects outbreak dynamics (Matthews, McKendrick, et al. 2006). Our study, however, cannot confirm or deny that super-shedders play a role in transmission dynamics.

Transmission of LPAIV generally occurs via defecating and feeding in bodies of water, but cloacal drinking and preening are also potential sources of infection (Wille et al. 2018). It has also been suggested that LPAIV can be transmitted via aerosol droplets (Slemons and Easterday 1978); however, it is unlikely virus aerosolized by the respiratory tract is a mode of transmission since LPAIV antigen was found in the epithelial cells of the intestines and bursa of Fabricius but not in the respiratory tract (Daoust et al. 2011; Franca, Stallknecht, et al. 2012; Wille et al. 2014). Aerosolized droplets are likely formed via wing flapping on the surface of virus contaminated water after an infected duck defecates and takes flight. These aerosolized droplets may enter the body through the nares then enter the throat where they are swallowed. These different inoculation methods could affect how LPAIV shedding impacts transmission, since proximity of susceptible ducks to infected ducks and viral load dilution in a body of water are transmission factors to consider. Future research is dependent upon understanding in what circumstances super-shedders are important in LPAIV transmission dynamics, and only then will control measures directed at the LPAIV super-shedders be effective.

The purpose of the research presented in this dissertation was to determine the host factors associated with intraspecific variation in pathogen shedding. We accomplished this goal by assessing intrinsic host factors of LPAIV-infected ducks; however, as was discussed in

chapter one, there are several wildlife host-pathogen systems in which intraspecific pathogen load variation has been observed. Not every host-pathogen system, however, is affected by the same host factor dynamics; therefore, it is important in future research to study the potential host factors for each host-pathogen system. For pathogens that require direct contact, perhaps the inoculation dose for infection is all that is needed to determine the required pathogen load for a super-shedder. For host-pathogen systems that require an arthropod vector or intermediate host for transmission, knowing the inoculation dose of the vector/intermediate host as well as the pathogen shedding variation of the vector/intermediate host will also be necessary. Other hostpathogen systems that are dependent upon the environment, like AIV, will require the use of quantitative microbial risk assessment and environmental factors. For instance, a recent analysis of the transmission dynamics for the respiratory pathogen MERS in humans determined that in addition to super-spreading, environmental conditions such as the size and air exchange rate of a hospital room also had an impact on the dose-response model for risk of infection (Adhikari et al. 2019). In order to adequately assess the importance of host factors on super-shedding dynamics in wildlife disease systems, it is also important to consider the other non-host factors affecting transmission.

In conclusion, the data and results presented in this dissertation provide a first look into the intrinsic host factors that are associated with intraspecific viral shedding variation in LPAIV-infected wild ducks. I have highlighted the main findings of this research, provided hypotheses for molecular mechanisms that may explain these findings, suggested how these data can be used in future LPAIV infection studies of wild ducks, and how these results will better inform the future of super-shedding research in wildlife disease systems. By increasing the knowledge in understanding the host factors involved in pathogen transmission heterogeneity, better

technology and tools can be developed that will aide public health officials and disease ecologists for use in disease management and control.

APPENDIX

APPENDIX

Table A2.1: Pearson's r correlation matrix for mallard lectin histochemistry scores. Crypts = crypt enterocytes, villi = villi enterocytes, and BB = brush border.

Tissue Section and Component	Proximal Crypts	Proximal BB	Proximal Villi	Heum Crypts	Heum BB	Heum Villi	Cecum Crypts	Cecum BB	Cecum Villi	Colon Crypts	Colon BB	Colon Villi
Proximal Crypts	1	0.81	0.81	0.43	0.38	0.39	0.25	0.27	0.24	0.16	0.32	0.48
Proximal BB	0.81	1	0.97	0.39	0.42	0.36	0.25	0.28	0.3	0.12	0.33	0.45
Proximal Villi	0.81	0.97	1	0.32	0.33	0.27	0.21	0.26	0.27	0.06	0.26	0.4
Ileum Crypts	0.43	0.39	0.32	1	0.61	0.82	0.73	0.6	0.71	0.76	0.46	0.61
Ileum BB	0.38	0.42	0.33	0.61	1	0.81	0.44	0.5	0.51	0.33	0.52	0.61
Ileum Villi	0.39	0.36	0.27	0.82	0.81	1	0.67	0.62	0.71	0.65	0.47	0.63
Cecum Crypts	0.25	0.25	0.21	0.73	0.44	0.67	1	0.83	0.91	0.73	0.45	0.59
Cecum BB	0.27	0.28	0.26	0.6	0.5	0.62	0.83	1	0.94	0.55	0.39	0.58
Cecum Villi	0.24	0.3	0.27	0.71	0.51	0.71	0.91	0.94	1	0.59	0.38	0.54
Colon Crypts	0.16	0.12	0.06	0.76	0.33	0.65	0.73	0.55	0.59	1	0.43	0.61
Colon BB	0.32	0.33	0.26	0.46	0.52	0.47	0.45	0.39	0.38	0.43	1	0.75
Colon Villi	0.48	0.45	0.4	0.61	0.61	0.63	0.59	0.58	0.54	0.61	0.75	1

Table A3.1: Mallard RNA integrity number (RIN) and sequencing pool at Michigan State University (MSU) and University of Minnesota (UMN). Ns = not sequenced.

bird	group	sex	bursa RIN	bursa pool	ileum RIN	ileum pool
2	I1	MALE	8.9	MSU_1	5.5	UMN
6	I1	FEMALE	9.8	MSU_1	9.4	UMN
14	I1	MALE	9.1	MSU_1	4.5	ns
28	I1	FEMALE	8.7	MSU_2	7.3	UMN
32	I1	MALE	8.5	MSU_2	3.5	ns
47	I1	FEMALE	10.0	MSU_3	4.9	ns
49	I1	FEMALE	10.0	MSU_3	5.8	UMN
54	I1	FEMALE	10.0	MSU_3	8.2	UMN
56	I1	MALE	10.0	MSU_4	8.8	UMN
62	I1	MALE	9.6	MSU_4	4.9	UMN
64	I1	FEMALE	9.9	MSU_4	4.9	UMN
66	I1	MALE	9.8	MSU_4	8.3	UMN
69	I1	MALE	9.5	MSU_4	5.6	UMN
70	I1	FEMALE	9.3	MSU_4	7.0	UMN
73	I1	FEMALE	10.0	MSU_5	6.0	UMN
7	I2	FEMALE	10.0	MSU_1	8.8	MSU_5
16	I2	FEMALE	9.4	MSU_1	9.1	MSU_5
20	I2	MALE	10.0	MSU_2	10.0	MSU_5
31	I2	FEMALE	9.1	MSU_2	8.7	MSU_5
38	I2	FEMALE	9.9	MSU_3	8.9	MSU_6
43	I2	FEMALE	10.0	MSU_3	8.7	MSU_6
52	I2	MALE	10.0	MSU_3	6.5	UMN
58	I2	MALE	9.9	MSU_4	9.7	MSU_6
71	I2	MALE	10.0	MSU_5	9.1	MSU_6
78	I2	FEMALE	10.0	MSU_5	5.1	UMN
15	I5	FEMALE	8.7	MSU_1	8.3	MSU_5
19	I5	FEMALE	9.5	MSU_2	9.6	MSU_5
22	I5	FEMALE	8.4	MSU_2	8.7	MSU_5
23	I5	FEMALE	9.4	MSU_2	8.6	MSU_5
26	I5	MALE	9.8	MSU_2	8.6	MSU_5
35	I5	MALE	9.6	MSU_2	8.6	MSU_6
42	I5	MALE	9.9	MSU_3	4.5	ns
48	I5	FEMALE	10.0	MSU_3	8.3	MSU_6
53	I5	FEMALE	10.0	MSU_3	8.2	MSU_6
55	I5	MALE	10.0	MSU_4	6.3	UMN
59	I5	MALE	10.0	MSU_4	9.1	MSU_6

Table A3.1 (cont'd)

63	I5	MALE	10.0	MSU_4	6.3	UMN
68	I5	FEMALE	10.0	MSU_4	9.5	MSU_6
74	I5	MALE	10.0	MSU_5	8.1	ns
75	I5	MALE	10.0	MSU_5	8.4	MSU_6
10	I15	FEMALE	9.4	MSU_1	6.5	ns
12	I15	MALE	8.8	MSU_1	5.1	ns
27	I15	MALE	8.8	MSU_2	6.0	ns
30	I15	MALE	9.0	MSU_2	6.4	ns
34	I15	MALE	5.0	MSU_2	5.1	ns
37	I15	MALE	8.9	MSU_2	6.3	ns
45	I15	FEMALE	10.0	MSU_3	7.5	ns
57	I15	FEMALE	10.0	MSU_4	5.9	ns
61	I15	FEMALE	10.0	MSU_4	8.8	ns
65	I15	FEMALE	10.0	MSU_4	5.1	ns
3	I29	MALE	8.9	MSU_1	5.8	ns
5	I29	MALE	10.0	MSU_1	6.1	ns
9	I29	MALE	9.0	MSU_1	7.7	ns
17	I29	MALE	9.2	MSU_1	5.4	ns
36	I29	FEMALE	9.7	MSU_2	6.6	ns
40	I29	MALE	9.0	MSU_3	5.4	ns
44	I29	FEMALE	8.2	MSU_3	5.7	ns
51	I29	FEMALE	9.0	MSU_3	5.7	ns
60	I29	FEMALE	10.0	MSU_4	5.4	ns
77	I29	MALE	10.0	MSU_5	9.1	ns
1	C1	FEMALE	7.2	MSU_1	9.0	UMN
13	C1	FEMALE	8.6	MSU_1	5.1	UMN
46	C1	MALE	10.0	MSU_3	9.8	MSU_6
67	C1	MALE	10.0	MSU_4	9.9	MSU_6
72	C1	FEMALE	7.2	MSU_5	10.0	MSU_6
4	C29	FEMALE	7.9	MSU_1	4.0	ns
8	C29	FEMALE	9.0	MSU_1	5.4	UMN
18	C29	MALE	9.3	MSU_2	8.1	UMN
39	C29	FEMALE	8.5	MSU_3	6.0	ns
50	C29	MALE	10.0	MSU_3	4.8	ns

Table A4.1: Mallard RNA integrity number (RIN) and sequencing pool at Michigan State University (MSU) and University of Minnesota (UMN).

1			bursa	bursa	ileum	ileum
bird	group	sex	RIN	pool	RIN	pool
4	I-1	M	9.2	Pool2	9.6	Pool2
9	I-1	F	9.7	Pool1	9	Pool2
15	I-1	M	9.5	Pool1	9.4	Pool2
16	I-1	M	7.9	Pool1	9.1	Pool2
20	I-1	F	9.4	Pool1	9.3	Pool2
23	I-1	F	9.5	Pool1	9.4	Pool3
27	I-1	F	9.6	Pool1	9.4	Pool3
28	I-1	F	9.5	Pool1	8.9	Pool2
32	I-1	M	9	Pool1	9	Pool3
41	I-1	M	9.3	Pool2	8.3	Pool3
44	I-1	F	8.9	Pool2	9.8	Pool2
55	I-1	M	9.1	Pool3	7.5	Pool3
1	I-3	M	9	Pool1	8.9	Pool2
3	I-3	M	9.5	Pool1	10	Pool2
5	I-3	F	9.3	Pool1	9	Pool2
14	I-3	F	9.6	Pool1	8.8	Pool2
17	I-3	M	9.6	Pool1	8.9	Pool2
25	I-3	M	9.8	Pool1	9.3	Pool3
33	I-3	F	9	Pool1	8.9	Pool3
37	I-3	F	9.8	Pool1	9.5	Pool3
46	I-3	M	9.6	Pool2	9.6	Pool3
47	I-3	F	9.7	Pool2	9.2	Pool3
51	I-3	F	9.6	Pool2	9.2	Pool3
57	I-3	F	9.7	Pool3	8.5	Pool3
6	I-5	M	9.7	Pool1	9	Pool2
8	I-5	M	9.6	Pool1	9.5	Pool2
12	I-5	M	9.4	Pool1	9.4	Pool2
21	I-5	F	9.6	Pool1	9.3	Pool3
30	I-5	M	9.4	Pool1	9.3	Pool3
31	I-5	F	9.1	Pool1	9.3	Pool3
34	I-5	F	9.2	Pool1	9.7	Pool3
43	I-5	M	9	Pool1	9.8	Pool3
49	I-5	F	9.8	Pool2	9	Pool3
50	I-5	M	9.8	Pool2	9.6	Pool3
54	I-5	F	9.3	Pool2	6	Pool3

Table A4.1 (cont'd)

56	I-5	F	5.8	Pool3	9.9	Pool3
2	I-14	M	8.9	Pool1	9.9	Pool2
22	I-14	M	9.2	Pool1	9.3	Pool3
24	I-14	M	9.4	Pool1	9.2	Pool3
29	I-14	F	7.3	Pool1	9.8	Pool3
36	I-14	F	9.7	Pool1	9.3	Pool3
38	I-14	F	9.8	Pool1	10	Pool3
40	I-14	F	9.6	Pool1	9.2	Pool3
52	I-14	M	9.4	Pool2	9.7	Pool3
19	C-1	F	9.4	Pool2	8.8	Pool2
42	C-1	M	8.8	Pool1	7.4	Pool2
45	C-1	F	7.9	Pool2	8.8	Pool3
48	C-1	F	9.1	Pool2	8.8	Pool3
53	C-1	M	9.5	Pool2	9.2	Pool3
7	C-14	F	9.7	Pool1	9.2	Pool2
10	C-14	M	10	Pool1	9.8	Pool3
11	C-14	M	9.9	Pool2	9.1	Pool2
18	C-14	F	9.7	Pool1	9	Pool2
35	C-14	M	9.6	Pool1	9.8	Pool3

REFERENCES

REFERENCES

- Adhikari, Umesh et al. 2019. "A Case Study Evaluating the Risk of Infection from Middle Eastern Respiratory Syndrome Coronavirus (MERS-CoV) in a Hospital Setting Through Bioaerosols." *Risk Analysis* 39(12): 2608–24.
- Al-Tawfiq, J. A., and A. J. Rodriguez-Morales. 2020. "Super-Spreading Events and Contribution to Transmission of MERS, SARS, and SARS-CoV-2 (COVID-19)." *The Journal of hospital infection* 105(2): 111–12.
- Alexa, A., and J. Rahnenfuhrer. 2020. "TopGO: Enrichment Analysis for Gene Ontology."
- Alonso, M. A., and S. M. Weissman. 1987. "CDNA Cloning and Sequence of MAL, a Hydrophobic Protein Associated with Human T-Cell Differentiation." *Proceedings of the National Academy of Sciences of the United States of America* 84(7): 1997–2001.
- Aly, Sharif S. et al. 2009. "Reliability of Environmental Sampling to Quantify Mycobacterium Avium Subspecies Paratuberculosis on California Free-Stall Dairies." *Journal of Dairy Science* 92(8): 3634–42.
- Aly, Sharif S. et al.. 2012. "Cost-Effectiveness of Diagnostic Strategies to Identify Mycobacterium Avium Subspecies Paratuberculosis Super-Shedder Cows in a Large Dairy Herd Using Antibody Enzyme-Linked Immunosorbent Assays, Quantitative Real-Time Polymerase Chain Reaction, and Bacte." *Journal of Veterinary Diagnostic Investigation* 24(5): 821–32.
- Amorim, M. J. et al. 2011. "A Rab11- and Microtubule-Dependent Mechanism for Cytoplasmic Transport of Influenza A Virus Viral RNA." *Journal of Virology* 85(9): 4143–56.
- Ampomah, Patrick Baah et al. 2018. "Annexins in Influenza Virus Replication and Pathogenesis." *Frontiers in Pharmacology* 9(1282): 1–9.
- Andrews, Simon. 2011. "FastQC: A Quality Control Tool for High Throughput Sequence Data."
- Angeletti, Dario, and Claudio Carere. 2014. "Comparative Ecogenotoxicology: Monitoring the DNA of Wildlife." *Current Zoology* 60(2): 252–54.
- Angelov, Dimitar et al. 2003. "The Histone Variant MacroH2A Interferes with Transcription Factor Binding and SWI/SNF Nucleosome Remodeling." *Molecular Cell* 11(4): 1033–41.
- Arsnoe, Dustin M., Hon S. Ip, and Jennifer C. Owen. 2011. "Influence of Body Condition on Influenza a Virus Infection in Mallard Ducks: Experimental Infection Data." *PLoS ONE* 6(8): 1–9.

- Ason, Brandon et al. 2006. "Differences in Vertebrate MicroRNA Expression." *Proceedings of the National Academy of Sciences of the United States of America* 103(39): 14385–89.
- Atarashi, Ryuichiro, Kazunori Sano, Katsuya Satoh, and Noriyuki Nishida. 2011. "Real-Time Quaking-Induced Conversion." 5(3): 150–53.
- Attardi, L. D. et al. 2000. "Erratum: PERP, an Apoptosis-Associated Target of P53, Is a Novel Member of the PMP-22/Gas3 Family (Genes and Development (2000) 14 (704-718))." *Genes and Development* 14(14): 1835.
- Baer, Alan, and Kylene Kehn-Hall. 2014. "Viral Concentration Determination through Plaque Assays: Using Traditional and Novel Overlay Systems." *Journal of Visualized Experiments* (93): 1–10.
- Bagashev, Asen et al. 2010. "Leucine-Rich Repeat (in Flightless I) Interacting Protein-1 Regulates a Rapid Type i Interferon Response." *Journal of Interferon and Cytokine Research* 30(11): 843–52.
- Bao, Jialing et al. 2018. "Serpin Functions in Host-Pathogen Interactions." *PeerJ* 6(e4557): 1–16.
- Barber, Megan R.W. et al. 2013. "Identification of Avian RIG-I Responsive Genes during Influenza Infection." *Molecular Immunology* 54(1): 89–97.
- Basters, Anja, Klaus Peter Knobeloch, and Günter Fritz. 2018. "USP18 A Multifunctional Component in the Interferon Response." *Bioscience Reports* 38(6): 1–9.
- Batra, Jyoti et al. 2018. "Protein Interaction Mapping Identifies RBBP6 as a Negative Regulator of Ebola Virus Replication." *Cell* 175(7): 1917-1930.e13.
- Bayoumi, Mahmoud, Mohammed A. Rohaim, and Muhammad Munir. 2020. "Structural and Virus Regulatory Insights Into Avian N6-Methyladenosine (M6A) Machinery." *Frontiers in Cell and Developmental Biology* 8(543): 1–14.
- Bazzigher, Luigi, Annette Schwartz, and Peter Staeheli. 1993. "No Enhanced Influenza Virus Resistance of Murine and Avian Cells Expressing Cloned Duck Mx Protein." *Virology* 195(1): 100–112.
- Beldomenico, Pablo M., and Michael Begon. 2010. "Disease Spread, Susceptibility and Infection Intensity: Vicious Circles?" *Trends in Ecology and Evolution* 25(1): 21–27.
- Benjamini, Yoav, and Yosef Hochberg. 1995. "Controlling the False Discovery Rate: A Practical and Powerful Approach to Multiple Testing." *Journal of the Royal Statistical Society B* 57(1): 289–300.
- Betakova, Tatiana, Anna Kostrabova, Veronika Lachova, and Lucia Turianova. 2017.

- "Cytokines Induced During Influenza Virus Infection." *Current Pharmaceutical Design* 23(18).
- Boddicker, Nick, and Dorian J Garrick. 2011. "Genetic Parameters and Chromosomal Regions Associated with Viral Load and Growth in Pigs Infected with Porcine Reproductive and Respiratory Syndrome Virus." *Iowa State University Animal Industry Report* 8(1).
- Bolger, Anthony M., Marc Lohse, and Bjoern Usadel. 2014. "Trimmomatic: A Flexible Trimmer for Illumina Sequence Data." *Bioinformatics* 30(15): 2114–20.
- Bonilla, Francisco A., and Hans C. Oettgen. 2010. "Adaptive Immunity." *Journal of Allergy and Clinical Immunology* 125(2): S33–40.
- Bonvin, Marianne et al. 2006. "Interferon-Inducible Expression of APOBEC3 Editing Enzymes in Human Hepatocytes and Inhibition of Hepatitis B Virus Replication." *Hepatology* 43(6): 1364–74.
- Brass, Abraham L. et al. 2009. "The IFITM Proteins Mediate Cellular Resistance to Influenza A H1N1 Virus, West Nile Virus, and Dengue Virus." *2Cell* 139(7): 1243–54.
- Bruce, Emily A., Paul Digard, and Amanda D. Stuart. 2010. "The Rab11 Pathway Is Required for Influenza A Virus Budding and Filament Formation." *Journal of Virology* 84(12): 5848–59.
- Byrd-Leotis, Lauren, Richard D. Cummings, and David A. Steinhauer. 2017. "The Interplay between the Host Receptor and Influenza Virus Hemagglutinin and Neuraminidase." *International Journal of Molecular Sciences* 18(7).
- Campbell, Lee K., and Katharine E. Magor. 2020. "Pattern Recognition Receptor Signaling and Innate Responses to Influenza A Viruses in the Mallard Duck, Compared to Humans and Chickens." *Frontiers in Cellular and Infection Microbiology* 10.
- Cao, M. et al. 2014. "DnaJA1/Hsp40 Is Co-Opted by Influenza A Virus To Enhance Its Viral RNA Polymerase Activity." *Journal of Virology* 88(24): 14078–89.
- Cao, Yingying et al. 2017. "Differential Responses of Innate Immunity Triggered by Different Subtypes of Influenza a Viruses in Human and Avian Hosts." *BMC Medical Genomics* 10(4): 41–54.
- Capparelli, R et al. 2009. "Heterogeneous Shedding of Brucella Abortus in Milk and Its Effect on the Control of Animal Brucellosis." *Journal of applied microbiology* 106(6): 2041–47.
- Cardona, Carol J., David A. Halvorson, Justin D. Brown, and Mary J. Pantin-Jackwood. 2014. "Conducting Influenza Virus Pathogenesis Studies in Avian Species." In *Animal Influenza Virus*, 169–83.

- Carey, Cynthia et al. 2006. "Experimental Exposures of Boreal Toads (Bufo Boreas) to a Pathogenic Chytrid Fungus (Batrachochytrium Dendrobatidis)." *EcoHealth* 3: 5–21.
- Carney, Samuel. 1992. "Species, Age and Sex Identification of Ducks Using Wing Plumage." 1-144.
- Carter, Deborah et al. 2019. "Influenza A Prevalence and Subtype Diversity in Migrating Teal Sampled Along the United States Gulf Coast." *Avian Diseases* 63(1): 165.
- Catalanotto, Caterina, Carlo Cogoni, and Giuseppe Zardo. 2016. "MicroRNA in Control of Gene Expression: An Overview of Nuclear Functions." *International Journal of Molecular Sciences* 17(10).
- Chase-Topping, Margo et al. 2008. "Super-Shedding and the Link between Human Infection and Livestock Carriage of Escherichia Coli O157." *Nature Reviews Microbiology* 6(12): 904–12.
- Chen, Huihui, and Zhengfan Jiang. 2013. "The Essential Adaptors of Innate Immune Signaling." *Protein and Cell* 4(1): 27–39.
- Chen, Song, Hedeel Guy Evan, and David R. Evans. 2011. "FAM129B/MINERVA, a Novel Adherens Junction-Associated Protein, Suppresses Apoptosis in HeLa Cells." *Journal of Biological Chemistry* 286(12): 10201–9.
- Chen, Xiaoyong et al. 2018. "Host Immune Response to Influenza A Virus Infection." *Frontiers in Immunology* 9: 320.
- Chen, Yun Wen et al. 2015. "Receptor-Type Tyrosine-Protein Phosphatase κ Directly Targets STAT3 Activation for Tumor Suppression in Nasal NK/T-Cell Lymphoma." *Blood* 125(10): 1589–1600.
- Cheng, Yo Ching et al. 2016. "Early and Non-Invasive Detection of Chronic Wasting Disease Prions in Elk Feces by Real- Time Quaking Induced Conversion." *PLoS ONE* 10: 1–18.
- Chesser, R. Terry et al. 2017. "Fifty-Eighth Supplement to the American Ornithological Society's Check-List of North American Birds." *Auk* 134(3): 751–73.
- Cheung, Timothy K W, and Leo L M Poon. 2007. "Biology of Influenza a Virus." *Annals of the New York Academy of Sciences* 1102: 1–25.
- Choi, Un Yung, Ji Seon Kang, Yune Sahng Hwang, and Young Joon Kim. 2015. "Oligoadenylate Synthase-like (OASL) Proteins: Dual Functions and Associations with Diseases." *Experimental & molecular medicine* 47: 1–6.
- Chuong, Edward B., Nels C. Elde, and Cédric Feschotte. 2016. "Regulatory Evolution of Innate Immunity through Co-Option of Endogenous Retroviruses." *Science* 351(6277): 1083–87.

- Ciriaco, Emilia, Pablo P. Píñera, Belén Díaz-Esnal, and Rosaria Laurà. 2003. "Age-Related Changes in the Avian Primary Lymphoid Organs (Thymus and Bursa of Fabricius)." *Microscopy Research and Technique* 62(6): 482–87.
- Cobbold, Rowland N et al. 2007. "Rectoanal Junction Colonization of Feedlot Cattle by Escherichia Coli O157:H7 and Its Association with Supershedders and Excretion Dynamics." *Applied and Environmental Microbiology* 73(5): 1563–68.
- Coleman, Macon D et al. 2018. "Cathepsin B Plays a Key Role in Optimal Production of the Influenza A- Virus." *Journal of Virology & Antiviral Research* 07(01): 1–16.
- Conover, W. J., Mark E. Johnson, and Myrle M. Johnson. 1981. "A Comparative Study of Tests for Homogeneity of Variances, with Applications to the Outer Continental Shelf Bidding Data." *Technometrics* 23(4): 351–61.
- Copois, Virginie et al. 2007. "Impact of RNA Degradation on Gene Expression Profiles: Assessment of Different Methods to Reliably Determine RNA Quality." *Journal of Biotechnology* 127(4): 549–59.
- Cornelissen, J. B.W.J. et al. 2012. "Differential Innate Responses of Chickens and Ducks to Low-Pathogenic Avian Influenza." *Avian Pathology* 41(6): 519–29.
- Costa, Federico, Elsio A Wunder, Daiana De Oliveira, and Vimla Bisht. 2015. "Patterns in Leptospira Shedding in Norway Rats (Rattus Norvegicus) from Brazilian Slum Communities at High Risk of Disease Transmission." *Plos neglected tropical diseases* 9(6): 1–14.
- Costa, Taiana P. et al. 2012. "Distribution Patterns of Influenza Virus Receptors and Viral Attachment Patterns in the Respiratory and Intestinal Tracts of Seven Avian Species." *Veterinary Research* 43(28): 1–13.
- Costa, Taiana P, Justin D. Brown, Elizabeth W. Howerth, and David E. Stallknecht. 2010. "The Effect of Age on Avian Influenza Viral Shedding in Mallards (Anas Platyrhynchos)." *Avian Diseases* 54: 581–85.
- Costa, Taiana P, Justin D Brown, Elizabeth W Howerth, and David E Stallknecht. 2011. "Variation in Viral Shedding Patterns between Different Wild Bird Species Infected Experimentally with Low-Pathogenicity Avian Influenza Viruses That Originated from Wild Birds." *Avian Pathology* 40(2): 119–24.
- Dai, Penggao et al. 2009. "Modulation of TLR Signaling by Multiple MyD88-Interacting Partners Including Leucine-Rich Repeat Fli-I-Interacting Proteins." *The Journal of Immunology* 182(6): 3450–60.
- Daoust, Pierre-Yves et al. 2011. "Replication of Low Pathogenic Avian Influenza Virus in Naturally Infected Mallard Ducks (Anas Platyrhynchos) Causes No Morphologic Lesions."

- *Journal of wildlife diseases* 47(2): 401–9.
- Das, Amaresh, Erica Spackman, Mary J Pantin-jackwood, and David L Suarez. 2009. "Removal of Real-Time Reverse Transcription Polymerase Chain Reaction (RT-PCR) Inhibitors Associated with Cloacal Swab Samples and Tissues for Improved Diagnosis of Avian Influenza Virus by RT-PCR." *Journal of Veterinary Diagnostic Investigation* 21: 771–78.
- Das, Anshuman, Phat Dinh, Debasis Panda, and Asit K. Pattnaik. 2014. "Interferon-Inducible Protein IFI35 Negatively Regulates RIG-I Antiviral Signaling and Supports Vesicular Stomatitis Virus Replication." *Journal of Virology* 88(6): 3103–13.
- Davies, Alexandra, and Peter J. Lachmann. 1993. "Membrane Defence against Complement Lysis: The Structure and Biological Properties of CD59." *Immunologic Research* 12(3): 258–75.
- Davis, Alvin E., Pedro Mejia, and Fengxin Lu. 2008. "Biological Activities of C1 Inhibitor." *Molecular Immunology* 45(16): 4057–63.
- Davison, Fred, Katherine E Magor, and Bernd Kaspers. 2008. "Structure and Evolution of Avian Immunoglobulins." *Avian Immunology* (1987): 107–27.
- Davison, Fred, Bernd Kaspers, and Karel A Schat. 2008. "The Avian Mucosal Immune System." *Avian Immunology*. (1987): 241-42.
- Deist, Melissa S. et al. 2017. "Resistant and Susceptible Chicken Lines Show Distinctive Responses to Newcastle Disease Virus Infection in the Lung Transcriptome." *BMC Genomics* 18(1): 1–15.
- DelGiudice, Glenn D. 2002. *Understanding Chronic Wasting Disease (CWD) and CWD Management Planning Background*.
- Denzin, Lisa K., and Peter Cresswell. 1995. "HLA-DM Induces Clip Dissociation from MHC Class II Aβ Dimers and Facilitates Peptide Loading." *Cell* 82(1): 155–65.
- Dobin, Alexander et al. 2013. "STAR: Ultrafast Universal RNA-Seq Aligner." *Bioinformatics* 29(1): 15–21.
- Dobin, Alexander, and Thomas R. Gingeras. 2015. "Mapping RNA-Seq Reads with STAR." *Current Protocols in Bioinformatics* 51(1): 11.14.1-11.14.19.
- Dolinski, Amanda, Jared Homola, Mark Jankowski, and Jennifer Owen. 2020. "De Novo Transcriptome Assembly and Data for the Blue-Winged Teal (Spatula Discors)." *Data in Brief* 30: 105380.
- Dolinski, Amanda, Mark Jankowski, Jeanne Fair, and Jennifer Owen. 2020. "The Association Between SAα2,3Gal Occurrence Frequency and Avian Influenza Viral Load in Mallards

- (Anas Platyrhynchos) and Blue-Winged Teals (Spatula Discors)." *BMC Veterinary Research* 16(430): 1–17.
- Duan, L. et al. 2007. "Characterization of Low-Pathogenic H5 Subtype Influenza Viruses from Eurasia: Implications for the Origin of Highly Pathogenic H5N1 Viruses." *Journal of Virology* 81(14): 7529–39.
- Dubois, Julia, Olivier Terrier, and Manuel Rosa-Calatrava. 2014. "Influenza Viruses and MRNA Splicing: Doing More with Less." *mBio* 5(3): 1–13.
- Dusek, Robert J. et al. 2009. "Surveillance for High Pathogenicity Avian Influenza Virus in Wild Birds in the Pacific Flyway of the United States, 2006–2007." *Avian Diseases Digest* 4(2): e9–10.
- Dushoff, Jonathan, and Simon Levin. 1995. "The Effects of Population Heterogeneity on Disease Invasion." *Mathematical Biosciences* 128: 25–40.
- Edinger, Thomas O., Marie O. Pohl, Emilio Yángüez, and Silke Stertz. 2015. "Cathepsin W Is Required for Escape of Influenza A Virus from Late Endosomes." *mBio* 6(3): 1–12.
- Edmunds, W. J., G. Kafatos, J. Wallinga, and J. R. Mossong. 2006. "Mixing Patterns and the Spread of Close-Contact Infectious Diseases." *Emerging Themes in Epidemiology* 3: 1–8.
- Ellstrom, Patrik et al. 2008. "Sampling for Low-Pathogenic Avian Influenza A Virus in Wild Mallard Ducks: Oropharyngeal versus Cloacal Swabbing." *Vaccine* 26(35): 4414–16.
- Evseev, Danyel, and Katharine E. Magor. 2019. "Innate Immune Responses to Avian Influenza Viruses in Ducks and Chickens." *Veterinary Sciences* 6(1).
- Fair, Jeanne Marie, Ellen Paul, and Jason Jones. 2010. "Guidelines to the Use of Wild Birds in Research." In *The Ornithological Council*, eds. Jeanne Marie Fair, Ellen Paul, and Jason Jones. Washington, D.C.
- Feng, Peter, Stephen Weagant, Michael A. Grant, and William Burkhardt. 2002. "BAM 4: Enumeration of Escherichia Coli and the Coliform Bacteria." In *Bacteriological Analytical Manual*,.
- Ferro, Pamela J. et al. 2010. "Multiyear Surveillance for Avian Influenza Virus in Waterfowl from Wintering Grounds, Texas Coast, USA." *Emerging Infectious Diseases* 16(8): 1224–30.
- Fleming-Canepa, Ximena et al. 2019. "Duck Innate Immune Responses to High and Low Pathogenicity H5 Avian Influenza Viruses." *Veterinary Microbiology* 228: 101–11.
- Florin, Luise, and Thorsten Lang. 2018. "Tetraspanin Assemblies in Virus Infection." *Frontiers in Immunology* 9: 1–9.

- Foletta, Victoria C., David H. Segal, and Donna R. Cohen. 1998. "Transcriptional Regulation in the Immune System: All Roads Lead to AP-1." *Journal of Leukocyte Biology* 63(2): 139–52
- Franca, M., D. E. Stallknecht, and E. W. Howerth. 2013. "Expression and Distribution of Sialic Acid Influenza Virus Receptors in Wild Birds." *Avian Pathology* 42(1): 60–71.
- Franca, M, R Poulson, et al. 2012. "Effect of Different Routes of Inoculation on Infectivity and Viral Shedding of LPAI Viruses in Mallards." *Avian Diseases* 56(4s1): 981–85.
- Franca, M, D E Stallknecht, et al. 2012. "The Pathogenesis of Low Pathogenic Avian Influenza in Mallards Research Note The Pathogenesis of Low Pathogenic Avian Influenza in Mallards." *Avian Diseases* 56(4s1): 976–80.
- Gallego Romero, Irene, Athma Pai, Jenny Tung, and Yoav Gilad. 2014. "Impact of RNA Degradation on Measurements of Gene Expression." *BMC biology* 12(42): 1–13.
- Galvani, Alison P, and Robert M May. 2005. "Epidemiology: Dimensions of Superspreading." *Nature* 438(7066): 293–95.
- Gambaryan, Alexandra et al. 2005. "Receptor Specificity of Influenza Viruses from Birds and Mammals: New Data on Involvement of the Inner Fragments of the Carbohydrate Chain." *Virology* 334(2): 276–83.
- Gambaryan, Alexandra et al. 2006. "Evolution of the Receptor Binding Phenotype of Influenza A (H5) Viruses." *Virology* 344: 432–38.
- Gao, Qingxia et al. 2020. "Eukaryotic Translation Elongation Factor 1 Delta Inhibits the Nuclear Import of Nucleoprotein and PA-PB1 Heterodimer of Influenza A Virus." *Journal of Virology* (October).
- Garrison, Keith E. et al. 2007. "T Cell Responses to Human Endogenous Retroviruses in HIV-1 Infection." *PLoS Pathogens* 3(11): 1617–27.
- Gatto, Mariele et al. 2013. "Serpins, Immunity and Autoimmunity: Old Molecules, New Functions." *Clinical Reviews in Allergy and Immunology* 45(2): 267–80.
- Gegear, Robert J. 2005. "Does Parasitic Infection Impair the Ability of Bumblebees to Learn Flower-Handling Techniques?" *Animal Behaviour* 70: 209–15.
- Geisler, Christoph, and Donald L Jarvis. 2011. "Effective Glycoanalysis with Maackia Amurensis Lectins Requires a Clear Understanding of Their Binding Speci Fi Cities." *Glycobiology* 21(8): 988–93.
- Gewurz, Benjamin E. et al. 2012. "Genome-Wide SiRNA Screen for Mediators of NF-KB Activation." Proceedings of the National Academy of Sciences of the United States of

- America 109(7): 2467–72.
- Godfrey, Stephanie S. 2013. "Networks and the Ecology of Parasite Transmission: A Framework for Wildlife Parasitology." *International Journal for Parasitology: Parasites and Wildlife* 2(1): 235–45.
- Gonzalez-Hernandez, Marta J. et al. 2012. "Expression of Human Endogenous Retrovirus Type K (HML-2) Is Activated by the Tat Protein of HIV-1." *Journal of Virology* 86(15): 7790–7805.
- Gonzalez, Javier, H. Düttmann, and M. Wink. 2009. "Phylogenetic Relationships Based on Two Mitochondrial Genes and Hybridization Patterns in Anatidae." *Journal of Zoology* 279(3): 310–18.
- Van der Goot, J. A., M. C.M. De Jong, G. Kochi, and M. Van Boven. 2003. "Comparison of the Transmission Characteristics of Low and High Pathogenecity Avian Influenza A Virus (H5N2)." *Epidemiology and Infection* 131(2): 1003–13.
- Grabherr, Manfred G. et al. 2013. "Trinity: Reconstructing a Full-Length Transcriptome without a Genome from RNA-Seq Data." *Nature Biotechnology* 29(7): 644–52.
- Grandi, Nicole, and Enzo Tramontano. 2018. "Human Endogenous Retroviruses Are Ancient Acquired Elements Still Shaping Innate Immune Responses." *Frontiers in Immunology* 9: 1–16.
- Gubler, Duane J. 2007. "The Continuing Spread of West Nile Virus in the Western Hemisphere." *Clinical Infectious Diseases* 45(8): 1039–46.
- Guermonprez, Pierre et al. 2002. "Antigen Presentation and T Cell Stimulation by Dendritic Cells." *Annual Review of Immunology* 20: 621–67.
- Guinea, R, and L Carrasco. 1995. "Requirement for Vacuolar Proton-ATPase Activity during Entry of Influenza Virus into Cells." *Journal of virology* 69(4): 2306–12.
- Gupta, Sunetra, Roy M. Anderson, and Robert M. May. 1989. "Networks of Sexual Contacts: Implications for the Pattern of Spread of HIV." *AIDS* 3: 807–17.
- Haas, Charles N., Joan B. Rose, and Charles P. Gerba. 2014. *Quantitative Microbial Risk Assessment*. John Wiley & Sons.
- Halvorson, David A. et al. 1983. "Epizootiology of Avian Influenza-Simultaneous Monitoring of Sentinel Ducks and Turkeys in Minnesota." *Avian Diseases* 27(1): 77–85.
- Halvorson, David A. 2008. "Control of Low Pathogenicity Avian Influenza." In *Avian Influenza*, 513–36.

- Hamann, Jorg et al. 2016. "Adhesion GPCRs as Modulators of Immune Cell Function." In *Handbook of Experimental Pharmacology*, eds. T. Langenhan and T. Schoneberg. Springer, 329–50.
- Han, Deping, Yanxin Hu, Kedao Teng, and Xuemei Deng. 2016. "Lower Expression of Sialic Acid Receptors in the Cecum of Silky Fowl (Gallus Gallus Domesticus Brisson) Compared to White Leghorn." *Poultry Science* 95(6): 1290–95.
- Hansell, Chris et al. 2007. "Unique Features and Distribution of the Chicken CD83 + Cell." *The Journal of Immunology* 179(8): 5117–25.
- Hanson, Britta a et al. 2005. "Avian Influenza Viruses and Paramyxoviruses in Wintering and Resident Ducks in Texas." *Journal of Wildlife Diseases* 41(3): 624–28.
- Hao, Linhui et al. 2008. "Drosophila RNAi Screen Identifies Host Genes Important for Influenza Virus Replication." *Nature* 454(7206): 890–93.
- Harduin-lepers, Anne. 2010. "Glycobiology Insights Comprehensive Analysis of Sialyltransferases in Vertebrate Genomes." *Glycobiology Insights* 2: 29–61.
- Hart, Kristen C. et al. 2000. "Transformation and Stat Activation by Derivatives of FGFR1, FGFR3, and FGFR4." *Oncogene* 19(29): 3309–20.
- Hayashi, Hideki et al. 2018. "Enterokinase Enhances Influenza a Virus Infection by Activating Trypsinogen in Human Cell Lines." *Frontiers in Cellular and Infection Microbiology* 8(MAR): 1–14.
- Hayden, M. S., A. P. West, and S. Ghosh. 2006. "NF-KB and the Immune Response." *Oncogene* 25(51): 6758–80.
- Heaton, Nicholas S. et al. 2016. "Targeting Viral Proteostasis Limits Influenza Virus, HIV, and Dengue Virus Infection." *Immunity* 44(1): 46–58.
- Heid, Christian A., Junko Stevens, Kenneth J. Livak, and P. Mickey Williams. 1996. "Real Time Quantitative PCR." *Genome Research* 6(10): 986–94.
- Henaux, Viviane, and Michael D. Samuel. 2011. "Avian Influenza Shedding Patterns in Waterfowl: Implications for Surveillance, Environmentaltransmission, and Disease Spread." *Journal of Wildlife Diseases* 47(3): 566–78.
- Henderson, Davin M et al. 2015. "Longitudinal Detection of Prion Shedding in Saliva and Urine by Induced Conversion." *Journal of Virology* 89(18): 9338–47.
- Hercus, Timothy R. et al. 2009. "The Granulocyte-Macrophage Colony-Stimulating Factor Receptor: Linking Its Structure to Cell Signaling and Its Role in Disease." *Blood* 114(7): 1289–98.

- Higgins, Kenneth F, Leo M Kirsch, and I. Joseph Ball Jr. 1969. "A Cable-Chain Device for Locating Duck Nests." *The Journal of Wildlife Management* 33(4): 1009–11.
- Hirota, Kiichi et al. 1997. "Ap-1 Transcriptional Activity Is Regulated by a Direct Association between Thioredoxin and Ref-1." *Proceedings of the National Academy of Sciences of the United States of America* 94(8): 3633–38.
- Hoeksema, Marloes et al. 2015. "Arginine-Rich Histones Have Strong Antiviral Activity for Influenza A Viruses." *Innate Immunity* 21(7): 736–45.
- Hogue, Brenda G., and Debi P. Nayak. 1992. "Synthesis and Processing of the Influenza Virus Neuraminidase, a Type II Transmembrane Glycoprotein." *Virology* 188(2): 510–17.
- Hong, Yeong Ho et al. 2006. "Molecular Cloning and Characterization of Chicken Lipopolysaccharide-Induced TNF-α Factor (LITAF)." *Developmental and Comparative Immunology* 30(10): 919–29.
- Hooper, P., and P Selleck. 2003. "Pathology of Low and High Virulent Influenza Virus Infections." *Avian Diseases* 47: 134–41.
- Howard, O. M. Zack, Jim A. Turpin, Robert Goldman, and William S. Modi. 2004. "Functional Redundancy of the Human CCL4 and CCL4L1 Chemokine Genes." *Biochemical and Biophysical Research Communications* 320(3): 927–31.
- Hu, Wei, and Chandrashekhar Pasare. 2013. "Location, Location, Location: Tissue-Specific Regulation of Immune Responses." *Journal of Leukocyte Biology* 94(3): 409–21.
- Hu, Xuming et al. 2017. "Expression Patterns of Endogenous Avian Retrovirus ALVE1 and Its Response to Infection with Exogenous Avian Tumour Viruses." *Archives of Virology* 162(1): 89–101.
- Huang, Ching Tai et al. 2004. "Role of LAG-3 in Regulatory T Cells." *Immunity* 21(4): 503–13.
- Huang, Yi-Wei et al. 2008. "Mammalian Septins Are Required for Phagosome Formation." *Molecular Biology of the Cell* 19: 1717–26.
- Huang, Yinhua et al. 2013. "The Duck Genome and Transcriptome Provide Insight into an Avian Influenza Virus Reservoir Species." *Nature genetics* 45(7): 776–83.
- Hudson, Peter J, Sarah E Perkins, and Isabella M Cattadori. 2010. "The Emergence of Wildlife Disease and the Application of Ecology." In *Infectious Disease Ecology: Effects of Ecosystems on Disease and of Disease on Ecosystems*, Princeton University Press, 347–67.
- Icardi, Laura et al. 2012. "The Sin3a Repressor Complex Is a Master Regulator of STAT Transcriptional Activity." *Proceedings of the National Academy of Sciences of the United States of America* 109(30): 12058–63.

- Ip, Hon S. et al. 2008. "Prevalence of Influenza A Viruses in Wild Migratory Birds in Alaska: Patterns of Variation in Detection at a Crossroads of Intercontinental Flyways." *Virology Journal* 5: 1–10.
- Ito, Toshihiro et al. 1997. "Receptor Specificity of Influenza A Viruses Correlates with the Agglutination of Erythrocytes from Different Animal Species." *Virology* 227(2): 493–99.
- Ito, Toshihiro et al. 2000. "Recognition of N-Glycolylneuraminic Acid Linked to Galactose by the A2,3 Linkage Is Associated with Intestinal Replication of Influenza A Virus in Ducks." *Journal of Virology* 74(19): 9300–9305.
- Iwasaki, Akiko, and Padmini S. Pillai. 2014. "Innate Immunity to Influenza Virus Infection." *Nature Reviews Immunology* 14(5): 315–28.
- Jankowski, Mark D. et al. 2010. "Testing Independent and Interactive Effects of Corticosterone and Synergized Resmethrin on the Immune Response to West Nile Virus in Chickens." *Toxicology* 269: 81–88.
- Jankowski, Mark D. et al. 2019. "Sialic Acid on Avian Erythrocytes." *Comparative Biochemistry and Physiology Part B: Biochemistry and Molecular Biology* 238: 110336.
- Jankowski, Mark D., Christopher J Williams, Jeanne M Fair, and Jennifer C Owen. 2013. "Birds Shed RNA-Viruses According to the Pareto Principle." *PLoS One* 8(8): e72611.
- Jimenez-Bluhm, Pedro et al. 2018. "Circulation of Influenza in Backyard Productive Systems in Central Chile and Evidence of Spillover from Wild Birds." *Preventive Veterinary Medicine* 153: 1–6.
- Jolly, P. E. et al. 2013. "Association between High Aflatoxin B1 Levels and High Viral Load in HIV-Positive People." *World Mycotoxin Journal* 6(3): 255–61.
- Jones, Kate E et al. 2008. "Global Trends in Emerging Infectious Diseases." *Nature* 451(7181): 990–93.
- Jorgensen, Sofie E. et al. 2020. "STK4 Deficiency Impairs Innate Immunity and Interferon Production Through Negative Regulation of TBK1-IRF3 Signaling." *Journal of Clinical Immunology*.
- Jourdain, Elsa et al. 2010. "Influenza Virus in a Natural Host, the Mallard: Experimental Infection Data." *PLoS ONE* 5(1).
- Juliarena, Marcela A. et al. 2008. "Association of BLV Infection Profiles with Alleles of the BoLA-DRB3.2 Gene." *Animal Genetics* 39(4): 432–38.
- Juliarena, Marcela A., Clarisa N. Barrios, M. Carolina Ceriani, and Eduardo N. Esteban. 2016. "Hot Topic: Bovine Leukemia Virus (BLV)-Infected Cows with Low Proviral Load Are

- Not a Source of Infection for BLV-Free Cattle." Journal of Dairy Science 99(6): 4586–89.
- Kaiser, Pete, and Peter Staheli. 2013. "Avian Cytokines and Chemokines." *Avian Immunology: Second Edition*: 189–204.
- Kalthoff, Donata, Anja Globig, and Martin Beer. 2010. "(Highly Pathogenic) Avian Influenza as a Zoonotic Agent." *Veterinary Microbiology* 140(3): 237–45.
- Kanehisa, Minoru, and Yoko Sato. 2020. "KEGG Mapper for Inferring Cellular Functions from Protein Sequences." *Protein Science* 29(1): 28–35.
- Kapczynski, Darrell R., Hai Jun Jiang, and Michael H. Kogut. 2014. "Characterization of Cytokine Expression Induced by Avian Influenza Virus Infection with Real-Time RT-PCR." *Methods in Molecular Biology* 1161: 217–33.
- Karlas, Alexander et al. 2010. "Genome-Wide RNAi Screen Identifies Human Host Factors Crucial for Influenza Virus Replication." *Nature* 463(7282): 818–22.
- Kasuya, Eiiti. 2019. "On the Use of r and r Squared in Correlation and Regression." *Ecological Research* 34(1): 235–36.
- Kelm, Sorge, and Roland Schauer. 1997. "Sialic Acids in Molecular and Cellular Interactions." *International Review of Cytology* 175: 137–240.
- Khaperskyy, Denys A. et al. 2016. "Selective Degradation of Host RNA Polymerase II Transcripts by Influenza A Virus PA-X Host Shutoff Protein." *PLoS Pathogens* 12(2): 1–25.
- Kida, Hiroshi, Ryo Yanagawa, and Yumiko Matsuoka. 1980. "Duck Influenza Lacking Evidence of Disease Signs and Immune Response." *Infection and Immunity* 30(2): 547–53.
- Killian, Mary Lea. 2014. "Avian Influenza Virus Sample Types, Collection, and Handling." In *Animal Influenza Virus*, ed. Erica Spackman. New York: Humana Press, 83–91.
- Kilpatrick, A Marm et al. 2006. "Predicting the Global Spread of H5N1 Avian Influenza." *Proceedings of the National Academy of Sciences* 103(51): 19368–73.
- Kim, Young Hoon, Jae Rin Lee, and Myong Joon Hahn. 2018. "Regulation of Inflammatory Gene Expression in Macrophages by Epithelial-Stromal Interaction 1 (Epsti1)." *Biochemical and Biophysical Research Communications* 496(2): 778–83.
- Kim, Young S., and Samuel B. Ho. 2010. "Intestinal Goblet Cells and Mucins in Health and Disease: Recent Insights and Progress." *Current Gastroenterology Reports* 12(5): 319–30.
- Kimble, Brian, Gloria Ramirez Nieto, and Daniel R Perez. 2010. "Characterization of Influenza Virus Sialic Acid Receptors in Minor Poultry Species." *Virology Journal* 7(365): 1–10.

- Kirui, James, Arindam Mondal, and Andrew Mehle. 2016. "Ubiquitination Upregulates Influenza Virus Polymerase Function." *Journal of Virology* 90(23): 10906–14.
- Klamp, Thorsten et al. 2003. "A Giant GTPase, Very Large Inducible GTPase-1, Is Inducible by IFNs." *The Journal of Immunology* 171(3): 1255–65.
- Klempner, Samuel J, and Sai-Hong Ou. 2017. "ROS1 (ROS Proto-Oncogene 1, Receptor Tyrosine Kinase)." *Atlas of Genetics and Cytogenetics in Oncology and Haematology* 19(5): 337–39.
- Knibbs, Randall N, Irwin J Goldstein, R Murray Ratcliffell, and Naoto Shibuyall. 1991. "Characterization of the Carbohydrate Binding Specificity of the Leukoagglutinating Lectin from Maackia Amurensis." *The Journal of Biological Chemistry* 266(1): 83–88.
- Ko, Jae Hong et al. 2004. "Characterization of the Chicken PKR: Polymorphism of the Gene and Antiviral Activity against Vesicular Stomatitis Virus." *Japanese Journal of Veterinary Research* 51(3–4): 123–33.
- Koch, G, and A R W Elbers. 2006. "Outdoor Ranging of Poultry: A Major Risk Factor for the Introduction and Development of High-Pathogenicity Avian Influenza." *NJAS Wageningen Journal of Life Sciences* 54(2): 179–94.
- König, Renate et al. 2010. "Human Host Factors Required for Influenza Virus Replication." *Nature* 463(7282): 813–17.
- Konno, Hiroyasu et al. 2009. "TRAF6 Establishes Innate Immune Responses by Activating NF-KB and IRF7 upon Sensing Cytosolic Viral RNA and DNA." *PLoS ONE* 4(5).
- Koretzky, G. A., J. Picus, T. Schultz, and A. Weiss. 1991. "Tyrosine Phosphatase CD45 Is Required for T-Cell Antigen Receptor and CD2-Mediated Activation of a Protein Tyrosine Kinase and Interleukin 2 Production." *Proceedings of the National Academy of Sciences of the United States of America* 88(6): 2037–41.
- Koyama, Shohei, Ken J. Ishii, Cevayir Coban, and Shizuo Akira. 2008. "Innate Immune Response to Viral Infection." *Cytokine* 43(3): 336–41.
- Krammer, Florian et al. 2018. "Influenza." Nature Reviews Disease Primers 4(1): 1–21.
- Kuchipudi, Suresh V. et al. 2014. "Highly Pathogenic Avian Influenza Virus Infection in Chickens but Not Ducks Is Associated with Elevated Host Immune and Pro-Inflammatory Responses." *Veterinary Research* 45(1): 1–18.
- Kuchipudi, Suresh V et al. 2009. "Differences in Influenza Virus Receptors in Chickens and Ducks: Implications for Interspecies Transmission." *Journal of molecular and genetic medicine: an international journal of biomedical research* 3(1): 143–51.

- Kudo, Kohya et al. 2016. "Phospholipase C Δ1 in Macrophages Negatively Regulates TLR4-Induced Proinflammatory Cytokine Production and Fcγ Receptor-Mediated Phagocytosis." *Advances in Biological Regulation* 61: 68–79.
- Kumar, N., Y. Liang, T. G. Parslow, and Y. Liang. 2011. "Receptor Tyrosine Kinase Inhibitors Block Multiple Steps of Influenza A Virus Replication." *Journal of Virology* 85(6): 2818–27.
- Kuwano, Yoshihiro et al. 2007. "CD83 Influences Cell-Surface MHC Class II Expression on B Cells and Other Antigen-Presenting Cells." *International Immunology* 19(8): 977–92.
- Langmead, B, C Trapnell, M Pop, and S Salzberg. 2009. "Ultrafast and Memory-Efficient Alignment of Short DNA Sequences to the Human Genome." *Genome biology* 10(3): R25.
- Larson, Gloria P. et al. 2019. "EPS8 Facilitates Uncoating of Influenza A Virus." *Cell Reports* 29(8): 2175-2183.e4.
- Lass, Sandra et al. 2013. "Generating Super-Shedders: Co-Infection Increases Bacterial Load and Egg Production of a Gastrointestinal Helminth." *Journal of the Royal Society Interface* 10(80).
- Law, C.W. et al. 2018. "RNA-Seq Analysis Is Easy as 1-2-3 with Limma, Glimma and EdgeR." *F1000Research* 5(1408): 1–29.
- Lawley, Trevor D et al. 2008. "Host Transmission of Salmonella Enterica Serovar Typhimurium Is Controlled by Virulence Factors and Indigenous Intestinal Microbiota." *Infection and Immunity* 76(1): 403–16.
- LeBouder, Fanny et al. 2008. "Annexin II Incorporated into Influenza Virus Particles Supports Virus Replication by Converting Plasminogen into Plasmin." *Journal of Virology* 82(14): 6820–28.
- Lee, Dong Hun et al. 2017. "Highly Pathogenic Avian Influenza A(H7N9) Virus, Tennessee, USA, March 2017." *Emerging Infectious Diseases* 23(11): 1860–63.
- Lei, Yu, and Yousuke Takahama. 2012. "XCL1 and XCR1 in the Immune System." *Microbes and Infection* 14(3): 262–67.
- Li, Bo, and Colin N Dewey. 2011. "RSEM: Accurate Transcript Quantification from RNA-Seq Data with or without a Reference Genome." *BMC bioinformatics* 12(1): 323.
- Li, Jinling et al. 2010. "Adaptation and Transmission of a Duck-Origin Avian Influenza Virus in Poultry Species." *Virus Research* 147(1): 40–46.
- Li, Zezhong et al. 2015. "MicroRNAs in the Immune Organs of Chickens and Ducks Indicate Divergence of Immunity against H5N1 Avian Influenza." *FEBS Letters* 589(4): 419–25.

- Lin, Lan et al. 2014. "HSPD1 Interacts with IRF3 to Facilitate Interferon-Beta Induction." *PLoS ONE* 9(12): 1–18.
- Lin, Ren-Jye et al. 2006. "Blocking of Interferon-Induced Jak-Stat Signaling by Japanese Encephalitis Virus NS5 through a Protein Tyrosine Phosphatase-Mediated Mechanism." *Journal of Virology* 80(12): 5908–18.
- Linden, S. K. et al. 2008. "Mucins in the Mucosal Barrier to Infection." *Mucosal Immunology* 1(3): 183–97.
- Liu, Bei et al. 2012. "Folding of Toll-like Receptors by the HSP90 Paralogue Gp96 Requires a Substrate-Specific Cochaperone." *Nature Communications* 3.
- Liu, Yunxia et al. 2018. "Chicken Interferon Regulatory Factor 1 (IRF1) Involved in Antiviral Innate Immunity via Regulating IFN-β Production." *Developmental and Comparative Immunology* 88: 77–82.
- Lloyd-Smith, James O, Sebastian J Schreiber, P Ekkehard Kopp, and W M Getz. 2005. "Superspreading and the Effect of Individual Variation on Disease Emergence." *Nature* 438(7066): 355–59.
- Loo, Yueh-Ming et al. 2008. "Distinct RIG-I and MDA5 Signaling by RNA Viruses in Innate Immunity." *Journal of Virology* 82(1): 335–45.
- Low, J Christopher et al. 2005. "Rectal Carriage of Enterohemorrhagic Escherichia Coli O157 in Slaughtered Cattle." 71(1): 93–97.
- Lu, Jian, and Andrew G. Clark. 2012. "Impact of MicroRNA Regulation on Variation in Human Gene Expression." *Genome Research* 22(7): 1243–54.
- MacDonald, M. R W et al. 2007. "Genomics of Antiviral Defenses in the Duck, a Natural Host of Influenza and Hepatitis B Viruses." *Cytogenetic and Genome Research* 117(1–4): 195–206.
- Mackenzie, N. M., and A. C. Pinder. 1987. "Flow Cytometry and Its Applications in Veterinary Medicine." *Research in veterinary science* 42(2): 131–39.
- MacPhee, Ross D. E., and Alex D. Greenwood. 2013. "Infectious Disease, Endangerment, and Extinction." *International Journal of Evolutionary Biology* 2013: 1–9.
- "Mallard Assembly and Gene Annotation." 2019. http://uswest.ensembl.org/Anas_platyrhynchos/Info/Annotation (November 24, 2020).
- Mamlouk, A et al. 2011. "Shedding and Intestinal Spread of Avian Influenza Virus H5N2 in Dabbling Ducks (Preliminary Study)." *Revue De Medecine Veterinaire* 162(10): 454–59.

- Manson, Jessamyn S, Michael C Otterstatter, and James D Thomson. 2010. "Consumption of a Nectar Alkaloid Reduces Pathogen Load in Bumble Bees." *Oecologia* 162(1): 81–89.
- Marshall, Jonathan, and Nigel French. 2011. *Modelling of Campylobacter Carriage and Transmission between and within Animal Groups*.
- Matrosovich, Mikhail, Georg Herrler, and Hans Dieter Klenk. 2013. "Sialic Acid Receptors of Viruses." In *SialoGlyco Chemistry and Biology II*, 1–28.
- Matthews, L, J C Low, et al. 2006. "Heterogeneous Shedding of Escherichia Coli O157 in Cattle and Its Implications for Control." *Proceedings of the National Academy of Sciences of the United States of America* 103(3): 547–52.
- Matthews, L, I J McKendrick, et al. 2006. "Super-Shedding Cattle and the Transmission Dynamics of Escherichia Coli O157." *Epidemiology and Infection* 134(01): 131–42.
- Maughan, Michele N et al. 2013. "Transcriptional Analysis of the Innate Immune Response of Ducks to Different Species-of-Origin Low Pathogenic H7 Avian Influenza Viruses." *Virology journal* 10(1): 1–11.
- McAuley, J. L. et al. 2017. "The Cell Surface Mucin MUC1 Limits the Severity of Influenza A Virus Infection." *Mucosal Immunology* 10(6): 1581–93.
- McCarthy, Davis J, Yunshun Chen, and Gordon K Smyth. 2012. "Differential Expression Analysis of Multifactor RNA-Seq Experiments with Respect to Biological Variation." *Nucleic acids research*: 1–10.
- McGinn, Owen J et al. 2011. "Modulation of Integrin A4β1 by ADAM28 Promotes Lymphocyte Adhesion and Transendothelial Migration." *Cell Biology International* 35(10): 1043–53.
- Meineke, Robert, Guus F. Rimmelzwaan, and Husni Elbahesh. 2019. "Influenza Virus Infections and Cellular Kinases." *Viruses* 11(2).
- Meyerholz, David K, and Amanda P Beck. 2018. "Principles and Approaches for Reproducible Scoring of Tissue Stains in Research." *Laboratory Investigation* 98: 844–55.
- Mi, Shuo Fu, Yan Li, Jing Hua Yan, and George Fu Gao. 2010. "Na+/K+-ATPase B1 Subunit Interacts with M2 Proteins of Influenza A and B Viruses and Affects the Virus Replication." *Science China Life Sciences* 53(9): 1098–1105.
- Minakuchi, M. et al. 2017. "Pre-MRNA Processing Factor Prp18 Is a Stimulatory Factor of Influenza Virus RNA Synthesis and Possesses Nucleoprotein Chaperone Activity." *Journal of Virology* 91(3): 1–11.
- Mohamed, Reda. 2017. "Sexual Dimorphism in the Anatomical Features of the Syrinx in the White Pekin Ducks (Anas Platyrhynchos)." *International Journal for Agricultural Sciences*

- and Veterinary Medicine 5(2): 78–85.
- Mok, B. W. Y. et al. 2012. "The NS1 Protein of Influenza A Virus Interacts with Cellular Processing Bodies and Stress Granules through RNA-Associated Protein 55 (RAP55) during Virus Infection." *Journal of Virology* 86(23): 12695–707.
- Monne, I. et al. 2014. "Emergence of a Highly Pathogenic Avian Influenza Virus from a Low-Pathogenic Progenitor." *Journal of Virology* 88(8): 4375–88.
- Mossong, Joël et al. 2008. "Social Contacts and Mixing Patterns Relevant to the Spread of Infectious Diseases." *PLoS Medicine* 5(3): 0381–91.
- Mulcahy, Dan, John Burke, Ron Pascho, and C. K. Jenies. 1982. "Pathogenesis of Infectious Hematopoietic Necrosis Virus in Adult Sockeye Salmon (Oncorhynchus Nerka)." *Canadian Journal of Fisheries and Aquatic Sciences* 39(8): 1144–49.
- Munday, James, Helen Floyd, and Paul R. Crocker. 1999. "Sialic Acid Binding Receptors (Siglecs) Expressed by Macrophages." *Journal of Leukocyte Biology* 66(5): 705–11.
- Munster, Vincent J. et al. 2005. "Mallards and Highly Pathogenic Avian Influenza Ancestral Viruses, Northern Europe." *Emerging Infectious Diseases* 11(10): 1545–51.
- Nadgir, Sagar V. et al. 2013. "Fifty Percent Tissue Culture Infective Dose Assay for Determining the Titer of Infectious Human Herpesvirus 8." *Journal of Clinical Microbiology* 51(6): 1931–34.
- Nair, Padmanabhan et al. 2003. "Coprocytobiology: On the Nature of Cellular Elements from Stools in the Pathophysiology of Colonic Disease." *Journal of Clinical Gastroenterology* 36(1): 84–93.
- Naito, Tadasuke, Fumitaka Momose, Atsushi Kawaguchi, and Kyosuke Nagata. 2007. "Involvement of Hsp90 in Assembly and Nuclear Import of Influenza Virus RNA Polymerase Subunits." *Journal of Virology* 81(3): 1339–49.
- Nguyen, Thang, Xikui K. Liu, Yongliang Zhang, and Chen Dong. 2006. "BTNL2, a Butyrophilin-Like Molecule That Functions to Inhibit T Cell Activation." *The Journal of Immunology* 176(12): 7354–60.
- Niu, Qiaona et al. 2019. "Chicken DDX3x Activates IFN-β via the CHSTING-ChiRF7-IFN-β Signaling Axis." *Frontiers in Immunology* 10: 1–13.
- O'Brien, Daniel J., Stephen M. Schmitt, Brent A. Rudolph, and Graham Nugent. 2011. "Recent Advances in the Management of Bovine Tuberculosis in Free-Ranging Wildlife." *Veterinary Microbiology* 151(1–2): 23–33.
- Oshiumi, Hiroyuki et al. 2015. "DDX60 Is Involved in RIG-I-Dependent and Independent

- Antiviral Responses, and Its Function Is Attenuated by Virus-Induced EGFR Activation." *Cell Reports* 11(8): 1193–1207.
- Papp, Zsuzsanna et al. 2017. "The Ecology of Avian Influenza Viruses in Wild Dabbling Ducks (Anas Spp.) in Canada." *PLoS ONE* 12(5): 1–18.
- Paull, Sara H. et al. 2012. "From Superspreaders to Disease Hotspots: Linking Transmission across Hosts and Space." *Frontiers in Ecology and the Environment* 10(2): 75–82.
- Payne, Anne F., Iwona Binduga-Gajewska, Elizabeth B. Kauffman, and Laura D. Kramer. 2006. "Quantitation of Flaviviruses by Fluorescent Focus Assay." *Journal of Virological Methods* 134(1–2): 183–89.
- Peacock, Thomas P., Carol M. Sheppard, Ecco Staller, and Wendy S. Barclay. 2019. "Host Determinants of Influenza RNA Synthesis." *Annual Review of Virology* 6: 215–33.
- Pearce, M. C. et al. 2004. "Temporal Shedding Patterns and Virulence Factors of Escherichia Coli Serogroups O26, O103, O111, O145, and O157 in a Cohort of Beef Calves and Their Dams." *Applied and Environmental Microbiology* 70(3): 1708–16.
- Peñaranda, Michelle D., Andrew R. Wargo, and Gael Kurath. 2011. "In Vivo Fitness Correlates with Host-Specific Virulence of Infectious Hematopoietic Necrosis Virus (IHNV) in Sockeye Salmon and Rainbow Trout." *Virology* 417: 312–19.
- Perusina Lanfranca, Mirna et al. 2016. "Biological and Pathological Activities of Interleukin-22." *Journal of Molecular Medicine* 94(5): 523–34.
- Petit, Daniel et al. 2018. "Reconstruction of the Sialylation Pathway in the Ancestor of Eukaryotes." *Scientific Reports* 8(1): 1–13.
- Pillai, Smitha P, and Chang W Lee. 2010. "Species and Age Related Differences in the Type and Distribution of Influenza Virus Receptors in Different Tissues of Chickens, Ducks and Turkeys." *Virology Journal* 7(5): 1–8.
- Pinheiro, Jose, Douglas Bates, Saikat DebRoy, and Deepayan Sarkar. 2007. "Linear and Nonlinear Mixed Effects Models." *R package version 3*: 1–97.
- Pleil, Joachim D. 2016. "Imputing Defensible Values for Left-Censored 'below Level of Quantitation' (LoQ) Biomarker Measurements." *Journal of Breath Research* 10(4): 45001.
- Plummer, Ian H et al. 2017. "Temporal Patterns of Chronic Wasting Disease Prion Excretion in Three Cervid Species." *Journal of General Virology* 98: 1932–42.
- Poveda, Jonay et al. 2017. "MXRA5 Is a TGF-B1-Regulated Human Protein with Anti-Inflammatory and Anti-Fibrotic Properties." *Journal of Cellular and Molecular Medicine* 21(1): 154–64.

- Predicala, Rey, and Yan Zhou. 2013. "The Role of Ran-Binding Protein 3 during Influenza A Virus Replication." *Journal of General Virology* 94: 977–84.
- Puertollano, Rosa et al. 1999. "The Mal Proteolipid Is Necessary for Normal Apical Transport and Accurate Sorting of the Influenza Virus Hemagglutinin in Madin-Darby Canine Kidney Cells." *Journal of Cell Biology* 145(1): 141–51.
- Purcell, Maureen K. et al. 2010. "Early Viral Replication and Induced or Constitutive Immunity in Rainbow Trout Families with Differential Resistance to Infectious Hematopoietic Necrosis Virus (IHNV)." Fish and Shellfish Immunology 28(1): 98–105.
- Qiu, X. B., Y. M. Shao, S. Miao, and L. Wang. 2006. "The Diversity of the DnaJ/Hsp40 Family, the Crucial Partners for Hsp70 Chaperones." *Cellular and Molecular Life Sciences* 63(22): 2560–70.
- Ranaware, Pradip B. et al. 2016. "Genome Wide Host Gene Expression Analysis in Chicken Lungs Infected with Avian Influenza Viruses." *PLoS ONE* 11(4): 1–16.
- Reed, L.J., and H. Muench. 1938. "A Simple Method of Estimating Fifty per Cent Endpoints." *American Journal of Hygiene* 27(3): 435–69.
- Reemers, Sylvia S. et al. 2010. "Early Host Responses to Avian Influenza A Virus Are Prolonged and Enhanced at Transcriptional Level Depending on Maturation of the Immune System." *Molecular Immunology* 47(9): 1675–85.
- Rio, Donald C. 2014. "Reverse Transcription–Polymerase Chain Reaction." *Cold Spring Harbor Protocols* 2014(11): 1207–16.
- Rishi, Arun K. et al. 2003. "Identification and Characterization of a Cell Cycle and Apoptosis Regulatory Protein-1 as a Novel Mediator of Apoptosis Signaling by Retinoid CD437." *Journal of Biological Chemistry* 278(35): 33422–35.
- Ritchie, M.E. et al. 2015. "Limma Powers Differential Expression Analyses for RNA-Sequencing and Microarray Studies." *Nuceic Acids Research* 43(7): e47.
- Rivas, Hembly G., Summer K. Schmaling, and Marta M. Gaglia. 2016. "Shutoff of Host Gene Expression in Influenza A Virus and Herpesviruses: Similar Mechanisms and Common Themes." *Viruses* 8(4): 1–26.
- Robinson, Mark D., Davis J. McCarthy, and Gordon K. Smyth. 2010. "EdgeR: A Bioconductor Package for Differential Expression Analysis of Digital Gene Expression Data." *Bioinformatics* 26(1): 139–40.
- Rohaim, Mohammed A. et al. 2018. "Chickens Expressing IFIT5 Ameliorate Clinical Outcome and Pathology of Highly Pathogenic Avian Influenza and Velogenic Newcastle Disease Viruses." *Frontiers in Immunology* 9: 1–17.

- Röhm, Carolin et al. 1995. "Do Hemagglutinin Genes of Highly Pathogenic Avian Influenza Viruses Constitute Unique Phylogenetic Lineages?" *Virology* 209(2): 664–70.
- Rohwer, Frank C, William P Johnson, and Elizabeth R Loos. 2002. "Blue-Winged Teal (Spatula Discors)." In *The Birds of North America*, eds. A. F. Poole and F. B. Gill. Ithaca, NY, USA: Cornell Lab of Orithology.
- Rong, Enguang, Jiaxiang Hu, et al. 2018. "Broad-Spectrum Antiviral Functions of Duck Interferon-Induced Protein with Tetratricopeptide Repeats (AvIFIT)." *Developmental and Comparative Immunology* 84: 71–81.
- Rong, Enguang, Xiaoxue Wang, et al. 2018. "Molecular Mechanisms for the Adaptive Switching between the OAS/RNase L and OASL/RIG-I Pathways in Birds and Mammals." *Frontiers in Immunology* 9: 1–14.
- Rosenberger, Carrie M. et al. 2017. "MiR-144 Attenuates the Host Response to Influenza Virus by Targeting the TRAF6-IRF7 Signaling Axis." *PLoS Pathogens* 13(4): 1–20.
- Rothenfusser, Simon et al. 2005. "The RNA Helicase Lgp2 Inhibits TLR-Independent Sensing of Viral Replication by Retinoic Acid-Inducible Gene-I." *The Journal of Immunology* 175(8): 5260–68.
- Rudnicka, Alina, and Yohei Yamauchi. 2016. "Ubiquitin in Influenza Virus Entry and Innate Immunity." *Viruses* 8(10): 1–15.
- Samji, Tasleem. 2009. "Influenza A: Understanding the Viral Life Cycle." *Yale Journal of Biology and Medicine* 82(4): 153–59.
- Sanchez, Erica L., and Michael Lagunoff. 2015. "Viral Activation of Cellular Metabolism." *Virology* 479–480: 609–18.
- Santhakumar, Diwakar, Dennis Rubbenstroth, Luis Martinez-Sobrido, and Muhammad Munir. 2017. "Avian Interferons and Their Antiviral Effectors." *Frontiers in Immunology* 8: 1–19.
- Sarais, Fabio et al. 2020. "Characterisation of the Teleostean KB-Ras Family: The Two Members NKIRAS1 and NKIRAS2 from Rainbow Trout Influence the Activity of NF-KB in Opposite Ways." Fish and Shellfish Immunology 106: 1004–13.
- Saunders, Samuel E., Shannon L. Bartlet-Hunt, and Jason C. Bartz. 2012. "Occurrence, Transmission, and Zoonotic Potential of Chronic Wasting Disease." *Emerging Infectious Diseases* 18(3): 369.
- Schmidt, Nora et al. 2019. "An Influenza Virus-Triggered SUMO Switch Orchestrates Co-Opted Endogenous Retroviruses to Stimulate Host Antiviral Immunity." *Proceedings of the National Academy of Sciences of the United States of America* 116(35): 17399–408.

- Schoggins, John W. 2019. "Interferon-Stimulated Genes: What Do They All Do?" *Annual Review of Virology* 6: 567–84.
- Schoggins, John W., and Charles M. Rice. 2011. "Interferon-Stimulated Genes and Their Antiviral Effector Functions." *Current Opinion in Virology* 1(6): 519–25.
- Searle, Shayle Robert, and Charles McCulloch. 2001. *Generalized, Linear and Mixed Models*. Wiley.
- Sen, Ganes C., and Gregory A. Peters. 2007. "Viral Stress-Inducible Genes." *Advances in Virus Research* 70(07): 233–63.
- Shapira, Sagi D. et al. 2009. "A Physical and Regulatory Map of Host-Influenza Interactions Reveals Pathways in H1N1 Infection." *Cell* 139(7): 1255–67.
- Shaw, Megan L., and Silke Stertz. 2017. "Role of Host Genes in Influenza Virus Replication." In *Roles of Host Gene and Non-Coding RNA Expression in Virus Infection*, Springer, Cham, 151–89.
- Shi, Zheng-zheng, Jia-wei Zhang, and Shu Zheng. 2007. "What We Know about ST13, a Co-Factor of Heat Shock Protein, or a Tumor Suppressor?" *Journal of Zhejiang University*. *Science B* 8(3): 170–76.
- Shim, Jung Min et al. 2017. "Influenza Virus Infection, Interferon Response, Viral Counter-Response, and Apoptosis." *Viruses* 9(8): 1–12.
- Shin, Amanda et al. 2008. "P2Y Receptor Signajing Regulates Phenotype and IFN-ά Secretion of Human Plasmacytoid Dendritic Cells." *Blood* 111(6): 3062–69.
- Singh, I., R. W. Doms, K. R. Wagner, and A. Helenius. 1990. "Intracellular Transport of Soluble and Membrane-Bound Glycoproteins: Folding, Assembly and Secretion of Anchor-Free Influenza Hemagglutinin." *EMBO Journal* 9(3): 631–39.
- Skehel, John J, and Don C Wiley. 2000. "Receptor Binding and Membrane Fusion in Virus Entry: The Influenza Hemagglutinin." *Annual Review of Biochemistry* 69(1): 539–69.
- Slemons, Richard D., and Bernard C. Easterday. 1978. "Virus Replication in the Digestive Tract of Ducks Exposed by Aerosol to Type-A Influenza." *Avian Diseases* 22(3): 367–77.
- Smith, Isobel A. et al. 2010. "BTN1A1, the Mammary Gland Butyrophilin, and BTN2A2 Are Both Inhibitors of T Cell Activation." *The Journal of Immunology* 184(7): 3514–25.
- Smith, Jacqueline et al. 2015. "A Comparative Analysis of Host Responses to Avian Influenza Infection in Ducks and Chickens Highlights a Role for the Interferon-Induced Transmembrane Proteins in Viral Resistance." *BMC genomics* 16(1): 1–19.

- Song, Guanhua et al. 2016. "E3 Ubiquitin Ligase RNF128 Promotes Innate Antiviral Immunity through K63-Linked Ubiquitination of TBK1." *Nature Immunology* 17(12): 1342–51.
- Soulat, Didier et al. 2008. "The DEAD-Box Helicase DDX3X Is a Critical Component of the TANK-Binding Kinase 1-Dependent Innate Immune Response." *EMBO Journal* 27(15): 2135–46.
- Spackman, Erica et al. 2002. "Development of a Real-Time Reverse Transcriptase PCR Assay for Type A Influenza Virus and the Avian H5 and H7 Hemagglutinin Subtypes." *Journal of Clinical Microbiology* 40(9): 3256–60.
- Spackman, Erica, and Mary Lea Killian. 2014. "Avian Influenza Virus Isolation, Propagation, and Titration in Embryonated Chicken Eggs." In *Animal Influenza Virus*, New York, NY: Humana Press, 125–40.
- Spackman, Erica, and David L. Suarez. 2008. "Type a Influenza Virus Detection and Quantitation by Real-Time RT-PCR." *Methods in Molecular Biology* 436(M): 19–26.
- Stahlschmidt, Zachary R., and Jordan R. Glass. 2020. "Life History and Immune Challenge Influence Metabolic Plasticity to Food Availability and Acclimation Temperature." *Physiological and biochemical zoology* 93(4): 271–81.
- Stallknecht, David E, et al. 1990. "Avian Influenza Viruses from Migratory and Resident Ducks of Coastal Louisiana." *Avian Diseases* 34(2): 398–405.
- Stallknecht, David E, and S M Shane. 1988. "Host Range of Avian Influenza Virus in Free-Living Birds." *Veterinary research communications* 12(2–3): 125–41.
- Stallknecht, David E, and Justin D Brown. 2008. "Ecology of Avian Influenza in Wild Birds." In *Avian Influenza*, 43–58.
- Stambas, John et al. 2017. "ADAMTS5 and Its Substrate Versican Play a Critical Role in Influenza Virus Immunity." *The Journal of Immunology* 198(1): 121–23.
- Stein, Richard A. 2011. "Super-Spreaders in Infectious Diseases." *International Journal of Infectious Diseases* 15(8): 510–13.
- Stertz, Silke, and Megan L. Shaw. 2011. "Uncovering the Global Host Cell Requirements for Influenza Virus Replication via RNAi Screening." *Microbes and Infection* 13(5): 516–25.
- Stricher, François, Christophe Macri, Marc Ruff, and Sylviane Muller. 2013. "HSPA8/HSC70 Chaperone Protein: Structure, Function, and Chemical Targeting." *Autophagy* 9(12): 1937–54.
- Su, Wen-Chi et al. 2015. "A Nucleolar Protein, Ribosomal RNA Processing 1 Homolog B (RRP1B), Enhances the Recruitment of Cellular MRNA in Influenza Virus Transcription."

- Journal of Virology 89(22): 11245–55.
- Suarez, David L., and S. Schultz-Cherry. 2000. "Immunology of Avian Influenza Virus: A Review." *Developmental and Comparative Immunology* 24(2–3): 269–83.
- Suarez, David L. 2009. "Influenza a Virus." In Avian Influenza, Blackwell Publishing Ltd., 1–22.
- Svobodová, Jana et al. 2020. "Differences in the Growth Rate and Immune Strategies of Farmed and Wild Mallard Populations." *PLoS ONE* 15(8 August): 1–19.
- Swayne, David E., ed. 2009. Avian Influenza. John Wiley & Sons.
- Tadiri, Christina P., Felipe Dargent, and Marilyn E. Scott. 2013. "Relative Host Body Condition and Food Availability Influence Epidemic Dynamics: A Poecilia Reticulata-Gyrodactylus Turnbulli Host-Parasite Model." *Parasitology* 140(3): 343–51.
- Takahashi, Yoshiyuki et al. 2008. "Regression of Human Kidney Cancer Following Allogeneic Stem Cell Transplantation Is Associated with Recognition of an HERV-E Antigen by T Cells." *Journal of Clinical Investigation* 118(3): 1099–1109.
- Takekawa, John Y. et al. 2010. "Migration of Waterfowl in the East Asian Flyway and Spatial Relationship to PHAI H5N1 Outbreaks." *Avian Diseases* 54(s1): 466–76.
- Team, R. Core. 2013. "R: A Language and Environment for Statistical Computing."
- Tokhtaeva, Elmira et al. 2015. "Septin Dynamics Are Essential for Exocytosis." *Journal of Biological Chemistry* 290(9): 5280–8297.
- Tolouei, Samira et al. 2019. "Assessing Microbial Risk through Event-Based Pathogen Loading and Hydrodynamic Modelling." *Science of the Total Environment* 693.
- Tripathi, Shashank et al. 2015. "Meta- and Orthogonal Integration of Influenza 'OMICs' Data Defines a Role for UBR4 in Virus Budding." *Cell Host and Microbe* 18(6): 723–35.
- Tsang, Kenneth W. et al. 2003. "A Cluster of Cases of Severe Acute Respiratory Syndrome in Hong Kong." *The New England Journal of Medicine* 348(20): 1977–85.
- Tummers, Bart et al. 2015. "The Interferon-Related Developmental Regulator 1 Is Used by Human Papillomavirus to Suppress NFκB Activation." *Nature Communications* 6: 1–12.
- Vanderven, Hillary A. et al. 2012. "Avian Influenza Rapidly Induces Antiviral Genes in Duck Lung and Intestine." *Molecular Immunology* 51(3–4): 316–24.
- Vanderwaal, Kimberly L, and Vanessa O Ezenwa. 2016. "Heterogeneity in Pathogen Transmission: Mechanisms and Methodology." *Functional Ecology* 30: 1606–22.

- Veillette, André, Michael A. Bookman, Eva M. Horak, and Joseph B. Bolen. 1988. "The CD4 and CD8 T Cell Surface Antigens Are Associated with the Internal Membrane Tyrosine-Protein Kinase P56lck." *Cell* 55(2): 301–8.
- Volmer, Christelle et al. 2011. "Immune Response in the Duck Intestine Following Infection with Low-Pathogenic Avian Influenza Viruses or Stimulation with a Toll-like Receptor 7 Agonist Administered Orally." *Journal of General Virology* 92(3): 534–43.
- Wang, Feng Xiang et al. 2008. "APOBEC3G Upregulation by Alpha Interferon Restricts Human Immunodeficiency Virus Type 1 Infection in Human Peripheral Plasmacytoid Dendritic Cells." *Journal of General Virology* 89(3): 722–30.
- Wang, Hongliang, and Chengyu Jiang. 2009. "Influenza A Virus H5N1 Entry into Host Cells Is through Clathrin-Dependent Endocytosis." *Science in China, Series C: Life Sciences* 52(5): 464–69.
- Wang, Ou et al. 2017. "Host Mechanisms Involved in Cattle Escherichia Coli O157 Shedding: A Fundamental Understanding for Reducing Foodborne Pathogen in Food Animal Production." *Scientific Reports* 7(1): 1–15.
- Wang, Yimeng, Jianhong Zhou, and Yuchun Du. 2014. "HnRNP A2/B1 Interacts with Influenza A Viral Protein NS1 and Inhibits Virus Replication Potentially through Suppressing NS1 RNA/Protein Levels and NS1 MRNA Nuclear Export." *Virology* 449: 53–61.
- Ward, C. L. et al. 2004. "Design and Performance Testing of Quantitative Real Time PCR Assays for Influenza A and B Viral Load Measurement." *Journal of Clinical Virology* 29(3): 179–88.
- Wargo, Andrew R et al. 2012. "Analysis of Host Genetic Diversity and Viral Entry as Sources of Between-Host Variation in Viral Load." *Virus Research* 165: 71–80.
- Wasserberg, Gideon, Erik E. Osnas, Robert E. Rolley, and Michael D. Samuel. 2009. "Host Culling as an Adaptive Management Tool for Chronic Wasting Disease in White-Tailed Deer: A Modelling Study." *Journal of Applied Ecology* 46(2): 457–66.
- Watanabe, Ken et al. 2006. "Identification of Hsc70 as an Influenza Virus Matrix Protein (M1) Binding Factor Involved in the Virus Life Cycle." *FEBS Letters* 580(24): 5785–90.
- Watanabe, Tokiko, Shinji Watanabe, and Yoshihiro Kawaoka. 2010. "Cellular Networks Involved in the Influenza Virus Life Cycle." *Cell Host and Microbe* 7(6): 427–39.
- Watanabe, Yohei, Madiha S Ibrahim, Yasuo Suzuki, and Kazuyoshi Ikuta. 2012. "The Changing Nature of Avian Influenza A Virus (H5N1)." *Trends in microbiology* 20(1): 11–20.
- Webster, Robert G. et al. 1978. "Intestinal Influenza: Replication and Characterization of Influenza Viruses in Ducks." *Virology* 84(2): 268–78.

- Webster, Robert G et al. 1992. "Evolution and Ecology of Influenza A Viruses." *Microbiological reviews* 56(1): 152–79.
- Weitzman, Chava L, Franziska C Sandmeier, and C Richard Tracy. 2017. "Prevalence and Diversity of the Upper Respiratory Pathogen Mycoplasma Agassizii in Mojave Desert Tortoises (Gopherus Agassizii)." *Herpetologica* 73(2): 113–20.
- Welsby, Iain et al. 2014. "PARP12, an Interferon-Stimulated Gene Involved in the Control of Protein Translation and Inflammation." *Journal of Biological Chemistry* 289(38): 26642–57.
- Whiteside, Simon T., Jean Charles Epinat, Nancy R. Rice, and Alain Israël. 1997. "I Kappa B Epsilon, a Novel Member of the IκB Family, Controls RelA and CRel NF-KB Activity." *EMBO Journal* 16(6): 1413–26.
- Whitlock, R. H. et al. 2006. "Johne's Disease: Mycobacterium Paratuberculosis Super-Shedders: Detection and Contribution to Passive Shedding (False-Posive Fecal Cultures)." In *American Association of Bovine Practioners*, 286.
- Whitlock, R. H., S. J. Wells, R. W. Sweeney, and J. Van Tiem. 2000. "ELISA and Fecal Culture for Paratuberculosis (Johne's Disease): Sensitivity and Specificity of Each Method." *Veterinary Microbiology* 77(3–4): 387–98.
- Wille, Michelle, Caroline Bröjer, Åke Lundkvist, and Josef D. Järhult. 2018. "Alternate Routes of Influenza A Virus Infection in Mallard (Anas Platyrhynchos)." *Veterinary Research* 49(1): 1–9.
- Wille, Michelle, Peter Van Run, Jonas Waldenström, and Thijs Kuiken. 2014. "Infected or Not: Are PCR-Positive Oropharyngeal Swabs Indicative of Low Pathogenic Influenza A Virus Infection in the Respiratory Tract of Mallard Anas Platyrhynchos?" *Veterinary Research* 45(53): 1–5.
- Wobeser, Gary A. 2007. Disease in Wild Animals. Berlin, Germany: Springer.
- Woolcock, Peter R. 2008. "Avian Influenza Virus Isolation and Propagation in Chicken Eggs." *Methods in Molecular Biology* 436: 35–46.
- Woolhouse, M E et al. 1996. "Heterogeneities in the Transmission of Infectious Agents: Implications for the Design of Control Programs." *Proceedings of the National Academy of Sciences of the United States of America* 94(1): 338–42.
- Xiong, Bin, Yiben Yang, Frank R. Fineis, and Ji Ping Wang. 2019. "DegNorm: Normalization of Generalized Transcript Degradation Improves Accuracy in RNA-Seq Analysis." *Genome Biology* 20(1): 1–18.
- Young, George R. et al. 2012. "Negative Selection by an Endogenous Retrovirus Promotes a

- Higher-Avidity CD4+ T Cell Response to Retroviral Infection." *PLoS Pathogens* 8(5).
- Yu, Ji Eun et al. 2011. "Expression Patterns of Influenza Virus Receptors in the Respiratory Tracts of Four Species of Poultry." *Journal of veterinary science* 12(1): 7–13.
- Yu, Jingyou, and Shan Lu Liu. 2019. "Emerging Role of LY6E in Virus-Host Interactions." *Viruses* 11(11): 1–11.
- Zeng, Miao et al. 2016. "Molecular Identification and Comparative Transcriptional Analysis of Myxovirus Resistance GTPase (Mx) Gene in Goose (Anser Cygnoide) after H9N2 AIV Infection." *Comparative Immunology, Microbiology and Infectious Diseases* 47: 32–40.
- Zhang, Junjie, Gang Li, and Xin Ye. 2010. "Cyclin T1/CDK9 Interacts with Influenza A Virus Polymerase and Facilitates Its Association with Cellular RNA Polymerase II." *Journal of Virology* 84(24): 12619–27.
- Zhang, Junqin et al. 2020. "Transcriptome Analysis Reveals the Neuro-Immune Interactions in Duck Tembusu Virus-Infected Brain." *International Journal of Molecular Sciences* 21(7).
- Zhang, Rong et al. 2014. "The Regulation of Autophagy by Influenza A Virus." *BioMed Research International*: 1–6.
- Zhang, Xiaolin et al. 2018. "Identification of New Type I Interferon-Stimulated Genes and Investigation of Their Involvement in IFN-β Activation." *Protein and Cell* 9(9): 799–807.
- Zhang, Yong et al. 2015. "PARP9-DTX3L Ubiquitin Ligase Targets Host Histone H2BJ and Viral 3C Protease to Enhance Interferon Signaling and Control Viral Infection." *Nature Immunology* 16(12): 1215–27.
- Zhang, Yong Zhen, and Edward C. Holmes. 2020. "A Genomic Perspective on the Origin and Emergence of SARS-CoV-2." *Cell* 181(2): 223–27.
- Zhao, Qiong et al. 2017. "Dual Roles of Two Isoforms of Autophagy-Related Gene ATG10 in HCV-Subgenomic Replicon Mediated Autophagy Flux and Innate Immunity." *Scientific Reports* 7(1): 1–15.
- Zheng, Min, Rajendra Karki, Peter Vogel, and Thirumala Devi Kanneganti. 2020. "Caspase-6 Is a Key Regulator of Innate Immunity, Inflammasome Activation, and Host Defense." *Cell* 181(3): 674-687.e13.
- Zhou, Yong, Juan Pu, and Yuping Wu. 2021. "The Role of Lipid Metabolism in Influenza A Virus Infection." *Pathogens* 10(3): 1–11.
- Zhu, L., H. Ly, and Y. Liang. 2014. "PLC- 1 Signaling Plays a Subtype-Specific Role in Postbinding Cell Entry of Influenza A Virus." *Journal of Virology* 88(1): 417–24.

- Zhuang, Shen et al. 2004. "Superspreading SARS Events, Beijing, 2003." *Emerging infectious diseases* 10(2): 256–60.
- Zuk, Marlene, and Kurt A. McKean. 1996. "Sex Differences in Parasite Infections: Patterns and Processes." *International Journal for Parasitology* 26(10): 1009–24.
- Zuur, Alain F, Elena N Ieno, and Chris S Elphick. 2010. "A Protocol for Data Exploration to Avoid Common Statistical Problems." *Methods in Ecology and Evolution* 1: 3–14.